Alexander Igamberdiev

A Duality Transform for Realizing Convex Polytopes with Small Integer Coordinates

2015

Informatik

A Duality Transform for Realizing Convex Polytopes with Small Integer Coordinates

Inaugural-Dissertation
zur Erlangung des Doktorgrades
der Naturwissenschaften im Fachbereich
Mathematik und Informatik
der Mathematisch-Naturwissenschaftlichen Fakultät
der Westfälischen Wilhelms-Universität Münster

vorgelegt von
Alexander Igamberdiev
aus Sankt Petersburg
2015

Dekan:	Prof. Dr. Martin Stein
Erster Gutachter:	Prof. Dr. André Schulz
Zweiter Gutachter:	Dr. habil. Ivan Izmestiev
Tag der mündlichen Prüfung:	11.02.2016
Tag der Promotion:	11.02.2016

Abstract

In this thesis we study realizations of convex polytopes with small integer coordinates. We develop an efficient duality transform that allows us to go from an efficient integer realization of a polytope to an efficient integer realization of its dual. Our algorithms are based on novel techniques based on braced stresses and a generalization of the Maxwell–Cremona lifting procedure.

Our methods prove to be especially efficient for realizing the class of polytopes dual to stacked polytopes, known as truncated polytopes. We show that every truncated polytope with n vertices can be realized on an integer grid of size $O(n^{9 \lg 6+1})$. This is only the second nontrivial class of polytopes, the first being the class of stacked polytopes, for which realizations on a polynomial size integer grid are known to exists.

More generally, our techniques are applicable to any simplicial polytope in the following sense. Given a simplicial polytope with n vertices and the maximal vertex degree Δ, realized on an integer grid of size L, we show how to realize its dual on an integer grid of size $O(nL^{3\Delta+9})$. Although this bound is not purely polynomial, it is a noticeable improvement over the exponential bound provided by standard polarity.

Our techniques can be generalized to higher dimensions. We present the generalizations of the duality transforms with all the necessary details and techniques.

The presented duality transform is in large part inspired by the work of Lovász on Colin de Verdière matrices of graphs of convex polytopes, and in particular by the generalization of the Maxwell–Cremona lifting procedure presented there. To make these techniques properly applicable, we develop new tools for operating with equilibrium and braced stresses, liftings, and interconnections among them.

In addition to the duality transforms, we present a direct embedding procedure for one special class of 3d polytopes, the class of prismatoids. We show that every prismatoid with n vertices can be realized on an integral grid of size $O(n^4) \times O(n^3) \times 1$.

Acknowledgements

This work would not be possible without the wise guidance of my advisor, André Schulz. I am grateful to him for introducing me to this topic, for hours of discussions and for his patience, I was a very lucky PhD student as my advisor always had time for me and for my questions. My second thanks goes to Ivan Izmestiev who agreed to be a co-referee for this work.

I'm indebted to everybody who taught me maths at all the stages of my life. I was always extremely lucky with my teachers, with each and every of you, I wish I could be as cool as you. One special gratitude goes to Konstantin Abramenko, who showed me the beauty of geometry under the very right angle from the very beginning. Another special thanks goes to Dmitry Chelkak for establishing the Chebyshev Lab, where I first witnessed an active mathematical lifeflow, and to everybody who participated in this project, it was a great fun.

I'm infinitely grateful to my family for the endless support that they provided me during all these years. I'm proud to have such a robust source of strength. It is invaluable.

My friends influenced me (and thus, this text) for the better a lot (imagine what it would be without you!). Love you all. We should meet more often, better in Rome. Those of you who made it to visit me during these years are my heroes.

Anton and Ksusha (in alphabetical order), you were always here when I was in doubts about yet another comma or what should be considered trivial. You are awesome.

Thanks to my Münster people. You brought life (and light!) to this place.

Contents

Introduction

Convex polytopes have a long history as a subject of mathematical research. They were systematically studied already back in ancient Greece with the efforts to classify the platonic solids. During the following centuries convex polytopes proved to be a fundamental geometrical concept, with a new wave of interest coming in the last hundred years. However, despite the seeming simplicity of the concept and a long history of attention, some immediate, striking questions are still open. One such question is the subject of our research.

A *convex 3-dimensional polytope* is a full dimensional convex hull of a finite set of points in $\mathbb{R}^3$. We reserve the word *polytope* for *convex* polytopes and usually omit the word *convex*. The surface of a polytope is formed by extreme points that are called *vertices*, straight-line segments connecting pairs of vertices called *edges* and 2d cells called *faces*. The vertices and edges of a polytope form the *graph of the polytope*.

Incidence relations between faces, edges and vertices define the *combinatorial structure*, or the *face structure*, of a polytope. The face structure of a 3d polytope is completely determined by its graph (see [45, Theorem 11]). We call two polytopes *combinatorially equivalent* if their face structures coincide, what is equivalent in 3d to that their graphs coincide.

The face structure of a polytope is a purely combinatorial object, namely a partially ordered set. By this, convex polytopes can be used to decode combinatorial structures. As a prominent example we mention the associahedron, which can be used to represent Catalan structures [25]. On the other hand, a polytope is a geometrical object. Thus, representing a combinatorial structure as a face lattice of a polytope allows us to analyze this structure from a new, geometrical viewpoint (which makes polytopes a central object in combinatorial optimization [36]). This raises the following question. Given the combinatorial structure of a polytope, how "nice" can be the geometry of a polytope, which *realizes* this combinatorial structure?

Depending on the goals, by "nice" one can desire the control over many different geometrical features: classical graph drawing features, such as the edge length ratio, the face area ratio, the aspect ratio of faces, the angular resolution [40]; or features specific to polytopes, such as the possibility to prescribe an arbitrarily shape to some of the faces [4]. One particularly intriguing feature is the realization with small integer vertex coordinates. Such realizations can be handled efficiently: In the standard computational RAM model with logarithmic costs [43] the complexity of every elementary arithmetical operation on a number with k bits depends on k at least linearly. Thus, efficiency of a realization directly influences complexity of any algorithm working with this realization. Moreover, a realization with integer vertex coordinates on a bounded grid guarantees bounds on other graph drawing quality measures. The final subject of our research is the following question:

> **Question.** Let $\mathcal{P}$ be a convex 3d polytope. Find a convex 3d polytope Q that is combinatorially equivalent to $\mathcal{P}$ and has small integer vertex coordinates.

The question above is traditionally phrased in terms of realizations of graphs. It can be traced back to the work by Steinitz of 1916 [38], which gives a combinatorial characterization

of the graphs of 3-dimensional polytopes. To proceed we need some graph theoretic notions.

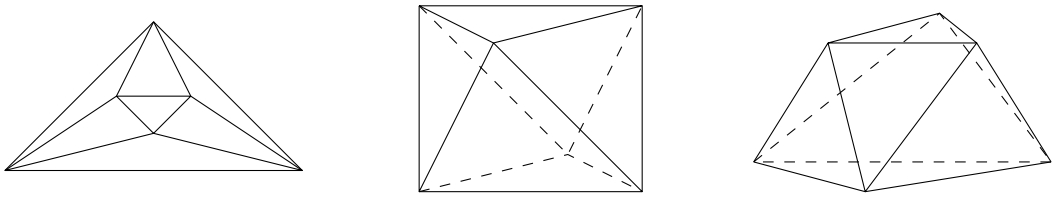

Figure 1: The graph and two different realizations of the octahedron.

A *graph* $G = (V, E)$ is a pair of a finite set of *vertices* V and a set of *edges* E connecting some pairs of the vertices. The graph is called *simple* if its edges are undirected, every two vertices are connected by no more than one edge, and none of the edges is a loop. A graph is called *connected* if every two vertices are connected by a path. A graph is called *k-connected* if it stays connected after removing of any $k-1$ of its vertices with all the incident edges. A graph is called *planar* if it can be drawn on a plane with all the edges drawn as Jordan curves so that every pair of edges do not intersect except at the common endpoints.

In 1916 Steinitz proved, that a graph G is the graph of a 3-dimensional polytope if and only if it is simple, planar, and 3-connected. Moreover, as we noticed above, a planar 3-connected graph defines the polytope uniquely up to combinatorial equivalence [45, Theorem 11]. Thus, our question can be rephrased as follows: given a planar 3-connected graph G, realize it as a graph of a convex polytope with small integer vertex coordinates.

State of the art

Best available general result. Although the original proof of Steinitz theorem is constructive and allows us to keep track of integrality of the coordinates of the resulting embedding, the produced grid size is double exponential in the number of vertices of the input graph. The first improvement over the double exponential bound was $O(n^{169n^3})$ due to Onn and Sturmfels [26]. The algorithm by Richter-Gebert reduced the bound down to $O(2^{18n^2})$ [30]. It was later improved to $O(2^{12n^2})$ by Ribó Mor [28].

The best nowadays existing algorithm for general 3d polytopes is due to Ribó Mor, Rote and Schulz [29] and it produces a realization of a polytope with n vertices within an integer grid of size $O(148^n)$. Although this is a huge improvement over the double exponential grid size produced by the original Steinitz approach, the grid size for general 3d polytopes is still exponential in the number of vertices.

Lower bound. On the other side, almost nothing is known about the lower bound on the size of the integral grid needed for realizing any 3d convex polytope with n vertices. The only known bound is $\Omega(n^{3/2})$ on each dimension [3], and it comes from the lower bound on the size of the 2d integer grid needed to support the orthogonal projection of a 3d realization.

Special classes of polytopes: stacked and simplicial. A natural direction of research is thus to try to find algorithms producing polynomial size grid realizations for special classes of polytopes. Recently, progress has been made for a special class of polytopes, called *stacked polytopes*. A 3-dimensional stacked polytope is produced from a tetrahedron by a sequence of stacking operation, where each stacking operation glues a triangular pyramid atop a triangular face of a polytope; see Fig. 2. Graphs of stacked polytopes are planar 3-trees. Demaine and Schulz showed that every stacked polytope with n vertices can be realized within an integer grid of size $O(n^{2\lg 6}) \times O(n^{2\lg 6}) \times O(n^{3\lg 6})$ [9]. This is however the only nontrivial class of polytopes for which an algorithm producing polynomial size integral realizations is known.

Another promising class of polytopes are *simplicial polytopes*. A polytope is called *simplicial* if every its face is a simplex, that is in 3d a triangle. Graphs of simplicial 3d polytopes are planar triangulations. This class is promising, since the position of every vertex of a simplicial polytope can be perturbed without breaking the combinatorial structure of the polytope. The question however stays open even for the simplicial polytopes. Recently, progress has been made in a paper by Pak and Wilson [27], which constructs realizations of simplicial 3d polytopes with coordinates polynomial in two dimensions (at the expense of the third dimension).

There exists many different approaches to realizing planar 3-connected graphs in the plane and in space, however none of them yet proved to be properly applicable to our problem. For a brief account of some of the existing approaches we redirect the reader to Chapter 1.

Other dimensions. In $\mathbb{R}^2$ the question is simple: every convex n-gon can be realized on $O(n)\times O(n^2)$ grid and no smaller realization is possible: any realization requires $O(n^3)$ area [3].

In any dimension higher than 3 there exist polytopes that *cannot* be realized with integral coordinates and there exist polytopes that *require* a double exponential integer grid size, which is a consequence of the universality theorem by Richter-Gebert [31]. Thus, only the study of special classes of polytopes is possible. The only studied class to date was the class of stacked d-dimensional polytopes, which are the d-dimensional counterparts of the 3d stacked polytopes: Demaine and Schulz showed that every stacked d-polytope with n vertices can be realized on the integer grid so that all the coordinates have size at most $10d^2R^2$, except for one axis, where the coordinates have size at most $6R^3$ for $R = n^{\lg(2d)}$ [10].

Main results

Realizing truncated polytopes. We present an efficient duality transformation that allows us to produce realizations with polynomial integer coordinates of polytopes dual to stacked polytopes, which are called *truncated polytopes*. A 3d truncated polytope can be produced from a tetrahedron by a sequence of *truncation operations*, where each truncation operation cuts off a degree-3 vertex of the polytope by replacing it with a new triangular face; see Fig. 2. We prove that:

Theorem (Theorem 2.5.3)**.** *Every truncated 3d polytope with n vertices can be realized with integer coordinates of size $O(n^{9\lg 6+1})$.*

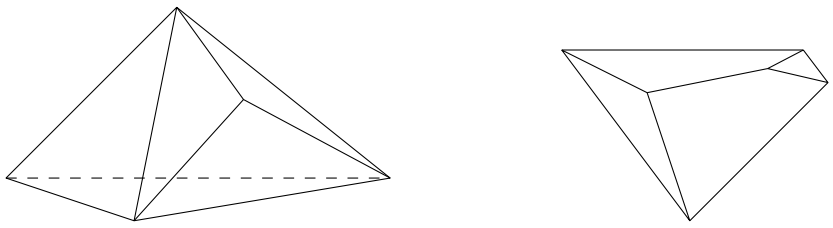

Figure 2: Left: a tetrahedron after one stacking operation. Right: a tetrahedron after the corresponding truncation.

Other duality results and the standard polarity approach. To produce realizations of truncated polytopes we develop an efficient duality transform. We remind that two 3d polytopes $\mathcal{P}$ and $\mathcal{P}^*$ are called *dual* if the vertices of $\mathcal{P}^*$ are in one-to-one correspondence with the faces of $\mathcal{P}$, and two vertices of $\mathcal{P}^*$ are connected by an edge if and only if the corresponding faces of $\mathcal{P}$ are adjacent.

One standard tool to construct a polytope dual to a given one is provided by polarity. However, for a polytope $\mathcal{P}$ with integer coordinates the coordinates of its polar dual are rationals and they acquire an exponential scaling factor when scaled to integers. Thus, for a polytope $\mathcal{P}$ with polynomial integer coordinates the coordinates of its polar dual are in general exponential.

We design a duality transform for simplicial polytopes that is more efficient than the standard polarity. To construct the realizations of truncated polytopes we use the rich structure of stacked polytopes discovered by Demaine and Schulz [9] in addition to our duality transform. For general simplicial polytopes we do not have such a rich structure and the efficiency of the duality transform depends on the maximal vertex degree of the polytope. We prove the following theorem

Theorem (Theorem 2.5.6)**.** *Let G be a triangulation of the plane with maximal vertex degree Δ_G and let $\mathcal{P} = (u_i)_{1\leq i\leq n}$ be a realization of G as a convex polytope with integer coordinates. Then there exists a realization $(\phi_f)_{f\in F(G)}$ of the dual graph G^* as a convex polytope with integer coordinates bounded by*

$$|\phi_f| = O(n \max |u_i|^{3\,\Delta_G\,+9}).$$

Our duality transforms for 3d polytopes are partially based on the ideas, presented by the author at the 21st International Symposium on Graph Drawing in Bordeaux, 2013 [16]. In particular, the embedding procedure for truncated 3d polytopes (Theorem 2.5.3) was presented in [16]. On the contrary, the duality transform for general simplicial polytopes presented in this thesis (Theorem 2.5.6) is based on a completely new approach in comparison to the conference version to provide better bounds in larger generality.

Generalizations to higher dimensions. Our results allow generalizations to higher dimensions. For truncated polytopes we prove that:

Theorem (Theorem 4.5.2)**.** *Let $\mathcal{P}$ be a truncated d-polytope with n faces. Then there exists a realization (ϕ_f) of $\mathcal{P}$ as a convex polytope with integer vertex coordinates bounded by*

$$|\phi_f| = n^{O(d^2 \lg(d))}.$$

The higher dimensional generalization of the duality transform for general simplicial polytopes is quite technical, we refer the reader directly to Theorem 4.6.2.

Main tool and further results

At its core our duality transform algorithms are based on the *Lovász duality transform*, which builds on the notion of *braced stresses*. To the best of our knowledge, it first appeared as an auxiliary construction in Lovász paper on Steinitz representations of polyhedra and the Colin de Verdière number [21]. The original paper did not give this construction any name. The term "braced stress", together with some further discussion of the concept and connections to other types of stresses can be found in the draft of a book on geometrical representations of graphs by the same author [22].

Let $\mathbf{u} = (u_i)$ be an embedding of a graph G to $\mathbb{R}^3$ and let $\omega : E(G) \to \mathbb{R}$ be an assignment of reals to the edges of G. We say that a vertex u_i is in *braced equilibrium* if there exists a real σ_i such that

$$\sum_{j\in N(i,G)} \omega_{ij}(u_j - u_i) + \sigma_i u_i = 0, \tag{1}$$

where the sum goes over the neighbours of u_i. (For simplicity we used a nonstandard form of Eq. (1) above. Later in the main part of the thesis we use a different, though equivalent,

standard form as the basic definition of braced stress.) We say that ω is a *braced stress* if every vertex is in braced equilibrium.

The braced stress is a natural 3d counterpart of the classical *equilibrium stress*. We remind, that a vertex u_i is said to be in *equilibrium* if

$$\sum_{j\in N(i)} \omega_{ij}(u_j - u_i) = 0, \tag{2}$$

where again the sum goes over the neighbours of u_i. An assignment ω is called an *equilibrium stress* if every vertex is in equilibrium. However, the notion of equilibrium stress is hardly applicable in the 3-dimensional setup; see Fig. 3. The notions of braced and equilibrium stresses are deeply interconnected: We establish different connections between braced and equilibrium stresses in Sect. 2.3.3, Sect. 2.3.4, and Sect. 2.3.6.

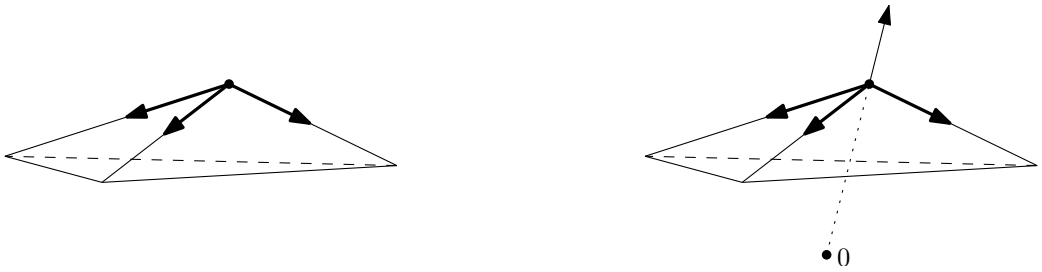

Figure 3: Left: for a realization of a graph in $\mathbb{R}^3$ a degree-3 vertex *cannot* be in classical equilibrium Eq. (2) unless it is coplanar with its neighbours. Right: the additional summand in the braced equilibrium condition Eq. (1) "solves" this problem.

The Lovász duality is an operation that transforms a pair $(\mathbf{u}, \omega)$ of a 3d embedding $\mathbf{u}$ of a planar 3-connected graph G with a braced stress ω into a realization of the dual to G graph G^* as a polytopal surface[1]. Moreover, under some additional assumption on the geometry of $\mathbf{u}$ (that we call "cone-convexity") and for a positive braced stresses the resulting realization is a convex polytope. This construction has a lot in common with the classical Maxwell–Cremona lifting procedure and can be viewed as a 3d counterpart of the latter.

The Lovász duality transforms the question of realizing a graph as a convex polytope to the question of finding a cone-convex realization of its dual graph with a positive braced stress. The latter will be our main target for the scope of this work. Thus, the genuine subject of our research are braced stresses and, deeply interconnected with them, equilibrium stresses.

Further results

Probably the most popular tool in operating with realizations of convex polytopes is provided by the pair of techniques of the equilibrium stresses and the Maxwell–Cremona lifting procedure. It transforms a planar realization of a graph equipped with an equilibrium stress to a polytopal surface in $\mathbb{R}^3$ by lifting every vertex along the vertical lines; Fig. 4. Furthermore, planar realizations with equilibrium stresses can be used to construct spacial realizations with braced stresses and we use these constructions extensively. Thus we give a comprehensive review of the Maxwell–Cremona lifting procedure and prove some new useful results concerning equilibrium stresses, such as *the wheel-decomposition theorem* and *the efficient reverse of the Maxwell–Cremona lifting procedure*.

[1] We remind that we reserved the word *polytope* for *convex* polytopes. However, the majority of constructions that we use and develop naturally operate with nonconvex objects as well. To avoid any confusion, we refer to nonconvex (and possibly self-intersecting) polytopes as *polytopal surfaces*. More precisely, a *polytopal surface* is an embedding of a planar 3-connected graph into $\mathbb{R}^3$ such that the vertices of every face are coplanar.

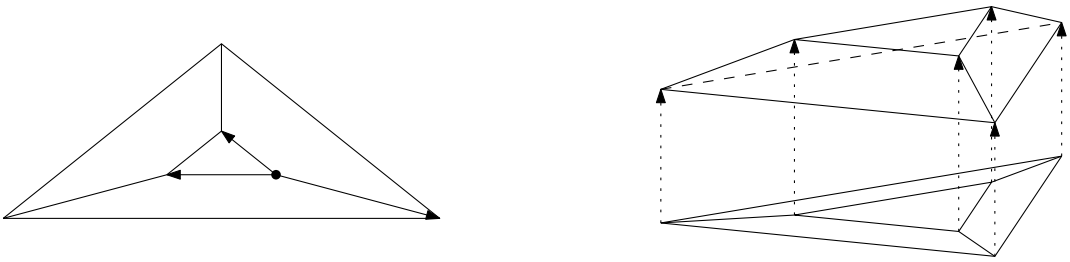

Figure 4: Left: an equilibrium stress. A vertex is in equilibrium if the weighted vectors connecting it to the neighbours sum up to zero. All interior edges in the figure are assigned with a stress equal to 1. Right: the Maxwell–Cremona lifting procedure lifts vertices of a stressed planar embedding along the vertical lines so that the result is a polytopal surface.

Wheel-decomposition theorems. Equilibrium stresses on an embedding of a graph to the plane form a linear space. We develop the *wheel-decomposition theorem*, which gives an explicit geometrical description of a basis of the linear space of equilibrium stresses on a given triangulation of the plane; see Fig. 5. That allows us to decompose every equilibrium stress on a triangulation into a linear combination of elementary equilibrium stresses and to efficiently operate with them. We present two versions of the wheel-decomposition theorem, for equilibrium and for braced stresses.

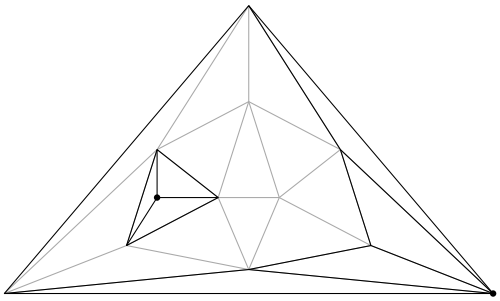

Figure 5: An equilibrium (or braced) stress on a triangulation is decomposed into a linear combination of stresses with support on *wheels*, which are small subgraphs of the initial triangulation. Two wheels are highlighted on the figure.

The efficient reverse of the Maxwell–Cremona lifting. The Maxwell–Cremona lifting procedure can be reversed: given a polytopal lifting of a planar realization of a graph, one can compute the equilibrium stress, such that the lifting is the Maxwell–Cremona lifting with respect to this stress.

The Maxwell–Cremona lifting procedure is computationally efficient: given a planar embedding with polynomial coordinates and a polynomial equilibrium stress, it produces a lifting with polynomial vertex coordinates as well. However, computing of the canonical equilibrium stress is not efficient: given a lifting with integer coordinates of polynomial size, the entries of the canonical equilibrium stress are rationals, and they require in general an exponential scaling factor when scaled to integers.

We present a perturbation argument that allows us to avoid scaling with an exponential scaling factor and produces an integral equilibrium stress ω on $\mathcal{P}$ such that $|\omega| \leq |\max u_i|^{\Delta_G}$, where Δ_G is the maximal vertex degree of the graph G. Our intuition in $\mathbb{R}^2$ is often stronger than in $\mathbb{R}^3$, thus, the possibility to transform a 3d embedding into a 2d embedding and a stress

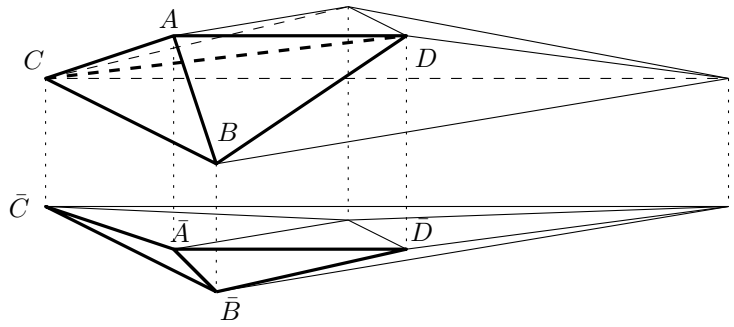

Figure 6: The standard reverse of the Maxwell–Cremona lifting computes the stress on the edge AB as the fraction of the volume of the tetrahedron $ABCD$ and the product of areas of the projections $\bar{A}\bar{B}\bar{C}$ and $\bar{A}\bar{B}\bar{D}$. An exponential scaling factor is in general unavoidable when scaling to integers.

is a desirable feature. Additional motivation for us is that we use this construction for one of our duality algorithms.

Fruitful symbiosis between braced and equilibrium stresses. We pay a lot of attention to interconnections between braced and equilibrium stresses. The majority of Sect. 2.3 is devoted to this subject. This equivalence can be used in two directions. First, it allows us to use the established machinery of equilibrium stresses to operate with braced stresses. Second, it gives a fresh point of view to the equilibrium stresses. As one example, we use braced stresses for a fresh geometrical view on how the equilibrium stresses of embeddings of graphs to a plane evolve under projective transformations; see Fig. 7.

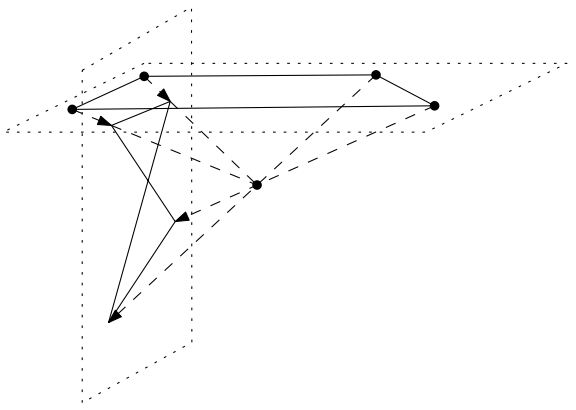

Figure 7: Braced stresses allow us to geometrically track equilibrium stresses under projective transformations.

Lovász lifting procedure. Lovász introduced a lifting procedure that is analogous to the Maxwell–Cremona procedure [21], but instead of an embedding of a graph to a plane with an equilibrium stress it starts with any embedding of a graph to $\mathbb{R}^3$ with a braced stress; and instead of lifting vertices along the vertical lines it lifts vertices along the rays emanating from the origin; see Fig. 8 and Fig. 4. The original paper gives this procedure no name, we refer to it as the *Lovász lifting procedure*.

This procedure is of independent interest. Moreover, a part of it constitutes the Lovász duality transform. In addition, the Lovász lifting procedure allows us to give a geometrical

sense to the wheel-decomposition theorem for braced stresses, which is one of the main tools in our duality transform for general simplicial polytopes.

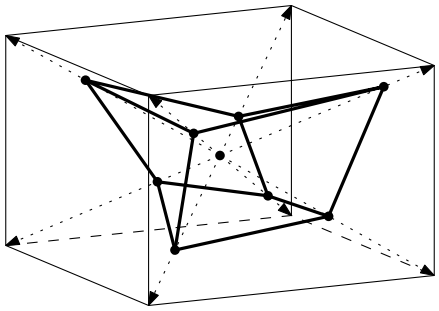

Figure 8: The Lovaśz lifting procedure lifts any 3d embedding of a graph (bold) with a braced stress to a polytopal surface by lifting every vertex along the rays through the origin.

We are not aware of any detailed presentations of the Lovász lifting procedure, the original paper [21] provides only the main ideas of the proof of a special case of "cone-convex" realization of the initial graph. So, for consistency of the presentation, we include an accurate handling of the Lovász lifting procedure and thus put the wheel-decomposition theorem for braced stresses and the Lovász duality transform in context.

Prismatoids. As a special example of a class of polytopes which allow especially efficient realizations we present an algorithm for realizing prismatoids. A prismatoid is a polytope, whose graph is a triangulated annulus, see Fig. 9. We present an algorithm that realizes every prismatoid with n vertices as a convex polytope on a $O(n^4)\times O(n^3)\times 1$ grid. This algorithm is a completely independent result, not relying on any of the previously discussed lifting techniques. This part of the work is based on the ideas presented by the author at the poster session of the 21st International Symposium on Graph Drawing in Bordeaux, 2013 [15].

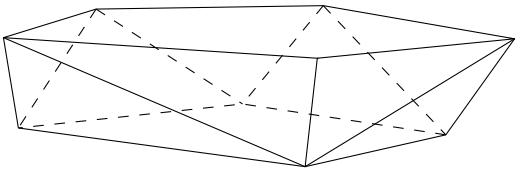

Figure 9: A prismatoid.

Higher dimensional generalizations. To generalize the duality transforms to higher dimensions we need to generalize the machinery of braced and equilibrium stresses that we use. To operate with equilibrium stresses in higher dimensions, we use the approaches based on the works by Rybnikov [32] and Demaine and Schulz [10]. We are, however, unaware of any available presentation of the theory of braced stresses in $\mathbb{R}^d$. Thus, we developed the necessary vocabulary and machinery from scratch. As a source of inspiration we used the work by Izmestiev on the Colin de Verdièr number of graphs of higher dimensional polytopes [17].

Structure

The main part of the work consists of three chapters. Chapter 2 is devoted to the constructions in $\mathbb{R}^3$ leading to the duality transforms. In Chapter 3 we present an embedding algorithm for prismatoids. Chapter 4 presents generalizations of the main 3d results to higher dimensions.

In presenting material of Chapter 2 we do not follow the shortest routes toward the main results. Instead, we organize the material by subject: We begin with the results concerning classical equilibrium stresses, Sect. 2.2. Then we proceed to the braced stresses and interconnections between braced and equilibrium stresses, Sect. 2.3. This is followed by the description of the main tool in the duality transformations, the Lovász duality transform, and of the connected to it Lovász lifting procedure, Sect. 2.4. Having all the machinery ready, we present the duality transforms for stacked and for general simplicial polytopes, Sect. 2.5.

Due to substantially more involved technical details, Chapter 4 has a more straightforward structure and only contains the technical material that is used for building the duality transforms. We begin with a section devoted to an accurate account of equilibrium and braced stresses in higher dimensions, Sect. 4.2. It is followed by a section describing the d-dimensional Maxwell–Cremona lifting procedure, Sect. 4.3. Then we present the Lovász duality transformation in $\mathbb{R}^d$, Sect. 4.4. We conclude with the duality transformations for stacked polytopes, Sect. 4.5, and for general simplicial polytopes, Sect. 4.6.

Chapter 1

Methods for realizing planar graphs: overview

To provide a broader picture, below we briefly overview some known methods for realizing planar graphs. This chapter is independent from the content of our work and might be skipped. Not all of these techniques are known to be applicable for realizing graphs as convex polytopes, however none of them is known to be in principle unmodifiable to be applicable. This list is not complete in any sense and only gives a brief introduction to the field.

We pay a special attention to approaches that produce realizations as convex polytopes. For the scope of this chapter we call an embedding of a graph to a plane *liftable* if its vertices can be assigned with the third coordinate so that the resulting 3d realization is a convex polytope, see Fig. 1.0.1. Another term commonly used for liftable embeddings is *regular*.

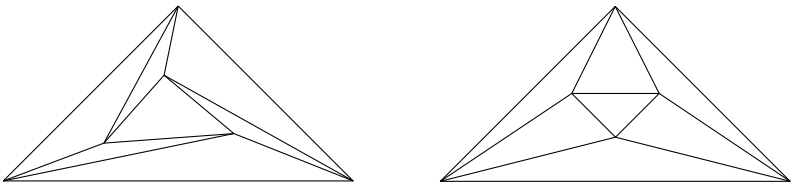

Figure 1.0.1: Two planar embeddings of the graph of the octahedron, left: nonliftable, right: liftable.

Equilibrium stresses and the Maxwell–Cremona lifting

We already mentioned the equilibrium stresses, see Eq. (2), and the Maxwell–Cremona lifting in the introduction. This technique is the most classical tool to construct a liftable planar realization and then to lift it to $\mathbb{R}^3$. Below we briefly put these techniques into context.

The Maxwell–Cremona lifting allows to control the 3d realization of a graph through an embedding of this graph to a plane with an equilibrium stress on it. Such embeddings can be produced in many ways. One of the classical constructions by Tutte [42] goes as follows: we start with an equilibrium stress, prescribe any face of the graph as the outerface and arbitrarily fix the locations of its vertices in convex position. Then we view Eq. (2) as the system of equations on the coordinates of the internal vertices of the graph. In other words, we view the left hand side of Eq. (2) as the Laplace operator and the locations of internal vertices as the harmonic functions with respect to this Laplacian.

This approach produces realizations with all the internal vertices in equilibrium, however, the vertices of the outerface can be set to equilibrium only if the outerface is triangular, or if

the locations of the vertices of the outerface are chosen with special precautions. One of such special modifications led to the currently best existing algorithm for general 3-dimensional polytopes by Ribó Mor, Rote, and Schulz [29].

Another kind of special treatment of this construction, which used on the fly modifications of the equilibrium stresses, was used by Schulz to construct realizations of convex polytopes with good vertex resolution [37].

Canonical order

The next approach to realizing planar graphs on the grid is based on the *canonical order* on triangulations of the plane, see Fig. 1.0.2. It was introduced by de Fraiysseix, Pach, and Pollack [8] to construct efficient planar realizations of triangulations. The so called *shift method*, presented by the authors in this paper, realizes every triangulation with n vertices on a $2n-4$ by $n-2$ grid [8, Theorem 1]. However, the planar realizations produced by the shift method are not always liftable.

Recently, Pak and Wilson [27] presented another construction based on the canonical order, that produces liftable 2d realizations, see Fig. 1.0.2. It realizes every simplicial 3d polytope with integer coordinates which are small in two dimensions (at the expense of the third dimension): in a general setup the layout requires a $4n^3 \times 8n^5 \times (500n^8)^n$ integer grid [27, Corollary 1.1]. For many special subclasses of simplicial polytopes the algorithm of Pak and Wilson allows a substantial decrease in the last coordinate.

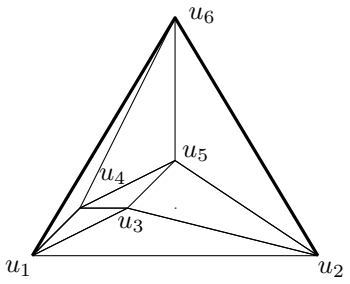

Figure 1.0.2: A triangulation with a canonical order on its vertices.

The canonical order labels the vertices of a triangulation in order they appear starting from one of the edges of the outerface, see Fig. 1.0.2. It allows to reconstruct the graph vertex by vertex starting from the base edge. The algorithm by Pak and Wilson performs this reconstruction so that every *horizon* is a convex polygonal chain, where a *horizon* is the boundary of the graph after an intermediate reconstruction step, on the figure: $u_1u_3u_2$, $u_1u_4u_3u_2$, $u_1u_4u_5u_2$ and $u_1u_6u_2$. This convexity guarantees liftability, since vertices that are being added can be assigned heights one after another so that the resulting surface is convex.

There exists an extension of the canonical order approach for planar 3-connected graphs by Chrobak and Kant [6]. It allows us to construct straight-line planar realizations with nonstrictly convex faces on an integral grid of size $(n-2) \times (n-2)$.

Schnyder realizer

The algorithm presented by Schnyder in his seminal work [34] allows to build realizations of planar graphs on a $2d$ integer grid of very small size. Namely, it produces a straight-line planar embedding of any planar graph with n vertices on $n-2$ by $n-2$ grid. There exists a generalization of Schnyder approach by Felsner, which produces realizations with nonstrictly convex faces [12]. For a planar 3-connected graph with f faces it requires a grid of size $f-1$ by $f-1$. We are not aware of any modifications of Schnyder construction that produce liftable planar embeddings. On the other hand, we are also not aware of any arguments that could

hinder such modifications. Due to the prominence of the construction, we briefly sketch it below.

The original construction is designed for a full triangulation of the plane G. We start with any planar embedding of G, see Fig. 1.0.3. Every vertex is connected to the three vertices of the outerface with disjoint paths, which are constructed following a purely combinatorial labeling procedure (labeling is present on the figure, we do not go into details). The paths divide the graph into three regions (white, rising and falling). The vertex is assigned with three coordinates, n_1, n_2, n_3, the number of faces in each of the regions.

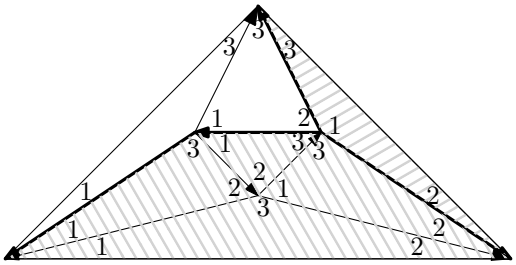

Figure 1.0.3: Schnyder construction. The vertex is assigned with coordinates $(1, 4, 2)$.

The coordinates are homogeneous, $n_1 + n_2 + n_3 = const$, thus they define an embedding of the graph into an affine plane in $\mathbb{R}^3$. This embedding turns out to be planar. An appropriate affine transformation finishes the construction.

Steinitz' construction

The construction behind the classical proof of Steinitz theorem is iterative and it constructs a realization of a graph directly as a convex polytope. It uses the following fact: every planar 3-connected graph can be transformed to a tetrahedron by a sequence of ΔY-operations followed by the elementary reductions: removing of double-edges and vertices of degree 2; see Fig. 1.0.4. The reversed deconstruction sequence can be carried out geometrically, starting from a tetrahedron. The construction requires a double exponential grid size.

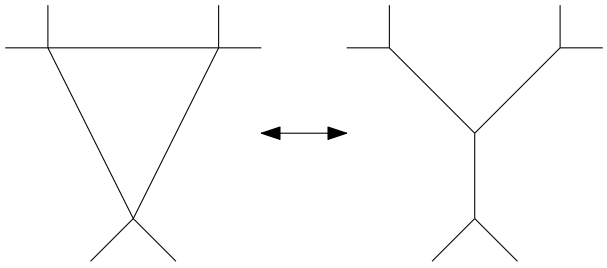

Figure 1.0.4: A series of ΔY transformations followed by the elementary reductions of double edges and vertices of degree 2 transforms any planar 3-connected graph down to a K_4.

Circle packing theorem

Yet another approach to realizations of graphs directly as convex polytopes is provided by the circle packing theorem, see Fig. 1.0.5. This theorem was first proven by Koebe [20] and rediscovered 50 years later by Thurston [41, Corollary 13.6.2], who found it as a consequence of previous works by Andreev [1] and [2]. A series of generalizations is known, the one that allows to realize a graph as a convex polytope is often referred to as the *primal-dual circle packing*.

This version is usually attributed to Brightwell and Scheinerman [5], for a constructive proof see Mohar [24]. We refer the reader to Ziegler [46, page 118] for a detailed historical overview.

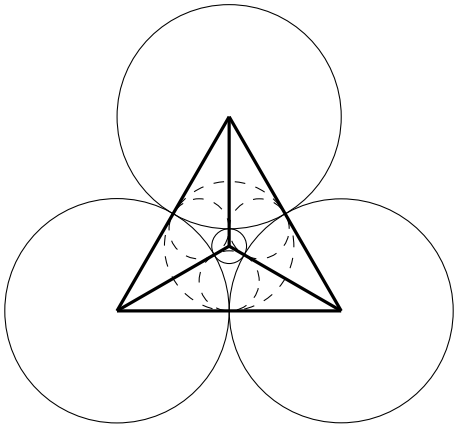

Figure 1.0.5: The primal-dual circle packing for the K_4.

The circle packing theorem represents every planar graph as a contact graph of a circle packing: Every vertex of a graph is represented as a circle in the plane. The circles are disjoint and two circles touch if and only if the vertices are connected by an edge. The stronger primal-dual circle packing is applicable to planar 3-connected graphs and it constructs a simultaneous circle packing representation of a graph and of its dual graph, so that the two circle packings are orthogonal (dual circles are dashed in Fig. 1.0.5). A convex polytope is produced by mapping a primal-dual circle packing from the plane to the sphere using the standard stereographic projection, and then intersecting the halfspaces bounded by the circles representing the dual graph.

The realizations produced by the primal-dual circle packing have an additional property, they *midscribe* a sphere: the unit sphere is tangent to every edge of the polytope. A generalization of this construction from the sphere to any smooth strictly convex body in $\mathbb{R}^3$ is provided by Schramm [35]. We remark that midscribing a sphere is "the best possible" behaviour of a polytope with respect to a sphere: It was shown by Steinitz in 1928 [39] that there exists 3-polytopes that are not inscribable, that is not realizable with all the vertices on a unit sphere. By duality that also means the existence of 3-polytopes that do not have realizations with all facets touching the unit sphere.

The circle packing theorem is an extremely elegant way of producing realizations that midscribe the sphere. However, these realizations are hardly geometrically readable: already for the simplest case of stacked polytopes the circle packing theorem produces realizations with exponentially small vertex resolution.

Colin de Verdière matrices

This approach originates from the spectral theory of graphs and realizes a graph directly as a convex polytope. It was developed by Lovász [21]. A Colin de Verdière matrix for a graph G is a weighted adjacency matrix, fulfilling some additional constraints. We refer to the original paper for details [21]. For a planar 3-connected graph any Colin de Verdière matrix has three independent eigenvectors (a basis of the nullspace), which define an embedding (u_i) of vertices of G to $\mathbb{R}^3$. This embedding is called a *nullspace representation of a graph*. It can then be rescaled in a canonical way to a realization of G as a convex polytope: there exist a set of real scaling factors λ_i for each vertex such that $\lambda_i u_i$ is a convex polytope with skeleton G, [21, Theorem 3]. The scaling factors λ_i can be derived from the initial matrix. We are not aware

of any successful attempts to analyze the geometrical properties of the realizations produced by this method.

Colin de Verdière matrices are directly related to braced stresses, a concept that we study extensively in this thesis: every Colin de Verdière matrix is a braced stress on its nullspace representation. In turn, every *negative* braced stress on a realization of a graph with some special geometry (we later define such realizations as *cone-convex*), is a Colin de Verdière matrix of this graph (see [21, Theorem 7] and the following discussion).

Chapter 2

Efficient duality transforms in $\mathbb{R}^3$

2.1 Preliminaries

2.1.1 Graphs

A *directed graph* is a pair $G = (V, E)$ of a finite set of vertices V and a subset $E \subset V \times V$ of the pairs of vertices that are called *edges*. An *undirected graph* contains with every edge $e = (u, v)$ its opposite edge $e' = (v, u)$; for an undirected graph we do not distinguish edges (u, v) and (v, u). A graph is called simple if it is undirected and none of the edges is a loop. All the graphs that we consider are simple. For a graph G we denote the set of its vertices as $V(G)$ and the set of its edges as $E(G)$. For a vertex $v \in V(G)$ we denote with $N(v, G)$ the set of neighbours of v, that is the vertices $u \in V(G)$ such that $(u, v) \in E(G)$. When it does not lead to confusion we abbreviate $N(v, G)$ with $N(v)$.

A *realization* or an *embedding* of a graph G in $\mathbb{R}^d$ is a map of the vertices of the graph to $\mathbb{R}^d$, $f : V(G) \to \mathbb{R}^d$, together with a set of curves in $\mathbb{R}^d$ connecting those pairs of the points which are connected by an edge of the graph (parametrization of the curve never plays a role). When all the curves representing edges are straight-line segments, the realization is called a *straight-line realization*. To define a straight-line realization of a graph it is clearly enough to define the positions of all its vertices $f : V(G) \to \mathbb{R}^d$. All the realizations that we study are straight-line realizations.

We call a realization of a graph in $\mathbb{R}^2$ *flat*. A realization of a graph in $\mathbb{R}^2$ is called *planar* if every two edges are disjoint except possibly at the common endpoint. Graphs that allow planar realizations are called *planar graphs*. Not every graph is planar: an immediate example of a nonplanar graph is given by a complete graph K_5 which contains 5 vertices and each pair of vertices is connected by an edge. By *Fary's theorem* every graph that allows some planar realization (or every planar graph) also allows a planar straight-line realization [11].

For a planar realization of a graph the connected regions of the plane bounded by the edges of the graph (including the unbounded region) are called *faces*. Generally speaking, the faces of a graph are not predefined by its combinatorics (by the graph itself), but are defined instead for every planar realization. However, for some graphs the face structure is predetermined by the graph. For such a graph G we denote the set of faces with $F(G)$.

A graph is called *connected* if every vertex is connected to any other vertex by a path. A graph is called *vertex k-connected* if the removal of any $k - 1$ vertices with all the adjacent edges does not break connectivity. The faces of a planar graph are uniquely predetermined by the graph if and only if the graph is 3-connected [45, Theorem 11]. In this case the cycles of edges that form a face allow a direct description: a cycle forms a face if an only if it does not separate the graph, that is the removal of the cycle from the graph keeps the graph connected. Thus, the planar realization of a planar 3-connected graph is combinatorially unique up to the

choice of the face that is realized as the unbounded face, that we call the *outerface*. In other words, using the standard bijection between the (one point compactification) of the plane and the sphere, the noncrossing realization of a planar 3-connected graph on the sphere is combinatorially unique.

An embedding of a planar 3-connected graph onto the sphere defines an orientation on the faces of the graph: we label the boundary cycle of every face in the clockwise order viewed from the outside of the sphere. (The choice of the clockwise labeling might seem unnatural, however we stick to it, as it is consistent with the natural choice of orientations in higher dimensions, which we use in Chapter 4.) Every planar 3-connected graph has exactly two nonhomeomorphic embeddings into the sphere, thus it can be oriented in exactly two different ways. We say that a planar 3-connected graph is *oriented* if one of the two orientations is chosen.

A choice of a cyclical order on the edges incident to every vertex of a graph is called a *combinatorial embedding* of a graph. Every embedding of a graph to a plane defines a combinatorial embedding of this graph. For a planar 3-connected graph there are exactly two combinatorial embeddings of this graph that correspond to planar realizations and differ by a symmetry. Thus, a choice of orientation on a planar 3-connected graph corresponds to a choice of one of two combinatorial embedding of this graph that correspond to planar realizations.

Given a planar realization of a graph G the *dual graph* G^* is defined as the graph whose vertices are the faces of G and two vertices of G^* are connected by an edge if and only if the corresponding faces of G^* share an edge. For a planar 3-connected graph the dual graph does not depend on the embedding and thus is a well-defined graph-theoretical object. The graph dual to a planar 3-connected graph is again planar and 3-connected and the graph, dual to the dual graph, is the initial graph, $(G^*)^* = G$.

2.1.2 Convex polytopes and polytopal surfaces

The notion of a convex d-dimensional polytope allows two dual definitions:

Definition 2.1.1. *(1) A* convex d-dimensional polytope *is the full dimensional convex hull of a finite set of points in* $\mathbb{R}^d$. *(2) A* convex d-dimensional polytope *is the full dimensional bounded intersection of a finite set of affine half-spaces of* $\mathbb{R}^d$.

These definitions are equivalent: a subset of $\mathbb{R}^d$ is a convex hull of a finite set of points if and only if it can be represented as an intersection of a finite set of half-spaces of $\mathbb{R}^d$ [46].

We remind that the *convex hull* of a finite set of points in $\mathbb{R}^d$ is defined as the set of all the *convex combinations* of these points:

$$\mathrm{Conv}(u_1, \dots u_n) = \left\{ \sum_{1 \le i \le n} \alpha_i u_i : \sum_{1 \le i \le n} \alpha_i = 1, \alpha_i \ge 0 \right\}.$$

We note that the points (half-spaces) from the above definition are not by default the extreme points (half-spaces) of the resulting polytope.

In the remaining of the chapter we work with 3-dimensional polytopes; polytopes of higher dimensions appear again in Chapter 4.

Faces, edges, vertices and the graph of polytope. We say that an affine plane $\alpha = \{x \in \mathbb{R}^3 : \langle n, x \rangle = c\}$ defined by a normal vector $n \in R^3$ and a constant $c \in \mathbb{R}$ is a *supporting plane* for a convex polytope $\mathcal{P}$ if

1. The intersection $\mathcal{P} \cap \alpha \neq \emptyset$ is nonempty; and
2. The whole polytope lies in one of the two halfspaces defined by the plane: $\mathcal{P} \subset \{x \in \mathbb{R}^3 : \langle n, x \rangle \le c\}$.

Definition 2.1.2. *The intersection $F = \alpha \cap \mathcal{P}$ of a supporting hyperplane α and a polytope $\mathcal{P}$ is called a* face *of a polytope.*

The dimension of a face is the dimension of its affine hull,

$$\mathrm{Aff}(F) = \{a + tb : a, b \in F, t \in \mathbb{R}\}.$$

The faces of the dimension 0 and 1 are called *vertices* and *edges* correspondingly and for 3-dimensional polytopes the faces of the maximal dimension 2 are simply referred to as *faces*. We denote the vertices of a polytope $\mathcal{P}$ with $V(\mathcal{P})$, the edges with $E(\mathcal{P})$ and the faces with $F(P)$.

Clearly, every face of a 3-dimensional polytope is a convex polygon. We call a polytope *simplicial* if every its face is a simplex, that is in the 3d case a triangle.

The edges and the vertices of a polytope $\mathcal{P}$ form the graph that we call the *graph of the polytope*, denoted with $G(\mathcal{P})$. In 1916 Steinitz showed that

Theorem 2.1.1 (Steinitz theorem, [38])**.** *A graph is the graph of a convex 3-dimensional polytope if and only if it is simple, planar, and 3-connected.*

Steinitz theorem allows us to study the *realizations* of polytopes — given a graph of a polytope, or simply any planar 3-connected graph G, realize it as a convex 3-polytope that has some special geometrical features. In this work we are looking for realizations with small integer coordinates.

Duality and the polar dual. We call two 3d polytopes $\mathcal{P}$ and $\mathcal{P}^*$ *dual* if there exists a bijection between the faces of $\mathcal{P}$ and the vertices of $\mathcal{P}^*$, $d : F(\mathcal{P}) \to V(\mathcal{P}^*)$ such that the faces f and g of $\mathcal{P}$ share an edge if and only if the vertices $d(f)$ and $d(g)$ are connected by an edge in $\mathcal{P}^*$. This is the translation of the duality of graphs to the language of polytopes: polytopes $\mathcal{P}$ and $\mathcal{P}^*$ are dual if and only if the graphs of these polytopes are dual, $G(\mathcal{P}^*) = (G(\mathcal{P}))^*$.

Given a convex polytope $\mathcal{P}$ that contains the origin in its interior there is a standard way of constructing a polytope dual to P called *polarity*. To every vertex v of $\mathcal{P}$ we put into correspondence an affine plane α_v defined by the equation

$$\alpha_v := \{x \in \mathbb{R}^3 : \langle v, x\rangle = 1\}$$

and a halfspace H_v bounded by α_v,

$$H_v := \{x \in \mathbb{R}^3 : \langle v, x\rangle \leq 1\}.$$

The polytope obtained as the intersection of the halfspaces H_v for all vertices v of $\mathcal{P}$ is called *the polar dual polytope* for $\mathcal{P}$, or simply the polar polytope, and is denoted with $\mathcal{P}^*$,

$$\mathcal{P}^* = \cap_{v \in V(\mathcal{P})} H_v.$$

Every defining plane α_v appears as a supporting plane for some facet f_v of $\mathcal{P}^*$, and by definition every facet of $\mathcal{P}^*$ in turn corresponds to some vertex of $\mathcal{P}$. Thus, there is a bijection between the vertices of $\mathcal{P}$ and the faces of $\mathcal{P}^*$ defined by $v \to f_v$ and, indeed, this bijection defines the duality between the polytope and its polar dual. Thus, the polar dual polytope is a dual polytope. The polar dual of the polar dual polytope is the initial polytope, $(\mathcal{P}^*)^* = P$.

Polarity between vectors and affine planes. Generally speaking, polarity is the bijective correspondence between the nonzero vectors and the affine planes not passing through the origin in $\mathbb{R}^3$:

Definition 2.1.3. *(1) Let $v \neq 0, v \in \mathbb{R}^3$. We call the plane α_v defined by*

$$\alpha_v = \{x \in \mathbb{R}^3 : \langle x, v \rangle = 1\}$$

the polar plane *of the vector v. (2) For an affine plane α in $\mathbb{R}^3$ we call the vector $v \in R^3$ such that $\alpha = \alpha_v$ the* polar vector *of the plane α.*

Polarity preserves incidence relations: a point v lies in a plane α if and only if the polar plane to v contains the polar point to α. As a consequence, points in $\mathbb{R}^3$ are coplanar if and only if their polar dual planes pass through one point — the polar dual to the plane containing the initial points.

Let $\mathcal{P}^*$ be the polar dual polytope for a polytope $\mathcal{P}$. Then the vertices of $\mathcal{P}^*$ are the polar duals of the faces of $\mathcal{P}$ and the faces of $\mathcal{P}^*$ are the polar duals of the vertices of $\mathcal{P}$. Thus, the polar dual polytope $\mathcal{P}^*$ can be alternatively viewed either as the convex hull of the polar dual vectors of faces of the initial polytope $\mathcal{P}$; or as the convex body bounded by the polar dual planes of vertices of the initial polytope $\mathcal{P}$.

Polytopal surfaces. In many cases the notion of convex polytope is too restrictive and the theory of stresses and liftings discussed further can be developed for larger classes of geometrical objects. We use the following generalization of the notion of convex polytope, that we call a *polytopal surface*

Definition 2.1.4. *A* polytopal surface *is a realization of a planar 3-connected graph G in $\mathbb{R}^3$ such that the vertices of every face are coplanar.*

A polytopal surface inherits the structure of the underlying planar 3-connected graph, thus the whole face structure of the surface is well-defined. Topologically, a polytopal surface is a sphere. Thus, there exists two orientations on a polytopal surface and we say that a polytopal surface is *oriented* if one of the two orientations is fixed. This corresponds to fixing an orientation of the underlying graph, or, in other words, a combinatorial embedding of the underlying graph.

A polytopal surface can thus be viewed as a nonconvex self-crossing polytope, whose faces are in turn polygonal chains that can be nonconvex and self-crossing. We do not use the term polytope instead of polytopal surface to highlight that we allow nonconvexity and self-intersections. We do not use the term polyhedral surface to highlight that we stick to the topology of the sphere.

The notion of polytopal surface allows us to take the polar dual: let $\mathcal{P}$ be a realization of a graph G as a polytopal surface such that no faces of $\mathcal{P}$ are coplanar with the origin. We define the polar $\mathcal{P}^*$ as the realization of the dual graph G^* with vertices — polar duals to the corresponding faces of $\mathcal{P}$. Clearly, $\mathcal{P}^*$ is in turn a polytopal surface.

Orientation on polytopes and polytopal surfaces. By default we consider all the polytopes oriented by the choice of the normal vector — the outer normal vector. Without going into formalities, we use the notions "left" and "right" on the surface of a polytope, meaning that the observer looks at the surface of the polytope from the outside.

In a more formal way, let f be a face of a polytope and n_f be the normal vector to f, oriented outside of the polytope. Let v_1^f, v_2^f be two independent vectors lying in the face f. We say that the pair of vectors (v_1^f, v_2^f) is positively oriented if together with the normal n_f they form a positively oriented basis (v_1^f, v_2^f, n_f) of $\mathbb{R}^3$.

For a general polytopal surface the notion of the outer normal vector is not defined. Thus we suppose that every polytopal surface comes with a chosen normal vector for each of its faces and this choice is consistent among the faces, so that the whole surface is oriented.

2.2 Equilibrium stresses

2.2.1 Maxwell–Cremona lifting and the canonical equilibrium stress

The main tool in operating with realizations of convex polytopes is the Maxwell–Cremona lifting procedure which is based on the notion of equilibrium stress:

Definition 2.2.1. *Let* $\mathbf{u} = (u_i)_{1\le i\le n}$ *be an embedding of a graph* G *into* $\mathbb{R}^d$*. We call an assignment of reals* $\omega\colon E(G) \to \mathbb{R}$ *to the edges of* G *(denoted by* $\omega(i,j) = \omega_{ij} = \omega_{ji}$*) an* equilibrium stress *on* $\mathbf{u}$ *if for every vertex* $u_i \in V(G)$

$$\sum_{u_j \in N(u_i,G)} \omega_{ij}(u_j - u_i) = 0. \tag{2.2.1}$$

We call an equilibrium stress on a planar embedding with a distinguished boundary face f_0 positive (negative) *if it is positive (negative) on every edge that does not belong to* f_0*.*

Let $\mathbf{u} = (u_i)_{1\le i\le n}$ be an embedding of a graph G onto $\mathbb{R}^2$. We call the assignment of reals $h : V(G) \to \mathbb{R}$ to the vertices of G a *lifting* of the embedding $\mathbf{u}$ and we view $h(u_i)$ as the third coordinate, height, of the vertex u_i, thus $(u_i, h(u_i)) \in \mathbb{R}^3$ defines an embedding of G to $\mathbb{R}^3$. We say that the lifting is *polyhedral*[1] if for every face f of G the liftings of the vertices of f are coplanar.

Maxwell–Cremona lifting

Given a 2d realization $\mathbf{p} = (p_i)_{1\le i\le n}$ of a graph G and an equilibrium stress ω on this realization there exists a standard way of constructing a polyhedral lifting of $\mathbf{p}$, that is called *Maxwell–Cremona lifting*. Let $u_i = (p_i, 1)$ be the vertical lifting of $\mathbf{p}$ to the affine plane[2] $\{z = 1\}$ of $\mathbb{R}^3$. For every face f of the graph G we define a vector $a_f \in \mathbb{R}^3$ in the following way: we start with any face f_0 of G and assign it with an arbitrarily vector a_{f_0}. Then we proceed iteratively: let faces f and g share an edge (u_iu_j) so that the face g lies to the left (we always assume that we "look" at the surface of the polytope from the outside) and f lies to the right from $\overrightarrow{u_ju_i}$ and let the vector a_f already be defined (see Fig.2.2.1).

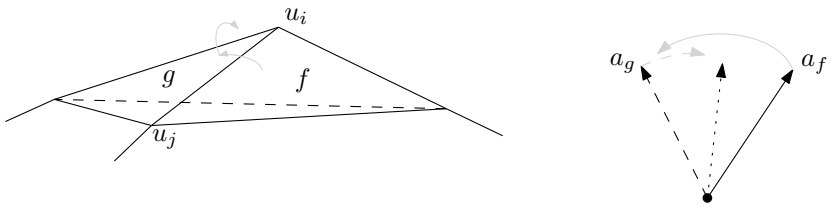

Figure 2.2.1: Iterative steps of the Maxwell–Cremona lifting procedure.

Then we define the vector a_g so that

$$a_g - a_f = -\omega_{ij}(u_j \times u_i). \tag{2.2.2}$$

Let $f_0f_1 \dots f_k = g$ and $f_0f_1' \dots f_l' = g$ be two different paths of adjacent faces leading from the initial face f_0 to some face g. To show the consistency of the vector assignment we need

[1] A *polyhedral* lifting is a *polytopal* surface as defined in Sect. 2.1. We use the word "polyhedral" instead of "polytopal" for liftings to comply with a tradition.

[2] Throughout the whole thesis we use a shortcut notation $\{x_k = c\}$ for the affine plane $\{(x_1 \dots x_d)^T \in \mathbb{R}^d : x_k = c\} \subset \mathbb{R}^d$.

to check that the value a_g does not depend on which path we choose. Thus, we should show that for every cycle $\Gamma = (f_1 \dots f_n = f_1)$ of adjacent faces the sum of increments equals zero:

$$\sum_{1 \le i \le n-1} \omega_{i'i''}(u_{i'} \times u_{i''}) = 0,$$

where the edge $u_{i'}u_{i''}$ separates faces f_i and f_{i+1}. Since we work only with planar graphs, this is equivalent to

$$\sum_{j \in N(i)} \omega_{ij}(u_i \times u_j) = 0$$

for every vertex u_i, where the sum goes over the neighbours of u_i. And this directly follows from the definition of equilibrium stress.

The nonhorizontal vectors in $\mathbb{R}^3$ are in one-to-one correspondence with the nonvertical affine planes of $\mathbb{R}^3$ through the following procedure: to a vector v we put into correspondence the affine plane $\{(x_1, x_2, \langle x, v\rangle)^T, x = (x_1, x_2, 1)^T \in \{z = 1\}\}$. In other words, we lift every point x of the standard affine plane $\{z = 1\}$ to the point with the height $h_v(x) = \langle x, v\rangle$ and these liftings form an affine plane.

We use this vector–plane correspondence to finalize the Maxwell–Cremona lifting: we lift every face f of the graph to the plane defined by the vector a_f, or in other words we assign every vertex u of a face f with a height $h_f(u) = \langle u, f\rangle$.

To finish the construction we show that for a vertex u_i that lies in the intersection of faces f and g the heights coming from the lifting of the face f and of the face g coincide. Indeed, this follows directly from the fact that for an edge (u_iu_j) separating faces f and g

$$h_g(u_i) - h_f(u_i) = \langle a_g - a_f, u_i\rangle = -\langle \omega_{ij}(u_j \times u_i), u_i\rangle = 0.$$

For a planar embedding $\mathbf{p}$ with an equilibrium stress ω the Maxwell–Cremona procedure defines the lifting uniquely up to the initial arbitrary choice of the vector a_{f_0} for some f_0, or, in other words, up to an arbitrary choice of lifting of any of the faces of the graph. This motivates the following definition:

Definition 2.2.2. *For a planar embedding of a graph $\mathbf{p} = (p_i)_{1 \le i \le n}$ we call two liftings h and h'* equivalent *if there exists a vector $a \in \mathbb{R}^3$ such that $h'(p_i) = h(p_i) + \langle a, (p_i, 1)\rangle$ for every $1 \le i \le n$.*

We call the *space of polyhedral liftings* of $\mathbf{p}$ the set of all the polyhedral liftings of $\mathbf{p}$ modulo the equivalence relation defined above. We denote this space with $\mathrm{Lift}(\mathbf{p})$. This space is clearly a linear space with respect to the pointwise addition and multiplication with scalars.

The Maxwell–Cremona lifting thus defines a map from the linear space of equilibrium stresses on $\mathbf{p}$ to the linear space of polyhedral liftings of $\mathbf{p}$ that we denote with

$$\mathrm{MC} : EQ(\mathbf{p}) \to \mathrm{Lift}(\mathbf{p}).$$

Lemma 2.2.1 (Maxwell [23], Whiteley [44])**.** *Maxwell–Cremona lifting is an isomorphism of linear spaces.*

This correspondence between stresses and liftings was first observed by Maxwell [23], the full proof is due to Whiteley [44], see also Crapo and Whiteley [7]. Since this is a classical result, we omit the formal proof and proceed directly to the description of the reverse map, which is an important component in our work.

Canonical equilibrium stress

The Maxwell–Cremona lifting procedure can be reversed. Let $\mathbf{u} = (u_i)_{1\le i\le n}$ be a realization of a graph G in $\mathbb{R}^3$ as a polytopal surface and let $\mathbf{p} = (p_i)_{1\le i\le n}$ be a projection of $\mathbf{u}$ to the plane $\{z = 0\}$. Then the embedding $\mathbf{p}$ can be assigned with an equilibrium stress that can be computed as

$$\omega_{ij} := \frac{[u_i u_j u_k u_l]}{[p_i p_j p_k][p_i p_j p_l]}, \tag{2.2.3}$$

where an edge (ij) separates faces spanned by the vertices (ijk) (on the left) and (ijl) (on the right) and we use the square bracket notation for signed volumes[3]:

$$[u_i u_j u_k u_l] := \det \begin{pmatrix} x_i & x_j & x_k & x_l \\ y_i & y_j & y_k & y_l \\ z_i & z_j & z_k & z_l \\ 1 & 1 & 1 & 1 \end{pmatrix}, \quad \text{where } u = \begin{pmatrix} x \\ y \\ z \end{pmatrix},$$

for 2d vectors $[p_i p_j p_k]$ is defined similarly. We remark that the faces do not have to be triangular and may contain other vertices in addition to u_i, u_j, u_k and u_i, u_j, u_l.

Definition 2.2.3. *We call the equilibrium stress defined above the* canonical equilibrium stress *on the orthogonal projection* $\mathbf{p}$ *of* $\mathbf{u}$.

Computing of the canonical equilibrium stress is the reverse operation to the Maxwell–Cremona lifting. The expression of Eq. (2.2.3) is a slight reformulation of the form presented in Hopcroft and Kahn [14, Equation 11]. We note that the canonical equilibrium stress is defined only when the denominators participating in Eq.(2.2.3) are nonzero, that is the points p_i, p_j, p_k and p_i, p_j, p_l are not collinear.

Signs of the stress and convexity of the lifting

Let $\mathbf{p}$ be a planar realization of a graph G and $\mathbf{u}$ be its lifting by an equilibrium stress ω. Then it is simple to see that the lifting is convex (concave) if and only if the stress is positive (negative) (see [30, Lemma 13.1.3] for details).

We do not define the notion of positive equilibrium stress for nonplanar embeddings of graphs to the plane, however the following property can be observed: Let $\mathbf{u}$ be a convex 3-polytope and $\mathbf{p}$ be its orthogonal projection to the plane $\{z = 0\}$. Then the canonical equilibrium stress on this projection is positive on all the internal edges of $\mathbf{p}$ and negative on the boundary edges of $\mathbf{p}$.

2.2.2 Wheel-decomposition for equilibrium stresses

We proceed with studying the structure of the linear space of equilibrium stresses in further details. In this subsection we restrict our attention to the graphs that are *full triangulations* of the plane — planar 3-connected graphs with every face (including the outerface) being a triangle. By Steinitz theorem these graphs are the graphs of simplicial 3-polytopes.

As we mentioned, the space of equilibrium stresses on a planar graph is a linear space. Below we explicitly present one basis of this linear space, which is simply computable and in addition has a clear geometrical meaning in context of the Maxwell–Cremona isomorphism between spaces of equilibrium stresses and polyhedral liftings.

The decomposition of an equilibrium stress into a linear combination of "local" equilibrium stresses will be the key for the next embedding algorithms. The wheel-decomposition theorem presented in this subsection provides the underlying theory.

[3] Throughout the thesis we use the word "volume" as the synonym of the corresponding determinant, without rescaling with $\frac{1}{d!}$, where d is the dimension of the space. Thus, the volume of the simplex formed by the vectors of an orthonormal basis equals 1, while the volume of the unite cube equals $d!$.

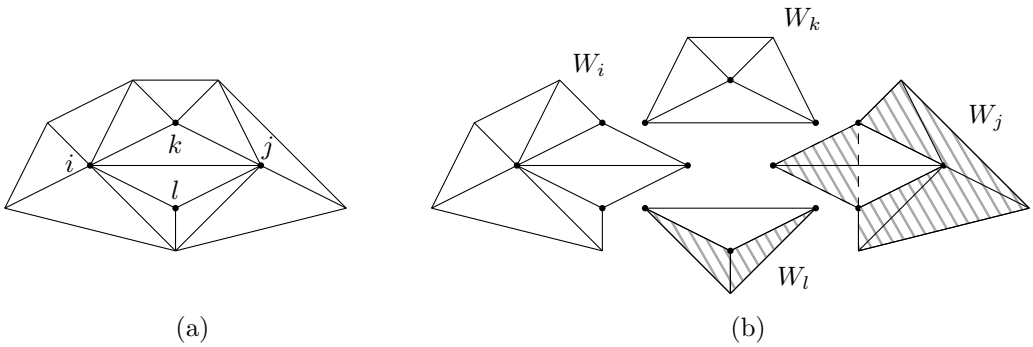

Figure 2.2.2: Part of a triangulation, participating in the wheel-decomposition of ω_{ij} (a); Wheels W_i, W_l, W_j, W_k ((b), c.c.w) with shadowed areas of the triangles participating in the definition of the *large atomic equilibrium stresses* for W_l and W_j.

Definition 2.2.4. *A graph formed by a vertex v_c, called* center*, connected to every vertex of a cycle $v_1, \dots, v_n$ (no other edge is present) is called a* wheel *(Fig. 2.2.2); we denote it as* $\mathrm{W}(v_c; v_1 \dots v_n)$*. We refer to the cycle $v_1 \dots v_n$ as the* base cycle *of the wheel* W*.*

Let G be a planar triangulation with $n > 3$ vertices. We denote the wheel that is a subgraph of the triangulation G with $v_i \in V(G)$ as a center as W_i. When G is oriented, we orient the base cycle of the wheel $W_i \subset G$ by labeling it in the counterclockwise order around the vertex u_i, see Fig. 2.2.3. Every triangulation can be "covered" with a set of wheels $(W_i)_{v_i \in V(G)}$, so that every edge is covered exactly four times (Fig. 2.2.2).

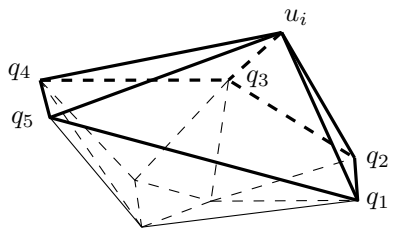

Figure 2.2.3: The subwheel $W_i \subset G$ centered at the vertex u_i of a triangulation G with the labeling of its base cycle, $W_i = W(u_i; q_1 \dots q_5)$. The wheel W_i is drawn bold.

Lemma 2.2.2. *Let $\mathbf{p} = (p_c, p_1, \dots p_n)$ be an embedding of a wheel $W(v_c; v_1 \dots v_n)$ in $\mathbb{R}^2$, such that for every $1 \le i \le n$ the points p_i, p_{i+1} and p_c are noncollinear (we use the cyclic notation for the vertices of the base of the wheel). Then the following expression defines an equilibrium stress:*

$$\omega_{ij} = \begin{cases} -1/[p_i p_{i+1} p_c], & j = i+1, 1 \le i \le n, \\ [p_{i-1} p_i p_{i+1}]/([p_{i-1} p_i p_c][p_i p_{i+1} p_c]), & j = c, 1 \le i \le n. \end{cases}$$

The equilibrium stress for the embedding $\mathbf{p}$ is unique up to a renormalization.

Proof. This stress coincides with the canonical equilibrium stress given by Eq. (2.2.3) from the lifting of $\mathbf{p}$ with $z_c = 1$ and $z_i = 0$ for $1 \le i \le n$ and so it is an equilibrium stress. The space of the equilibrium stresses is 1-dimensional, since the space of the polyhedral liftings is 1-dimensional. □

We note that the equilibrium stress defined in Lemma 2.2.2 depends on the orientation of the wheel: The reverse of the order on the base cycle $(p_1 \dots p_n) \to (p_n \dots p_1)$ of the wheel

$W(p_c; p_1 \dots p_n)$ does not change the geometry of the embedding, but multiplies the equilibrium stress of Lemma 2.2.2 with -1.

Definition 2.2.5. *1. In the setup of Lemma 2.2.2, we call the equilibrium stress ω the* small atomic equilibrium stress *of the wheel W and denote it as $\omega^a(W)$.*

2. We call the stress $\omega^A(W)$ that is obtained by the multiplication of $\omega^a(W)$ by the factor $\prod_{1\le j\le n}[p_j p_{j+1} p_c]$, the large atomic equilibrium stress *of W.*

We point out that the large atomic stresses are products of $\deg(v_c) - 1$ triangle areas multiplied by 2, and so, all the stresses $\omega^A_{ij}(W)$ are integers if W is realized with integer coordinates.

Theorem 2.2.1 (Wheel-decomposition theorem for equilibrium stresses)**.** *Let G be a triangulation and $\mathbf{p} = (p_i)_{1\le i\le n}$ be an embedding of G to $\mathbb{R}^2$ such that every face of G is realized as a nondegenerate triangle. Then every equilibrium stress ω on $\mathbf{p}$ can be expressed as a linear combination of the small atomic equilibrium stresses on the wheels $(W_i)_{1\le i\le n}$*

$$\omega = \sum_{1\le i\le n} \alpha_i \omega^a(W_i).$$

The decomposition is not unique: valid coefficients α_i are given by the heights (i.e., z-coordinates) of the corresponding vertices p_i in any of the Maxwell–Cremona liftings of $\mathbf{p}$ induced by ω, thus for every $v \in \mathbb{R}^2$ and $c \in \mathbb{R}$ the map $\alpha_i \to \alpha_i + \langle v, p_i\rangle + c$ sends a set of valid coefficients to a set of valid coefficients and any two sets of valid coefficients are connected this way.

Proof. The Maxwell–Cremona lifting procedure defines a linear isomorphism between the linear spaces of equilibrium stresses and of polyhedral liftings of a planar embedding of a graph.

As shown in Lemma 2.2.2, the atomic equilibrium stress $\omega^a(W_i)$ corresponds to a lifting that lifts the vertex p_i to the height 1 and leaves all the other vertices untouched. Thus the stress that lifts the i-th vertex to z_i is exactly the linear combination $\sum_{1\le i\le n} z_i \omega^a(W_i)$. □

2.2.3 An efficient reverse of the Maxwell–Cremona lifting

A direct way to reverse the Maxwell–Cremona lifting procedure would be to project the 3d embedding of a graph to a plane and to compute the canonical equilibrium stress using Eq. (2.2.3). If the 3d embedding has polynomial size integer coordinates, the computed stresses are, generally speaking, rational, and when scaled to integers may increase by an exponential factor. The following theorem provides a more careful method by allowing a small perturbation of the canonical equilibrium stress as given by Eq. (2.2.3) using the wheel-decomposition theorem.

Theorem 2.2.2 (Reverse of the Maxwell–Cremona lifting)**.** *Let $\mathbf{u} = (u_i)_{1\le i\le n}$ be an embedding of a triangulation G into $\mathbb{Z}^3$ such that none of the planes supporting the faces of G is orthogonal to the plane $\{z = 0\}$ and no pair of adjacent faces is coplanar. Let $\mathbf{p} = (p_i)_{1\le i\le n}$ be the orthogonal projection of $\mathbf{u}$ to the plane $\{z = 0\}$. Then one can construct an integer equilibrium stress ω on $\mathbf{p}$ such that*

$$|\omega_{ij}| < 8 \cdot (2 \max_{i\le n} |u_i|)^{2\,\Delta_G + 5}$$

and $\operatorname{sign}(\omega_{ij}) = \operatorname{sign}(\widetilde{\omega}_{ij})$ for the canonical equilibrium stress $\widetilde{\omega}$ on $\mathbf{p}$ as defined by Eq. (2.2.3). In particular, for an embedding of $\mathbf{u}$ as a convex polytope such that the projection $\mathbf{p}$ is non-crossing the constructed stress is positive.

Proof. Let $L := \max_{i,j} |u_i - u_j|$ be the size of the grid containing the initial embedding. We start with the canonical equilibrium stress $\widetilde{\omega}$ as specified by Eq. (2.2.3) for the embedding $\mathbf{p}$.

Since all the coordinates are integers, and the embedding $\mathbf{u}$ has no flat edges, all stresses are bounded by

$$\frac{1}{L^4} \leq \frac{1}{|[p_i p_j p_k]||[p_l p_j p_i]|} \leq |\widetilde{\omega}_{ij}| \leq |[u_i u_j u_k u_l]| \leq L^3.$$

We are left with making these stresses integral while preserving a polynomial bound. The faces of $\mathbf{u}$ are nonvertical, thus the faces of $\mathbf{p}$ are nondegenerate and we may apply the wheel-decomposition theorem to the stress $\widetilde{\omega}$: we rewrite it as a linear combination of the *large* atomic equilibrium stresses of the wheels,

$$\widetilde{\omega} = \sum_{1 \leq k \leq n} \alpha_k \omega^A(W_k).$$

We remark that since we use *large* atomic equilibrium stresses, coefficients α_k are not the z coordinates of u_k, but these z coordinates divided by the multiplicative factor from the definition of the large atomic equilibrium stress. Since all the points p_i have integer coordinates, the large atomic equilibrium stresses are integers as well. Moreover, each of them, as a product of $\deg(u_k) - 1$ triangle areas, is bounded by $|\omega^A_{ij}(W_k)| \leq L^{2(\Delta_G - 1)}$.

To make the $\widetilde{\omega}_{ij}$s integral we round the coefficients α_k down. To guarantee that the rounding does not alter the signs of the stress, we scale the atomic equilibrium stresses (before rounding) with the factor

$$C = 4 \max_{i,j,k} |\omega^A_{ij}(W_k)| / \min_{i,j} |\widetilde{\omega}_{ij}|$$

and define as the new stress:

$$\omega := \sum_{1 \leq k \leq n} \lfloor C\alpha_k \rfloor \omega^A(W_k).$$

Clearly,

$$\begin{aligned} |\omega_{ij} - C\widetilde{\omega}_{ij}| &= \left| \sum_{1 \leq k \leq n} (\lfloor C\alpha_k \rfloor - C\alpha_k) \omega^A_{ij}(W_k) \right| \\ &< \sum_{1 \leq k \leq n} |\omega^A_{ij}(W_k)| \leq 4 \max_{i,j,k} |\omega^A_{ij}(W_k)| = C \min_{i,j} |\widetilde{\omega}_{ij}| \leq C|\widetilde{\omega}_{ij}|, \end{aligned}$$

where the third inequality holds since exactly four wheels participate in the wheel decomposition of every single edge. Thus, $\operatorname{sign}(\omega_{ij}) = \operatorname{sign}(C\widetilde{\omega}_{ij}) = \operatorname{sign}(\widetilde{\omega}_{ij})$. From the last equation it also follows that none of the stresses ω_{ij} are zero.

Therefore, the constructed equilibrium stress ω is integral and of the same sign structure as the canonical equilibrium stress. We conclude the proof with an upper bound on its size. Since $C < 4L^{2(\Delta_G - 1)} L^4$,

$$\begin{aligned} |\omega_{ij}| &\leq \left| \sum_{1 \leq k \leq n} (C\alpha_k \pm 1) \omega^A_{ij}(W_k) \right| \leq C|\widetilde{\omega}_{ij}| + \sum_{1 \leq k \leq n} |\omega^A_{ij}(W_k)| \\ &\leq C \max |\widetilde{\omega}_{ij}| + 4 \max |\omega^A_{ij}(W_k)| \leq 4L^{2\Delta_G + 2} \cdot L^3 + 4L^{2\Delta_G - 2} \leq 8L^{2\Delta_G + 5}. \end{aligned}$$

□

2.3 Braced stresses

This section is devoted to another kind of stress that we heavily use in our constructions.

2.3.1 Definition

Definition 2.3.1. *Let* $\mathbf{u} = (u_i)_{1\le i\le n}$ *be an embedding of a graph* G *into* $\mathbb{R}^d$. *We call an assignment of reals* $\omega : E(G) \to \mathbb{R}$ *to the edges of* G *a* braced stress *on the embedding* $\mathbf{u}$ *if there exists an assignment of reals* $\sigma : V(G) \to \mathbb{R}$ *to the vertices of* G *(to unify notation we denote* $\sigma(u_i)$ *by* ω_{ii}*) such that*

$$\sum_{j\in N(i,G)} \omega_{ij}u_j + \omega_{ii}u_i = 0 \quad \forall 1 \le i \le n.$$

We call a braced stress positive *if it is positive on every edge.*

Trivially, the definition of braced stress is equivalent to that

$$\sum_{j\in N(i,G)} \omega_{ij}u_j \parallel u_i \quad \forall 1 \le i \le n. \tag{2.3.1}$$

We refer to the equilibrium condition in the above definition as the *braced equilibrium condition.*

The braced stresses of an embedding form a linear space with respect to the pointwise addition and multiplication with scalars. We denote the space of braced stresses of an embedding $\mathbf{u}$ with $\mathrm{Br}(\mathbf{u})$.

A braced stress is naturally expressed in a matrix form: we define a *braced stress matrix* as a symmetric matrix $[M_{ij}]_{1\le i,j\le n}$ by

$$\begin{aligned} &M_{ij} = \omega_{ij}, \quad (ij) \in E(G), \text{ or } i = j,\\ &M_{ij} = 0, \quad \text{otherwise.}\end{aligned}$$

In the matrix form the braced equilibrium condition is rewritten as

$$Mu = 0,$$

where $u = (u_1, \dots, u_n)^T$. In the following we freely switch between braced stresses and braced stress matrices.

The braced equilibrium condition can also be expressed in a slightly different form similar to the standard equilibrium stress condition:

$$\sum_{j\in N(i,G)} \omega_{ij}(u_j - u_i) = -\left(\sum_{j\in N(i,G)} \omega_{ij} + \omega_{ii}\right) u_i \quad \forall 1 \le i \le n. \tag{2.3.2}$$

Thus, a braced stress becomes an equilibrium stress as soon as

$$\sum_{j\in N(i,G)} \omega_{ij} + \omega_{ii} = 0 \quad \forall 1 \le i \le n. \tag{2.3.3}$$

and every equilibrium stress is always a braced stress.

To the best of our knowledge, *braced stresses* were introduced by Lovász [21] in connection with studies of Colin de Verdière matrices of graphs of 3-polytopes. Since we are interested only in geometrical results of [21] we do not discuss the notion of Colin de Verdière matrices which has roots in spectral graph theory. We only remark, that by [21, Theorem 7] and the following discussion, every positive braced stress of a cone-convex embedding (see Definition 2.4.1) of a planar 3-connected graph G written as a braced stress matrix is a Colin de Verdière matrix of G, whose entries are multiplied with -1.

2.3.2 Canonical braced stresses

Before we proceed with properties of the braced stresses, we provide an additional motivation for why the notion of braced stress is natural: To every 3d embedding of a graph G as a polytopal surface one can naturally assign a braced stress defined only by the geometry of the embedding. We call this stress the *canonical braced stress*. For a convex polytope containing the origin in its interior the canonical braced stress is positive. The construction is due to Lovász [21], we repeat the proof due to its simplicity.

Lemma 2.3.1 ([21], Sect.5)**.** *Let $\mathcal{P} = (u_i)_{1\leq i\leq n}$ be an embedding of a planar 3-connected graph G into $\mathbb{R}^3$ as a polytopal surface (the vertices of each face are coplanar) such that none of the planes supporting the faces of $\mathcal{P}$ passes through the origin. Let $(\phi_f)_{f\in F(G)}$ be the polar vectors to the faces of $\mathcal{P}$: the normal vectors normalized so that $\langle \phi_f, x\rangle = 1$ for every point x of the face f.*

Then there exists a unique braced stress $b\omega$ for (u_i) such that

$$\phi_g - \phi_f = b\omega_{ij}(u_j \times u_i) \tag{2.3.4}$$

for every pair of dual edges $(u_i, u_j) \in E(G)$ and $(\phi_f, \phi_g) \in E(G^*)$.

Definition 2.3.2. *We call the braced stress $b\omega$ defined above the* canonical braced stress *of an embedding.*

We remark that the definition of the canonical braced stress is local: to define the stress on the edge (u_iu_j) one uses only the positions of its endpoints u_i and u_j and the polar vectors to its two incident faces.

Proof of Lemma 2.3.1. First, we check that the left and right hand sides of Eq. (2.3.4) are parallel vectors and $u_i \times u_j \neq 0$ and thus the equation correctly defines $b\omega_{ij}$. Indeed, for $k \in \{i, j\}$

$$\langle \phi_f - \phi_g, u_k\rangle = \langle \phi_f, u_k\rangle - \langle \phi_g, u_k\rangle = 1 - 1 = 0$$

by the chosen normalization of normals, and

$$\langle u_i \times u_j, u_k\rangle = 0$$

by the definition of cross product. The vectors u_i and u_j span the plane since, if they were parallel, planes supporting both faces f and g would pass through the origin. So, both sides of Eq. (2.3.4) are orthogonal to the plane spanned by the vectors u_i and u_j and thus are parallel. Since the vectors u_i and u_j are not parallel, $u_i \times u_j \neq 0$. Thus, Eq. (2.3.4) uniquely defines $b\omega_{ij}$ for $(i, j) \in E(G)$.

To show that $b\omega$ is a braced stress, it remains to check that $\sum_{j\in N(i,G)} b\omega_{ij}u_j \parallel u_i$ for every $1 \leq i \leq n$. This is however straightforward:

$$\left(\sum_{j\in N(i,G)} b\omega_{ij}u_j\right) \times u_i = \sum_{j\in N(i,G)} b\omega_{ij}(u_j \times u_i) = \sum_{1\leq k\leq \deg(v_i)} \phi_{f_k} - \phi_{f_{k+1}} = 0,$$

where $(\phi_1, \phi_2, \ldots, \phi_{\deg(u_i)})$ is the cyclic sequence of faces incident to u_i. □

2.3.3 Braced stresses and equilibrium stresses: flat embeddings

Braced stresses are a natural generalization of equilibrium stresses for nonflat embeddings: Trivially, from Eq. (2.3.2), an equilibrium stress is always a braced stress. Moreover, for flat embeddings the reverse also holds:

Lemma 2.3.2. *1. Let $\mathbf{u} = (u_i)_{1\le i\le n}$ be an embedding of a graph G into $\mathbb{R}^3$. Then every equilibrium stress on $\mathbf{u}$ is a braced stress and the additional weights ω_{ii} can be computed with $\omega_{ii} = -\sum_{j\in N(i,G)} \omega_{ij}$;*

2. Let $\mathbf{u} = (u_i)_{1\le i\le n}$ be a flat embedding of G that lies in a plane α not containing the origin. Then every braced stress on $\mathbf{u}$ is an equilibrium stress.

Proof. 1. That is trivial considering the braced equilibrium condition in the form of Eq. (2.3.2).

2. Consider the braced equilibrium condition in form of Eq. (2.3.2). If the left and right hand sides are nonzero, then the left hand side is parallel to the plane α while the right hand side is not. So both must equal zero and thus

$$\sum_{j\in N(i,G)} \omega_{ij}(u_j - u_i) = 0.$$

□

2.3.4 Braced stresses and stresses of braced graphs

An additional geometrical meaning to the notion of braced stress gives the fact that the braced stresses are in 1-to-1 correspondence with equilibrium stresses on *braced graphs*:

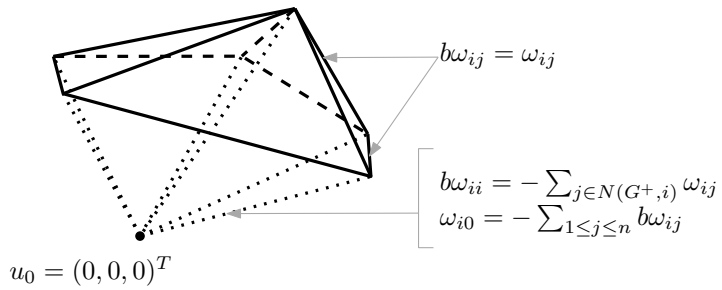

Figure 2.3.1: The graph G^+, with its subgraph G depicted bold. The edges of G^+ that do not belong to G, are dotted. We denote with ω an equilibrium stress on G^* and with $b\omega$ the corresponding braced stress on G.

Lemma 2.3.3. *Let $\mathbf{u} = (u_i)_{1\le i\le n}$ be an embedding of a graph G into $\mathbb{R}^3$. Let G^+ be the graph G with one additional vertex u_0 connected with every vertex in G, and let this additional vertex be embedded at the origin: $u_0 = (0,0,0)^T$ (see Fig. 2.3.1) Then the following two statements hold:*

1. Let ω be an equilibrium stress for the embedding $\mathbf{u}^+ = (u_i)_{0\le i\le n}$ of G^+. Then the restriction of ω to G is a braced stress on the embedding $\mathbf{u}$ of G, and the additional weights can be computed with

$$\omega_{ii} := -\sum_{j\in N(i,G^+)} \omega_{ij}, \quad \forall 1 \le i \le n;$$

2. Let ω be a braced stress on the embedding $\mathbf{u}$ of G. Then the extension of ω to the embedding $\mathbf{u}^+$ of G^+ with

$$\omega_{i0} := -\sum_{j\in N(i,G)\cup\{i\}} \omega_{ij} \quad \forall 1 \le i \le n$$

is an equilibrium stress for the embedding $\mathbf{u}^+$ of G^+.

Proof. 1. We check the braced equilibrium condition in form of Eq. (2.3.2):

$$\sum_{j\in N(i,G)} \omega_{ij}(u_j - u_i) + \left(\sum_{j\in N(i,G)} \omega_{ij} + \omega_{ii}\right) u_i$$
$$= \sum_{j\in N(i,G^+)} \omega_{ij}(u_j - u_i) - \omega_{i0}(u_0 - u_i) + (-\omega_{i0})u_i = 0.$$

The last transition holds since ω is a braced stress on G and $u_0 = 0$.

2. We first check that the equilibrium condition holds at the vertices of G: for every $1 \le i \le n$

$$\sum_{j\in N(i,G^+)} \omega_{ij}(u_j - u_i) = \sum_{j\in N(i,G)} \omega_{ij}(u_j - u_i) + \omega_{i0}(u_0 - u_i)$$
$$= -\left(\sum_{j\in N(i,G)} \omega_{ij} + \omega_{ii}\right) u_i + \left(-\sum_{j\in N(i,G)\cup\{i\}} \omega_{ij}\right)(-u_i) = 0.$$

The second transition used the braced equilibrium condition in form of Eq. (2.3.2), the definition of ω_{i0} and that $u_0 = 0$.

Next we check that it also holds at the additional vertex u_0 of G^+. To simplify the notation we use the braced stress matrix M, thus $\omega_{i0} := -\sum_{1\le i\le n} M_{ij}$ and

$$\sum_{i\in N(0,G^+)} \omega_{0i}(u_i - u_0) = \sum_{1\le i\le n} \omega_{0i}u_i = -\sum_{1\le i\le n}\left(\sum_{1\le j\le n} M_{ij}\right) u_i = -\sum_{1\le j\le n}\left(\sum_{1\le i\le n} M_{ij}u_i\right) = 0,$$

where the last equation holds by the definition of braced stress in terms of braced stress matrix. □

2.3.5 Scalability of braced stresses

Another useful property of braced stresses is that they can be arbitrarily rescaled together with the embedding. This result was noted by Lovász [21]; we include the proof for completeness. The graphs in this subsection are not necessarily planar nor 3-connected.

Lemma 2.3.4. *Let* $\mathbf{u} = (u_i)_{1\le i\le n}$ *and* $\mathbf{r} = (r_i)_{1\le i\le n}$ *be two embeddings of a graph* G *into* $\mathbb{R}^3$ *such that* $\mathbf{r}$ *is a rescaling of* $\mathbf{u}$*:*

$$r_i = \lambda_i u_i, \quad \lambda_i \in \mathbb{R}\setminus\{0\},\ 1 \le i \le n.$$

Then the map $\mathrm{pr}_{u\to r} : \mathbb{R}^{E(G)} \to \mathbb{R}^{E(G)}$ *defined as*

$$(\mathrm{pr}_{u\to r}\,\omega)_{ij} = \frac{1}{\lambda_i\lambda_j}\omega_{ij}, \qquad (i,j) \in E(G)$$

is a linear isomorphism between the linear spaces of braced stresses on $\mathbf{u}$ *and* $\mathbf{r}$ *with* $\mathrm{pr}_{u\to r}\,\mathrm{pr}_{r\to u} = \mathrm{Id}$.

Proof. For simplicity we work with braced stress matrices: we extend the map to the whole matrix using the same formula:

$$(\mathrm{pr}_{u\to r}\,M)_{ij} = \frac{1}{\lambda_i\lambda_j}M_{ij}, \qquad 1 \le i,j \le n$$

We first show that for every braced stress matrix M of $\mathbf{u}$ the image $\mathrm{pr}_{u\to r}(M)$ is a braced stress matrix for $\mathbf{r}$. Indeed,

$$\sum_{j=1}^{n} \frac{1}{\lambda_i\lambda_j} M_{ij} r_j = \frac{1}{\lambda_i} \sum_{j=1}^{n} M_{ij} \frac{1}{\lambda_j} r_j = \frac{1}{\lambda_i} \sum_{j=1}^{n} M_{ij} u_j = 0, \quad 1 \le i \le n.$$

Next, trivially, $\mathrm{pr}_{u\to r}\,\mathrm{pr}_{r\to u} = \mathrm{Id}$:

$$(\mathrm{pr}_{r\to u}\,\mathrm{pr}_{u\to r}\,M)_{ij} = \lambda_i\lambda_j(\mathrm{pr}_{u\to r}\,M)_{ij} = \lambda_i\lambda_j \frac{1}{\lambda_i\lambda_j} M_{ij} = M_{ij}.$$

Finally, in the matrix form

$$\mathrm{pr}_{u\to r}\,M = \begin{pmatrix} 1/\lambda_1, & \dots, & 1/\lambda_n \end{pmatrix} M \begin{pmatrix} 1/\lambda_1 \\ \cdots \\ 1/\lambda_n \end{pmatrix}$$

and thus $\mathrm{pr}_{u\to r}$ is trivially linear. □

2.3.6 Projective equivalence with equilibrium stresses

We already mentioned that the spaces of braced and equilibrium stresses coincide for flat embeddings of a graph. The scalability property now allows us to describe an isomorphism between the linear space of braced stresses on any embedding and the linear space of equilibrium stresses on any of the flat rescalings of this embedding. Thus, we can use for braced stresses all the machinery available for equilibrium stresses.

We thus show now that the linear spaces of braced stresses and of equilibrium stresses are isomorphic by presenting a projective correspondence between these two spaces. This correspondence is also of independent interest as it highlights the projective nature of the notion of equilibrium stress.

Lemma 2.3.5. *Let $\mathbf{u} = (u_i)_{1\le i\le n}$ be an embedding of a graph G in $\mathbb{R}^3$ such that none of its vertices is at the origin. Let α be any plane that does not contain the origin and is not parallel to any of the vectors u_i. Let $\mathbf{p} = (p_i)_{1\le i\le n}$ be the central projection of $\mathbf{u}$ to α:*

$$p_i := \lambda_i u_i, \quad \lambda_i \in \mathbb{R},\, p_i \in \alpha.$$

Then the map $\mathrm{pr}_\alpha : \mathbb{R}^{E(G)} \to \mathbb{R}^{E(G)}$ defined as

$$(\mathrm{pr}_\alpha\,\omega)_{ij} = \frac{1}{\lambda_i}\frac{1}{\lambda_j}\omega_{ij}, \quad (ij) \in E(G)$$

is a linear isomorphism between the linear space of braced stresses on $\mathbf{u}$ and the linear space of equilibrium stresses on $\mathbf{p}$.

Proof. Due to Lemma 2.3.4, the map $pr_{u\to p} : \mathbb{R}^{E(G)} \to \mathbb{R}^{E(G)}$ defined as $pr_{u\to p}(\omega)_{ij} = \frac{1}{\lambda_i\lambda_j}\omega_{ij}$ is a linear isomorphism between the spaces of braced stresses of $\mathbf{u}$ and $\mathbf{p}$. To finish the proof we remark that $\mathbf{p}$ is a flat embedding and thus by Lemma 2.3.2 the spaces of braced stresses and of equilibrium stresses on $\mathbf{p}$ coincide. □

We remark that the previous lemma gives a fresh perspective on how the space of equilibrium stresses behaves under projective transformations of the plane. We discuss it in Sect. 2.3.8.

2.3.7 Free lunch: wheel-decomposition for braced stresses

We use the correspondence between equilibrium stresses and braced stresses to define the concept of *atomic braced stress* and to formulate and prove the *wheel-decomposition theorem* for braced stresses, which is the braced analogue of the wheel-decomposition theorem for equilibrium stresses, Theorem 2.2.1.

Definition 2.3.3. *Let $W = W(v_c; v_1, \dots v_n)$ be a wheel with center v_c. Let $\mathbf{u} = (u_c; u_1, \dots u_n)$ be an embedding of W to $\mathbb{R}^3$ such that for every $1 \le i \le n$ the points u_i, u_{i+1} and u_c are noncoplanar with the origin (as usual, we use the cyclic notation for the vertices of the base of the wheel). Then we call the assignment of reals to the edges of W*

$$b\omega^a_{ij} := \begin{cases} -\frac{1}{\det(u_i u_{i+1} u_c)}, & j = i+1, 1 \le i \le n, \\ \frac{\det(u_{i-1} u_i u_{i+1})}{\det(u_{i-1} u_i u_c)\det(u_i u_{i+1} u_c)}, & j = c, 1 \le i \le n \end{cases} \tag{2.3.5}$$

the atomic braced stress *on* $\mathbf{u}$.

We call the rescaling of $b\omega^a$ with the factor $\prod_{1\le i\le n} \det(u_i u_{i+1} u_c)$ the large atomic braced stress *and denote it with*

$$b\omega^A := \left(\prod_{1\le i\le n} \det(u_i u_{i+1} u_c) \right) \cdot b\omega^a.$$

Note that for a wheel with integer vertex coordinates, $u_i \in \mathbb{Z}^3$, the large atomic braced stress $b\omega^A$ is integer.

Lemma 2.3.6. *In the setup of Definition 2.3.3,*

1. *The atomic braced stress on $\mathbf{u}$ is a braced stress on $\mathbf{u}$.*
2. *A braced stress on $\mathbf{u}$ is unique up to scaling.*
3. *Let $\alpha = \{z = 1\}$ be an affine plane and let none of u_i be parallel to α. Let $\mathbf{p}$ be the central projection of $\mathbf{u}$ to this plane, $p_i = \lambda_i u_i \in \alpha$, $\lambda_i \in \mathbb{R}$. Then, in the notation of Lemma 2.3.5,*

$$b\omega^a = \lambda_c \operatorname{pr}_\alpha^{-1}(\omega^a),$$
$$b\omega^A = \frac{1}{\lambda_c^n (\prod_{1\le i\le n} \lambda_i)^2} \operatorname{pr}_\alpha^{-1}(\omega^A),$$

where ω^a and ω^A are the small *and* large *atomic equilibrium stresses on $\mathbf{p}$ correspondingly.*

We note that the requirement $\alpha = \{z = 1\}$ in the last statement of the lemma is excessive: the rotation of coordinates in $\mathbb{R}^3$ allows α to be any plane with distance 1 to the origin and after an appropriate rescaling α can be any plane not passing through the origin. We state the lemma for $\alpha = \{z = 1\}$ to avoid complications with defining coordinates (and orientation) on α that we need to compute the atomic equilibrium stresses of flat realizations of wheels.

Proof of Lemma 2.3.6. Pick any affine plane β that does not contain the origin and such that none of u_i is parallel to β. Let $\mathbf{p}$ be the central projection of $\mathbf{u}$ to this plane, $p_i = \lambda_i u_i \in \beta$. Due to Lemma 2.3.5 the braced stresses of $\mathbf{u}$ are in 1-to-1 correspondence with the equilibrium stresses of $\mathbf{p}$, which proves the uniqueness (part 2 of the lemma).

To finish the proof we check the expressions in part 3. Due to Lemma 2.3.5, $\operatorname{pr}_\alpha^{-1}(\omega^a)$ is a braced stress, which also proves part 1 of the lemma. We check only the equation for small atomic stresses. The case of large atomic stresses can be checked similarly. Since none of the

triples of points u_i, u_{i+1}, u_c for $1 \leq i \leq n$ is coplanar with the origin, none of the triples of points p_i, p_{i+1}, p_c is collinear. Thus we can construct the small atomic stress for $\mathbf{p}$:

$$\omega^a_{ij} := \begin{cases} -\frac{1}{[p_i p_{i+1} p_c]}, & j = i+1, 1 \leq i \leq n, \\ \frac{[p_{i-1} p_i p_{i+1}]}{[p_{i-1} p_i p_c][p_i p_{i+1} p_c]}, & j = c, 1 \leq i \leq n. \end{cases}$$

By Lemma 2.3.5, the image of ω^a under the reverse projection $b\omega := \mathrm{pr}_\alpha^{-1}(\omega^a)$ of $\mathbf{p}$ to $\mathbf{u}$ is a braced stress for $\mathbf{u}$ with

$$b\omega_{ij} := \lambda_i \lambda_j \omega^a_{ij}.$$

We additionally rescale it with a factor λ_c to

$$b\omega^a := \lambda_c b\omega$$

and remark that

$$\frac{[p_i p_k p_l]}{\lambda_i \lambda_k \lambda_l} = \det(u_i u_k u_l).$$

A straightforward computation finishes the proof. □

The wheel-decomposition theorem for braced stresses is now in context of Lemma 2.3.5 a straightforward consequence of the wheel-decomposition theorem for equilibrium stresses as given in Theorem 2.2.1:

Theorem 2.3.1 (Wheel-decomposition theorem for braced stresses)**.** *Let $\mathbf{u} = (u_i)_{1 \leq i \leq n}$ be an embedding of a triangulation G with $n > 3$ vertices in $\mathbb{R}^3$ such that none of the planes supporting the faces of $\mathbf{u}$ passes through the origin. Let $b\omega$ be a braced stress for $\mathbf{u}$. Then there exists a set of real coefficients $(\alpha_i)_{1 \leq i \leq n}$ such that*

$$b\omega = \sum_{1 \leq i \leq n} \alpha_i b\omega^a(W_i),$$

where $b\omega^a(W_i)$ is the atomic braced stress for the wheel $W_i \subset G$ centered at the vertex u_i. The set of coefficients is unique up to the "parallel translation" transformation

$$\alpha_i \to \alpha_i + \langle v, u_i \rangle \qquad \forall i$$

for any vector v in $\mathbb{R}^3$.

Proof. Let α be any affine plane at the distance 1 from the origin that is not parallel to any of the vectors u_i. We rotate coordinates in $\mathbb{R}^3$ so that $\alpha = \{z = 1\}$, what does not affect the statement of the theorem. Let $\mathbf{p} = (p_i)_{1 \leq i \leq n}$ be the central projection of $\mathbf{u}$ to this plane and $\omega = \mathrm{pr}_\alpha(b\omega)$ be the central projection of $b\omega$ (see Lemma 2.3.5):

$$\begin{aligned} p_i = \lambda_i u_i : \quad & p_i \in \alpha, && 1 \leq i \leq n, \\ \omega_{ij} = \frac{1}{\lambda_i \lambda_j} & b\omega_{ij}, && (i,j) \in E(G). \end{aligned}$$

Due to Lemma 2.3.5, ω is an equilibrium stress for $\mathbf{p}$. Since the faces of $\mathbf{u}$ are not coplanar with the origin, the faces of $\mathbf{p}$ are nondegenerate triangles. Thus we can apply the wheel-decomposition theorem for equilibrium stresses (Theorem 2.2.1) to get

$$\omega = \sum_{1 \leq k \leq n} \alpha_k \omega^a(W_k), \tag{2.3.6}$$

where $\omega^a(W_k)$ is the small atomic equilibrium stress for the wheel centered at the vertex p_k. We use the second part of Lemma 2.3.5 and project both sides of Eq. (2.3.6) back to $\mathbf{u}$:

$$\mathrm{pr}_\alpha^{-1}\,\omega = \sum_{1\le k\le n} \alpha_k\,\mathrm{pr}_\alpha^{-1}\,\omega^a(W_k).$$

By construction, the left-hand side equals $b\omega$. By the third part of Lemma 2.3.6, the summands on the right-hand side equal the rescaled atomic braced stresses of the wheels,

$$\mathrm{pr}_\alpha^{-1}\,\omega^a(W_k) = \frac{1}{\lambda_k} b\omega^a(W_k), \quad 1 \le k \le n.$$

Thus,

$$b\omega = \sum_{1\le k\le n} \mathrm{pr}_\alpha^{-1}(\alpha_k) b\omega^a(W_k),$$

where we denote $\mathrm{pr}_\alpha^{-1}(\alpha_k) = \frac{\alpha_k}{\lambda_k}$.

To finish the proof we analyze the uniqueness of the coefficients. The coefficients in the planar decomposition, Eq. (2.3.6), are the heights of the corresponding vertices in any of the Maxwell–Cremona liftings of $\mathbf{p}$ with help of ω. They are unique up to the transformation $\alpha_k \to \alpha'_k = \alpha_k + \langle v, p_k\rangle$, where v is any vector in $\mathbb{R}^3$. The corresponding transformation for the coefficients of the wheel-decomposition of braced stresses is:

$$\begin{aligned}\mathrm{pr}_\alpha^{-1}(\alpha_k) \to \mathrm{pr}_\alpha^{-1}(\alpha'_k) = \frac{\alpha'_k}{\lambda_k} &= \frac{\alpha_k + \langle v, p_k\rangle}{\lambda_k} \\ &= \mathrm{pr}_\alpha^{-1}(\alpha_k) + \langle v, \frac{p_k}{\lambda_k}\rangle = \mathrm{pr}_\alpha^{-1}(\alpha_k) + \langle v, u_k\rangle.\end{aligned}$$

□

2.3.8 Free lunch: projective properties of equilibrium stresses

In this subsection we want to observe one trivial consequence of the connection between braced and equilibrium stresses developed above. We present a very geometric view on how equilibrium stresses on a planar embedding of a graph behave under projective transformations of the plane. This is in no way a new result, but the point of view might be new.

Pure projective transformation

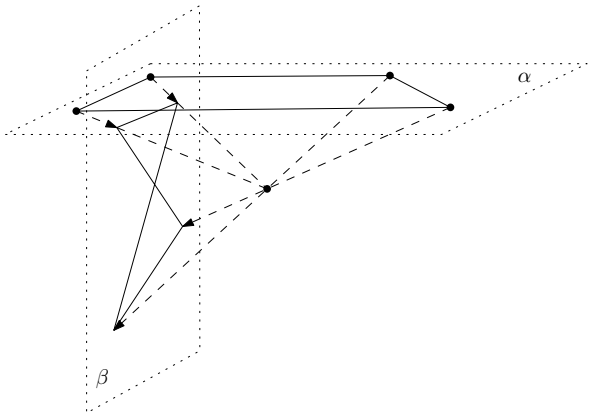

Figure 2.3.2: Projective transformation of a plane.

One standard way to geometrically view a projective transformation is depicted on Fig. 2.3.2: let α and β be two affine planes in $\mathbb{R}^3$, then the central projection from α to β via lines through the origin defines a projective transformation of the plane.

Lemmas 2.3.3 and 2.3.4 allow to track equilibrium stresses during the central projection: Let ω be an equilibrium stress on the embedding of a graph G to α. We denote the central projection from α to β with $\mathrm{pr}_{\alpha\to\beta}$ and the corresponding scaling coefficient of each point $u \in \alpha$ with $c(u)$:

$$\mathrm{pr}_{\alpha\to\beta}(u) = c(u)u \in \beta.$$

Then by combining Lemma 2.3.4 and Lemma 2.3.2

$$\mathrm{pr}_{\alpha\to\beta}(\omega)_{ij} := c(u_i)c(u_j)\omega_{ij}$$

is an equilibrium stress on the projective image — the embedding $\mathrm{pr}_{\alpha\to\beta}(u)$ of G to β.

The disadvantage of this interpretation of projective transformation is that the points of α that are parallel to β are not properly projected and form a line at infinity that is not properly observable in β. The braced stresses provide a fix to this problem: unlike the equilibrium stresses they are also defined for embeddings of graphs to the sphere, thus one may use the natural model of projective plane as a sphere with glued opposite points, where the line at infinity is just another large circle on the sphere. We discuss this fix below.

Projective transformation seen through the sphere

Before we proceed, we introduce a notation: let α be an affine plane in $\mathbb{R}^3$. We denote the central projection from α to the unit sphere with π_α:

$$\pi_\alpha(u) = \frac{u}{|u|}.$$

The reverse of π_α is then directly defined only on the half sphere bounded by the large circle parallel to α. We define it on the other side of the sphere symmetrically $\pi_\alpha^{-1}(x) = \pi_\alpha^{-1}(-x)$ and thus it is defined (and is 2-to-1) on the whole sphere except the large circle parallel to α.

Any projective transformation of the plane $f : \mathbb{R}^2 \to \mathbb{R}^2$ can now be geometrically viewed in the following way:

1. Embed the initial plane to $\mathbb{R}^3$ as some affine plane α;
2. Project points of α to the unit sphere via lines through the origin:
$$u \to \pi_\alpha(u);$$
3. Pick some other affine plane $\beta \in \mathbb{R}^3$ and project the points of the sphere to β:
$$s \to \pi_\beta^{-1}(s).$$

Thus, for every f one finds α and β such that $f = \pi_\beta^{-1} \circ \pi_\alpha$.

Fig. 2.3.3 illustrates the process, first (1) the graph is drawn on a plane, then we project it to the sphere and it is stored on the sphere (2), and in the end (3) it is projected to the other plane.

The notion of braced stress makes it possible to assign stresses directly to the embedding of a graph to the sphere. This allows us to avoid difficulties, connected with the infinite line of the projective plane: from the point of view of the sphere the infinite line is a large circle and is indistinguishable from any other line.

By this we can look at the behavior of stresses during the projective transformation of the plane once again: Let ω be an equilibrium stress on an embedding of a graph G onto a plane α. Then, $\mathrm{pr}_\alpha^{-1}(\omega)$ is a braced stress on an embedding of G onto the sphere. And finally, $\mathrm{pr}_\beta \mathrm{pr}_\alpha^{-1}(\omega)$ is an equilibrium stress on the embedding of G to β, projective image of the initial embedding.

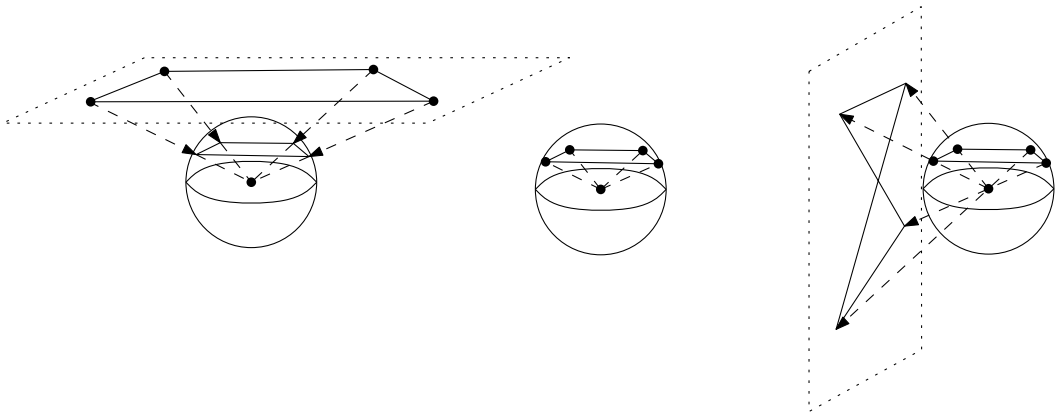

Figure 2.3.3: Projective transformation with one intermediate step, embedding to the sphere.

2.3.9 Canonical braced stresses as Hessians of volume

A different approach to the construction of canonical braced stresses was developed by Izmestiev [17] in his work on the Colin de Verdière matrices of skeletons of d-polytopes.

Let $(v_i)_{1\le i\le n}$ be a set of vectors in $\mathbb{R}^3$. The polytope with normal vectors (v_i) and support parameters $\mathbf{x} = (x_i)_{1\le i\le n}$ is the intersection of half-spaces defined by $\langle p, v_i\rangle \le x_i$,

$$P(\mathbf{x}) = \cap_{1\le i\le n}\{p \in \mathbb{R}^3 : \langle p, v_i\rangle \le x_i\}.$$

Let $\mathcal{P}$ be a convex polytope with a set of normals to faces $(v_f)_{f\in F(P)}$ and faces lying in planes $\{p \in \mathbb{R}^3 : \langle p, v_f\rangle = x_f\}_{f\in F(P)}$. Then with respect to the set of vectors (v_f) we can write $P = P(\mathbf{x})$. By varying the support parameters x_f we change the polytope and its volume. The following holds:

Lemma 2.3.7 (Lemma 2.3, [17])**.** *Let P be a convex polytope and let $\mathcal{P}^* = (v_f)_{f\in F(P)}$ be its polar dual, thus $P = P(\mathbf{1})$. Then for the canonical braced stress ω^c on P^**

$$\omega^c_{fg} = \left.\frac{\partial \operatorname{Vol}(P(x))}{\partial x_f \partial x_g}\right|_{\mathbf{x}=\mathbf{1}} \qquad f \sim g \in F(P).$$

Moreover the whole Hessian matrix

$$M_{fg} := \left.\frac{\partial \operatorname{Vol}(P(x))}{\partial x_f \partial x_g}\right|_{\mathbf{x}=\mathbf{1}} \qquad \forall f, g \in F(P)$$

is a braced stress matrix for $\mathcal{P}^*$, and a Colin de Verdière matrix for the skeleton of $\mathcal{P}^*$.

We do not repeat the whole proof, the part about braced stresses is a straightforward geometrical check that (the equation is informal and we ignore signs)

$$\frac{\phi_f - \phi_g}{u_i \times u_j} = \frac{|\phi_f - \phi_g|}{|u_i||u_j|\sin(u_i, u_j)} = \left.\frac{\partial \operatorname{Vol}(P(x))}{\partial x_f \partial x_g}\right|_{\mathbf{x}=\mathbf{1}}.$$

We only remark, that the representation as a Hessian matrix makes the braced equilibrium condition trivial: the well known Minkowski theorem asserts that

$$\sum_{g\in F(G)} \operatorname{Vol}_2(g)\frac{\phi_g}{|\phi_g|} = 0.$$

By differentiating this equality with respect to x_f and noticing that $\mathrm{Vol}_2(f) = \frac{\partial \mathrm{Vol}(P(x))}{\partial x_f}|\phi_f|$ we deduce

$$\sum_{g \neq f} \frac{\partial \mathrm{Vol}(P(x))}{\partial x_f \partial x_g}\phi_g = -\frac{\partial \mathrm{Vol}(P(x))}{(\partial x_f)^2}\phi_f,$$

what is exactly the braced equilibrium condition.

2.3.10 Orthogonal projection of the canonical braced stresses

The notion of the canonical braced stress is not translationally invariant: when one moves the origin, the canonical braced stress changes. In this section we study what happens when we send the origin to infinity.

Specifically, let $\mathcal{P}$ be a polytopal surface in $\mathbb{R}^3$. In this section we do not require $\mathcal{P}$ to be convex, nor we require it to be non-self-intersecting; we only need that the canonical braced stress and the canonical dual braced stress (see Definition 2.3.4 below) are defined, what is guaranteed as soon as all the faces of $\mathcal{P}$ are flat and not coplanar with the origin.

Let us consider the canonical braced stress $\omega(t)$ of the parallelly translated polytopal surface $\mathcal{P}(t) = \mathcal{P} + tv$, where $v \in \mathbb{R}^3$ and $t \in \mathbb{R}$. And then let $t \to \infty$. The intuition is that the "additional" stresses $\omega_{ii}(t)$ from the definition of the braced stress, Definition 2.3.1, on the "additional" edges from the origin will now cancel with the v components of the forces on the "real" edges of $\mathcal{P}$; thus the braced stress becomes an equilibrium stress on the projection of $\mathcal{P}$ to the plane orthogonal to v. This is indeed the case and moreover this equilibrium stress coincides with the canonical equilibrium stress of the orthogonal projection $\mathcal{P}^v$ of $\mathcal{P}$ to this plane, Theorem 2.3.2.

We begin our exposition with an even stronger version of the limit statement above: In fact, the limit of braced stresses $\omega(t)$ on $\mathcal{P}(t)$ is an equilibrium stress on $\mathcal{P}^v$ for any converging sequence of braced stresses $\omega(t)$ and not only for the canonical ones:

Lemma 2.3.8. *Let $\mathcal{P}$ be a polytopal surface in $\mathbb{R}^3$, let $\mathcal{P}(t) = \mathcal{P} + tv$ with $t \in \mathbb{R}$ and a fixed vector $v \in \mathbb{R}^3$ be a family of its parallel translations. Let $\omega(t_k)$ be a braced stress on $\mathcal{P}(t_k)$ for some sequence of times $t_k \xrightarrow[k\to\infty]{} \infty$. Suppose this sequence of stresses converge: for every edge (i,j) of $\mathcal{P}$ there exists the finite limit $\lim_{k\to\infty} \omega_{ij}(t_k)$ which we denote with ω^v_{ij}. Then this limit is an equilibrium stress on the orthogonal projection $\mathcal{P}^v$ of $\mathcal{P}$ to the plane orthogonal to v.*

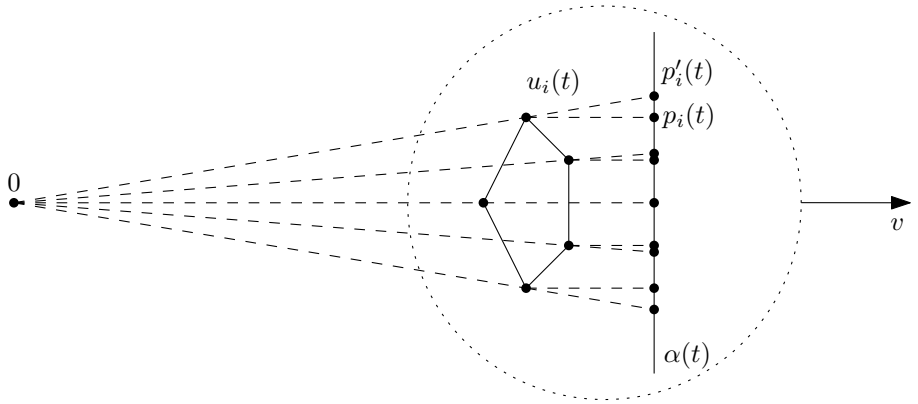

Figure 2.3.4: The limiting braced stress is an equilibrium stress.

Proof. To clarify the notation we shortcut $t_k \xrightarrow[k\to\infty]{} \infty$ with $t \to \infty$, what does not lead to any confusion in our setup.

Let α be any affine plane orthogonal to v. We fix the relative position of α and $\mathcal{P}$ and when $\mathcal{P}(t)$ goes to infinity, we move α simultaneously, $\alpha(t) := \alpha + tv$; Fig. 2.3.4. We denote the vertices of $\mathcal{P}(t)$ with $u_i(t)$. Let $p_i'(t)$ be the central projection of the vertex $u_i(t)$ to the plane $\alpha(t)$,

$$p_i'(t) = \lambda_i(t)u_i(t) \in \alpha(t), \quad \lambda_i(t) \in \mathbb{R}.$$

For every t the stress $\omega(t)$ is a braced stress on $u_i(t)$. Thus, by Lemma 2.3.5, the central projection $\mathrm{pr}_{\alpha(t)}\,\omega(t)$ of this stress to the plane $\alpha(t)$, defined as

$$(\mathrm{pr}_{\alpha(t)}\,\omega(t))_{ij} = \frac{1}{\lambda_i(t)}\frac{1}{\lambda_j(t)}\omega_{ij}(t)$$

is an equilibrium stress on the embedding $\mathbf{p}'(t) = (p_i'(t))$. We denote this projected stress with $\omega^p(t) := \mathrm{pr}_{\alpha(t)}\,\omega(t)$. Since the relative position of $\mathcal{P}(t)$ and $\alpha(t)$ is fixed, $\lambda_i(t) \to 1$. Thus, the limit of $\omega^p(t)$ exists and it equals the limit ω^v of the braced stresses $\omega(t)$:

$$\lim_{t\to\infty} \omega_{ij}^p(t) = \lim_{t\to\infty} (\mathrm{pr}_{\alpha(t)}\,\omega(t))_{ij} = \lim_{t\to\infty} \frac{1}{\lambda_i(t)}\frac{1}{\lambda_j(t)}\omega_{ij}(t) = \lim_{t\to\infty} \omega_{ij}(t) = \omega_{ij}^v.$$

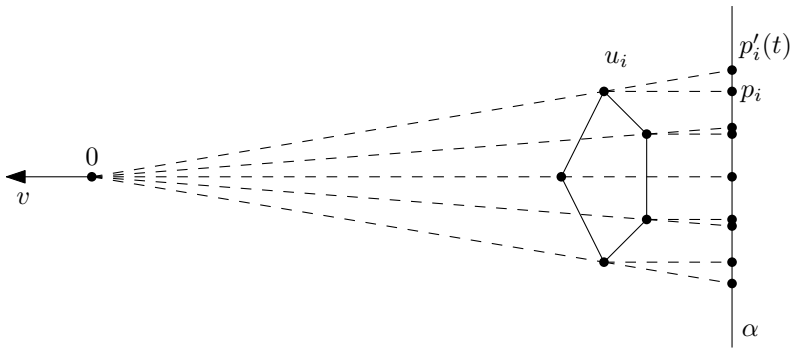

Figure 2.3.5: After the change of coordinates.

We show next that the constructed limit stress ω^v is an equilibrium stress on $\mathcal{P}^v$. Let $p_i(t)$ be the orthogonal projection of $u_i(t)$ to the plane $\alpha(t)$. Trivially, $p_i'(t) \to p_i(t)$ with $t \to \infty$. Let us now change the system of coordinates (use the reverse parallel translation $x \to x - tv$) so that $\alpha(t) = \alpha$ and $\mathcal{P}(t) = \mathcal{P}$ are fixed. Thus the orthogonal projection $p_i(t) = p_i$ of $\mathcal{P}$ to α is fixed as well, and it is the projection $\mathcal{P}^v$ of the polytopal surface $\mathcal{P}$ to the plane orthogonal to the vector v from the statement of the theorem, thus $(p_i) = \mathcal{P}^v$. And we have a family of embeddings $\mathbf{p}'(t) = (p_i'(t))$ that converge to $\mathcal{P}^v = (p_i)$ (see Fig.2.3.5),

$$\mathbf{p}'(t) = (p_i'(t)) \to \mathcal{P}^v = (p_i).$$

The notion of equilibrium stress is invariant under translations, thus after the change of coordinates the stress $\omega^p(t)$ is still an equilibrium stress on $\mathbf{p}'(t)$. Thus, since $\mathbf{p}'(t) \to \mathcal{P}^v$, the limit $\lim_{t\to\infty} \omega^p(t)$ is an equilibrium stress on $\mathcal{P}^v$. And as we established before, this limit exactly equals ω^v. Thus, ω^v is an equilibrium stress on $\mathcal{P}^v$. □

As we established the general limit result we move on to the behavior of the canonical braced stresses:

Theorem 2.3.2. *Let $\mathcal{P} = (u_i)$ be a polytopal surface in $\mathbb{R}^3$ and let $\mathcal{P}(t) = \mathcal{P} + tv$ be a family of parallel translations of $\mathcal{P}$, where $t \in \mathbb{R}$ and $v \in \mathbb{R}^3$ is a fixed unit vector not parallel to any face of $\mathcal{P}$. Let $\omega^c(t)$ be the canonical braced stress on $\mathcal{P}(t)$ and let $\mathcal{P}^v$ be the orthogonal projection of $\mathcal{P}$ to the plane orthogonal to v. Then*

(1) For every edge (i,j) there exists the finite limit $\lim_{t\to\infty} t^2\omega^c_{ij}(t)$, which we denote with ω^v_{ij}, and this limit equals

$$\omega^v_{ij} := \lim_{t\to\infty} t^2\omega^c_{ij}(t) = \frac{1}{\langle v, \phi_f\rangle\langle v, \phi_g\rangle}\omega^c_{ij}, \tag{2.3.7}$$

where ϕ_f and ϕ_g are the polar vectors to the faces f and g of $\mathcal{P}$ separated by the edge (i,j), and $\omega^c = \omega^c(0)$ is the canonical braced stress on the initial polytopal surface $\mathcal{P}$;

(2) This limit is a nonzero equilibrium stress on the projection $\mathcal{P}^v$ of $\mathcal{P}$;

(3) And moreover, this equilibrium stress coincides with the canonical equilibrium stress on the projection $\mathcal{P}^v$ of $\mathcal{P}$.

Before proving Theorem 2.3.2 we explicitly compute $\omega^c(t)$ in terms of ω^c, $\mathcal{P}$ and t. To facilitate this computation we use the reciprocity of the canonical braced stresses of the polytopal surface and of its polar dual as noticed by Lovász [21]:

Definition 2.3.4. *Let $\mathcal{P} = (u_i)$ be a polytopal surface in $\mathbb{R}^3$ such that none of its faces is coplanar with the origin, let $\mathcal{P}^* = (\phi_f)$ be its polar dual. We call the canonical braced stress ω^{*c} of the polar dual $\mathcal{P}^*$ the* canonical dual braced stress *of $\mathcal{P}$. Thus,*

$$\omega^{*c}_{fg} = \frac{u_j - u_i}{\phi_f \times \phi_g} \tag{2.3.8}$$

for every pair of dual edges (i,j) of $\mathcal{P}$ and (f,g) of $\mathcal{P}^*$.

We remark that the polytopal surfaces $\mathcal{P}$ and $\mathcal{P}^*$ generally may be nonconvex and self-intersecting. Though, the equation Eq. (2.3.8) defines ω^{*c} as soon as the points of every face are coplanar, which always holds. The following was noticed by Lovász in [21, part 7]:

Lemma 2.3.9. *Let $\mathcal{P}$ be a polytopal surface in $\mathbb{R}^3$, let ω^c be its canonical braced stress and let ω^{*c} be its canonical dual braced stress. Then*

$$\omega^{*c}_{fg} = \frac{1}{\omega^c_{ij}},$$

for every pair of dual edges (i,j) of $\mathcal{P}$ and (f,g) of $\mathcal{P}^*$.

For the purpose of completeness and due to its simplicity we repeat the original proof.

Proof. We build the cross product of both sides of the equation $\phi_g - \phi_f = \omega^c_{ij}(u_j \times u_i)$ with ϕ_g to get $(\phi_g - \phi_f) \times \phi_g = -\phi_f \times \phi_g$ on the left hand side and

$$\omega^c_{ij}(u_j \times u_i) \times \phi_g = \omega^c_{ij}(\langle u_j, \phi_g\rangle u_i - \langle u_i, \phi_g\rangle u_j) = \omega^c_{ij}(u_i - u_j)$$

on the right hand side. Thus

$$(u_j - u_i) = \frac{1}{\omega^c_{ij}}(\phi_f \times \phi_g),$$

what by the definition of the canonical dual braced stress ω^{*c} finishes the proof. □

We use the reciprocity established above to explicitly compute $\omega^c(t)$. For all but finitely many t the shifted polytopal surface $\mathcal{P}(t)$ is in general position: none of the planes of its faces contains the origin, and thus the polar dual, the canonical braced stress and the canonical dual braced stress are well-defined. Since we are interested in the behaviour of the system with $t \to \infty$, we are free to consider all but these finitely many values of t.

Lemma 2.3.10. *In the setup of Theorem 2.3.2*

$$\omega^c_{ij}(t) = \frac{1}{(1+t\langle v,\phi_f\rangle)(1+t\langle v,\phi_g\rangle)}\omega^c_{ij},$$

where ϕ_f and ϕ_g are the polar vectors to the faces f and g incident to the edge (i,j) and $\omega^c = \omega^c(0)$ is the canonical braced stress on the initial polytopal surface $\mathcal{P}$.

Proof. As usual the vertices of $\mathcal{P}(t)$ are denoted with $u_i(t)$. By the definition of the canonical braced and dual braced stresses,

$$\omega^c_{ij}(t) = \frac{\phi_f(t)-\phi_g(t)}{u_i(t)\times u_j(t)}, \quad \omega^{*c}_{fg}(t) = \frac{u_j(t)-u_i(t)}{\phi_f(t)\times\phi_g(t)},$$

where $u_i(t)$ are the vertices of $\mathcal{P}(t)$ and $\phi_f(t)$ are the polar vectors to the faces of $\mathcal{P}(t)$.

First, we notice that by construction $u_i(t) = u_i + tv$. Second, we recompute $\phi_f(t)$. Since $\mathcal{P}(t)$ is a translation of $\mathcal{P}$, the faces of $\mathcal{P}(t)$ are parallel to the corresponding faces of $\mathcal{P}$ and thus the polar vectors to the corresponding faces are collinear. So,

$$\phi_f(t) = \lambda_f(t)\phi_f,\ \lambda_f(t)\in\mathbb{R}$$

for some real scalar $\lambda_f(t)\in\mathbb{R}$. To determine these scalars we use the definition of the polar:

$$\langle\phi_f, u\rangle = \langle\phi_f(t), u(t)\rangle = 1$$

for any vertex u that belongs to the face f. Thus,

$$1 = \langle\phi_f(t), u(t)\rangle = \lambda_f(t)\langle\phi_f, u+tv\rangle = \lambda_f(t)(1+t\langle v,\phi_f\rangle)$$

and we derive

$$\lambda_f(t) = \frac{1}{1+t\langle v,\phi_f\rangle}, \qquad \phi_f(t) = \frac{1}{1+t\langle v,\phi_f\rangle}\phi_f.$$

Thus, for the canonical dual braced stress of the shifted polytopal surface:

$$\begin{aligned}\omega^{*c}_{fg}(t) = \frac{u_j(t)-u_i(t)}{\phi_f(t)\times\phi_g(t)} &= (1+t\langle v,\phi_f\rangle)(1+t\langle v,\phi_g\rangle)\frac{u_j-u_i}{\phi_f\times\phi_g}\\ &= (1+t\langle v,\phi_f\rangle)(1+t\langle v,\phi_g\rangle)\omega^{*c}_{fg},\end{aligned}$$

and for the canonical braced stress:

$$\begin{aligned}\omega^c_{ij}(t) = \frac{1}{\omega^{*c}_{fg}(t)} &= \frac{1}{(1+t\langle v,\phi_f\rangle)(1+t\langle v,\phi_g\rangle)\omega^{*c}_{fg}}\\ &= \frac{1}{(1+t\langle v,\phi_f\rangle)(1+t\langle v,\phi_g\rangle)}\omega^c_{ij}.\end{aligned}$$

□

Now we are ready to move on to the proof of the first two parts of Theorem 2.3.2.

Proof of Theorem 2.3.2, parts (1) and (2). (1) We use the translation formula of Lemma 2.3.10:

$$\lim_{t\to\infty} t^2\omega_{ij}(t) = \lim_{t\to\infty}\frac{1}{(1/t+\langle v,\phi_f\rangle)(1/t+\langle v,\phi_g\rangle)}\omega_{ij} = \frac{1}{\langle v,\phi_f\rangle\langle v,\phi_g\rangle}\omega_{ij}.$$

We remind that the direction v is chosen so that it is not parallel to any of the faces of $\mathcal{P}$, thus $\langle v,\phi_f\rangle\neq 0$ and the denominator above is nonzero.

(2) To show that ω^v is an equilibrium stress on $\mathcal{P}^v$ we use Lemma 2.3.8 for the family of braced stresses $t^2\omega^c(t)$, which converge to ω^v due to part (1) of the theorem. □

Before we move on to part (3) of Theorem 2.3.2 we revisit the notion of the canonical equilibrium stress on an orthogonal projection. We introduced the canonical equilibrium stress in Sect. 2.2.1 with Eq. (2.2.3), as an equilibrium stress on the orthogonal projection of a polytopal surface to the plane $\{z = 0\}$. Below we briefly discuss the notation for projecting to any plane.

Let $\mathcal{P} = (u_i)_{1\le i\le n}$ be a polytopal surface with a graph G. Let α be a plane in $\mathbb{R}^3$ with fixed orientation (with a chosen normal vector v), and $\mathcal{P}^v = (u_i^v)_{1\le i\le n}$ be the orthogonal projection of $\mathcal{P}$ to α. Then, the *canonical equilibrium stress* is the assignment of reals $\omega_{ij}^\alpha : E(G) \to \mathbb{R}$ to the edges of G

$$\omega_{ij}^\alpha := \frac{[u_iu_ju_ku_l]}{[\![u_iu_ju_k]\!]_\alpha [\![u_iu_ju_l]\!]_\alpha}, \tag{2.3.9}$$

where as always we use the *square bracket notation* for the oriented volume, and the *double square bracket notation* is for the oriented area of the projection:

$$[\![u_iu_ju_k]\!]_\alpha := [u_i^v u_j^v u_k^v],$$

where the coordinates on α to compute the area are chosen in accordance with the orientation of α and the coordinates in $\mathbb{R}^3$: the ordered set of vectors $\{(1,0)_\alpha, (0,1)_\alpha, v\}$ is a positively oriented orthonormal basis in $\mathbb{R}^3$.

For part (3) of Theorem 2.3.2 we use the following geometrical observation:

Lemma 2.3.11. *Let the vectors u_i, u_j, u_k, u_l define four affinely independent points in $\mathbb{R}^3$. Let ϕ_f and ϕ_g be the polar vectors to the planes f and g spanned by $(u_iu_ju_k)$ and $(u_iu_ju_l)$ correspondingly. We also fix a projection plane α with a unit normal vector v. Then,*

$$\frac{1}{\langle v, \phi_f\rangle\langle v, \phi_g\rangle}\frac{\phi_f \times \phi_g}{u_j - u_i} = \frac{[u_iu_ju_ku_l]}{[\![u_iu_ju_k]\!]_\alpha [\![u_iu_ju_l]\!]_\alpha}. \tag{2.3.10}$$

Proof. We assume that the faces $(u_iu_ju_k)$ and $(u_iu_ju_l)$ are oriented by this order of vertices. Since the left hand side of Eq. (2.3.10) is invariant under rescalings of ϕ_f and ϕ_g, we replace ϕ_f and ϕ_g with positively oriented unit normal vectors to f and g correspondingly.

We show that both sides of Eq. (2.3.10) are equal to

$$\frac{\sin(\phi_f, \phi_g)}{\cos(v, \phi_f)\cos(v, \phi_g)|u_j - u_i|},$$

where $\sin(v_1, v_2)$ and $\cos(v_1, v_2)$ are the sine and cosine of the angle between the two vectors and the angle $\angle(\phi_f, \phi_g)$ is counted counterclockwise around the edge $\overrightarrow{u_ju_i}$.

On the left hand side we use that $\langle v, \phi_f\rangle = |v||\phi_f|\cos(v, \phi_f)$ and that

$$\frac{\phi_f \times \phi_g}{u_j - u_i} = \frac{|\phi_f||\phi_g|\sin(\phi_f, \phi_g)}{|u_j - u_i|}.$$

On the right hand side we use geometrical relations between volumes, areas and distances:

$$\begin{aligned}[u_iu_ju_ku_l] &= \operatorname{dist}(u_l, (u_iu_ju_k))\operatorname{Area}(u_iu_ju_k)\\ &= \big(\operatorname{dist}(u_l, (u_iu_j))\sin(\phi_f, \phi_g)\big)\operatorname{Area}(u_iu_ju_k)\\ &= \left(\frac{\operatorname{Area}(u_iu_ju_l)}{|u_j - u_i|}\right)\sin(\phi_f, \phi_g)\operatorname{Area}(u_iu_ju_k),\end{aligned}$$

where $\operatorname{dist}(u_l, (u_iu_ju_k))$ is the signed distance between u_l and the plane spanned by $(u_iu_ju_k)$; the area $\operatorname{Area}(u_iu_ju_k)$ is positive, since the orientation on the plane $(u_iu_ju_k)$ is set by exactly

this order of the points; and $\operatorname{dist}(u_l, (u_i u_j))$ is the nonsigned, positive distance between u_l and the line through u_i and u_j. Thus,

$$[u_i u_j u_k u_l] = \frac{\operatorname{Area}(u_i u_j u_k)\operatorname{Area}(u_i u_j u_l)\sin(\phi_f, \phi_g)}{|u_j - u_i|}.$$

To finalize the proof we use that

$$\operatorname{Area}(u_i u_j u_k) = \frac{[\![u_i u_j u_k]\!]_\alpha}{\cos(\phi_f, v)},$$
$$\operatorname{Area}(u_i u_j u_l) = \frac{[\![u_i u_j u_l]\!]_\alpha}{\cos(\phi_g, v)}.$$

□

Proof of Theorem 2.3.2, part (3). Lemma 2.3.11 and the reciprocal representation for the canonical braced stress ω^c of Lemma 2.3.9 show that the expressions for the limit of the braced stresses of Eq. (2.3.7) and for the canonical equilibrium stress of Eq. (2.3.9) coincide. □

2.4 Lovász lifting procedure

In the paper on the Colin de Verdière number of graphs of polytopes and Steinitz representations [21] Lovász introduced a procedure that is analogous to the Maxwell–Cremona lifting, but instead of a flat embedding with an equilibrium stress it takes as an input a 3d embedding with a braced stress, and instead of lifting the vertices along the vertical lines, it lifts the vertices along the lines through the origin. The original paper gives this procedure no name, we refer to it as the *Lovász lifting*. In this section we review the Lovász lifting procedure, and use it to give the wheel-decomposition theorem for braced stresses a geometrical meaning. Half of the Lovász lifting algorithm will later be a key instrument in our algorithms for constructing realizations of graphs as convex polytopes.

Cone-convex embeddings. In the Lovász lifting procedure an important role is played by special 3d realizations of graphs that we call *cone-convex*:

Definition 2.4.1. *We call an embedding* $\mathbf{u} = (u_i)_{i\leq 1\leq n}$ *of a planar 3-connected graph* G *to* $\mathbb{R}^3$ *a* cone-convex embedding*, if its projection onto the sphere* $\left(\frac{u_i}{|u_i|}\right)_{1\leq i\leq n}$ *with edges drawn as geodesic arcs is a strictly convex embedding of* G *into the sphere.*

We remark that the embedding of a graph G into the sphere is strictly convex if the faces of the embedding are strictly convex spherical polygons, or, in other words, the faces are the intersections of pointed convex disjoint polyhedral cones with the sphere. So, an embedding is cone-convex if the cones over its faces are pointed, convex and disjoint. Note that the vertices of a cone-convex embedding are not supposed to form a convex polytope.

In the analogy between the Lovász and the Maxwell–Cremona lifting procedures the cone-convex realizations in the construction of Lovász play the same role as the planar (noncrossing) realizations in the Maxwell–Cremona construction.

2.4.1 Lovász dual transform

The following lemma is due to Lovász [21]:

Lemma 2.4.1 (Lemma 4, Lemma 5, [21])**.** *(1) Let* $\mathbf{u} = (u_i)_{1\leq i\leq n}$ *be any embedding of a planar 3-connected graph* G *in* $\mathbb{R}^3$*, let* ω *be a braced stress on* $\mathbf{u}$*. Then there exists a realization* (ϕ_f) *in* $\mathbb{R}^3$ *of the graph* G^* *dual to* G *such that*

$$\phi_g - \phi_f = \omega_{ij}(u_j \times u_i) \tag{2.4.1}$$

for every pair of dual edges (i, j) *of* G *and* (f, g) *of* G^**, this realization is unique up to translations, and any such realization is a realization of* G^* *as a polytopal surface (the vertices of each face are coplanar).*

(2) Moreover, for a cone-convex *realization* $\mathbf{u}$ *and a* positive *braced stress* ω *any* (ϕ_f) *satisfying Eq.* (2.4.1) *is a realization of* G^* *as a* convex polytope*.*

Proof. (1) This is Lemma 4 of [21]. We repeat the proof since it illustrates one of the basic algorithms that we use to construct realizations of graphs as convex polytopes.

To construct the family of vectors (ϕ_f), we start by assigning an arbitrary value to ϕ_{f_0} (for an arbitrary face f_0); then we proceed iteratively picking ϕ vectors such that Eq. (2.4.1) is fulfilled. To prove the consistency of the construction, we show that the differences $(\phi_g - \phi_f)$ sum to zero over every cycle in G^*. Since G as well as G^* is planar and 3-connected, it suffices to check this condition for all elementary cycles of G^*, which are the faces of G^*. Let $\tau(i)$ denote the set of counterclockwise oriented edges of the face in G^* dual to $u_i \in V(G)$. Then,

combining Eq. (2.4.1) and the definition of braced stress yields

$$\sum_{(f,g)\in\tau(i)} (\phi_g - \phi_f) = \sum_{j\in N(i,G)} \omega_{ij}(u_j \times u_i) = \left(\sum_{j\in N(i,G)} \omega_{ij}u_j\right) \times u_i$$
$$= (-\omega_{ii}u_i) \times u_i = 0.$$

The vectors (ϕ_f) are unique up to the initial choice for ϕ_{f_0}.

To show that (ϕ_f) is a polytopal surface, let F be some face of G^*. The graph G^* is dual to G, thus the face F corresponds to some vertex u of G and we can denote $F = F_u$. Let $f_1, \dots f_n$ be the cyclic sequence of faces of G incident to the vertex u, let the edge uu_i separate f_i and f_{i+1}. Then by Eq. (2.4.1)

$$\langle \phi_{f_{i+1}} - \phi_{f_i}, u\rangle = \langle \omega_{uu_i}(u \times u_i), u\rangle = 0,$$

thus, for all the faces f_i incident to the vertex u the dot products $\langle u, \phi_f\rangle$ coincide, so, all the vertices ϕ_f of G^* that belong to the face F_u of G^* lie in the same affine plane orthogonal to the vector u.

(2) This is Lemma 5 of [21]. Lovász formulates this result with an additional constraint $|u_i| = 1$ for all the vertices of G, that is for an embedding of a graph onto the sphere. However, he never uses this constraint in the proof. Additionally he formulates the rescaling property of braced stresses showing why the renormalization of $\mathbf{u}$ doesn't change the result (we have reviewed this property in details in Lemma 2.3.4). □

The construction of Lemma 2.4.1 is a natural reverse to the canonical braced stress construction that we presented in Sect. 2.3.2 and it uses the same defining equation Eq. (2.4.1). The part (2) of Lemma 2.4.1 is the key ingredient of the duality transforms for polytopes that we present in Sect. 2.5.

2.4.2 Lovász lifting procedure: convex case

The following result is the core geometrical argument in [21]:

Theorem 2.4.1 (Theorem 3, [21]). *Let $\mathbf{u} = (u_i)_{1\le i\le n}$ be a cone-convex realization of a planar 3-connected graph G in $\mathbb{R}^3$ and let ω be a positive braced stress on it. Then there exists a positive rescaling $\mathbf{q} = (q_i)_{1\le i\le n}$ of $\mathbf{u}$,*

$$q_i = \lambda_i u_i, \quad \lambda_i \in \mathbb{R}_+ \, \forall 1 \le i \le n,$$

such that $\mathbf{q}$ is a realization of G as a convex polytope.

The Lovász lifting is a "braced" analogue of the Maxwell–Cremona lifting. Indeed, the rescaling property of the braced stresses, Lemma 2.3.4, allows to reformulate the Lovász lifting procedure for the initial embeddings $\mathbf{u}$ of graphs lying in some fixed convex surface, for example, the unit sphere. Then, the Lovász lifting procedure lifts every vertex of a graph from the unit sphere somewhere along the ray through the origin so that the lifting is a convex polytope. While the Maxwell–Cremona lifting lifts every vertex of a graph from the horizontal plane somewhere along the vertical line so that the lifting is a convex polytope. Thus, the Maxwell–Cremona lifting procedure may be geometrically (informally) seen as the Lovász lifting procedure with the origin at the infinity.

Below we sketch the original construction by Lovász. We then also present a slightly different point of view to this construction, which highlights its local nature and the (very strong) analogy with the Maxwell–Cremona lifting.

Proof of Theorem 2.4.1. We follow Lemma 2.4.1 to construct the embedding (ϕ_f) of the dual to G graph G^* such that for every pair of dual edges (u_iu_j) of G and (ϕ_f, ϕ_g) of G^* Eq. (2.4.1) holds:

$$\phi_g - \phi_f = \omega_{ij}(u_j \times u_i).$$

Due to the part (2) of Lemma 2.4.1 the embedding (ϕ_f) of G^* is a convex polytope $\mathcal{P}^*$. The polytope $\mathcal{P}^*$ is unique up to parallel translation, if necessary, we shift $\mathcal{P}^*$ so that it contains the origin in its interior.

Let $P = (r_i)_{1\le i\le n}$ be the polar dual to $\mathcal{P}^*$. Then it is straightforward from the definition of the polar dual that $r_i = \lambda_i u_i$ for some $\lambda_i \in \mathbb{R}_+$. The origin in the interior of $\mathcal{P}^*$ guarantees that these $\lambda_i > 0$. By the construction the graph of P is G, what finishes the proof. □

The last step of taking the polar dual from the previous proof can be seen from a slightly different point of view, which makes the construction a full analogue of Maxwell–Cremona lifting. Moreover, this alternative point of view is easily generalized to any (non cone-convex) 3d embeddings $\mathbf{u}$, to nonpositive braced stresses ω and to abandoning the condition of the origin lying inside $\mathcal{P}^*$.

2.4.3 Lovász lifting procedure: general case

Let $\mathbf{u}$ be any 3d embedding of a planar 3-connected graph G and let ω be any braced stress on $\mathbf{u}$. We mimic the Maxwell–Cremona procedure. For every face f of $\mathbf{u}$ we define an affine plane α_f, to which we lift this face: we define the lifting of the face f as the intersection of the cone over this face with the plane α_f. The details are presented below:

We start as usual and use Lemma 2.4.1 to construct an embedding (ϕ_f) of the graph G^* dual to G as a polytopal surface such that for every pair of dual edges Eq. (2.4.1) holds.

For every face f let α_f be the affine plane, polar to the vector ϕ_f: an affine plane with the normal vector ϕ_f normalized so that $\langle x, \phi_f\rangle = 1$ for every $x \in \alpha_f$. We lift every vertex u_i of the face f to the plane α_f along the ray $\{tu_i : t \in \mathbb{R}\}$ through the origin and u_i:

$$u_i \to q_i^f := \alpha_f \cap \{tu_i : t \in \mathbb{R}\} = \frac{1}{\langle \phi_f, u_i\rangle} u_i. \tag{2.4.2}$$

Eq. (2.4.1) guarantees that if a vertex u_i belongs to both faces f and g, the liftings q_i^f and q_i^g of u_i constructed using the liftings of faces f and g correspondingly coincide: Let $f_1, \dots f_{\deg(u_i)}$ be the cyclic sequence of all the faces incident to u_i, then

$$\langle \phi_{f_l} - \phi_{f_{l+1}}, u_i\rangle = \langle \omega_{ij_l}(u_i \times u_{j_l}), u_i\rangle = 0,$$

where the edge $(u_iu_{j_l})$ is dual to (f_lf_{l+1}), so all of $\langle \phi_{f_l}, u_i\rangle$ for $1 \le l \le \deg(u_i)$ coincide and thus all the $q_i^{f_l}$ coincide as well.

Thus, the vector $q_i := q_i^f$ does not depend on the choice of the face f incident to u_i and so it is well-defined. Thus, the lifting of every vertex is well-defined. By definition, every face of G is lifted to some plane, thus the lifting is a polytopal surface. A simple check shows that if we start with a cone-convex embedding $\mathbf{u}$ and a positive braced stress ω, and if we then pick $\mathcal{P}^*$ with the origin in its interior, the positiveness of the braced stress guarantees convexity on every edge, thus the lifting is a convex polytope.

It is clear that the construction presented above is the original Lovász's proof of Theorem 2.4.1 where the last step of taking the polar dual polytope is replaced by taking the polar dual planes for each of the vertices of the polytope and then studying how these planes intersect. Thus, the two constructions give the same result.

Definition 2.4.2. *We call the embedding* $\mathbf{q}$ *of a graph* G *into* $\mathbb{R}^3$ *constructed above the* Lovász lifting *of* $\mathbf{u}$ *by the braced stress* ω.

The result of the Lovász lifting is not necessarily a convex polytope, but some polytopal surface that is a rescaling $q_i = \lambda_i u_i$ of $\mathbf{u}$. Analogously to the Maxwell–Cremona liftings, we call any such rescaling a *central lifting* and those forming a polytopal surface — a *central polytopal lifting*.

The result of the Lovász lifting is not uniquely defined: In the construction we had the freedom to choose any initial value ϕ_f for one of the faces f. Thus, all the vectors (ϕ_f) are defined up to a parallel translation

$$\phi_f \to \phi_f + \phi, \quad \forall f \in F(G)$$

for any vector $\phi \in \mathbb{R}^3$. This corresponds to the following transformation on the set of central polytopal liftings: two liftings $\mathbf{q}$ and $\mathbf{r}$ of the same embedding $\mathbf{u}$ correspond to the same braced stress if and only if there exists a vector $\phi \in \mathbb{R}^3$ such that

$$\frac{u_i}{q_i} - \frac{u_i}{r_i} = \langle u_i, \phi \rangle$$

for every vertex u_i of G. (The left hand side of the equation above is well-defined since u_i, q_i and r_i are collinear.) The last condition defines an equivalence relation on the set of all the central polytopal liftings of $\mathbf{u}$; and the two Lovász liftings of $\mathbf{u}$ are equivalent if and only if they are produced by the same braced stress ω. We denote the class of equivalence of all the Lovász liftings of $\mathbf{u}$ by the braced stress ω with $L(\mathbf{u}, \omega)$. We call the set of all the central polytopal liftings modulo this equivalence relation the *space of central polytopal liftings* and denote with $L(\mathbf{u})$. Thus, $L(\mathbf{u}, \omega) \in L(\mathbf{u})$ for any braced stress ω on $\mathbf{u}$.

The Lovász lifting procedure is clearly reversible: Let $\mathbf{u}$ be a 3d embedding of a graph G and let $q_i = \lambda_i u_i$ be a rescaling of $\mathbf{u}$ such that $\mathbf{q} = (q_i)$ is a polytopal surface. Then there exists a unique braced stress ω on $\mathbf{u}$ such that $\mathbf{q} \in L(\mathbf{u}, \omega)$. Moreover, this braced stress is the canonical braced stress $\omega^c(\mathbf{q})$ on $\mathbf{q}$ rescaled to $\mathbf{u}$; in the notation of Sect. 2.3

$$\omega = \mathrm{pr}_{q \to u}(\omega^c(\mathbf{q})).$$

In particular, the Lovász lifting of a polytopal surface $\mathbf{u}$ with its canonical braced stress is this polytopal surface itself.

We summarize the remarks above into the following observation:

Lemma 2.4.2. *Let $\mathbf{u} = (u_i)_{1 \le i \le n}$ be any realization of a planar 3-connected graph G in $\mathbb{R}^3$. Then the Lovász lifting procedure is a bijection $L : \mathrm{BR}(\mathbf{u}) \to L(\mathbf{u})$ between the space of braced stresses $\mathrm{BR}(\mathbf{u})$ on $\mathbf{u}$ and the space of polytopal central liftings $L(\mathbf{u})$ of $\mathbf{u}$.*

2.4.4 Geometry of the wheel-decomposition

We are ready to provide a geometrical meaning to the wheel-decomposition theorem for braced stresses, Theorem 2.3.1. In the remainder of the section we suppose that the graph G is a triangulation.

Lemma 2.4.3. *Let $\mathbf{u} = (u_i)_{1 \le i \le n}$ be 3d embedding of a triangulation G with $n > 3$ vertices. Let ω^0 be a braced stress on $\mathbf{u}$ and let $\omega := \omega_0 + \alpha \omega^a(W_k)$ for some $1 \le k \le n$, where $\omega^a(W_k)$ is the atomic braced stress on the wheel $W_k \subset G$ centered at the vertex u_k of G.*

Let f_0 be any face of G that does not contain u_k. Let $\mathbf{q} = (q_i)_{1 \le i \le n} \in L(\mathbf{u}, \omega_0)$ and $\mathbf{r} = (r_i)_{1 \le i \le n} \in L(\mathbf{u}, \omega)$ be two Lovász liftings of $\mathbf{u}$ by stresses ω_0 and ω respectively that coincide on the face f_0. Then

$$\begin{aligned} &q_i = r_i, && i \neq k, \\ &\frac{1}{q_k} - \frac{1}{r_k} = \alpha \frac{1}{u_k}, \end{aligned}$$

where the last equation is an informal equivalent of $\frac{u_k}{q_k} - \frac{u_k}{r_k} = \alpha$ and the left hand side fractions make sense since u_k, q_k and r_k are collinear.

Proof. For the proof we follow the construction of the Lovász lifting step by step. For the liftings $\mathbf{q}$ and $\mathbf{r}$ we denote the vectors ϕ_f and the planes α_f from the lifting procedure with $\phi_f(q), \alpha_f(q)$ and $\phi_f(r), \alpha_f(r)$ correspondingly.

We start with defining vectors $\phi_f(q)$ and $\phi_f(r)$. Since the liftings $\mathbf{q}$ and $\mathbf{r}$ coincide on the face f_0, the vectors $\phi_{f_0}(q)$ and $\phi_{f_0}(r)$ also coincide, $\phi_{f_0}(q) = \phi_{f_0}(r) = \phi_{f_0}$. The vectors $\phi_f(q)$ and $\phi_f(r)$ for other faces of G are computed iteratively using Eq. (2.4.1).

Let f be any face of G that does not contain the vertex u_k. Then $\phi_f(q) = \phi_f(r)$ and thus the lifting planes also coincide $\alpha_f(q) = \alpha_f(r)$. Indeed, the faces incident to u_k form an elementary cycle (boundary of a face) Γ_k in the graph G^* dual to G. Since G and thus G^* are planar 3-connected, there is a path $f_0, f_1, \dots f_m = f$ in the dual graph G^* connecting f_0 with f not passing through Γ_k. We use this path to compute the values $\phi_f(q)$ and $\phi_f(r)$ from $\phi_{f_0}(q)$, $\phi_{f_0}(r)$ and the iterative Eq. (2.4.1). Since the braced stresses ω and ω_0 coincide on edges of G not containing u_k, the right hand sides of Eq. (2.4.1) along the path $f_0, f_1, \dots f_m = f$ coincide for the liftings r and q. Thus

$$\phi_f(q) = \phi_f(r) \quad \forall f : u_k \notin f.$$

Thus, the lifting planes $\alpha_f(q)$ and $\alpha_f(r)$ also coincide for all the faces f not containing u_k.

Since every vertex u_l that is not u_k lies in at least one (in fact, in at least two, but we need only one) face f that does not contain u_k, the liftings of u_l can be defined from the face f as

$$q_l := \alpha_f(q) \cap \{tu_l : t \in \mathbb{R}\},$$
$$r_l := \alpha_f(r) \cap \{tu_l : t \in \mathbb{R}\}.$$

Since the planes $\alpha_f(q)$ and $\alpha_f(r)$ coincide, $q_l = r_l$ for every $l \neq k$.

The last step is to compute the liftings of u_k. Let $g = (u_i u_j u_k)$ be any face adjacent to u_k and $f = (u_j u_i u_l)$ be the other face adjacent to the edge $(u_j u_i)$, thus f does not contain u_k. We assume that g lies to the left and f to the right of $(u_j u_i)$, otherwise we relabel. Then,

$$\phi_g(q) - \phi_f(q) = \omega^0_{ij}(u_j \times u_i),$$
$$\phi_g(r) - \phi_f(r) = \omega_{ij}(u_j \times u_i).$$

Since $\phi_f(q) = \phi_f(r)$,

$$\phi_g(r) - \phi_g(q) = (\omega_{ij} - \omega^0_{ij})(u_j \times u_i).$$

Thus,

$$\begin{aligned}\langle \phi_g(r) - \phi_g(q), u_k \rangle &= (\omega_{ij} - \omega^0_{ij})\langle u_j \times u_i, u_k \rangle \\ &= \omega^a_{ij}(W_k)\langle u_j \times u_i, u_k \rangle \\ &= -\alpha \frac{1}{\det(u_j u_i u_k)} \langle u_j \times u_i, u_k \rangle = -\alpha.\end{aligned}$$

The third transition holds, since we assumed that the face $g = (u_i u_j u_k)$ lies to the left of the edge $(u_j u_i)$, thus the vertex u_j precedes the vertex u_i in the order on vertices of the base cycle of the wheel W_k, thus by the definition of the atomic braced stress $\omega^a_{ij}(W_k) = -\frac{1}{\det(u_j u_i u_k)}$.

By the definition of the Lovász lifting, Eq (2.4.2),

$$q_k = \frac{1}{\langle \phi_g(q), u_k \rangle} u_k,$$
$$r_k = \frac{1}{\langle \phi_g(r), u_k \rangle} u_k.$$

Thus,

$$\frac{u_k}{r_k} - \frac{u_k}{q_k} = \langle \phi_g(r), u_k \rangle - \langle \phi_g(q), u_k \rangle = -\alpha,$$

where the left hand side makes sense since u_k, q_k and r_k are collinear. □

In the remaining of the section we use the fractions $\frac{u}{v}$ for collinear u and v without additionally mentioning it.

Lemma 2.4.4. *Let $\mathbf{q} = (q_i)_{1 \le i \le n} \in L(\mathbf{u}, \omega^q)$ and $\mathbf{r} = (r_i)_{1 \le i \le n} \in L(\mathbf{u}, \omega^r)$ be two Lovász liftings of a 3d embedding $\mathbf{u} = (u_i)_{1 \le i \le n}$ of a triangulation G with $n > 3$ vertices. Then,*

$$\omega^r - \omega^q = \sum_{1 \le i \le n} \left(\frac{u_i}{q_i} - \frac{u_i}{r_i} \right) \omega^a(W_i),$$

where $\omega^a(W_i)$ is the atomic braced stress on the wheel $W_i \subset G$ centered at the vertex u_i of G.

Proof. The proof is in two steps: (1) first we prove the lemma when the liftings differ only at one vertex and (2) then the general case.

(1) First, let $\mathbf{q}$ and $\mathbf{r}$ differ only at one vertex: $q_i = r_i$, $i \neq k$. Then, by Lemma 2.4.3

$$\mathbf{r} \in L \left(\mathbf{u}, \omega^q + \left(\frac{u_k}{q_k} - \frac{u_k}{r_k} \right) \omega^a(W_k) \right).$$

Though, the braced stress is uniquely defined by the lifting, so

$$\omega^r = \omega^q + \left(\frac{u_k}{q_k} - \frac{u_k}{r_k} \right) \omega^a(W_k).$$

(2) Now we move on to the general case. Let

$$\begin{aligned} Q^0 &= (q_1, q_2, q_3, \dots q_n), \\ Q^1 &= (r_1, q_2, q_3, \dots q_n), \\ Q^2 &= (r_1, r_2, q_3, \dots q_n), \\ &\dots \\ Q^n &= (r_1, r_2, r_3, \dots r_n) \end{aligned}$$

be a sequence of liftings such that each two consecutive differ only on one vertex, $Q^0 = \mathbf{q}$ and $Q^n = \mathbf{r}$. Let $\omega^0, \dots, \omega^n$ be the corresponding braced stresses, $Q^k \in L(\mathbf{u}, \omega^k)$.

Then by the first part of the proof,

$$\omega^k - \omega^{k-1} = \left(\frac{u_k}{q_k} - \frac{u_k}{r_k} \right) \omega^a(W_k) \qquad \forall 1 \le k \le n,$$

and to finish the proof we sum up the equations above for $1 \le k \le n$ and note that $\omega^0 = \omega^q$ and $\omega^n = \omega^r$. □

Theorem 2.4.2 (Geometry of the wheel-decomposition)**.** *Let $\mathbf{q} = (q_i)_{1 \le i \le n} \in L(\mathbf{u}, \omega)$ be a Lovász lifting of a 3d embedding $\mathbf{u} = (u_i)_{1 \le i \le n}$ of a triangulation G with $n > 3$ vertices by a braced stress ω. Then,*

$$\omega = \sum_{1 \le i \le n} -\frac{u_i}{q_i} \omega^a(W_i),$$

where $\omega^a(W_i)$ is the atomic braced stress on the wheel $W_i \subset G$ centered at the vertex u_i of G.

Proof. Let $\mathbf{q}(t) = t\mathbf{q}$ for $t \in \mathbb{R}_+$ be a continuous family of rescalings of $\mathbf{q}$, thus $q_i(t) = tq_i$. Let $\phi_f(t) = \frac{1}{t}\phi_f$ be the corresponding polar vectors from the Lovász lifting construction and let $\omega(t)$ be the corresponding braced stresses, $\mathbf{q}(t) \in L(\mathbf{u}, \omega(t))$. Then

$$\phi_g(t) - \phi_f(t) = \omega_{ij}(t)(q_j(t) \times q_i(t))$$

and thus

$$\omega_{ij}(t) = \frac{1}{t^3}\omega_{ij}.$$

By Lemma 2.4.4

$$\omega - \omega(t) = \sum_{1 \le i \le n} \left(\frac{u_i}{q_i(t)} - \frac{u_i}{q_i} \right) \omega^a(W_i).$$

With $t \to \infty$ the left hand side goes to

$$\omega - \omega(t) = \omega - \frac{1}{t^3}\omega \to \omega$$

and the right hand side goes to

$$\sum_{1 \le i \le n} \left(\frac{u_i}{q_i(t)} - \frac{u_i}{q_i} \right) \omega^a(W_i) = \sum_{1 \le i \le n} \left(\frac{u_i}{tq_i} - \frac{u_i}{q_i} \right) \omega^a(W_i) \to \sum_{1 \le i \le n} -\frac{u_i}{q_i}\omega^a(W_i).$$

□

2.4.5 Geometry of the wheel-decomposition: equilibrium stresses

Lemma 2.3.3 allows to restate the wheel-decomposition theorem for braced stresses (Theorem 2.3.1) in terms of equilibrium stresses on braced simplicial polytopes.

Let G be a graph. We call the graph G^+ formed by G with one additional vertex v_0 connected with every vertex of G (no other edge is present) the *bracing of* G and we denote $G^+ = \mathrm{br}(v_0, G)$. In a symbolic notation, G^+ is a join of G and one vertex v_0, $G^+ = G + \{v_0\}$. We call a bracing of a triangulation a *braced triangulation.*

We call a *biwheel* a graph G formed by a cycle $(v_1, \dots v_n)$ and two additional vertices A and B connected to every vertex of the cycle and to each other (no other edge is present, see Fig. 2.4.1). We denote it with $\mathrm{bW}(A, B; v_1, \dots v_n)$. While the wheel is a graph of a pyramid, the biwheel is a graph of a bipyramid. Clearly, a biwheel $\mathrm{bW}(A, B; v_1, \dots v_n)$ is the bracing of the wheel $\mathrm{W}(B; v_1, \dots v_n)$ with the vertex A and simultaneously the bracing of the wheel $\mathrm{W}(A; v_1, \dots v_n)$ with the vertex B.

Giving an order on the cycle $(v_1, \dots v_n)$ and on the apexes A, B, the biwheel $\mathrm{bW}(A, B, (v_1, \dots v_n))$ can be considered oriented. We however do not track orientations of the biwheels and thus also partly omit the discussion of signs of equilibrium stresses on biwheels.

Before we proceed with the wheel-decomposition theorem for braced triangulations, we study equilibrium stresses on biwheels.

Lemma 2.4.5. *Let $U = \mathrm{bW}(A, B; u_1, \dots u_n)$ be a biwheel with apexes A and B embedded in $\mathbb{R}^3$.*

Then the assignment

$$\begin{aligned}
\omega_{i,i+1} &:= -\frac{1}{[Au_iu_{i+1}B]} && 1 \le i \le n, \\
\omega_{i,B} &:= \frac{[Au_{i-1}u_iu_{i+1}]}{[Au_{i-1}u_iB][Au_iu_{i+1}B]} && 1 \le i \le n, \\
\omega_{i,A} &:= \frac{[Bu_{i+1}u_iu_{i-1}]}{[Bu_{i-1}u_iA][Bu_iu_{i+1}A]} && 1 \le i \le n
\end{aligned}$$

defines an equilibrium stress on U and this stress is unique up to rescaling.

We do not define the stress on the edge AB since we do not have a nice closed formula for it and since it can be immediately derived from the other stresses using elementary geometry. Indeed, suppose that the lemma holds and ω is an equilibrium stress. Then for the value ω_{AB}

$$\omega_{AB}(B-A) = -\sum_{1\le i\le n} \omega_{iA}(u_i - A).$$

Thus, to find ω_{AB} we can use the formula

$$\omega_{AB} = -\frac{\sum_{1\le i\le n} \omega_{iA}\langle u_i - A, B - A\rangle}{|B-A|^2}.$$

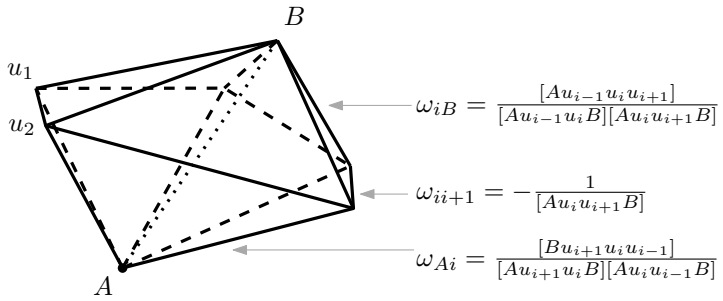

Figure 2.4.1: A biwheel with the atomic equilibrium stress.

Proof of Lemma 2.4.5. Let $\mathrm{bW}^a = \mathrm{bW} - A$ be the parallel translation of the biwheel such that one of its apexes, A, coincides with the origin.

By Lemma 2.3.3 the equilibrium stresses on the translated biwheel bW^a are in 1-to-1 correspondence with the braced stresses on a (translated) wheel $\mathrm{W}^a(B; u_1, \dots u_n)$, obtained from the biwheel bW^a by removing the apex A. The braced stress on a wheel is unique up to rescaling, what proves the uniqueness.

To compute the braced stress on the wheel $\mathrm{W}^a(B; u_1, \dots u_n)$ we use the atomic braced stress $b\omega^a$ on the wheel, Eq. (2.3.5):

$$b\omega^a_{i,i+1} := -\frac{1}{\det(u^a_i u^a_{i+1} B^a)} \qquad 1 \le i \le n,$$

$$b\omega^a_{iB} := \frac{\det(u^a_{i-1} u^a_i u^a_{i+1})}{\det(u^a_{i-1} u^a_i B^a)\det(u^a_i u^a_{i+1} B^a)} \qquad 1 \le i \le n,$$

where we denote with $u^a_i := u_i - A$, $B^a := B - A$ and $A^a := A - A = (0,0,0)^T$ the translated vertices of the initial biwheel.

Though, for any three vectors u, v, w, $\det(u,v,w) = \mathrm{Vol}((0,0,0)^T, u, v, w)$ and since $A^a = (0,0,0)^T$ we rewrite the formulas in terms of $\mathrm{Vol}(A^a, u^a_i, u^a_j, u^a_k)$. The volumes are translational invariant, so we omit superscripts.

Finally, we use Lemma 2.3.3 to go from the braced stress on the wheel to the equilibrium stress ω^0 on the biwheel bW^0. The transition map is identical on edges (Bi) and $(i, i+1)$ thus we get:

$$\omega^a_{i,i+1} = -\frac{1}{[Au_iu_{i+1}B]},$$

$$\omega^a_{iB} = \frac{[Au_{i-1}u_iu_{i+1}]}{[Au_{i-1}u_iB][Au_iu_{i+1}B]}.$$

We do not compute stress ω^a for edges (Ai) and (AB) since these computations are involved and require computing of additional coefficients $b\omega^a_{ii}$ which we omitted. Instead, we consider a second parallel translation of the initial biwheel $\mathrm{bW}^b = \mathrm{bW} - B$ such that this time the other apex B is at the origin.

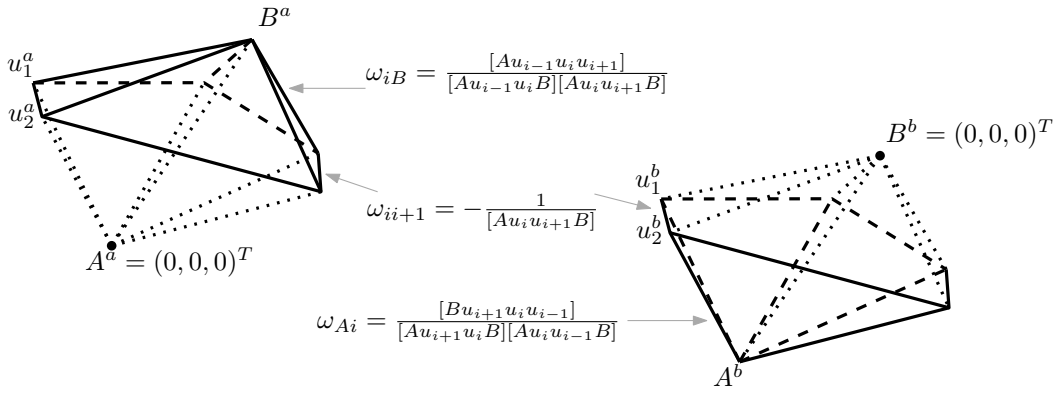

Figure 2.4.2: Two translations of the biwheel with the stresses computed from each of them.

Again by Lemma 2.3.3 the equilibrium stresses on the biwheel are in 1-to-1 correspondence with the braced stresses on the wheel $W(A; u_n, \dots u_1)$ (for convenience in this wheel we reoriented the cycle $u_1, \dots u_n$). We compute the atomic braced stress on the wheel $W(A; u_n, \dots u_1)$ as we did for the wheel $W(B; u_1, \dots u_n)$ and use Lemma 2.3.3 to transform it into an equilibrium stress ω^b on the whole biwheel bW^b. Again we compute only the easily computable edges (Ai) and $(i, i+1)$:

$$\omega^b_{i,i+1} = -\frac{1}{[Bu_{i+1}u_iA]},$$
$$\omega^b_{Ai} = \frac{[Bu_{i+1}u_iu_{i-1}]}{[Bu_{i+1}u_iA][Bu_iu_{i-1}A]}.$$

The notion of equilibrium stress is translational invariant thus both equilibrium stresses ω^a and ω^b are equilibrium stresses on the initial biwheel bW. Though, as the computation showed, the stresses ω^a and ω^b coincide on the edges $(i, i+1)$ of the biwheel. Moreover, as we already discussed, the space of equilibrium stresses on the biwheel is 1-dimensional. Thus, the stresses ω^a and ω^b are equal and we denote them simply as $\omega = \omega^a = \omega^b$. □

Let $G = (u_i)_{1 \le i \le n}$ be a triangulation of the plane with $n > 3$ vertices. Then, as we already discussed in the wheel-decomposition theorem, the edges and faces of G incident to any vertex u_i of G form a wheel, that we denote $\mathrm{W}_i(G)$. When we brace a triangulation G with a vertex A, we automatically brace every wheel $\mathrm{W}_i(G)$, thus every wheel $\mathrm{W}_i(G)$ turns into a biwheel that we denote with $\mathrm{bW}_i(G)$.

Translated by Lemma 2.3.3 to the language of equilibrium stresses on braced graphs, the wheel-decomposition theorem states that every equilibrium stress on a braced triangulation is a linear combination of stresses on biwheels:

Theorem 2.4.3. *Let $U^+ = \mathrm{br}(A, (u_i)_{1 \le i \le n})$ be an embedding of a braced triangulation $G^+ = \mathrm{br}(A; G)$ into $\mathbb{R}^3$, where G is a planar triangulation with n vertices. Then every equilibrium stress ω on U^+ is a linear combination of atomic equilibrium stresses on the biwheels bW^i for*

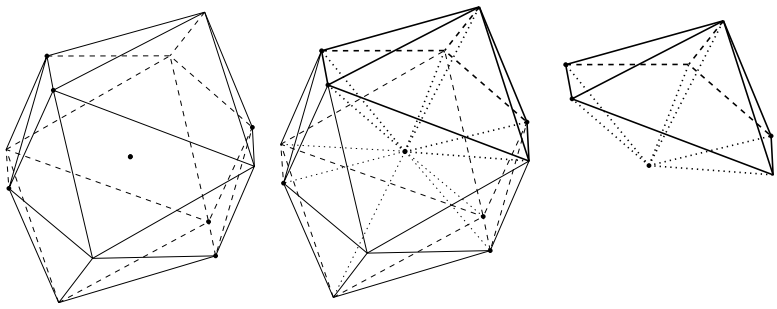

Figure 2.4.3: Covering a braced triangulation with biwheels: a triangulation (left), a braced triangulation (center) and one biwheel of this braced triangulation (right).

$1 \leq i \leq n$:

$$\omega = \sum_{1 \leq i \leq n} \alpha_i \omega^a(\mathrm{bW}^i).$$

The decomposition is unique up to an automorphism of the set of coefficients

$$\alpha_i \to \alpha_i + \langle u_i, v \rangle$$

for any vector v in $\mathbb{R}^3$.

Proof. This is an immediate consequence of the wheel-decomposition theorem for braced stresses Theorem 2.3.1 and Lemma 2.3.3. □

2.5 Duality transforms

In this section we use the techniques developed above to efficiently construct the duals of convex polytopes.

2.5.1 High level description

Our duality transform algorithms are based on the Lovász duality transformation that we introduced in Lemma 2.4.1. In the theorem below we sum up the results of Lemma 2.4.1 in a form that we use for duality transforms together with the estimates on the size of the integer grid required by the algorithm:

Theorem 2.5.1 (Lovász duality construction)**.** *Let G be a planar 3-connected graph, let $\mathbf{u} = (u_i)_{1\le i\le n}$ be its cone-convex embedding with integer coordinates and let ω be an integer positive braced stress on $\mathbf{u}$. Then there exists a realization $(\phi_f)_{f\in F(G)}$ of the dual graph G^* as a convex polytope with integer coordinates bounded by*

$$|\phi_f| < 2n \cdot \max_{(i,j)\in E(G)} |\omega_{ij}(u_j \times u_i)|.$$

Proof. We use Lemma 2.4.1 to construct $(\phi_f)_{f\in F(G)}$ that satisfy Eq. (2.4.1) and such that $\phi_{f_0} = (0,0,0)^T$ for a distinguished face $f_0 \in F(G)$. The part (2) of Lemma 2.4.1 guaranties that $(\phi_f)_{f\in F(G)}$ form a convex polytope with graph G^*. Since (ϕ_f) satisfy Eq. (2.4.1), $\phi_{f_0} = (0,0,0)^T$ and all ω_{ij} as well as all u_i are integral, all ϕ_f have integer coordinates as well.

To finish the proof we estimate how large the vectors (ϕ_f) are. We evaluate ϕ_{f_k} for some face $f_k \in F(G)$. The following algebraic expression holds for all values ϕ_{f_i}:

$$\phi_{f_k} = \phi_{f_0} + (\phi_{f_1} - \phi_{f_0}) + \ldots + (\phi_{f_{k-1}} - \phi_{f_{k-2}}) + (\phi_{f_k} - \phi_{f_{k-1}}).$$

Let us now consider the shortest path $f_0, f_1, \ldots, f_k$ in G^* connecting the faces f_0 and f_k. Clearly, k is less than $2n$, and hence

$$|\phi_{f_k}| \le 2n \cdot \max_{(f_a,f_b)\in E(G^*)} |\phi_{f_a} - \phi_{f_b}| = 2n \cdot \max_{(i,j)\in E(G)} |\omega_{ij}(u_i \times u_j)|.$$

□

Then, all our duality algorithms follow the same two-stage approach:

- Construct a cone-convex embedding of a graph G^* dual to G with a positive braced stress ω;
- Apply the construction from Theorem 2.5.1.

In this section we present a duality transform for three types of polytopes: stacked polytopes, simplicial polytopes with a degree 3 vertex and special geometry, and general simplicial polytopes.

The second stage of the algorithms for all types of polytopes is the same and is described in Theorem 2.5.1. The first stages of the algorithms for different types of polytopes differ a lot. Thus in the remainder of this section we describe the different first stages of the algorithms for the different types of polytopes: we present three different approaches to constructing small integer cone-convex realizations of graphs with small positive integer braced stresses.

2.5.2 The stacking approach

Here we present an approach for constructing 3d cone-convex embeddings with braced stresses out of 2d planar realizations with equilibrium stress by stacking an additional vertex (tetrahedron) to the graph. This approach leads to the embedding algorithm for truncated polytopes, and for a special class of simple polytopes with a degree 3 vertex, however proves to be inefficient for general simple polytopes.

Let G be a planar graph with a triangular face f. We say that the graph G^+ is build by *stacking* a vertex u atop a face f of G and we denote with $G^+ = \mathrm{Stack}(G, f, u)$ if the graph G^+ is formed by the graph G with one additional vertex u which is connected by edges to the three corners of the face f. Clearly, the graph $\mathrm{Stack}(G, f, u)$ is planar, and for a 3-connected graph G the result of stacking operation is again 3-connected.

Lemma 2.5.1. *Let $\mathbf{p}^\uparrow = (p_i)_{2\le i\le n}$ be a 2d integer planar convex embedding of a planar 3-connected graph $G^\uparrow$ with a designated triangular face $f = (p_2p_3p_4)$ embedded as the boundary face. Let ω be a positive integer equilibrium stress for $\mathbf{p}^\uparrow$.*

Then the embedding $\mathbf{u} = (u_i)_{1\le i\le n}$ of the graph $G = \mathrm{Stack}(G^\uparrow, (v_2v_3v_4), v_1)$ defined as

$$\begin{aligned} u_i &= (3p_i - (p_2 + p_3 + p_4), 1)^T \quad 2 \le i \le n,\\ u_1 &= (0, 0, -3)^T, \end{aligned}$$

where $(p, 1)^T = (p_x, p_y, 1)^T \in \mathbb{R}^3$ for $p = (p_x, p_y) \in \mathbb{R}^2$, is an integral cone-convex embedding and there exists a positive integer braced stress $b\omega$ for $\mathbf{u}$ such that

$$\begin{aligned} &b\omega_{ij} = \omega_{ij} \quad \text{for each internal edge } (i,j) \text{ of the original embedding of } G^\uparrow,\\ &|b\omega_{ij}| \le \max_{(i,j)\in E(G^\uparrow)} |\omega_{ij}| + 1 \qquad \forall (i,j) \in E(G). \end{aligned}$$

Proof. The embedding $\mathbf{u}$ can be described as follows: The planar embedding $\mathbf{p}^\uparrow$ of $G^\uparrow$ is realized in the plane $\{z = 1\}$, scaled 3 times, and translated so that the barycenter of the boundary face coincides with the origin. The stacked vertex u_1 is then placed at $(0, 0, -3)^T$. The embedding is cone-convex since it describes a tetrahedron containing the origin with one face that is refined with a plane convex subdivision.

Following the structure of $G = \mathrm{Stack}(G^\uparrow, (v_2v_3v_4), v_1)$, we decompose G into two subgraphs: $G^\uparrow = G[\{v_2, \ldots, v_n\}]$ and $G^\downarrow := G[\{v_1, v_2, v_3, v_4\}]$.

We first compute a braced stress $b\omega'$ for the embedding $\mathbf{u}^\uparrow = (u_i)_{2\le i\le n}$ of $G^\uparrow$. The plane embedding $\mathbf{p}^\uparrow$ of $G^\uparrow$ has an integer equilibrium stress ω. Since $\mathbf{u}^\uparrow$ is just a rescaling and translation of $\mathbf{p}^\uparrow$, clearly, ω is also an equilibrium stress for $\mathbf{u}^\uparrow$ and thus it is a braced stress for this embedding.

As a second step we compute a braced stress $b\omega''$ for the embedding (u_1, u_2, u_3, u_4) of the tetrahedron $G^\downarrow$. By the construction, $u_1 + u_2 + u_3 + u_4 = 0$. Thus, the matrix

$$b\omega'' := \begin{pmatrix} 1 & 1 & 1 & 1\\ 1 & 1 & 1 & 1\\ 1 & 1 & 1 & 1\\ 1 & 1 & 1 & 1 \end{pmatrix}$$

is a braced stress matrix for the embedding (u_1, u_2, u_3, u_4) of $G^\downarrow$.

In the final step we extend the two braced stresses $b\omega'$ and $b\omega''$ to G and combine them. Clearly, a braced stress on a subgraph is a braced stress on the whole graph. Furthermore, braced stresses form a linear space and thus any linear combination of braced stresses is again a braced stress. Thus, we form an integer braced stress for the whole embedding $\mathbf{u}$ of G by setting:

$$b\omega := b\omega' + \lambda b\omega'',$$

where λ is a positive integer chosen so that $b\omega$ is a positive braced stress. This can be done as follows. Recall that ω is a positive equilibrium stress and $b\omega''$ is a positive braced stress. Hence, the only three entries in $b\omega$ that may be negative are: $b\omega_{23}$, $b\omega_{34}$ and $b\omega_{42}$, for which $b\omega_{ij} := b\omega'_{ij} + \lambda b\omega''_{ij}$ with $b\omega'_{ij} = \omega_{ij} < 0$ and $b\omega''_{ij} = 1$. Thus, we choose λ such that $b\omega$ is positive at these entries. To satisfy this condition we pick

$$\lambda := \max_{(i,j)\in\{(2,3),(3,4),(4,2)\}} |b\omega'_{ij}| + 1.$$

The bound $|b\omega_{ij}| \leq \max_{(k,l)\in E(G^\uparrow)} |\omega_{kl}| + 1$ for every edge (i,j) of G trivially follows. □

Combining Lemma 2.5.1 and the Lovász duality transform, Theorem 2.5.1, leads to

Theorem 2.5.2. *Let $G = \mathrm{Stack}(G^\uparrow; v_1; v_2v_3v_4)$ and let $\mathbf{p}^\uparrow = (p_i)_{2\leq i\leq n}$ be a planar 2d embedding of $G^\uparrow$ with integer coordinates, boundary face $(v_2v_3v_4)$, and a positive integer equilibrium stress ω. Then there exists a realization $(\phi_f)_{f\in F(G^*)}$ of the graph G^*, dual to G, as a convex polytope with integer coordinates such that*

$$|\phi_f| = O(n \cdot \max|\omega_{ij}| \cdot \max|p_i|^2).$$

Proof. We first apply Lemma 2.5.1 to obtain a cone-convex embedding $\mathbf{u} = (u_i)_{1\leq i\leq n}$ of G with integer coordinates and a positive integral braced stress ω. We then apply Theorem 2.5.1 and obtain a family of vectors $(\phi_f)_{f\in F(G^*)}$ that forms a desired realization of G^* as a convex polytope with integer coordinates.

To estimate how large the coordinates of the embedding (ϕ_f) are, we combine bounds for (ϕ_f) given by Theorem 2.5.1 with the bounds for the entries of ω given by Lemma 2.5.1:

$$\begin{aligned}|\phi_f| \leq 2n \cdot \max_{(i,j)\in E(G)} |\omega_{ij}(u_j \times u_i)| &\leq 2n \cdot (\max|\omega_{ij}| + 1) \cdot \max|u_i|^2 \\ &= O(n \cdot \max|\omega_{ij}| \cdot \max|p_i|^2).\end{aligned}$$

□

Realizations of Truncated Polytopes

The framework presented in Theorem 2.5.2 can now be used to construct an integer polynomial size grid embedding for truncated polytopes.

We remind, that given a convex polytope $\mathcal{P}$ with a triangular face f the operation of *stacking* a vertex u atop the face f glues to $\mathcal{P}$ atop the face f a triangular pyramid with base f and apex u so that the resulting polytope is convex again. This operation is the polytope language translation of stacking a vertex to a graph. We call a polytope *stacked polytope* if it can be produced from a tetrahedron by a sequence of stacking operations. The graphs of stacked polytopes are planar 3-trees.

The *truncated polytopes* are dual to stacked. Another description is possible through the truncation operation. A *truncation operation* cuts off a vertex of a polytope by intersecting the polytope with a half space bounded by a plane that separates this vertex from all the other vertices of the polytope. The truncation operation is clearly dual to stacking. Thus, *truncated polytopes* are those that can be produced from a tetrahedron by a series of truncation operations.

We realize truncated polytopes as dual to stacked polytopes using the framework of Theorem 2.5.2. To construct an input for the framework of Theorem 2.5.2 we use a result by Demaine and Schulz [9]:

Lemma 2.5.2. *Any graph of a stacked polytope with n vertices and any distinguished face f_0 can be embedded on a $O(n^{2\lg 6}) \times O(n^{2\lg 6})$ grid with boundary face f_0 and with integral positive equilibrium stress ω such that, for every edge (i,j), we have $|\omega_{ij}| = O(n^{5\lg 6})$.*

Proof. This lemma is not explicitly stated in [9] but it is a by-product of the presented constructions. In particular, the estimates for the coordinate size are stated there in Theorem 1 and the integer stresses are defined there by Lemma 9.

Recently, a flaw was discovered in [9], which affected the estimates. The flaw was within the balancing procedure, Sect. 3.1 of [9]. It was corrected in the latest version of the paper [10, Lemma 7].

The fix affected the estimate of Eq. (3.3) in [9] and the numbers in the following computations (but not the arguments). Since we need the corrected computations for the bounds of this lemma we report briefly the necessary changes using the exact notations of the original paper. The updated bound of Eq. (3.3) is $w(f_0) \leq n^{\lg 6}$ [10, Lemma 7] instead of n^2. We denote this bound with R. To correct the values in Sect. 3.3 we replace in the computations n with $\sqrt{R} = n^{(\lg 6)/2}$. In particular, in Subsect. 3.3.1 the (preliminary) boundary face is now given by $\mathbf{p}_1 = (0,0), \mathbf{p}_2 = (\sqrt{R}, 0), \mathbf{p}_3 = (0, \sqrt{R})$. In Subsect. 3.3.2 the (final) boundary face is now given by $\mathbf{p}_1 = (0,0), \mathbf{p}_2 = (10R^2, 0), \mathbf{p}_3 = (0, 10R^2)$; and the corrected scaling factor for the stress is $Y = 4R$. The lemma follows by taking the updated values from [9]. □

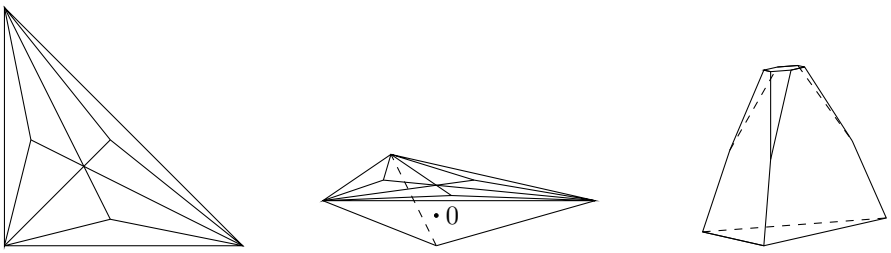

Figure 2.5.1: The 2d embedding of $G_\uparrow$ (a), the cone-convex embedding of G (b), and the resulting embedding of the dual (c).

Theorem 2.5.3. *Any truncated 3d polytope with n vertices can be realized with integer coordinates of size* $O(n^{9 \lg 6+1})$.

Proof. Let G^* be the graph of the truncated polytope and let $G := (G^*)^*$ be its dual. Clearly, G is the graph of a stacked polytope with $(n+4)/2$ vertices. We denote the last stacking operation (for some sequence of stacking operations producing G) as the stacking of the vertex v_1 onto the face $(v_2 v_3 v_4)$ of the graph $G^\uparrow := G[V \setminus \{v_1\}]$. The graph $G^\uparrow$ is again a graph of a stacked polytope, and hence, by Lemma 2.5.2, there exists an embedding $(p_i)_{2 \leq i \leq n}$ of $G^\uparrow$ into $\mathbb{Z}^2$ with an equilibrium stress ω satisfying the properties of Theorem 2.5.2. We apply Theorem 2.5.2 and obtain a polytope embedding (ϕ_f) of G^* with bound

$$|\phi_f| = O(n \cdot \max |\omega_{ij}| \cdot \max |p_i|^2) = O(n^{9 \lg 6+1}).$$

□

Fig. 2.5.1 shows an example of our algorithm. The computations for this example are presented below.

Example of the algorithm for truncated polytopes

As an example for our embedding algorithm for truncated polytopes we show how to embed the *truncated tetrahedron*. This polytope is obtained from the tetrahedron by truncating all of its four vertices. The graph G^* of this polytope and its dual G are depicted in Fig. 2.5.1. We start with the planar embedding of $G^\uparrow = G[v_2, \ldots, v_8]$ that is defined on Fig. 2.5.2.

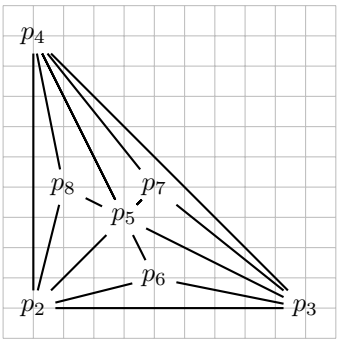

$p_2 = (-3, -3)^T$
$p_3 = (6, -3)^T$
$p_4 = (-3, 6)^T$
$p_5 = (0, 0)^T$
$p_6 = (1, -2)^T$
$p_7 = (1, 1)^T$
$p_8 = (-2, 1)^T$

Figure 2.5.2: The original plane embedding of $G^{\uparrow}$.

The embedding has the integer equilibrium stress $\omega_{52} = \omega_{53} = \omega_{54} = 1$, $\omega_{23} = \omega_{34} = \omega_{42} = -2$, and all the other entries have value 3.

Following Lemma 2.5.1, we embed the drawing of $G^{\uparrow}$ onto the plane $\{z = 1\}$. Unlike the general case of Lemma 2.5.1, we do not have to scale 3 times and translate, since the barycenter of p_2, p_3, p_4 is initially at the origin. We add the stacked point $u_1 := (0, 0, -3)^T$.

The corresponding braced stresses $[b\omega''_{ij}]_{1 \le ij \le 4}$ and $[b\omega'_{ij}]_{2 \le ij \le 8}$ (in the braced stress matrix form) are:

$$b\omega'' = \begin{pmatrix} 1 & 1 & 1 & 1 \\ 1 & 1 & 1 & 1 \\ 1 & 1 & 1 & 1 \\ 1 & 1 & 1 & 1 \end{pmatrix}, \quad b\omega' = \begin{pmatrix} -3 & -2 & -2 & 1 & 3 & 0 & 3 \\ -2 & -3 & -2 & 1 & 3 & 3 & 0 \\ -2 & -2 & -3 & 1 & 0 & 3 & 3 \\ 1 & 1 & 1 & -12 & 3 & 3 & 3 \\ 3 & 3 & 0 & 3 & -9 & 0 & 0 \\ 0 & 3 & 3 & 3 & 0 & -9 & 0 \\ 3 & 0 & 3 & 3 & 0 & 0 & -9 \end{pmatrix}. \tag{2.5.1}$$

We extend $b\omega'$ and $b\omega''$ to the whole graph G and form the final braced stress $b\omega = b\omega' + 3b\omega''$:

$$b\omega = \begin{pmatrix} 3 & 3 & 3 & 3 & 0 & 0 & 0 & 0 \\ 3 & 0 & 1 & 1 & 1 & 3 & 0 & 3 \\ 3 & 1 & 0 & 1 & 1 & 3 & 3 & 0 \\ 3 & 1 & 1 & 0 & 1 & 0 & 3 & 3 \\ 0 & 1 & 1 & 1 & -12 & 3 & 3 & 3 \\ 0 & 3 & 3 & 0 & 3 & -9 & 0 & 0 \\ 0 & 0 & 3 & 3 & 3 & 0 & -9 & 0 \\ 0 & 3 & 0 & 3 & 3 & 0 & 0 & -9 \end{pmatrix}.$$

We can now apply Theorem 2.5.1 and compute the vectors (ϕ_f). We first assign $\phi_{(236)} = (0, -18, 27)^T$. (One can start with assigning of any vector to any face — the resulting embedding will be the same up to translation. This assignment makes the resulting coordinates look slightly nicer.) The remaining vectors are then iteratively computed with Eq. (2.4.1). We

obtain as a result:

$$
\begin{aligned}
\phi_{(265)} - \phi_{(236)} &= M_{26}(u_2 \times u_6) = (-3, 12, 27)^T & \phi_{(236)} &= (0, -18, 27)^T \\
\phi_{(258)} - \phi_{(265)} &= M_{25}(u_2 \times u_5) = (-3, 3, 0)^T & \phi_{(265)} &= (-3, -6, 54)^T \\
\phi_{(284)} - \phi_{(258)} &= M_{28}(u_2 \times u_8) = (-12, 3, -27)^T & \phi_{(258)} &= (-6, -3, 54)^T \\
\phi_{(485)} - \phi_{(284)} &= M_{48}(u_4 \times u_8) = (15, 3, 27)^T & \phi_{(284)} &= (-18, 0, 27)^T \\
\phi_{(457)} - \phi_{(485)} &= M_{45}(u_4 \times u_5) = (6, 3, 0)^T & \phi_{(485)} &= (-3, 3, 54)^T \\
\phi_{(473)} - \phi_{(457)} &= M_{47}(u_4 \times u_7) = (15, 12, -27)^T & \phi_{(457)} &= (3, 6, 54)^T \\
\phi_{(375)} - \phi_{(473)} &= M_{37}(u_3 \times u_7) = (-12, -15, 27)^T & \phi_{(473)} &= (18, 18, 27)^T \\
\phi_{(356)} - \phi_{(375)} &= M_{35}(u_3 \times u_5) = (-3, -6, 0)^T & \phi_{(375)} &= (6, 3, 54)^T \\
\phi_{(362)} - \phi_{(356)} &= M_{36}(u_3 \times u_6) = (-3, -15, -27)^T & \phi_{(356)} &= (3, -3, 54)^T \\
\phi_{(321)} - \phi_{(362)} &= M_{32}(u_3 \times u_2) = (0, -9, -27)^T & \phi_{(362)} &= (0, -18, 27)^T \\
\phi_{(124)} - \phi_{(321)} &= M_{12}(u_1 \times u_2) = (-27, 27, 0)^T & \phi_{(321)} &= (0, -27, 0)^T \\
\phi_{(143)} - \phi_{(124)} &= M_{14}(u_1 \times u_4) = (54, 27, 0)^T & \phi_{(124)} &= (-27, 0, 0)^T \\
& & \phi_{(143)} &= (27, 27, 0)^T.
\end{aligned}
$$

The final result is depicted in Fig. 2.5.3. The embedding requires a $54 \times 54 \times 54$ grid.

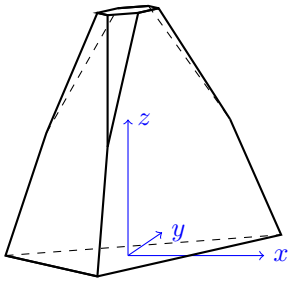

Figure 2.5.3: The final embedding of the truncated tetrahedron.

A duality transform for simplicial polytopes with degree-3 vertex

As an immediate consequence of the framework of Theorem 2.5.2 and of the efficient reverse of the Maxwell–Cremona lifting, Theorem 2.2.2, we state the following result:

Theorem 2.5.4. *Let $G^\uparrow$ be a triangulation and let $\mathbf{u}^\uparrow = (u_i)_{2 \le i \le n}$ be its realization as a convex polytope with integer coordinates, such that its orthogonal projection into the plane $\{z = 0\}$ is a planar embedding $\mathbf{p}^\uparrow = (p_i)_{2 \le i \le n}$ of $G^\uparrow$ with boundary face $(v_2 v_3 v_4)$. Then the exists a realization $(\phi_f)_{f \in F(G)}$ of a graph dual to $G = \mathrm{Stack}(G^\uparrow; v_1; v_2 v_3 v_4)$ with integer coordinates bounded by*

$$|\phi_f| = O(n \max |u_i|^{2\,\Delta_G + 7}).$$

Proof. By combining Theorem 2.5.2 with Theorem 2.2.2 we obtain the statement of the theorem. □

We remark that the algorithms following the lifting approach, e.g. [30], generate embeddings that fulfill the geometrical conditions of the above theorem. Although the theorem proved above can be seen as a special case of a more general Theorem 2.5.6, the bounds for this special case are better. The approach that led to the theorem above can be modified for

general simplicial polytopes without restrictions on the geometry and without a degree-3 vertex. However, such a modification requires a substantial amount of technicalities and leads to worse estimates than the 3-dimensional techniques developed in the next subsection.

2.5.3 A duality transform for general simplicial polytopes

The last type of 3-dimensional polytopes for which we present the duality transform are simplicial polytopes. As usual, the duality transform goes in two stages described in Subsec. 2.5.1. In the second stage we apply as usual the Lovász duality transform, Theorem 2.5.1.

The first stage for this class of polytopes is however completely different from the stacking approach discussed above. Unlike the algorithms of stacking approach, the algorithm of this section is intrinsically 3-dimensional and use neither planar (flat) embeddings in intermediate steps, nor 2-dimensional equilibrium stresses. Instead, it operates directly with braced stresses and uses the techniques developed in Sect. 2.3 with the main tool being the wheel-decomposition theorem for braced stresses, Theorem 2.3.1.

The main content of this subsection is the following theorem, which is the first stage of the duality transform scheme presented in Sect. 2.5.1:

Theorem 2.5.5. *Let $\mathcal{P} = (u_i)_{1\le i\le n}$ be a convex simplicial polytope in $\mathbb{R}^3$ with integer coordinates, containing the origin in its interior. Then there exists an integral positive braced stress ω on $\mathcal{P}$ such that its entries are bounded by*

$$|\omega_{ij}| = O(\max_{1\le i\le n} |u_i|^{3\,\Delta_{\mathrm{G}}+7})$$

where Δ_{G} is the maximal vertex degree of the graph G of $\mathcal{P}$.

Proof. The proof goes through 3 steps:

(I) We construct as ω^c the canonical braced stress for $\mathcal{P}$ and bound its entries;

(II) We use the wheel-decomposition theorem to decompose $\omega^c = \sum_{1\le k\le n} \alpha_k \omega^a(W_k)$ and bound the entries of atomic braced stresses;

(III) We define the final braced stress $\omega := \sum_{1\le k\le n} \lfloor C\alpha_k \rfloor \omega^a(W_k)$ with $C = 4\frac{\max(\omega^a(W_k))}{\min(\omega^c)}$ and check its correctness.

Throughout the proof we set $L := \max_{ij} |u_i - u_j|$.
Step (I): Let ω^c be the canonical braced stress for $\mathcal{P}$:

$$\phi_g - \phi_f = \omega^c_{ij}(u_j \times u_i)$$

for every pair of dual edges (u_iu_j) and $(\phi_f\phi_g)$. On the next steps we need to bound $|\omega^c_{ij}|$. Obviously,

$$\frac{\max|\phi_g - \phi_f|}{\min|u_j \times u_i|} \ge |\omega^c_{ij}| \ge \frac{\min|\phi_g - \phi_f|}{\max|u_j \times u_i|}.$$

To bound $|\omega^c_{ij}|$ further we need a lower bound for $|\phi_g - \phi_f|$ (estimate a) and an upper bound for $|\phi_f|$ (estimate b).

(estimate a) We remark that ϕ_f is the solution of the linear system

$$\langle \phi_f, u^f_1\rangle = 1, \langle \phi_f, u^f_2\rangle = 1, \langle \phi_f, u^f_3\rangle = 1,$$

where the vertices $u^f_1u^f_2u^f_3$ belong to the face f. Thus, since u_i are integral,

$$\phi_f = \frac{1}{\det(u^f_1u^f_2u^f_3)} Z_3$$

for Z_3 being some vector in $\mathbb{Z}^3$. Similarly,

$$\phi_g = \frac{1}{\det(u_1^g u_2^g u_3^g)} Z_3'.$$

Again, Z_3' is some vector in $\mathbb{Z}^3$. Thus, going to the common denominator,

$$|\phi_g - \phi_f| = \frac{1}{\det(u_1^f u_2^f u_3^f)\det(u_1^g u_2^g u_3^g)} Z_3''$$

for some third Z_3'' in $\mathbb{Z}^3$. So, since $\phi_f \neq \phi_g$,

$$|\phi_g - \phi_f| \geq \frac{1}{\det(u_1^f u_2^f u_3^f)\det(u_1^g u_2^g u_3^g)} \geq \frac{1}{L^6}. \tag{2.5.2}$$

(estimate b) To bound $|\phi_f|$ from above we consider the pyramid over the face $f = (u_1^f u_2^f u_3^f)$ with the tip at $\mathbf{0} = (0,0,0)^T$. Its (nonoriented) volume $\mathrm{Vol}(\mathbf{0}, u_1^f, u_2^f, u_3^f)$ can be computed as

$$h_f \,\mathrm{Area}(u_1^f, u_2^f, u_3^f) \;= \mathrm{Vol}(\mathbf{0}, u_1^f, u_2^f, u_3^f),$$

where h_f is the height to the base f. Since all u_is are integral, $\mathrm{Vol}(\mathbf{0}, u_1^f, u_2^f, u_3^f) \geq 1$. Trivially, $\mathrm{Area}(u_1^f u_2^f u_3^f) \leq L^2$. Since ϕ_f is the polar vector for the plane supporting the face f, and $|h_f|$ is the distance from the origin to this plane, $|h_f| = \frac{1}{|\phi_f|}$. Thus,

$$|\phi_f| \leq \frac{\mathrm{Area}(u_1^f, u_2^f, u_3^f)}{\mathrm{Vol}(\mathbf{0}, u_1^f, u_2^f, u_3^f)} \leq L^2. \tag{2.5.3}$$

Using the two bounds of Eq. (2.5.2) and Eq. (2.5.3) gives:

$$|\omega_{ij}^c| \geq \frac{\min|\phi_g - \phi_f|}{\max|u_j \times u_i|} \geq \frac{1/L^6}{L^2} = \frac{1}{L^8},$$
$$|\omega_{ij}^c| \leq \frac{\max|\phi_g - \phi_f|}{\min|u_j \times u_i|} \leq 2\max|\phi_f| \leq 2L^2.$$

Step (II): We use the wheel-decomposition theorem for braced stresses, Theorem 2.3.1, to decompose ω^c into a linear combination of the *large* atomic braced stresses of wheels:

$$\omega^c = \sum_{1 \leq k \leq n} \alpha_k \omega^A(W_k). \tag{2.5.4}$$

As a next step we bound the entries $|\omega_{ij}^A|$ from above. By definition,

$$|\omega_{ij}^A(W_k)| \leq (\max_{o,p,q} |\det(u_o u_p u_q)|)^{\deg(u_k)-1} \leq L^{3(\deg(u_k)-1)}.$$

Step (III): The large atomic braced stresses in the decomposition Eq. (4.6.3) are integers. To make the whole sum integral we round the coefficients. Though, direct rounding may influence the sign of the resulting stresses. To overcome this effect we scale the coefficients before rounding. We pick the scaling factor

$$C := 4 \left\lceil \frac{\max_{i,j,k} |\omega_{ij}^A(W_k)|}{\min_{i,j} |\omega_{ij}^c|} \right\rceil$$

and construct a braced stress

$$\omega := \sum_{1 \leq k \leq n} \lfloor C\alpha_k \rfloor \omega^A(W_k).$$

The braced stress ω is integral. It remains to prove that the signs of ω_{ij} and ω^c_{ij} coincide, which would validate that ω is positive. Indeed,

$$\begin{aligned}|\omega_{ij} - C\omega^c_{ij}| &= \left| \sum_{1\leq k\leq n} (\lfloor C\alpha_k \rfloor - C\alpha_k)\omega^A_{ij}(W_k) \right| \\ &\leq \sum_{1\leq k\leq n} |\omega^A_{ij}(W_k)| \leq 4 \max |\omega^A_{ij}(W_k)| \leq C \min |\omega^c_{ij}|.\end{aligned}$$

The third transition holds since exactly 4 wheels participate in the wheel-decomposition of any single edge. In the remainder of the proof we bound the entries of ω. Due to the bounds on ω^c and ω^A, the constant C is bounded by

$$C \leq 4L^{3(\Delta_G - 1)+8}.$$

The constructed braced stress ω is therefore bounded by

$$\begin{aligned}|\omega_{ij}| \leq& |C\omega^c_{ij}| + 4 \max |\omega^A_{ij}(W_k)| \\ \leq& |C| \max |\omega^c_{ij}| + 4 \max |\omega^A_{ij}(W_k)| \\ \leq& 4L^{3(\Delta_G - 1)+8} 2L^2 + 4L^{3(\Delta_G - 1)}.\end{aligned}$$

□

The duality transform theorem is now a direct consequence of Theorem 2.5.1 and 2.5.5:

Theorem 2.5.6. *Let G be a triangulation with maximal vertex degree Δ_G and let $\mathcal{P} = (u_i)_{1\leq i\leq n}$ be a realization of G as a convex polytope with integer coordinates. Then there exists a realization $(\phi_f)_{f\in F(G)}$ of the dual graph G^* as a convex polytope with integer coordinates bounded by*

$$|\phi_f| < O(n \max |u_i|^{3\,\Delta_G + 9}).$$

Chapter 3

Prismatoid

The algorithms for realizing large classes of polytopes on the integer grid usually require a large grid size. However, for special classes of polytopes more effective algorithms exist. Below we present an embedding algorithm for one particular type of polytopes called prismatoids.

A *prismatoid* is a polytope whose graph is a triangulated annulus. We show how to embed such a graph with n vertices as a convex polytope on a $O(n^4) \times O(n^3) \times 1$ grid.

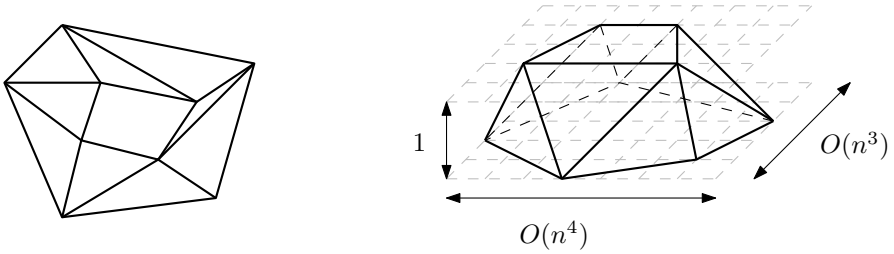

3.0.1 Analysis

The graph of a prismatoid has two special faces that form the exterior of the annulus. We call one (any) of these faces *the outerface* and the other *the innerface*. In our algorithm we first construct a planar realization of a prismatoid in the plane, and the outerface will indeed be an outerface of this planar realization. The remaining faces of the prismatoid are n triangular faces that form the triangulation of the annulus.

The n triangular faces of the prismatoid are of two types: some are adjacent to the outerface and some to the innerface. We call the triangular faces adjacent to the outerface *grey* and those adjacent to the innerface *white*. Then we replace each group of consecutive triangles of the same colour by one triangle. We call the result the *reduced prismatoid*. The reduction is depicted on Fig. 3.0.1.

We denote the vertices of the outerface of the reduced prismatoid with $A_1 \dots A_k$ and the vertices of the innerface with $B_1, \dots B_k$ so that $A_i B_i A_{i+1}$ is a face of the reduced prismatoid. We denote the number of vertices removed from the edge $A_i A_{i+1}$ during the initial reduction with a_i and from the edge $B_i B_{i+1}$ with b_i.

We call a prismatoid a (k, m)-*prismatoid* if the inner- and the outerface of the reduced prismatoid are k-gons and $a_i = b_i = m$ for all $1 \leq i \leq k$, see Fig. 3.0.2. We note that the reduced prismatoid is a $(k, 0)$-prismatoid. We present an algorithm that realizes every (k, m)-prismatoid on the integer grid of size

$$2\lceil k/4 \rceil \left(\lceil k/4 \rceil + 1\right) \left\lceil \frac{1}{4} m(15m + 13) \right\rceil \times 4\lceil k/4 \rceil \left\lceil \frac{1}{4} m(15m + 13) \right\rceil \times 1.$$

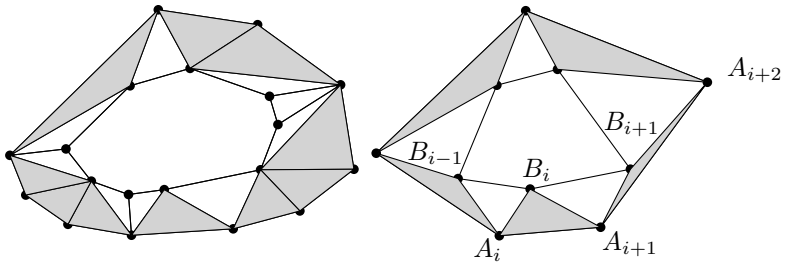

Figure 3.0.1: The initial prismatoid (left) and the reduced prismatoid (right). The triangles adjacent to the outerface (innerface) are colored grey (white).

Then every prismatoid with n vertices is, trivially, a subpolytope of a (k, m)-prismatoid with $m = \max_{1 \leq i \leq k}(\max(a_i, b_i))$, see Fig. 3.0.2, and thus can be realized on a grid of size $O(n^4) \times O(n^3) \times 1$.

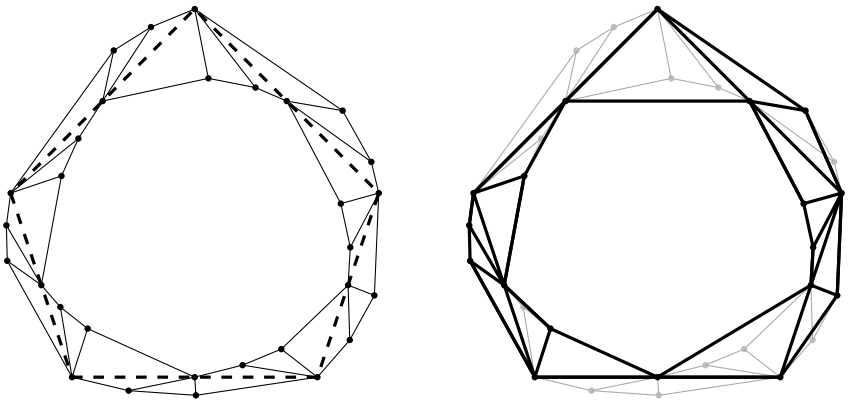

Figure 3.0.2: Left: a (k, m)-prismatoid with $k = 5, m = 2$. The dashed edges represent the border between grey and white faces and simultaneously the outerface of the reduced prismatoid. Right: the realization of the initial prismatoid (bold black) induced by a realization of a (k, m)-prismatoid (grey). Some of the grey faces of the final realization are vertical and thus not visible.

3.0.2 Realization of the (k, m)-prismatoid

The algorithm follows a two stages approach. First we realize the reduced prismatoid (see Fig. 3.0.1) and then we reintroduce the missing vertices.

Realization of the reduced prismatoid

We realize the outerface of the reduced prismatoid as a convex polygon with k vertices on a $O(k^2) \times O(k^1)$ grid (we note that a convex polygon cannot be realized on an asymptotically smaller grid, see [3]). One possible construction is given by the following procedure: let first

$k = 4l$ for some $l \in \mathbb{Z}$. We define a chain (see Fig. 3.0.3)

$$\begin{aligned} A_k &= (0, -l), \\ A_1 &= A_k + (l, 1), \\ A_2 &= A_1 + (l-1, 1), \\ &\dots \\ A_l &= A_{l-1} + (1, 1) = (l(l+1)/2, 0). \end{aligned}$$

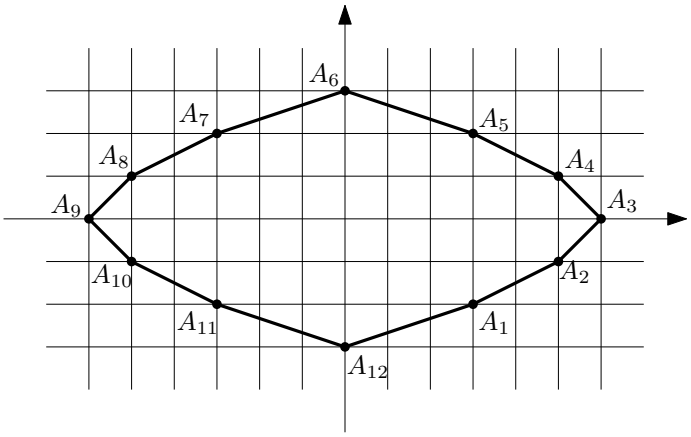

Figure 3.0.3: The grid realization of the 12-gon.

Four mirror w.r.t the axes copies of the above chain give a convex $4l$-gon. For k not divisible by 4 we construct a $4\lceil k/4 \rceil$-gon and pick any k-vertex subpolygon. Our construction requires the grid of size $\lceil k/4 \rceil (\lceil k/4 \rceil + 1) \times 2\lceil k/4 \rceil$.

We scale the realization of the outerface by a factor of 2 so that the midpoints of its edges have integer coordinates. We realize the innerface of the reduced prismatoid as the middle k-gon (the k-gon whose vertices are the middle points of the edges of the initial k-gon) of the outerface (see Fig. 3.0.4). To finish the realization of the reduced prismatoid as a convex polytope, we lift the innerface to the $\{z = 1\}$ plane, the outerface stays in the $\{z = 0\}$. Thus we realized the reduced $(k, 0)$-prismatoid on the grid of size

$$2\lceil k/4 \rceil (\lceil k/4 \rceil + 1) \times 4\lceil k/4 \rceil \times 1. \tag{3.0.1}$$

Reintroduction of missing points: general idea

The second step is the reintroduction of the points removed during the reduction. We reintroduce the vertices to the outer- and innerface of the reduced prismatoid by replacing the edges of these faces with the convex chains of length $m + 1$, see Fig. 3.0.4. We replace every edge A_iA_{i+1} by a convex chain $A_iA_i^1 \dots A_i^mA_{i+1}$ and every edge B_iB_{i+1} by a convex chain $B_iB_i^1 \dots B_i^mB_{i+1}$.

The resulting embedding is convex if and only if the following condition holds: For every edge A_iB_i or B_iA_{i+1} separating grey and white triangles, the angle between this edge and the innerface is larger than the angle between this edge and the outerface, that is for every $1 \le i \le k$ (we use the cyclic notation for indices)

1. $\angle(A_iB_iB_{i-1}^m) > \angle(B_iA_iA_i^1)$, and
2. $\angle(A_{i+1}B_iB_i^1) > \angle(B_iA_{i+1}A_i^m)$.

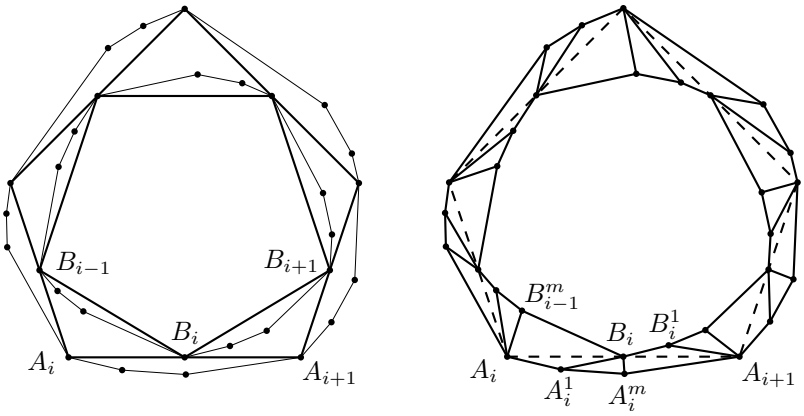

Figure 3.0.4: Reintroducing the points removed during the initial reduction. Left: bold is the reduced prismatoid and thin are the chains with the reintroduced vertices. Right: dashed are the edges separating the white and grey triangles.

We refer to the conditions above as the *convexity conditions*. We briefly discuss why these two convexity conditions suffice for the convexity of the prismatoid. To show convexity of the prismatoid we show that it is convex on every edge. We have edges of four types and we handle them separately:

- Edges that belong to the outer- or inner- face are convex, since we deploy the outerface in the $\{z = 0\}$ and the innerface in the $\{z = 1\}$ affine planes correspondingly;
- Edges that separate two white triangular faces are convex, since for every $1 \leq i \leq k$ the chain $B_iB^1_i \dots B^m_iB_{i+1}$ is a convex chain lying inside the triangle $B_iA_{i+1}B_{i+1}$;
- Edges that separate two grey triangular faces are convex, since for every $1 \leq i \leq k$ the chain $A_iA^1_i \dots A^m_iA_{i+1}$ is a convex chain built on the edge A_iA_{i+1};
- Edges that separate a grey and a white triangular faces. Consider the edge A_iB_i. It is incident to two faces $A_iB_iB^m_{i-1}$ and $A_iB_iA^1_i$. We argue that the edge A_iB_i is convex if on the flat drawing of the prismatoid, Fig. 3.0.4, the angle $\angle(A_iB_iB^m_{i-1})$ is larger than the angle $\angle(B_iA_iA^1_i)$. The spatial realization of the prismatoid is obtained by lifting the innerface to the $\{z = 1\}$ affine plane. Let us consider this lifting. Let us fix the face $A^1_iA_iB_i$ and allow the plane containing the face $A_iB_iB^m_{i-1}$ to rotate around the edge A_iB_i. When the edge A_iB_i is flat, the points $A^1_iA_iB_iB^m_{i-1}$ lie on one plane. This plane dissects two parallel planes $\{z = 0\}$ and $\{z = 1\}$ along the edge $A^1_iA_i$ and $B_iB^m_{i-1}$, thus these edges are parallel and the angles $\angle(A_iB_iB^m_{i-1}) = \angle(B_iA_iA^1_i)$ are equal. The rotation of the face $B^m_{i-1}B_iA_i$ around the edge A_iB_i, that makes the edge A_iB_i convex, increases the angle $A_iB_iB^m_{i-1}$.

Further we present an algorithm that constructs convex chains satisfying these conditions. The construction that we present is trivial but contains some technical computations. One can instead use any other construction satisfying the convexity conditions listed above.

Reintroduction of missing points: details

Expansion of the innerface. First we expand the edges of the innerface. Consider one edge of the innerface, $(B_{i-1}B_i)$. We will replace it with a convex chain $B_{i-1}B^1_{i-1} \dots B^m_{i-1}B_i$ that lies within the triangle $B_{i-1}A_iB_i$, Fig. 3.0.4 (left) and Fig. 3.0.5.

We start with a realization of the reduced prismatoid. First we scale this realization with a large factor N, that will be accurately estimated later. Before scaling, the points B_{i-1}, A_i, B_i are integral, thus after scaling the vectors

$$e_1 := \frac{1}{N}\overrightarrow{B_{i-1}A_i}$$
$$e_2 := \frac{1}{N}\overrightarrow{A_iB_i}$$

are integral and define an integer grid, see Fig. 3.0.5.

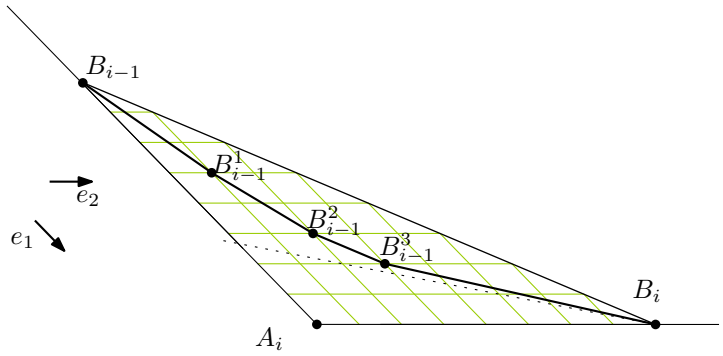

Figure 3.0.5: The grid generated by the triangle $B_{i-1}A_iB_i$, expansion of an edge of the inner-face. To guarantee the convexity condition (1), the last point B^m_{i-1} lies above the dotted line with the slope $(1, m)$ through the point B_i.

We use this grid to construct a convex chain inside the triangle $B_{i-1}A_iB_i$:

$$B^1_{i-1} = B_{i-1} + (m, 1),$$
$$B^2_{i-1} = B^1_{i-1} + (m-1, 1),$$
$$B^3_{i-1} = B^2_{i-1} + (m-2, 1),$$
$$\dots$$
$$B^m_{i-1} = B^{m-1}_{i-1} + (1, 1),$$

where $(x, y) = xe_1 + ye_2$. The slope of the last edge $B^m_{i-1}B_i$ is thus not predetermined by the construction and we control it later with the choice of the scaling factor N.

The point B^m_{i-1} (and thus, the whole chain) lies inside the triangle $B_{i-1}A_iB_i$ if and only if

$$N > m + (m-1) + (m-2) + \ldots + 1 = m(m+1)/2. \tag{3.0.2}$$

This gives the first bound on the scaling factor N. The two convexity conditions (1) and (2), that we discussed above, later will give us two more bounds on N. In the end of the proof we will combine these three bounds and define the final scaling factor.

To guarantee the convexity condition (1) on the next step, we need as an additional requirement that the slope of the last edge $(B^m_{i-1}B_i)$ is at least $(1, m)$ w.r.t. the (e_1, e_2)-grid, or equivalently that the point B^m_{i-1} lies above the line from B_i in the direction $e_1 + me_2$, see Fig. 3.0.5. That is,

$$\frac{N - m(m+1)/2}{N - m} > \frac{1}{m}$$

or

$$N > \frac{m^2(m+1)/2 - m}{m-1} = m\frac{m(m+1)/2 - 1}{m-1} = \frac{1}{2}m(m+2). \tag{3.0.3}$$

This gives the second bound on the scaling factor N.

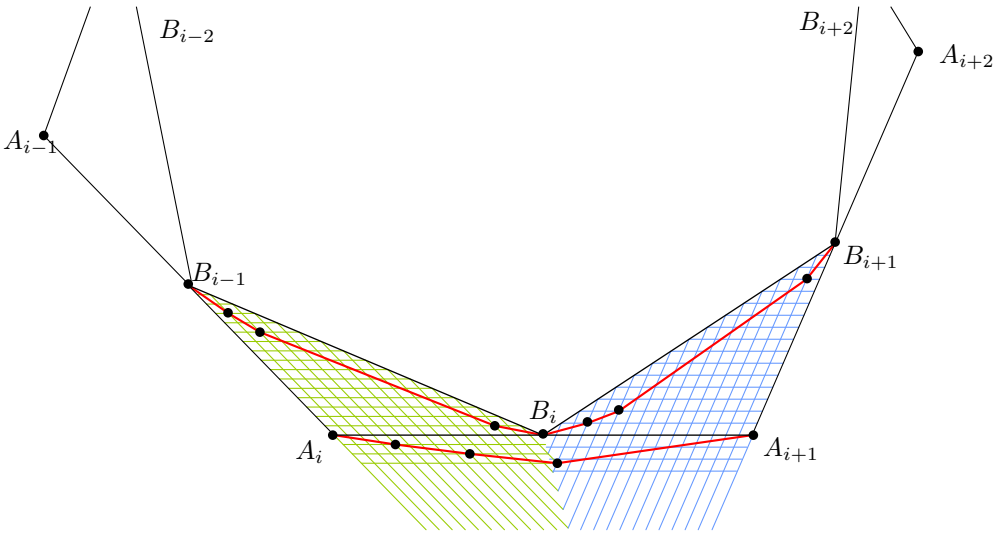

Figure 3.0.6: The example shows how to expand an edge of the outerface with $m = 3$ new vertices. The available subgrid is big enough to realize any chain of up to m vertices while guaranteeing the convexity conditions (1) and (2).

Expansion of the outerface. Now we are ready to expand the outerface. We consider an edge A_iA_{i+1} and replace it with a convex chain $A_iA_i^1 \dots A_i^m A_{i+1}$, Fig. 3.0.6. On the previous step we generated two integer grids adjacent to this edge (see Fig. 3.0.7) — one coming from the "left" triangle $B_{i-1}A_iB_i$ with the basis vectors

$$e_1^l := \frac{1}{N}\overrightarrow{B_{i-1}A_i}$$
$$e_2^l := \frac{1}{N}\overrightarrow{A_iB_i},$$

the other coming from the "right" triangle $B_iA_{i+1}B_{i+1}$ with the basis vectors

$$e_1^r := \frac{1}{N}\overrightarrow{B_iA_{i+1}},$$
$$e_2^r := \frac{1}{N}\overrightarrow{A_{i+1}B_{i+1}}.$$

We use the grid coming from the left to define the convex chain $A_iA_i^1 \dots A_i^m A_{i+1}$ and the grid coming from the right to control the convexity condition (2).

We define the convex chain:

$$A_i^1 = A_i + (1, m+1)_l,$$
$$A_i^2 = A_i^1 + (1, m+2)_l,$$
$$A_i^3 = A_i^2 + (1, m+3)_l,$$
$$\dots$$
$$A_i^m = A_i^{m-1} + (1, 2m)_l,$$

where $(x, y)_l = xe_1^l + ye_2^l$, see Fig. 3.0.7.

The convexity condition (1) states that the slope of the first edge $A_iA_i^1$ should be smaller than the slope of the last edge $B_{i-1}^m B_i$ of the chain ending at the vertex B_i. By condition (2)

the slope of the last edge $A_i^m A_{i+1}$ should be smaller than the slope of the first edge $B_i B_i^1$ of the chain starting from the vertex B_i,

$$\angle(A_i^m A_{i+1} B_i) < \angle(A_{i+1} B_i B_i^1).$$

The condition (1) is guaranteed by the bound of Eq. (3.0.3) on the scaling factor N that we discussed above, since the slope of $A_i A_i^1$ w.r.t. the left grid is $(1, m+1)$ and the slope of $B_{i-1}^m B_i$ is at least $(1, m)$. We thus proceed with the convexity condition (2) and we rephrase this condition so that it provides a bound on N. The remainder of the section is devoted to this computation. The resulting bound on N is presented in Eq. (3.0.4).

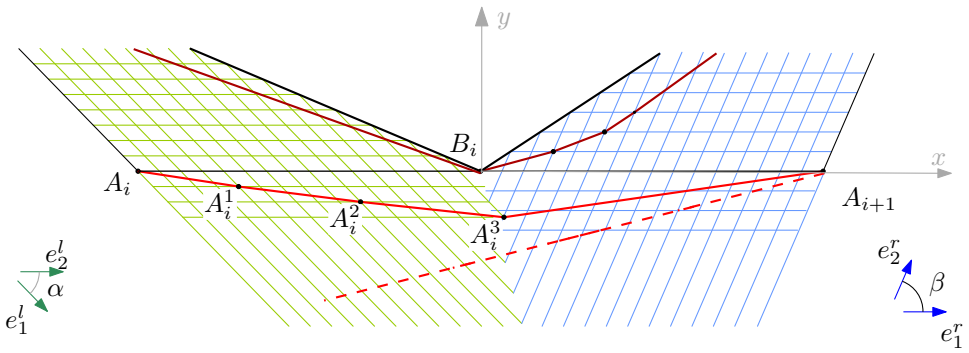

Figure 3.0.7: The expansion of an edge of the outerface with $m = 3$ new vertices. The left grid is light green and the right grid is light blue.

To provide the computations we introduce the euclidean coordinates on the plane: the x-axis is set parallel to the vector $\overrightarrow{A_i A_{i+1}}$, the origin is at the point B_i, see Fig. 3.0.7. We denote the lengths $c := |A_i A_{i+1}|$, $c_l := |A_{i-1} A_i|$, $c_r := |A_{i+1} A_{i+2}|$ and the oriented angles $\alpha = \angle(e_1^l, e_2^l)$ and $\beta = \angle(e_1^r, e_2^r)$. In these coordinates:

$$A_i = \left(-\frac{c}{2}, 0\right), \qquad A_{i+1} = \left(\frac{c}{2}, 0\right),$$
$$e_1^l = \left(\frac{c_l}{2N}\cos(\alpha), -\frac{c_l}{2N}\sin(\alpha)\right), \qquad e_2^l = \left(\frac{c}{2N}, 0\right),$$
$$e_1^r = \left(\frac{c}{2N}, 0\right), \qquad e_2^r = \left(\frac{c_r}{2N}\cos(\beta), \frac{c_r}{2N}\sin(\beta)\right).$$

The coordinates of the point A_i^m with respect to the left grid are

$$A_i^m = A_i + (1, m+1)_l + (1, m+2)_l + \ldots + (1, 2m)_l = A_i + (m, m^2 + m(m+1)/2)_l,$$

where $(x, y)_l = x e_1^l + y e_2^l$. Thus, in euclidean coordinates

$$(A_i^m)_x = -\frac{c}{2} + m\frac{c_l}{2N}\cos(\alpha) + (m^2 + m(m+1)/2)\frac{c}{2N},$$
$$(A_i^m)_y = -m\frac{c_l}{2N}\sin(\alpha).$$

So the slope of the edge $A_i^m A_{i+1}$ is

$$\frac{(A_{i+1} - A_i^m)_y}{(A_{i+1} - A_i^m)_x} = \frac{m\frac{c_l}{2N}\sin(\alpha)}{c - m\frac{c_l}{2N}\cos(\alpha) - (m^2 + m(m+1)/2)\frac{c}{2N}}.$$

The point B_i^1 with respect to the right grid has coordinates

$$B_i^1 = B_i + (m, 1)_r,$$

where $(x,y)_r = xe_1^r + ye_2^r$. Thus, in euclidean coordinates

$$(B_i^1)_x = m\frac{c}{2N} + \frac{c_r}{2N}\cos(\beta),$$
$$(B_i^1)_y = \frac{c_r}{2N}\sin(\beta),$$

and the slope of the edge $B_iB_i^1$ is

$$\frac{(B_i^1 - B_i)_y}{(B_i^1 - B_i)_x} = \frac{\frac{c_r}{2N}\sin(\beta)}{m\frac{c}{2N} + \frac{c_r}{2N}\cos(\beta)}.$$

The convexity condition (2) is satisfied if and only if the slope of the edge $A_i^m A_{i+1}$ is smaller than the slope of the edge $B_iB_i^1$, that is

$$\frac{(A_{i+1} - A_i^m)_y}{(A_{i+1} - A_i^m)_x} < \frac{(B_i^1 - B_i)_y}{(B_i^1 - B_i)_x}.$$

We substitute the computed values, go to the common denominator and obtain

$$\begin{aligned}
& mc_l\sin(\alpha)[mc + c_r\cos(\beta)] < c_r\sin(\beta)[(2Nc - mc_l\cos(\alpha) - (m^2 + m(m+1)/2)c] \\
\Leftrightarrow \quad & \frac{mc_l\sin(\alpha)[mc + c_r\cos(\beta)] + c_r\sin(\beta)[mc_l\cos(\alpha) + (m^2 + m(m+1)/2)c]}{2c_rc\sin(\beta)} < N \\
\Leftarrow \quad & \frac{c_l\sin(\alpha)[m^2c + mc_r] + c_r\sin(\beta)[mc_l + (m^2 + m(m+1)/2)c]}{2c_rc\sin(\beta)} < N \\
\Leftarrow \quad & \frac{1}{2}\frac{c_l}{c_r}\frac{\sin\alpha}{\sin\beta}m^2 + \frac{1}{2}\frac{c_l}{c}\frac{\sin\alpha}{\sin\beta}m + \frac{1}{2}\frac{c_l}{c}m + \frac{1}{2}(m^2 + m(m+1)/2) < N.
\end{aligned}$$

The first transition holds since the polygon $A_1, \dots A_k$ is convex and thus $\sin(\beta) > 0$. On the second transition we replace $\cos(\beta)$ and $\cos(\alpha)$ on the left hand side with its maximal value 1. Since $\sin\alpha > 0$ and $\sin\beta > 0$ it makes the inequality stronger.

In the construction of the outer- and innerface k-gons presented above, the lengths of any two consecutive edges differ by no more than a factor of 2 and of any three consecutive edges by no more than a factor of 3,

$$\frac{c_l}{c} < 2, \qquad \frac{c_l}{c_r} < 3,$$

and the sines of any two consecutive angles differ by no more than a factor of 2,

$$\frac{\sin\alpha}{\sin\beta} < 2.$$

Thus the last inequality holds if

$$N > 3m^2 + 2m + m + \frac{1}{2}\left(m^2 + \frac{m(m+1)}{2}\right) = \frac{1}{4}m(15m+13). \tag{3.0.4}$$

We finally collected all the three constraints on the scaling factor N, Eq. (3.0.2), Eq. (3.0.3) and Eq. (3.0.4) and the first two of them clearly follow form the third, thus we pick as the scaling factor

$$N := \left\lceil \frac{1}{4}m(15m+13) \right\rceil.$$

Combining this bound with the bound of Eq. (3.0.1) on the size of the grid we used to realize the reduced prismatoid, we deduce that our algorithm realizes a (k,m)-prismatoid on the integer grid of size

$$2\lceil k/4\rceil\,(\lceil k/4\rceil + 1)\left\lceil \frac{1}{4}m(15m+13)\right\rceil \times 4\lceil k/4\rceil\left\lceil \frac{1}{4}m(15m+13)\right\rceil \times 1.$$

Since every prismatoid with n vertices is a subpolytope of a (k, m)-prismatoid with $k, m < n$, every prismatoid can be realized on an integer grid of size

$$O(n^4) \times O(n^3) \times 1.$$

Chapter 4

Efficient duality transforms in $\mathbb{R}^d$

4.1 Preliminaries

4.1.1 Combinatorics and notation of d-polytopes: overview

Before we proceed with d-dimensional polytopes we review the basic combinatorial properties and introduce the notation that we use further without additional references. For a comprehensive review of d-dimensional polytopes we refer the reader to the book by Ziegler [46]. In our terminology polytopes are always considered convex, thus we often omit the word "convex" and write simply a d-polytope. For nonconvex polytopes we later introduce the notion of *polytopal surface*.

The notion of convex polytopes allows two equivalent approaches, as the convex hull of a set of points and as the intersection of a set of halfspaces.

Let $(u_1, \dots u_n)$ be a finite set of points in $\mathbb{R}^d$. We remind that the *convex hull* of this set of points, $\mathrm{Conv}(u_1, \dots u_n)$ is the set of all the convex combinations of (u_i):

$$\mathrm{Conv}(u_1, \dots u_n) = \left\{ \sum_{1 \le i \le n} \alpha_i u_i : \sum_{1 \le i \le n} \alpha_i = 1, \alpha_i \ge 0 \right\}.$$

Definition 4.1.1 (Convex polytope as a convex hull)**.** *The full-dimensional convex hull of a finite set of points in $\mathbb{R}^d$ is called a d-dimensional* convex polytope*.*

A polytope as the convex hull of a set of points is often referred to as a *V-polytope*. We note that the points from the definition above are not by default the vertices of the resulting polytope, however the vertices of the polytope form a subset of the initial set of points.

Definition 4.1.2 (Convex polytope as an intersection of halfspaces)**.** *A bounded full-dimensional subset of $\mathbb{R}^d$ which is the intersection of a finite set of halfspaces of $\mathbb{R}^d$ is called a d-dimensional* convex polytope*.*

A polytope as the intersection of a set of halfspaces is often referred to as an *H-polytope*. Again we note that the hyperplanes bounding the halfspaces from the definition above are not by default supporting the resulting polytope, however the set of hyperplanes supporting the $(d-1)$-dimensional faces of the polytope is a subset of the initial set of bounding hyperplanes.

The two definitions of a convex polytope are equivalent (we refer to [46] for details).

Faces. We say that an affine hyperplane $\alpha = \{x \in \mathbb{R}^d : \langle n, x \rangle = c\}$ defined by a normal vector $n \in R^d$ and a constant $c \in \mathbb{R}$ is a *supporting hyperplane* for a convex polytope $\mathcal{P}$ if

1. The intersection $\mathcal{P} \cap \alpha \neq \emptyset$ is nonempty and

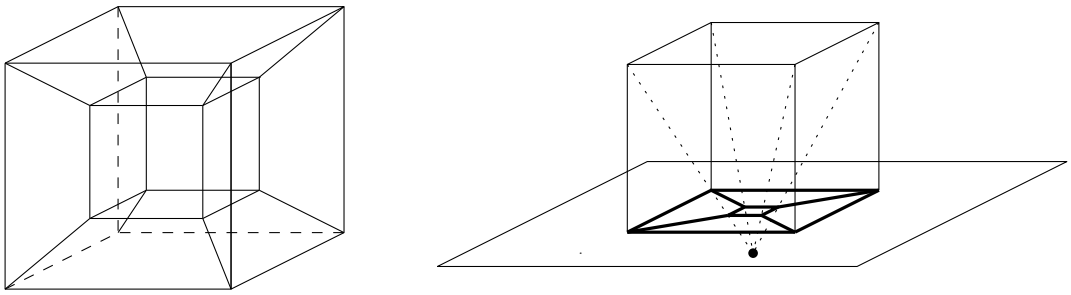

Figure 4.1.1: There is not much hope to visualize a higher dimensional polytope. Though, 4-dimensional polytopes can be viewed through *Schlegel diagrams*. A polytope $\mathcal{P}$ is centrally projected to the hyperplane of one of its facets f. The center of projection is chosen outside the polytope close to the barycenter of f. The right figure illustrates the construction of a Schlegel diagram (bold) of the 3d cube. The left figure shows a Schlegel diagram of the 4d cube. Schlegel diagrams are a special case of *flat realizations* that we discuss in the end of the section.

2. The whole polytope lies in one of the two halfspaces defined by the hyperplane: $\mathcal{P} \subset \{x \in \mathbb{R}^d : \langle n, x\rangle \leq c\}$ or $\mathcal{P} \subset \{x \in \mathbb{R}^d : \langle n, x\rangle \geq c\}$.

Definition 4.1.3. *The intersection $F = \alpha \cap \mathcal{P}$ of a supporting hyperplane α and a polytope $\mathcal{P}$ is called a* face *of a polytope. For convenience and to comply with tradition we also consider the whole polytope $\mathcal{P}$ and the empty set $\emptyset$ being faces of $\mathcal{P}$.*

The dimension of a face is the dimension of its affine hull,

$$\mathrm{Aff}(F) = \{a + t(b - a) : a, b \in F, t \in \mathbb{R}\}.$$

We refer to the faces of the dimension k as *k-faces* and denote the set of all the k-faces with $\mathcal{F}_k(\mathcal{P})$. The faces of dimension $d-1$ are called *facets*. The faces of dimension $d-2$ are called *ridges*. The faces of dimensions 0 and 1 are called *vertices* and *edges* correspondingly.

Face lattice and combinatorial equivalence. The faces of a convex polytope form a partially ordered set with respect to the inclusion as a subset. This poset is called *the face lattice* of the polytope. The face lattice of a polytope represents the combinatorial structure of the polytope: We say that two polytopes $\mathcal{P}$ and $\mathcal{Q}$ are *combinatorially equivalent* if their face lattices are isomorphic.

The combinatorial equivalence of polytopes corresponds to a topological equivalence: the polytopes $\mathcal{P}$ and $\mathcal{Q}$ are combinatorially equivalent if and only if there exist of a homeomorphism $h : \mathcal{P} \to \mathcal{Q}$ such that $h(F)$ is a k-face of Q if and only if F is a k-face of P.

Let F be a k-face of a polytope $\mathcal{P}$. We call *the boundary* of F and denote with ∂F the set of $(k-1)$-faces of $\mathcal{P}$ that are subsets of F. We call *the coboundary* of F and denote with δF the set of $(k+1)$-faces of $\mathcal{P}$, that contain F as a subset.

Polytopal complexes and the skeleton of a polytope. In defining the notion of *polytopal complex* we follow Ziegler [46, chapter 5]:

Definition 4.1.4. *A* polytopal complex *C is a finite collection of polytopes in $\mathbb{R}^d$ such that*

- *the empty polytope is in C;*
- *if $P \in C$, then all the faces of P are also in C;*
- *the intersection $P \cap Q$ of two polytopes P, Q in C is a face both of P and of Q.*

The dimension of a complex $dim(C)$ *is the largest dimension of a polytope in* C*.*

An immediate example of a polytopal complex is provided by the set of all faces of a convex polytope. Thus, a convex polytope can be viewed as a polytopal complex.

We call *the face lattice* of a polytopal complex the polytopal complex itself with the partial order given by the relation of inclusion as a subset. Thus the notion of face lattice of a polytopal complex naturally generalizes the notion of face lattice of a polytope. In particular, the face lattice of a polytope is the face lattice of the polytopal complex of faces of this polytope.

For a convex polytope $\mathcal{P}$ we call the *k-skeleton* of P the polytopal complex of all the faces of $\mathcal{P}$ of dimension smaller or equal than k and we denote with $\mathrm{Sk}_k(\mathcal{P})$. Thus,

$$\mathrm{Sk}_k(\mathcal{P}) = \cup_{0\leq i\leq k}\mathcal{F}_i(\mathcal{P}).$$

The k-skeleton of a polytopal complex C is the union of the k-skeletons of the polytopes contained in it, $\mathrm{Sk}_k(C) = \cup_{\mathcal{P}\in C}(\mathrm{Sk}_k(\mathcal{P}))$.

Polarity between points and affine hyperplanes in $\mathbb{R}^d$. Polarity is a bijective correspondence between nonzero vectors (points) and affine hyperplanes not containing the origin in $\mathbb{R}^d$. Let $v \in \mathbb{R}^d$ be a nonzero vector. We put into correspondence to v the affine hyperplane $\alpha_v \subset \mathbb{R}^d$ defined by the equation

$$v \to \alpha_v := \{x \in \mathbb{R}^d : \langle v, x\rangle = 1\}.$$

We call the hyperplane α_v the *polar dual* hyperplane to v. Conversely, for an affine hyperplane α we call the vector $v \in \mathbb{R}^d$ the *polar dual vector* to α if $\alpha = \alpha_v$.

Polarity preserves incidence relations: let the point $v \in \mathbb{R}^d$ lie in an affine hyperplane $\alpha \subset \mathbb{R}^d$. Then the polar dual hyperplane to v contains the polar dual point to α. As a consequence, polarity maps a set of coplanar points to a set of hyperplanes passing through one point, which is the polar dual point to the hyperplane containing the initial points.

Duality and the polar dual polytope. We say that a lattice L is dual to a lattice L^* if L^* is equivalent to L with all the arrows inverted. We say that a polytope $\mathcal{P}^*$ is dual to a polytope $\mathcal{P}$ if their face lattices $\mathcal{L}(\mathcal{P})$ and $\mathcal{L}(\mathcal{P}^*)$ are dual face lattices. Thus, to every k-face f of $\mathcal{P}$ there corresponds a unique dual $(d-k-1)$-face f^* of $\mathcal{P}^*$. By definition, the dual of the dual polytope $(\mathcal{P}^*)^*$ is combinatorially equivalent to the initial polytope $\mathcal{P}$.

Given a convex polytope $\mathcal{P}$ that contains the origin in its interior, there is a standard way of constructing a polytope dual to P which uses polarity. To every vertex v of $\mathcal{P}$ we put into correspondence the polar dual affine hyperplane α_v defined by the equation

$$\alpha_v := \{x \in \mathbb{R}^d : \langle v, x\rangle = 1\}$$

and a halfspace H_v bounded by α_v,

$$H_v := \{x \in \mathbb{R}^d : \langle v, x\rangle \leq 1\}.$$

The polytope obtained as an intersection of the halfspaces H_v for all vertices v of $\mathcal{P}$ is called *the polar dual polytope* for $\mathcal{P}$, or simply the polar polytope, and is denoted with $\mathcal{P}^*$,

$$\mathcal{P}^* = \cap_{v\in\mathcal{F}_0(\mathcal{P})}H_v.$$

Every defining hyperplane α_v is indeed a supporting hyperplane for some facet f_v of $\mathcal{P}^*$ and by definition every facet of $\mathcal{P}^*$ in turn corresponds to some vertex of $\mathcal{P}$. Indeed, the polar dual polytope is a dual polytope and the isomorphism between the face lattices is generated by the correspondence $v \to f_v$.

Since the polarity in $\mathbb{R}^d$ preserves incidences between points and planes, the vertices of the polar dual polytope are the polar dual points to the faces of the primal polytope. Thus, the polar dual polytope can be alternatively defined as the convex hull of points that are polar duals to the faces of the primal polytope. The polar dual to the polar dual polytope is the primal polytope $(\mathcal{P}^*)^* = P$.

Details on the structure of $(d-1)$- and $(d-2)$-faces of a polytope. Let F be a $(d-2)$-face of $\mathcal{P}$. Then the face dual to F is an edge F^* of $\mathcal{P}^*$ connecting two vertices f^* and g^* of $\mathcal{P}^*$, which in turn are dual to facets f and g of $\mathcal{P}$. Thus, every $(d-2)$-face of $\mathcal{P}$ is incident to exactly two facets f and g (and separates them) and can be denoted as (fg). The notation (fg) assumes an order of f and g, mnemonically $(fg) = -(gf)$, see Fig. 4.1.2 and Sect. 4.1.3 for details on orientations.

For every $(d-3)$-face F of $\mathcal{P}$ the set $\delta(F)$ of adjacent $(d-2)$-faces has a natural cyclic order. Indeed, the dual to F face is a 2-face F^* of $\mathcal{P}^*$, that is a simple polygon, whose boundary is a cycle $(f_1^*, f_2^*, \dots, f_k^*, f_{k+1}^* = f_1^*)$, consisting of 0-faces f_i^* and 1-faces $(f_i^* f_{i+1}^*)$ incident to F^*. Thus, the $(d-1)$-faces incident to F are

$$(f_1, f_2, \dots, f_k, f_{k+1} = f_1)$$

and the $(d-2)$-faces incident to F are

$$(f_1 f_2), (f_2 f_3), \dots, (f_k, f_1)$$

and there is a natural cyclic order on them.

4.1.2 Conventions on orientations

Orientation on a real vector space. Let L be a d-dimensional real vector space, we say that it is oriented if a positively oriented basis $e_1, \dots e_d$ is chosen. Two orders on the same set of vectors that differ by a permutation σ define the same orientation if and only if σ is an even permutation. Two bases $\mathbf{e} = (e_i)$ and $\mathbf{f} = (f_i)$ define the same orientation if and only if the determinant

$$\det(f_1, \dots f_d) > 0,$$

where the columns are the coordinates of the vectors f_i in the basis $\mathbf{e}$. We also say that the basis $\mathbf{e} = (e_i)$ is *positively (negatively) oriented* (or simply positive (negative)) with respect to the basis $\mathbf{f} = (f_i)$ and use the notation

$$\mathrm{sign}_{\mathbf{f}}(\mathbf{e}) = \pm 1.$$

The standard euclidean space $\mathbb{R}^d$ is naturally oriented with the basis

$$e_1 = \begin{pmatrix} 1 \\ 0 \\ \dots \\ 0 \end{pmatrix}, e_2 = \begin{pmatrix} 0 \\ 1 \\ \dots \\ 0 \end{pmatrix}, \dots, e_d = \begin{pmatrix} 0 \\ 0 \\ \dots \\ 1 \end{pmatrix}.$$

When some standard basis is assumed, we write simply $\mathrm{sign}(\mathbf{e}) = \pm 1$ to denote that a basis $\mathbf{e}$ is positive (negative) w.r.t this standard basis.

Orientation on an (affine) hyperplane by a choice of normal. Let α be an (affine) hyperplane in $\mathbb{R}^d$. Then the orientation on α can be prescribed by a choice of a positively oriented normal vector and we use the "normal - last" rule:

Let n be a normal vector to α. Then the basis $(e_1, \dots e_{d-1})$ in α is *positively oriented w.r.t the chosen normal* n if $(e_1, \dots e_{d-1}, n)$ is a positively oriented basis in $\mathbb{R}^d$, or in the notation of the previous paragraph

$$\operatorname{sign}(e_1, \dots e_{d-1}, n) = 1.$$

Conversely, given a basis $\mathbf{e} = (e_1, \dots e_{d-1})$ in α we say that the normal vector n is a *positive normal vector* w.r.t $\mathbf{e}$ if $(e_1, \dots e_{d-1}, n)$ is a positively oriented basis in $\mathbb{R}^d$.

Orientation on an (affine) subspace of $\mathbb{R}^d$ of any dimension by an ordered set of points. Let α be a k-dimensional (affine) subspace of $\mathbb{R}^d$. Then the orientation on α can be prescribed by a choice of an ordered set of points $u_1, \dots u_{k+1}$ in α: we map a set of points to a basis

$$e_1 := u_1 - u_{k+1}, \dots, e_k := u_k - u_{k+1}$$

and appoint this basis as a positively oriented.

This definition complies with the sign of the signed volume (see Subsec. 4.1.4 for an overview): Let $(u_1, \dots u_{k+1})$ be points in $\mathbb{R}^k$. Then the signed volume of the simplex generated by these points

$$\operatorname{Vol}(u_1, \dots, u_{k+1}) := \det \begin{pmatrix} u_1 & u_2 & \dots & u_{k+1} \\ 1 & 1 & \dots & 1 \end{pmatrix} = \det \begin{pmatrix} u_1^1 & u_2^1 & \dots & u_{k+1}^1 \\ u_1^2 & u_2^2 & \dots & u_{k+1}^2 \\ \dots & & & \\ u_1^k & u_2^k & \dots & u_{k+1}^k \\ 1 & 1 & \dots & 1 \end{pmatrix},$$

where $u_i = (u_i^1, u_i^2, \dots, u_i^k)^T$, is exactly the determinant of the basis generated by these points:

$$\det(u_1 - u_{k+1}, \dots, u_k - u_{k+1}) = \det \begin{pmatrix} u_1 & u_2 & \dots & u_{k+1} \\ 1 & 1 & \dots & 1 \end{pmatrix}. \tag{4.1.1}$$

The equation above motivates the following useful observation:

Lemma 4.1.1. *Let α be a k-dimensional real vector space. Given two orders on the same set of points $(u_1 \dots u_{k+1})$ and $(u_{\sigma(1)} \dots u_{\sigma(k+1)})$ they define the same orientation if and only if σ is an even permutation.*

Proof. We fix any euclidean structure on α so that $\alpha = \mathbb{R}^k$. Then two bases $(e_1, \dots e_k)$ and $(e'_1 \dots e'_k)$ defined by the given sets of points have the same orientation if and only if the determinants $\det(e_1, \dots e_k)$ and $\det(e'_1, \dots e'_k)$ have the same sign. The reference to Eq. (4.1.1) finishes the proof. □

We say that the set of points $\mathbf{u} = (u_1 \dots u_{k+1})$ is *positively (negatively) oriented* w.r.t some basis $\mathbf{e} = (e_1, \dots e_k)$ and write

$$\operatorname{sign}_{\mathbf{e}}(\mathbf{u}) = 1$$

if the orientation defined by the set of points $\mathbf{u}$ coincides with the orientation of the basis $\mathbf{e}$. If the orientation defined by $\mathbf{u}$ is opposite to the orientation of $\mathbf{e}$, we say that $\mathbf{u}$ is *negatively* oriented w.r.t e and write $\operatorname{sign}_{\mathbf{e}}(\mathbf{u}) = -1$. When some standard basis $\mathbf{e}$ is assumed, we write simply $\operatorname{sign}(\mathbf{u}) = \pm 1$.

We remark that this definition might appear counterintuitive in $\mathbb{R}$: the orientation on the line through two points A and B given by an order of the points (A, B) corresponds to the orientation given by the basis vector $\overrightarrow{BA}$.

4.1.3 Orientation on faces of a polytope

Orientation on facets. Let $\mathcal{P}$ be a convex polytope. Then for every facet f the outer normal vector n_f is defined as a vector normal to f and directed outside of the polytope $\mathcal{P}$. Thus every facet is canonically oriented by this choice of the normal vector, see Fig. 4.1.2.

In particular, let $(u_1^f, \dots u_d^f)$ be a sequence of affinely independent points in f. Then these points define positive orientation on f if and only if $(u_1^f - u_d^f, \dots u_{d-1}^f - u_d^f, n_f)$ is a positively oriented basis in $\mathbb{R}^d$,

$$\det(u_1^f - u_d^f, \dots u_{d-1}^f - u_d^f, n_f) > 0. \tag{4.1.2}$$

Orientation on $(d-2)$-faces. Let f and g be two adjacent facets and let (fg) be the $(d-2)$-face separating them. The facets f and g are canonically oriented by the outer normal vectors of $\mathcal{P}$. We define the canonical orientation on (fg) as follows. Let $(u_1, \dots u_{d-1})$ be any set of affinely independent points in (fg), let u_f be a vertex of $f \setminus (fg)$ and u_g be a vertex of $g \setminus (fg)$, see Fig. 4.1.2.

Definition 4.1.5. *We say that the ordered set of points $(u_1, \dots u_{d-1})$ defines a positive orientation on (fg) and denote with $\operatorname{sign}_{(fg)}(u_1, \dots u_{d-1}) = 1$ if*

$$\operatorname{sign}_f(u_1, \dots u_{d-1}, u_f) = -1,$$
$$\operatorname{sign}_g(u_1, \dots u_{d-1}, u_g) = 1,$$

where by $\operatorname{sign}_f(u_1, \dots u_{d-1}, u_f) = 1(-1)$ we denote that the ordered set $(u_1, \dots u_{d-1}, u_f)$ is positively (negatively) oriented in f.

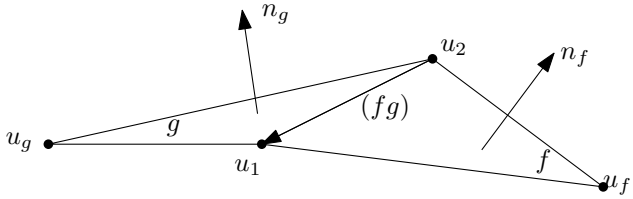

$(fg) = (u_1, u_2) = \overrightarrow{u_2 u_1}$,
$(f) = -(u_1, u_2, u_f)$,
$(g) = (u_1, u_2, u_g)$.

Figure 4.1.2: The orientation on $(d-1)$- and $(d-2)$-dimensional faces in the case $d = 3$. The order (u_1, u_2, u_g) defines the positive orientation on g w.r.t the positive normal n_g. The order (u_1, u_2, u_f) defines the negative orientation on f w.r.t the positive normal n_f. Thus, the order (u_1, u_2) defines a positive orientation on (fg). Counterintuitively, but by definition, the positive basis vector on the line spanned by (u_1, u_2) that corresponds to the orientation given by the order (u_1, u_2) is directed from u_2 to u_1.

Clearly, the two conditions of the above definition are equivalent. Moreover, by the definition

$$\operatorname{sign}_{(fg)}(u_1, \dots u_{d-1}) = -\operatorname{sign}_{(gf)}(u_1, \dots u_{d-1}).$$

4.1.4 Volumes

Signed volume of a full dimensional simplex. Let $\mathbf{u} = (u_1 \dots u_{d+1})$ be a set of points in $\mathbb{R}^d$. Then the signed volume is the determinant of the set of vectors generating the simplex $\mathbf{u}$, where as a convention we subtract the last point u_{d+1} from all the others to go from the set of points to a set of vectors, and we use the standard notations:

$$\begin{aligned}\operatorname{Vol}_d(u_1, \dots u_{d+1}) &= \det(u_1 - u_{d+1}, u_2 - u_{d+1}, \dots, u_d - u_{d+1}) \\ &= \det \begin{pmatrix} u_1 & u_2 & \dots & u_{d+1} \\ 1 & 1 & \dots & 1 \end{pmatrix}.\end{aligned}$$

We note that analogously to the 3d setup, we use a nonstandard rescaling for volume, as we do not multiply the determinant with $\frac{1}{d!}$. Thus, the volume of the simplex formed by the vectors of an orthonormal basis equals 1, while the volume of the unite cube equals $d!$. We use as a shortcut notation:

$$[u_1, \dots u_{d+1}] := \mathrm{Vol}_d(u_1, \dots u_{d+1}).$$

Signed volume of a k-dimensional simplex in $\mathbb{R}^d$. Let $\alpha \subset \mathbb{R}^d$ be a k-dimensional affine subspace with a chosen orientation and let $(u_1 \dots u_{k+1})$ be a sequence of affinely independent points in α, thus forming a k-dimensional simplex T. Then we naturally compute the volume of T as follows: We choose an orthonormal basis $\mathbf{e} = (e_1 \dots e_k)$ in α that is positively oriented with respect to the initial orientation on α. Then α has a structure of $\mathbb{R}^k$ and we compute the standard signed volume

$$\mathrm{Vol}_k(u_1, \dots u_{k+1}) = \det \begin{pmatrix} u_1 & u_2 & \dots & u_{k+1} \\ 1 & 1 & \dots & 1 \end{pmatrix},$$

where the coordinates of points u_i are in the basis $\mathbf{e}$.

Special case: volumes of facets of a polytope. As described in the Sect. 4.1.3, every facet f of a polytope has an orientation defined by the outernormal vector n_f. Then for a simplicial facet $f = (u_1, \dots u_d)$ the signed volume equals

$$\mathrm{Vol}_{d-1}(u_1, \dots u_d) = \det(u_1 - u_d, \dots, u_{d-1} - u_d, n_f).$$

Nonsigned volumes. The signed volumes require the containing space to be oriented. However in many cases the orientation on the containing space is not prescribed. In this case we compute the nonsigned volumes, that is effectively the signed volume with respect to the orientation defined by the set of points itself.

Let $(u_1 \dots u_{k+1})$ be affinely independent points in $\mathbb{R}^d$, thus forming a k-dimensional simplex T lying in a k-dimensional affine subspace α of $\mathbb{R}^d$. When α is not oriented, we compute the nonsigned volume of T as follows. We define an orientation on α by the given set of points $(u_1 \dots u_{k+1})$ and then compute the signed volume with respect to this orientation.

We choose an orthonormal basis $\mathbf{e} = (e_1 \dots e_k)$ in α that is positively oriented with respect to the set of points (u_i). Then α has a structure of $\mathbb{R}^k$ and we compute the standard signed volume

$$\mathrm{Vol}^+_k[u_1, \dots u_{k+1}] = \det \begin{pmatrix} u_1 & u_2 & \dots & u_{k+1} \\ 1 & 1 & \dots & 1 \end{pmatrix},$$

where the coordinates of points u_i are in the basis $\mathbf{e}$. Thus, by definition, the nonsigned volume $\mathrm{Vol}^+_k[u_1, \dots u_{k+1}]$ is always nonnegative (and positive for a nondegenerate set of points), what motivates the notation.

4.1.5 Realizations of polytopes

The main question of this chapter is the following: given a convex d-polytope $\mathcal{P}$, find a convex d-polytope $\mathcal{Q}$ that is combinatorially equivalent to $\mathcal{P}$ and that has small integer coordinates of its vertices. In other words, we are looking for *realizations* of a given polytope $\mathcal{P}$ as a convex polytope with small integer coordinates. To attack this problem, we use many other types of *realizations* of polytope, which we introduce below.

Realizations of polytopes allow two equivalent natural approaches: as polytopal complexes and as maps. We present both. As usual, we use a strong analogy with the 3d case, where the combinatorics of the polytope is predetermined by its graph and thus where we studied the realizations of graphs of polytopes in $\mathbb{R}^3$.

Realizations of polytopes as polytopal complexes

Definition 4.1.6. *Let P be a convex d-polytope.*

- *We call a convex d-polytope that is combinatorially equivalent to P a* realization of P as a convex polytope*;*
- *We call a $(d-1)$-dimensional polytopal complex whose face lattice is equivalent to the $(d-1)$-skeleton of P a* realization of P as a polytopal surface*;*
- *We call a $(d-2)$-dimensional polytopal complex whose face lattice is equivalent to the $(d-2)$-skeleton of P a* ridged realization of P*.*

By the higher dimensional generalization of Whitney's theorem [13, Theorem 12.3.1], the combinatorial structure of a d-polytope is predetermined by its $(d-2)$-skeleton. Thus, the combinatorial structure of a polytope is recoverable from its ridge realization as well as from its realization as a polytopal surface. (A realization as a convex polytope tells the combinatorial structure by definition.) In particular, that allows us to use the terms *polytopal surface* and *ridged realization* without mentioning the underlying polytope.

Counterintuitively, we say that a polytopal surface is d-dimensional if the underlying polytope is d-dimensional. A *polytopal surface* can be viewed as a nonconvex self-intersecting generalization of a convex polytope.

Ridged realizations of a polytope is the least restrictive class of realizations which we use and on which we are able to define the notions of stress. We remark, that for polytopes with simplicial $(d-2)$-faces, in particular, for simplicial polytopes, the notion of ridged realization is tautological: every embedding of vertices of such a polytope P in $\mathbb{R}^d$, $\mathbb{R}^{d-1}$ or $\mathbb{R}^{d-2}$ of general position realizes every $(d-2)$-face as a convex polytope and thus defines a ridged realization of P. Ridged realizations generalize to $\mathbb{R}^d$ the straight-line embeddings of graphs in $\mathbb{R}^3$.

We make an intense use of realizations of d-polytopes in $\mathbb{R}^{d-1}$ thus we introduce two "flat" types of realizations. The *planar realization* below generalizes the planar embedding of a graph to a plane:

Definition 4.1.7. *Let P be a convex d-polytope.*

- *We call the realization of P as a polytopal surface in $\mathbb{R}^{d-1}$ a* flat realization*.*
- *We call a flat realization* planar *if it lies within the realization of one distinguish outerfacet f and the realizations of all the other facets are pairwise interiorly disjoint.*

Realizations of polytopes as maps

Another natural approach to realizations of polytopes, which directly generalizes the notion of realizations of graphs, and allows to track orientations, is given by maps:

Definition 4.1.8. *Let P be a convex d-polytope. We say that a continuous map $h : P \to \mathbb{R}^m$* realizes *P in $\mathbb{R}^m$. In particular,*

- *A map h realizes P* as a convex polytope *if h is a homeomorphism onto its image, $h(P)$ is a convex polytope and $h(f)$ is a k-face of $h(P)$ if and only if f is a k-face of P for every $0 \leq k \leq d$;*
- *A map h realizes P* as a polytopal surface *if for every facet f of P the map h realizes f as a convex $(d-1)$-polytope;*
- *A map h defines a* ridged realization *of P if for every $(d-2)$-face f of P the map h realizes f as a convex $(d-2)$-polytope;*

Due to the topological description of combinatorial equivalence of polytopes, the definition above is consistent with the definition in terms of polytopal complexes: a polytope (or a polytopal complex) is a *realization* (as a convex polytope / as a polytopal surface / a ridged realization) in terms of Definition 4.1.6 if and only if it is the image of some *realizing map* (of the corresponding type) in terms of Definition 4.1.8.

Orientations on realizations

We always assume that the d-polytope P that is being realized comes oriented. In particular every facet of P comes with an ordered set of d points on it, that define the positive orientation of this facet. Though, the combinatorial structure of a polytope does not contain any information about the orientation. Thus the realizations of a polytope viewed as polytopal complexes do not inherit the orientation of the underlying polytope. However, realizations seen as images of maps do. Thus, when we work with orientations on realizations, we always assume that some realizing map h is fixed. As a consequence, every facet of a realization is oriented with an ordered set of points.

4.2 Approaches to stresses in higher dimensions

In this subsection we review some of the existing approaches to the notions of equilibrium and braced stresses in higher dimensions and the interconnections between them.

4.2.1 Equilibrium stress

We start with a generalization to higher dimensions of the concept of equilibrium stress on an embedding of a graph to a plane. We follow the approach presented by Rybnikov [32].

Let $\mathcal{P}$ be a ridged realization of a d-polytope P in $\mathbb{R}^{d-1}$. Let (fg) be a $(d-2)$-face separating two facets f and g. Then the face (fg) spans a $(d-2)$-dimensional hyperplane in $\mathbb{R}^{d-1}$ and it has two opposite unit normal vectors n_1 and n_2. The face (fg) is as usual oriented, thus one of the normal vectors is the positive normal vector. We denote the positive unit normal vector to (fg) within $\mathbb{R}^{d-1}$ with n_{fg}, see Fig. 4.2.1. Naturally, $n_{fg} = -n_{gf}$.

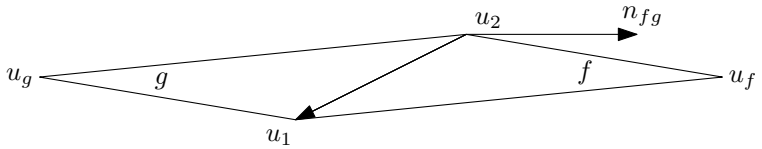

Figure 4.2.1: The positive normal n_{fg} to a $(d-2)$-face $(fg) = (u_1, u_2)$ in the case $d = 3$.

Definition 4.2.1 (Equilibrium stress)**.** *Let $\mathcal{P}$ be a ridged realization of a d-polytope in $\mathbb{R}^{d-1}$. The assignment $\Omega : \mathcal{F}_{d-2}(\mathcal{P}) \to \mathbb{R}$ of reals to $(d-2)$-faces of $\mathcal{P}$ (we shortcut $\Omega(F)$ with Ω_F) is called an equilibrium stress if*

$$\sum_{(f_i f_{i+1}) \in \delta(F)} \Omega_{f_i f_{i+1}} \operatorname{Vol}^+_{d-2}(f_i f_{i+1}) n_{f_i f_{i+1}} = 0 \tag{4.2.1}$$

for every $(d-3)$-face F of $\mathcal{P}$, where the sum goes over the cycle $\delta(F)$ of $(d-2)$-faces adjacent to F.

We remark that the notation that we use in the definition above is different from the notation that we use in the 3d case, Definition 2.2.1: In the 3d case every $(d-2)$-face is an edge and we denote it through its endpoints. In the higher dimensions this notation is inapplicable and we use the notation through the incident faces. However the two definitions are consistent, see Fig. 4.2.2 and the discussion of the 3d case below.

We call the equation Eq. (4.2.1) the *local equilibrium condition.* The stresses are assigned to nonoriented faces, for a $(d-2)$-face (fg), $\Omega_{(fg)} = \Omega_{(gf)}$. We also note that the volumes in the definition are unsigned (positive).

The notion of equilibrium stress is clearly invariant under isometries of $\mathbb{R}^{d-1}$: Let $\mathcal{P}$ be a ridged realization of a d polytope P in $\mathbb{R}^{d-1}$, let $h : \mathbb{R}^{d-1} \to \mathbb{R}^{d-1}$ be an isometry, let $\mathcal{Q} = h(\mathcal{P})$ be the image of $\mathcal{P}$ under the isometry h. Then any equilibrium stress on $\mathcal{P}$ is an equilibrium stress on $\mathcal{Q}$.

Equilibrium stresses on $\mathcal{P}$ form a linear space w.r.t. the pointwise addition and multiplication with real scalars. We denote this space with $\mathrm{EQ}(\mathcal{P})$. For a planar realization $\mathcal{P}$ we call and equilibrium stress Ω *positive* if it is positive on every nonboundary $(d-2)$-face, that is $\Omega_{fg} > 0$, $\forall (fg) \in \mathcal{F}_{d-2}(\mathcal{P}), f, g \neq f_0$, where f_0 is the outerfacet. In applications we mainly need the following global reformulation of the equilibrium condition:

Lemma 4.2.1 (Global equilibrium condition)**.** *In the setup of Definition 4.2.1, Ω is an equilibrium stress if and only if it satisfies the* global equilibrium condition

$$\sum_{(f_i f_{i+1}) \in \Gamma} \Omega_{f_i f_{i+1}} \operatorname{Vol}^+_{d-2}(f_i f_{i+1}) n_{f_i f_{i+1}} = 0, \tag{4.2.2}$$

where Γ *is any cycle* $\Gamma = \{f_1, f_2, \dots, f_n = f_1\}$ *of adjacent facets* $f_i \sim f_{i+1}$ *of* $\mathcal{P}$.

Proof. The implication from global to local is trivial. To check the reverse we show that any cycle Γ in the graph of a dual polytope $\Gamma \in \mathrm{Sk}_1(\mathcal{P}^*)$ can be decomposed into a collection of elementary cycles — boundaries of 2-faces. This is true since the 1-homologies of $\mathcal{P}$ are null. □

The link to the 3d case. For $d = 3$, the $(d-2)$-dimensional faces are edges, so the stress defined by Definition 4.2.1 assigns reals to the edges. An edge e can be denoted through its two endpoints, $e = (u_i u_j)$ or through two incident faces, $e = (gf)$. In the 3-dimensional setup of Definition 2.2.1 we follow a well established tradition and use the notation through the endpoints. In the higher dimensional setup of Definition 4.2.1, the $(d-2)$-face is an arbitrary $(d-2)$-dimensional convex polytope and the notation through the endpoints in not applicable. Thus we use the notation through the incident faces. In case $d = 3$ both definitions are applicable and define the same object. Indeed, by definition

$$\mathrm{Vol}^+_{d-2}(fg) n_{gf} = (u_j - u_i)^\perp$$

for an edge $(u_i u_j)$ incident to faces f and g so that g lies to the left and f lies to the right of $\overrightarrow{u_j u_i}$. Thus the d-dimensional equilibrium condition of Eq. (4.2.1) is the $\pi/2$ rotation of the 3-dimensional equilibrium condition of Eq. (2.2.1), see Fig. 4.2.2.

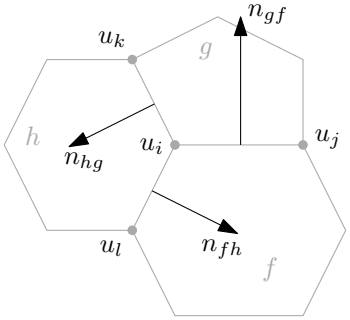

$$n_{gf} = (u_j - u_i)^\perp / |u_j - u_i|$$

$$\begin{aligned} 0 &= \textstyle\sum_{(f_i f_{i+1}) \in \delta(u_i)} \omega_{f_i f_{i+1}} Vol^+_{d-2}(f_i f_{i+1}) n_{f_i f_{i+1}} \\ &= \omega_{gf}|u_j - u_i| n_{gf} + \omega_{hg}|u_k - u_i| n_{hg} + \omega_{fh}|u_l - u_i| n_{fh} \\ &= (\omega_{gf}(u_j - u_i) + \omega_{hg}(u_k - u_i) + \omega_{fh}(u_l - u_i))^\perp = 0 \end{aligned}$$

Figure 4.2.2: The link between the 3-dimensional and the higher dimensional setups.

4.2.2 Braced stress

Below we generalize to higher dimensions the notion of braced stress that we introduced in Sect. 2.3. As for the equilibrium stress, the generalization contains the 3d case as a special case. We do not follow in our presentation any previously published text as we are not aware of any that describes the object that satisfies our needs. However the object that we define is closely connected to Colin de Verdière matrices for graphs of d-polytopes and as a source of inspiration we used the work of Izmestiev on the subject [17].

Our generalization is direct and to use the definition of 3d braced stress in higher dimensions we start with reviewing some approaches to generalizing the notion of cross product.

Generalization of cross product to higher dimensions

Let e be a convex k-polytope in $\mathbb{R}^d$. We remind that we call e *oriented* if it comes with an ordered set of $k+1$ affinely independent points $(e_1, e_2, \dots, e_{k+1})$ in it.

For a $(d-2)$-dimensional embedding of a $(d-2)$-polytope e in $\mathbb{R}^d$ that is oriented by a chosen set of points $e_1, \dots e_{d-1}$, and any additional point $v \in \mathbb{R}^d$ we define the oriented volume

of the convex hull of e, v and the origin as

$$\mathrm{Vol}_d(e, v, \mathbf{0}) = \det(e_1, \dots e_{d-1}, v) \frac{\mathrm{Vol}^+_{d-2}(e)}{\mathrm{Vol}^+_{d-2}(e_1, \dots e_{d-1})}$$

and we use a natural shortcut notation $[e, v, \mathbf{0}] := \mathrm{Vol}_d(e, v, \mathbf{0})$. Clearly, $[e, v, \mathbf{0}]$ is linear on v and thus there exists a vector $U_e \in \mathbb{R}^d$ such that $[e, v, \mathbf{0}] = \langle U_e, v\rangle$ for every $v \in \mathbb{R}^d$. This motivates the definition (see Fig. 4.2.3):

Definition 4.2.2 (Generalization of cross product)**.** *Let e be an oriented $(d-2)$-polytope in $\mathbb{R}^d$. We define the vector $U_e \in \mathbb{R}^d$ such that*

$$\langle U_e, v\rangle = \mathrm{Vol}_d(e, v, \mathbf{0}) \quad \forall v \in \mathbb{R}^d.$$

In the case of $d = 3$, the polytope e is a directed line segment $e = (a, b)$ and $U_e = a \times b$, thus U_e is a natural generalization of the cross product. The vector U_e is clearly orthogonal to the hyperplane $(\mathbf{0}, e)$ spanned by the origin and the $(d-2)$-polytope e. Indeed, a stronger geometrical property holds:

Lemma 4.2.2. *Let e be an oriented $(d-2)$-polytope in $\mathbb{R}^d$ lying in the affine hyperplane $\{x_d = 1\}$. Then*

$$\mathrm{pr}_{\{x_d=0\}} U_e = -\mathrm{Vol}^+_{d-2}(e) n_e, \tag{4.2.3}$$

where $\mathrm{pr}_{\{x_d=0\}}$ is the orthogonal projection to the hyperplane $\{x_d = 0\} \subset \mathbb{R}^d$ and n_e is the positively oriented unit normal to e inside the hyperplane $\{x_d = 1\}$.

As an immediate corollary we also have that

Corollary 4.2.1. *In the setup of the lemma above*

$$\langle U_e, n_e\rangle = -\mathrm{Vol}^+_{d-2}(e).$$

Proof of Lemma 4.2.2. By the definition of U_e and n_e it is enough to prove the lemma for the case e is a simplex with the orientation given by an order on its vertices $e = (e_1, \dots e_{d-1})$.

Trivially U_e is orthogonal to the hyperplane $(\mathbf{0}, e)$ spanned by the origin and e. Thus, $\mathrm{pr}_{\{x_d=0\}} U_e$ is parallel to n_e, and it remains to show that

$$\langle U_e, n_e\rangle = -\mathrm{Vol}^+_{d-2}(e).$$

Let $e_k = \bar{e}_k + n_d$ where $\bar{e}_k$ lies in $\{x_d = 0\}$ and $n_d = (0, \dots, 0, 1)^T$ is the unit normal to $\{x_d = 0\}$. Then by the definition of U_e the right hand side equals

$$\begin{aligned}
\langle U_e, n_e\rangle &= \det(e_1, \dots, e_{d-1}, n_e) \\
&= \det(\bar{e}_1 + n_d, \dots, \bar{e}_{d-1} + n_d, n_e) \\
&= \det(\bar{e}_1, \dots, \bar{e}_{d-1}, n_e) + \sum_{1 \le i \le d} (-1)^{d-k} \det\left((\bar{e}_1, \dots \bar{e}_{d-1}) \setminus \bar{e}_k, n_e, n_d\right) \\
&= \sum_{1 \le i \le d-1} (-1)^{d-k} \det\left((\bar{e}_1, \dots \bar{e}_{d-1}) \setminus \bar{e}_k, n_e, n_d\right),
\end{aligned}$$

where we denote with $(\bar{e}_1, \dots \bar{e}_{d-1}) \setminus \bar{e}_k$ the ordered set of points with missing $\bar{e}_k$. The last equation holds since $\det(\bar{e}_1, \dots, \bar{e}_{d-1}, n_e) = 0$ as a determinant of d vectors lying in a $(d-1)$-dimensional hyperplane $\{x_d = 0\}$. On the other hand $\mathrm{Vol}^+_{d-2}(e)$ equals the volume of the projection of e onto $\{x_d = 0\}$:

$$\begin{aligned}
\mathrm{Vol}^+_{d-2}(e) &= \mathrm{Vol}^+_{d-2}(\bar{e}_1 \dots \bar{e}_{d-1}) \\
&= \det(\bar{e}_1 - \bar{e}_{d-1}, \dots, \bar{e}_{d-2} - \bar{e}_{d-1}, n_e, n_d) \\
&= \sum_{1 \le i \le d-1} (-1)^{d-1-k} \det((\bar{e}_1, \dots, \bar{e}_{d-1}) \setminus \bar{e}_k, n_e, n_d).
\end{aligned}$$

□

Braced stress

Let $\mathcal{P}$ be a ridged realization of a d-polytope $\mathcal{P}$. Then for every $(d-2)$-face (fg) of $\mathcal{P}$ we can define the generalized cross product $U_{(fg)}$, see Fig. 4.2.3.

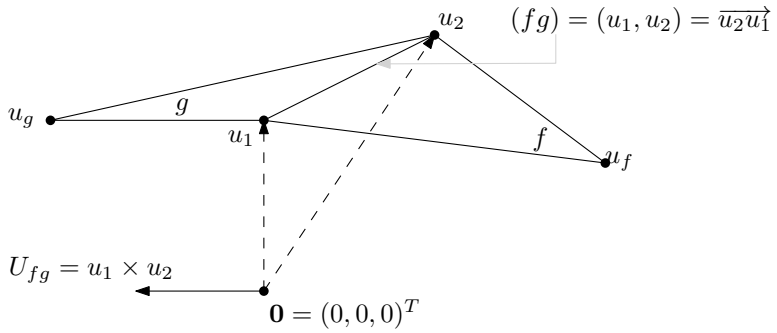

Figure 4.2.3: The generalized cross product U_{fg} of a $(d-2)$-face (fg) of a ridged realization of a d-polytope in case $d = 3$. In $3d$ case the face (fg) is an oriented edge (u_1, u_2) and $U_{fg} = u_1 \times u_2$. We remind that an edge oriented with an order on its vertices is directed counterintuitive.

We use the generalized cross product $U_{(fg)}$ very often, so, when it does not lead to confusion we use a shortcut notation which omits brackets and write U_{fg} instead of $U_{(fg)}$. With the generalization of the cross product in hands we can define braced stresses in $\mathbb{R}^d$:

Definition 4.2.3 (Braced stress)**.** *Let $\mathcal{P}$ be a ridged realization of a d-polytope in $\mathbb{R}^d$. The assignment $\Omega : \mathcal{F}_{d-2}(\mathcal{P}) \to \mathbb{R}$ of reals to $(d-2)$-faces of $\mathcal{P}$ is called a* braced stress *if*

$$\sum_{(f_i f_{i+1}) \in \delta(F)} \Omega_{f_i f_{i+1}} U_{f_i f_{i+1}} = 0 \tag{4.2.4}$$

for every $(d-3)$-face F of $\mathcal{P}$, where the sum goes over the cycle $\delta(F)$ of $(d-2)$-faces adjacent to F and we denote with U_{fg} the generalized cross product for a $(d-2)$-face (fg) of $\mathcal{P}$.

We call Eq. (4.2.4) from the definition above the *local braced equilibrium condition.*

Lemma 4.2.3 (Global property of the braced stresses)**.** *In the setup of Definition 4.2.3, Ω is a braced stress if and only if it satisfies the* global *braced equilibrium condition:*

$$\sum_{(f_i f_{i+1}) \in \Gamma} \Omega_{f_i f_{i+1}} U_{f_i f_{i+1}} = 0,$$

where Γ is any cycle $\Gamma = \{f_1, f_2, \ldots, f_n = f_1\}$ of adjacent facets $f_i \sim f_{i+1}$ of $\mathcal{P}$.

Proof. The proof mimics the proof of Lemma 4.2.1. □

Braced stresses on $\mathcal{P}$ form a linear space w.r.t. the pointwise addition and multiplication with real scalars. We denote this space with $\mathrm{BR}(\mathcal{P})$.

A second notation for the cross product and the braced equilibrium condition

A slightly different point of view on the generalization of the cross product is possible, that produces a binary operation.

Let F be a $(d-3)$-dimensional polytope in $\mathbb{R}^d$ and let u be any vector in $\mathbb{R}^d$. Then we define the cross product

$$F \times u := U_{(F,u)},$$

where we denote with (F, u) the convex hull $\mathrm{Conv}(F, u)$. The defined operation is linear on the second argument: Indeed, by definition $F \times u = U_{(F,u)}$ is such a vector that

$$U_{(F,u)}x = \mathrm{Vol}_d((F, u), x, \mathbf{0}) = \det(u_1^F, \ldots, u_{d-2}^F, u, x)\frac{\mathrm{Vol}^+_{d-3}(F)}{\mathrm{Vol}^+_{d-3}(u_1^F, \ldots u_{d-2}^F)}$$

for any $x \in \mathbb{R}^d$, where $(u_1^F, \ldots u_{d-2}^F)$ is any set of affinely independent points in F. The right hand side is linear on u, thus

$$\begin{aligned} U_{F,\lambda u+\beta v}x = \lambda \det(F, u, x) + \beta \det(F, v, x) = \lambda U_{(F,u)}x + \beta U_{(F,v)}x, \quad \forall x \in \mathbb{R}^d \\ \Leftrightarrow U_{F,\lambda u+\beta v} = \lambda U_{(F,u)} + \beta U(F, v) \\ \Leftrightarrow F \times (\lambda u + \beta v) = \lambda F \times u + \beta F \times v. \end{aligned}$$

So we have the 3-dimensional cross product of two vectors $a \times b$ generalized to $\mathbb{R}^d$ with $F \times u$ where F is a $(d-3)$-dimensional polytope and u is a vector in $\mathbb{R}^d$. (We remark, that for the definition F can be any $(d-3)$-dimensional measurable subset of $\mathbb{R}^d$, however we never use generality more than of a polytope.)

Braced equilibrium condition revisited

A binary operation introduced above allows a convenient restatement of the braced equilibrium condition for simplicial polytopes. Let e be a $(d-2)$-dimensional face of a polytope $\mathcal{P}$. Then it allows two points of views: (1) as a $(d-2)$-face separating two facets f and g and then we use the notation $e = (fg)$ or (2) as a $(d-2)$-face spanned by one of its subfaces, a $(d-3)$ face F, and the vertex u of e that does not lie in this subface, $u \in e \setminus F$ Then we use the notation $e = (F, u)$, see Fig. 4.2.4. These two points of view are equivalent and we use the freedom to switch between them depending on the context.

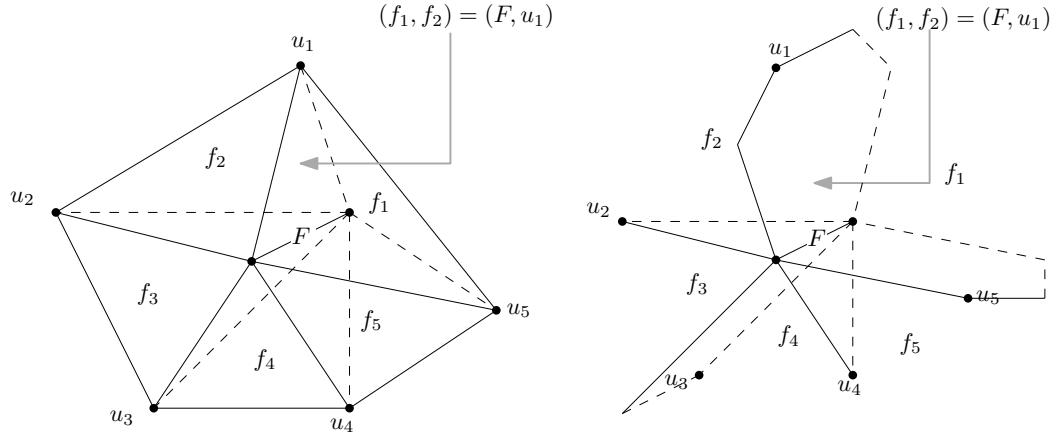

Figure 4.2.4: The cycle of $(d-2)$-faces (F, u_i) incident to a $(d-3)$-face F, in simplicial case (left) and in general case (right), for $d = 4$.

Let us now return to the definition of braced stress. The braced equilibrium condition states that

$$\sum_{(f_i f_{i+1}) \in \delta(F)} \Omega_{f_i f_{i+1}} U_{f_i f_{i+1}} = 0$$

for every $(d-3)$-face F of $\mathcal{P}$, where the sum goes over the cycle of $(d-2)$-faces adjacent to F. Thus, every $(d-2)$-face $(f_i f_{i+1})$ is in fact a face spanned by the $(d-3)$-face F and some vertex u_i that does not lie in F, thus $(f_i f_{i+1}) = (F, u_i)$, see Fig. 4.2.4. The equation $(f_i f_{i+1}) = (F, u_i)$

assumes an orientation on F, we choose it so that the equation holds: as usual we orient F with an order on its vertices $F = (u_1^f, \dots u_{d-2}^f)$ so that adding the vertex u_i to the end makes the orientation on $(F, u_i) = (u_1^f, \dots, u_{d-1}^f, u_i)$ coincide with the orientation on $(f_i f_{i+1})$. It is a straightforward check that the orientation on F induced by the equation $(f_i f_{i+1}) = (F, u_i)$ does not depend on the index i.

The above notation allows us to operate with d-dimensional braced stresses in exactly the same way as in 3-dimensional case: We rewrite the left hand side of Eq. (4.2.4):

$$\sum_{(f_i f_{i+1}) \in \delta(F)} \Omega_{f_i f_{i+1}} U_{f_i f_{i+1}} = \sum_{u_j \in N(F)} \Omega_{(F,u_j)} F \times u_j$$
$$= F \times \left(\sum_{u_j \in N(F)} \Omega_{(F,u_j)} u_j \right),$$

where the last transition holds since the generalized cross product is linear on the second argument; and where $N(F)$ denotes the set of vertices of $\mathcal{P}$ that are "neighbours" of the $(d-3)$-face F, that is whose convex hull with F form a $(d-2)$-face of $\mathcal{P}$. Thus, the local braced equilibrium condition of Eq. (4.2.4) is equivalent to

$$F \times \left(\sum_{u_j \in N(F)} \Omega_{(F,u_j)} u_j \right) = 0.$$

This in turn is equivalent to that the sum $\sum_{u_j \in N(F)} \Omega_{(F,u_j)} u_j$ lies in the $(d-2)$-dimensional plane spanned by the face F and the origin, what we can denote as

$$\sum_{u_j \in N(F)} \Omega_{(F,u_j)} u_j \parallel F. \tag{4.2.5}$$

So, the notion of braced stress in $\mathbb{R}^d$ is indeed a straightforward generalization of the braced stress for graphs in $\mathbb{R}^3$, where instead of the set of neighbours $(u_j)_{j \in N(i)}$ of a vertex u_i we have a set of $(d-2)$-faces $(F, u_j)_{j \in N(F)}$ incident to a given $(d-3)$-face F, see Fig. 4.2.4. For $d = 3$ the $(d-3)$-face F of $\mathcal{P}$ is a vertex u and Eq. (4.2.5) is exactly the braced equilibrium condition in 3d.

For nonsimplicial polytopes we also can use the cross-product notation in higher dimensions. The definition of the cross product $F \times u$ does not use the fact that F is simplicial. For a nonsimplicial $(d-2)$-face e that has a $(d-3)$-dimensional subface F we can select any point u that does not lie in this subface, $u \in e \setminus F$ and then clearly

$$U_{f_i f_{i+1}} = \frac{\mathrm{Vol}^+_{d-2}(e_i \in \delta(F) : u_i \in e_i)}{\mathrm{Vol}^+_{d-2}(\mathrm{Conv}(F, u_i))} F \times u_i,$$

where in the nominator we compute the volume of the $(d-2)$-face adjacent to F that contains the vertex u_i.

Thus for nonsimplicial polytopes the braced equilibrium condition is equivalent to

$$\sum_{u_i \in N(F)} \Omega_{(F,u_i)} \frac{\mathrm{Vol}^+_{d-2}(e_i \in \delta(F) : u_i \in e_i)}{\mathrm{Vol}^+_{d-2}(\mathrm{Conv}(F, u_i))} u_i \parallel F.$$

This however looks pretty monstrous and we never have to use it.

4.2.3 From equilibrium stresses to braced stresses and back

A braced stress on a flat embedding is an equilibrium stress

Lemma 4.2.4. *Let $\mathcal{P}$ be a ridged realization of a d-polytope P in some hyperplane α of $\mathbb{R}^d$ that does not contain the origin. Then every braced stress ω on $\mathcal{P}$ is an equilibrium stress on $\mathcal{P}$.*

Proof. W.l.o.g we assume that $\alpha = \{x_d = 1\}$. Then by Lemma 4.2.2

$$\mathrm{pr}_{\{x_d=0\}} U_{(fg)} = -\operatorname{Vol}^+_{d-2}(fg) n_{fg}.$$

This completes the proof. □

An equilibrium stress on a flat embedding is a braced stress

Lemma 4.2.5. *Let $\mathcal{P}$ be a ridged realization of a d-polytope $\mathcal{P}$ in the $(d-1)$-dimensional Euclidean space X and let ω be an equilibrium stress on $\mathcal{P}$. Then for any realization of X as an affine hyperplane in $\mathbb{R}^d$, ω is a braced stress on $\mathcal{P}$.*

Proof. Let X be realized as a hyperplane in $\mathbb{R}^d$. We choose the Euclidean coordinates so that this hyperplane is $X = \{x_d = 1\}$.

We prove that for every $(d-3)$-face F of $\mathcal{P}$

$$\sum_{(f_i f_{i+1}) \in \delta(F)} \Omega_{f_i f_{i+1}} U_{f_i f_{i+1}} = 0.$$

We do it in two steps: (1) we prove that the projection of the sum onto the $\{x_d = 0\}$ hyperplane is zero and (2) we prove that the component orthogonal to $\{x_d = 0\}$ is zero as well.

(1) Indeed, by Lemma 4.2.2

$$\mathrm{pr}_{\{x_d=0\}} \left(\sum_{(f_i f_{i+1}) \in \delta(F)} \Omega_{f_i f_{i+1}} U_{f_i f_{i+1}} \right) = - \sum_{(f_i f_{i+1}) \in \delta(F)} \Omega_{f_i f_{i+1}} \operatorname{Vol}(f_i f_{i+1}) n_{f_i f_{i+1}} = 0$$

by the definition of equilibrium stress.

(2) We prove that

$$\mathrm{pr}_{\{x^d=0\}^T} \left(\sum_{(f_i f_{i+1}) \in \delta(F)} \Omega_{f_i f_{i+1}} U_{f_i f_{i+1}} \right) = 0.$$

First we prove that the notion of braced stress is invariant under parallel translations within the affine hyperplane $\{x_d = 1\}$: Let $h_a : \mathbb{R}^d \to \mathbb{R}^d$ be the affine transformation of $\mathbb{R}^d$ that sends every $x \in \{x_d = 1\}$ to $h_a(x) = x + a$ for some vector $a \in \{x_d = 0\}$ and such that $h_a(\mathbf{0}) = \mathbf{0}$. This transformation is trivially volume preserving. Thus,

$$\begin{aligned} \langle U_{(h_a(fg))}, v \rangle &= \operatorname{Vol}_d(h_a(fg), v, \mathbf{0}) \\ &= \operatorname{Vol}_d((fg), h_a^{-1}(v), h_a^{-1}(\mathbf{0})) = \langle U_{fg}, h_a^{-1}(v) \rangle \qquad \forall v \in \mathbb{R}^d, \end{aligned}$$

where the second transition holds since h_a preserves volumes and the last transition holds since $h_a(\mathbf{0}) = \mathbf{0}$. The stress ω is a braced stress on the translated polytope $h_a(\mathcal{P}) = \mathcal{P} + a$ if and

only if

$$\begin{aligned}
&\sum_{(f_if_{i+1})\in\delta(F)} \Omega_{f_if_{i+1}} U_{h_a(f_if_{i+1})} = 0 \\
\Leftrightarrow &\sum_{(f_if_{i+1})\in\delta(F)} \Omega_{f_if_{i+1}} \langle U_{h_a(f_if_{i+1})}, v\rangle = 0 \qquad \forall v \in \mathbb{R}^d \\
\Leftrightarrow &\sum_{(f_if_{i+1})\in\delta(F)} \Omega_{f_if_{i+1}} \langle U_{f_if_{i+1}}, h_a^{-1} v\rangle = 0 \qquad \forall v \in \mathbb{R}^d \\
\Leftrightarrow &\sum_{(f_if_{i+1})\in\delta(F)} \Omega_{f_if_{i+1}} U_{f_if_{i+1}} = 0,
\end{aligned}$$

and the last condition is the definition of ω being a braced stress on $\mathcal{P}$.

Thus, the braced stress is translational invariant within $\{x_d = 1\}$ and w.l.o.g we suppose that $\mathcal{P}$ is embedded into $\{x_d = 1\}$ so that $e_d = (0, 0, \ldots, 0, 1) \in F$, or, equivalently, so that the origin lies inside the orthogonal projection of F onto $\{x_d = 0\}$. Then

$$\langle U_{(f_if_{i+1})}, e_d\rangle = \mathrm{Vol}_d((f_if_{i+1}), e_d, \mathbf{0}) = 0$$

for any (f_if_{i+1}) since e_d lies in F and thus in every (f_if_{i+1}). But by definition

$$\mathrm{pr}_{\{x_d=0\}^T} U_{fg} = \langle U_{fg}, e_d\rangle,$$

which means that every summand of the sum in question is zero, thus the whole sum is zero as well.

□

4.2.4 Scalability of braced stresses

Analogously with the 3-dimensional case, any braced stress of an embedding can be rescaled together with the embedding:

Lemma 4.2.6. *Let $C = (u_i)_{1\le i\le n}$ be a ridged realization of a simplicial d-polytope in $\mathbb{R}^d$ and let $\Omega : \mathcal{F}_{d-2}(C) \to \mathbb{R}$ be a braced stress for C. Let $C' := (\lambda(u_i)u_i)_{1\le i\le n}$ be any rescaling of C with $\lambda(u_i) \in \mathbb{R}$.*

Then the map $\mathrm{pr}_{C\to C'} : \mathbb{R}^{|\mathcal{F}_{d-2}(C)|} \to \mathbb{R}^{|\mathcal{F}_{d-2}(C)|}$ defined as

$$(\mathrm{pr}_{C\to C'}\,\Omega)_{(u_1^f,\ldots u_{d-1}^f)} = \frac{1}{\prod_{1\le i\le d-1}(\lambda(u_i^f))}\Omega_{(u_1^f,\ldots u_{d-1}^f)}, \qquad \forall (u_1^f, \ldots u_{d-1}^f) \in \mathcal{F}_{d-2}(C)$$

is a linear isomorphism between the linear spaces of braced stresses on C and C' with $\mathrm{pr}_{C\to C'} \circ \mathrm{pr}_{C'\to C} = \mathrm{Id}$.

Proof. The linearity of the map is trivial. Since the map is symmetric w.r.t C and C', to prove the lemma it is enough to show that for every braced stress Ω on C the image $\mathrm{pr}_{C\to C'}\,\Omega$ is a braced stress on C'. We prove that for every $(d-3)$-face F' of C'

$$F' \times \left(\sum_{u'_j\in N(F')} (\mathrm{pr}_{C\to C'}\,\Omega)_{(F',u'_j)} u'_j \right) = 0.$$

This holds since, for F' being the image of the face F of $\mathcal{P}$,

$$F' \times \left(\sum_{u'_j \in N(F')} (\mathrm{pr}_{C \to C'} \Omega)_{(F',u'_j)} u'_j \right) = \left(\prod_{u_i \in \mathcal{F}_0(F)} \lambda(u_i) \right) F \times \left(\sum_{u_j \in N(F)} \frac{1}{\prod_{u_i \in \mathcal{F}_0(F) \cup u_j} \lambda(u_i)} \Omega_{(F,u_j)} \lambda(u_j) u_j \right) = F \times \left(\sum_{u_j \in N(F)} \Omega_{(F,u_j)} u_j \right) = 0.$$

□

4.2.5 Canonical braced stress

Analogously to the 3d case with every d-dimensional polytopal surface $\mathcal{P}$ one associates the canonical braced stress Ω^c.

Definition 4.2.4. *Let $\mathcal{P}$ be a d-dimensional polytopal surface such that none of its facets lies on a hyperplane passing through the origin. The* canonical braced stress Ω^c *is the assignment of reals to the $(d-2)$-faces of $\mathcal{P}$ such that*

$$\phi_g - \phi_f = \Omega^c_{fg} U_{fg} \tag{4.2.6}$$

for every $(d-2)$-face (fg) separating facets f and g, where ϕ_g and ϕ_f are the polar vectors to the facets f and g.

A priory the existence of such an assignment is not guaranteed, thus we prove the existence and that the defined object is indeed a braced stress of the embedding:

Lemma 4.2.7. *The canonical braced stress is well-defined and is a braced stress on the underlying polytopal surface.*

Proof. By the definition of canonical braced stress none of the facets of $\mathcal{P}$ lie in a hyperplane passing through the origin, thus $U_{fg} \neq 0$ for every $(d-2)$-face of $\mathcal{P}$. It remains to show that

$$\phi_g - \phi_f \parallel U_{fg}.$$

For every point $u \in (fg)$

$$\langle \phi_g - \phi_f, u \rangle = \langle \phi_g, u \rangle - \langle \phi_f, u \rangle = 1 - 1 = 0$$

and

$$\langle U_{fg}, u \rangle = 0$$

by the definition of U_{fg}. Thus U_{fg} and $\phi_g - \phi_f$ are orthogonal to the hyperplane spanned by the origin and the face (fg), so they are parallel. Thus the canonical braced stress is well-defined by Eq. (4.2.6).

To show that Ω^c is a braced stress on $\mathcal{P}$ we check the braced equilibrium condition: let $\Gamma = (f_1, f_2, \dots f_n = f_1)$ be any cyclic sequence of adjacent facets of $\mathcal{P}$, then by definition

$$\sum_{(f_i f_{i+1}) \in \Gamma} \Omega^c_{f_i f_{i+1}} U_{f_i f_{i+1}} = \sum_{\Gamma} (\phi_{f_i} - \phi_{f_{i+1}}) = 0.$$

□

Lemma 4.2.8. *Let $\mathcal{P}$ be a convex d-polytope that contains the origin in its interior. Then the canonical braced stress on $\mathcal{P}$ is positive.*

Proof. Let f and g be two adjacent facets of $\mathcal{P}$, let u_g be a vertex of $g \setminus (fg)$. Then, since $\mathcal{P}$ is convex and contains the origin in its interior, $\langle u_g, \phi_f \rangle < 1$ while $\langle u_g, \phi_g \rangle = 1$, thus

$$\langle u_g, \phi_g - \phi_f \rangle > 0. \tag{4.2.7}$$

Then we compute the sign of $\langle U_{fg}, u_g \rangle$. Let $(fg) = (u_1, \dots u_{d-1})$, then

$$\begin{aligned} \langle U_{fg}, u_g \rangle &= \mathrm{Vol}_d((fg), u_g, \mathbf{0}) \\ &= \det(u_1, \dots, u_{d-1}, u_g) \\ &= \det(u_1 - u_g, \dots, u_{d-1} - u_g, u_g), \end{aligned}$$

and since $\mathcal{P}$ is convex and contains the origin,

$$\mathrm{sign}(\det(u_1 - u_g, \dots, u_{d-1} - u_g, u_g)) = \mathrm{sign}(\det(u_1 - u_g, \dots, u_{d-1} - u_g, n_g)) > 0,$$

where n_g is the outernormal vector of the facet g and the last inequality is the definition of orientation on (fg). Thus,

$$\langle u_g, U_{fg} \rangle > 0. \tag{4.2.8}$$

The statement of the lemma follows by combining Eq. (4.2.7), Eq. (4.2.8) and the definition of the canonical braced stress, Eq. (4.2.6). □

4.3 Maxwell–Cremona lifting

The lifting approach is a very common tool to operate with convex polytopes and, more generally, with polytopal surfaces. It takes as an input a flat realization of a polytope (we remind, that in the d-dimensional setup flat means $(d-1)$-dimensional) and assigns every point of the flat realization the last coordinate following some lifting procedure. Thus the lifting approach allows us to control the geometrical features of the final d-dimensional realization through controlling the geometry of a flat realization, what is often simpler, especially in case $d = 3$ where the flat realization is a drawing on the plane.

In our presentation we generally follow the presentation by Demaine and Schulz [10].

Definition 4.3.1. *Let $\mathcal{P}$ be a flat realization of a d-polytope P in $\mathbb{R}^{d-1} = \{x_d = 0\} \subset \mathbb{R}^d$. We call an assignment of reals $h : \mathcal{F}_0(\mathcal{P}) \to \mathbb{R}$ to vertices of $\mathcal{P}$ a* lifting.

We regard $h(p)$ as a new (last) coordinate of a point $p \in \mathbb{R}^{d-1}$. Thus h lifts a point $p \in \mathbb{R}^{d-1}$ to $(p, h(p)) \in \mathbb{R}^d$.

We call a lifting *polyhedral* if the lifting of every facet is a $(d-1)$-polytope. We remark that every lifting of a simplicial polytope is polyhedral. We denote the set of all the polyhedral liftings of $\mathcal{P}$ as $L^0(\mathcal{P})$.

The lifting procedure $p \to (p, h(p))$ is complemented by the projection operation $\pi : R^d \to \mathbb{R}^{d-1}$ that simply removes the last coordinate

$$\pi(p, h(p)) \to p,$$

where $p \in \mathbb{R}^{d-1}$. Throughout the section we use $\mathrm{pr}_\alpha(u)$ for the orthogonal projection of a point $u \in \mathbb{R}^d$ to an affine hyperplane $\alpha \subset \mathbb{R}^d$. In particular, $\mathrm{pr}_{\{x_d=c\}}(u)$ for a real $c \in \mathbb{R}$ projects $u \in \mathbb{R}^d$ to the affine hyperplane $\{x_d = c\} \subset \mathbb{R}^d$, and in terms of the projection π defined above

$$\mathrm{pr}_{\{x_d=c\}}(u) = (\pi(u), c).$$

Bijection between the nonhorizontal vectors and the nonvertical affine hyperplanes in $\mathbb{R}^d$: To every nonvertical affine hyperplane α in $\mathbb{R}^d$ we put in one-to-one correspondence a vector $a \in \mathbb{R}^d$ (we say that the vector a *defines the affine hyperplane* α) and a function $h : \mathbb{R}^d \to \mathbb{R}$ that we call the *height function*. The function h computes the last coordinate of the orthogonal projection of a point $u \in \mathbb{R}^d$ to the affine hyperplane α. Thus $h(u)$ is such a number that

$$(\pi(u), h(u)) \in \alpha.$$

The vector a is such a vector that

$$h(u) = \langle a, \mathrm{pr}_{\{x_d=1\}} u \rangle \quad \forall u \in \mathbb{R}^d.$$

Such a vector exists since h restricted to the horizontal hyperplane $\{x_d = 0\}$ is an affine function. Thus the vector a defines the lifting of the affine hyperpane $\{x_d = 1\}$ to α through the assignment

$$u \to (\pi(u), \langle u, a \rangle) \quad \forall u \in \{x_d = 1\}.$$

Thus, for every polyhedral lifting of a flat realization of a polytope $\mathcal{P}$, to every face f of $\mathcal{P}$ that is lifted to an affine hyperplane α_f we associate a vector $a_f \in \mathbb{R}^d$ and a height function $h_f : \mathbb{R}^d \to \mathbb{R}$.

Conversely, a set of vectors $(a_f)_{f \in \mathcal{F}_{d-1}(\mathcal{P})}$ (or, equivalently, a set of functions h_f or of hyperplanes α_f) defines a polyhedral lifting of $\mathcal{P}$ if and only if $h_f(u) = h_g(u)$ (or, equivalently, $\langle \mathrm{pr}_{\{x_d=1\}} u, a_f \rangle = \langle \mathrm{pr}_{\{x_d=1\}} u, a_g \rangle$) for every $u \in (fg)$ for every pair of adjacent facets f and g.

4.3.1 Maxwell–Cremona lifting

The Maxwell–Cremona lifting is a lifting algorithm that produces a polyhedral lifting given a flat embedding and an equilibrium stress on this embedding. The Maxwell–Cremona lifting allows us to efficiently control the geometry of the lifting through the properties of the stress, in particular, the convexity of the resulting lifting is directly controlled by the signs of the equilibrium stress. Below we describe the algorithm.

Let $\mathcal{P}$ be a flat realization of a d-polytope, and let Ω be an equilibrium stress on $\mathcal{P}$. First we embed the $\mathbb{R}^{d-1}$ containing $\mathcal{P}$ into $\mathbb{R}^d$ as the $\{x_d = 1\}$ affine hyperplane. We denote the vertices of this homogenized embedding of $\mathcal{P}$ with u_i. Second, we assign a vector $a_f \in \mathbb{R}^d$ to every facet f of $\mathcal{P}$ in such a way that for any two adjacent facets f and g

$$a_g - a_f = -\Omega_{fg} U_{fg}. \tag{4.3.1}$$

To produce this assignment we start with assigning an arbitrarily value a_{f_0} to an arbitrarily facet f_0 and proceed iteratively. To verify that this assignment process is well-defined we show that

$$\sum_{(f_i f_{i+1}) \in \Gamma} U_{f_i f_{i+1}} \Omega_{f_i f_{i+1}} = 0$$

for every cycle $\Gamma = (f_1 \dots f_m = f_1)$ in $\mathrm{Sk}_1(\mathcal{P}^*)$. This is however guaranteed by the definition of braced stress, and due to Lemma 4.2.5, every equilibrium stress on a realization in $\{x_d = 1\}$ is a braced stress.

We use the correspondence between the affine hyperplanes and the vectors in $\mathbb{R}^d$ discussed above to assign to every facet f of $\mathcal{P}$ the lifting plane α_f defined by the vector a_f through

$$u \to (\pi(u), \langle a_f, \mathrm{pr}_{\{x_d=1\}}(u) \rangle),$$

where u is any vertex of f. In terms of the height function, we assign to every vertex u_i of $\mathcal{P}$ a new height $h_f(u_i) = \langle a_f, \mathrm{pr}_{\{x_d=1\}}(u_i) \rangle$ where f is any facet containing u_i in its boundary.

To prove the consistency of the lifting procedure we show that for any two facets f and g such that each of them contains a vertex u, the liftings of u defined by the facets f and g coincide:

$$h_f(u) = h_g(u).$$

By connectivity arguments, this is enough to check for the case when f and g share a common $(d-2)$-face (fg) and $u \in (fg)$. Then

$$h_g(u) - h_f(u) = \langle u, a_g - a_f \rangle = \langle u, \Omega_{fg} U_{fg} \rangle = \Omega_{fg} \langle u, U_{fg} \rangle = 0,$$

where the last equation holds since $u \in (fg)$.

Given a flat realization $\mathcal{P}$ of a d-polytope P and an equilibrium stress Ω on $\mathcal{P}$ the Maxwell–Cremona lifting of $\mathcal{P}$ by Ω is defined uniquely up to the initial choice of lifting of any one facet f_0 of $\mathcal{P}$. This motivates the following definitions:

Definition 4.3.2. *(1) Let $\mathcal{P}$ be a flat realization of a d-polytope P in $\{x_d = 1\} \subset \mathbb{R}^d$. We call two polyhedral liftings h_1 and h_2 of $\mathcal{P}$* equivalent *and denote it with $h_1 \sim h_2$ if there exists a vector $v \in \mathbb{R}^d$ such that*

$$h_1(u_i) = h_2(u_i) + \langle v, u_i \rangle$$

for every vertex u_i of $\mathcal{P}$.

(2) Let $\mathcal{P}$ be a flat realization of a d-polytope $\mathcal{P}$ in $\mathbb{R}^{d-1}$. The space of polyhedral liftings *$L(\mathcal{P})$ is the set of polyhedral liftings $L_0(\mathcal{P})$ modulo the equivalence relation,*

$$L(\mathcal{P}) := L^0(\mathcal{P}) / \sim .$$

Lemma 4.3.1. *The space of polyhedral liftings is a linear space with respect to the pointwise addition and multiplication to scalars.*

Proof. The lemma is equivalent to that

$$\begin{aligned} &h_1 + h_2 \sim h_1' + h_2' && \forall h_1 \sim h_1', h_2 \sim h_2' \in L^0(\mathcal{P}), \\ &ch_1 \sim ch_1' && \forall h_1 \sim h_1' \in L^0(\mathcal{P}), c \in \mathbb{R}, \end{aligned}$$

what follows immediately from the definition of the equivalence relation. □

Theorem 4.3.1. *Let $\mathcal{P}$ be a flat realization of a d-polytope P. Then the Maxwell–Cremona lifting procedure defines a linear map from the linear space of equilibrium stresses* $\mathrm{EQ}(\mathcal{P})$ *to the linear space of polyhedral liftings $L(\mathcal{P})$ of $\mathcal{P}$,*

$$\mathrm{MC} : \mathrm{EQ}(\mathcal{P}) \to L(\mathcal{P}).$$

Proof. We prove that

$$\begin{aligned} &\mathrm{MC}(\Omega_1 + \Omega_2) = \mathrm{MC}(\Omega_1) + \mathrm{MC}(\Omega_2), && \forall \Omega_1, \Omega_2 \in \mathrm{EQ}(\mathcal{P}), \\ &\mathrm{MC}(c\Omega) = c\,\mathrm{MC}(\Omega), && \forall \Omega \in \mathrm{EQ}(\mathcal{P}), c \in \mathbb{R}. \end{aligned}$$

We start with additivity. Let f_0 be any facet of $\mathcal{P}$. We pick an element (a lifting) of each of the equivalence classes of liftings $\mathrm{MC}(\Omega_1)$, $\mathrm{MC}(\Omega_2)$ and $\mathrm{MC}(\Omega_1 + \Omega_2)$:

$$h_1 \in \mathrm{MC}(\Omega_1), h_2 \in \mathrm{MC}(\Omega_2), h_s \in \mathrm{MC}(\Omega_1 + \Omega_2)$$

such that the face f_0 is lifted to the hyperplane $\{x_d = 0\}$ in each of h_1, h_2, h_s,

$$a_f^1 = a_f^2 = a_f^s = 0,$$

where the vectors a_f^1, a_f^2 and a_f^s define the liftings of the face f by h^1, h^2 and h^s correspondingly. We show that

$$h_1 + h_2 = h_s.$$

We prove it iteratively, and mimic the Maxwell–Cremona construction. We show that for every facet f

$$a_f^1 + a_f^2 = a_f^s.$$

As a base we use the face f_0, for which both sides are zero. Consider the iterative step going from the lifting of a facet f, for which $a_f^1 + a_f^2 = a_f^s$ to the lifting of the facet g adjacent to f, using the iterative equation Eq. (4.3.1)

$$\begin{aligned} a_f^1 - a_g^1 &= -\Omega_{fg}^1 U_{fg}, \\ a_f^2 - a_g^2 &= -\Omega_{fg}^2 U_{fg}, \\ a_f^s - a_g^s &= -(\Omega^1 + \Omega^2)_{fg} U_{fg}. \end{aligned}$$

Thus

$$a_g^1 + a_g^2 - a_g^s = (a_f^1 + a_f^2 - a_f^s) - (\Omega_{fg}^1 + \Omega_{fg}^2 - (\Omega^1 + \Omega^2)_{fg}) U_{fg} = 0 - 0 = 0,$$

what finishes the proof of additivity.

The scalability with scalars

$$\mathrm{MC}(c\Omega) = c\,\mathrm{MC}(\Omega), \quad \forall \Omega \in \mathrm{EQ}(\mathcal{P}), c \in \mathbb{R}$$

is trivial. □

4.3.2 Canonical equilibrium stress

Let $\mathcal{P}^l$ be a polytopal surface in $\mathbb{R}^d$ and $\mathcal{P}$ be its projection to an affine hyperplane α. Then this projection is naturally equipped with an equilibrium stress that we call *canonical equilibrium stress*. In this subsection we present a construction of the canonical equilibrium stress which is the direct reverse of the Maxwell–Cremona lifting procedure. Later in Subsect. 4.3.4 we present a formula for the canonical equilibrium stress based on the notion of *creasing*.

Let $\mathcal{P}^l$ be a polytopal surface in $\mathbb{R}^d$ and $\mathcal{P}$ be its projection to the affine hyperplane $\{x_d = 1\}$. Then we can try to reverse-engineer the Maxwell–Cremona lifting construction to find an equilibrium stress on $\mathcal{P}$ that would lead from the flat realization $\mathcal{P}$ to the polytopal surface $\mathcal{P}^l$.

For every facet f of $\mathcal{P}$ we can compute the vector a_f from the Maxwell–Cremona lifting procedure. Then the reverse-engineering expects that $a_g - a_f \parallel U_{fg}$ for every pair of adjacent facets f and g, and that the scaling coefficients between $a_g - a_f$ and U_{fg} constitute an equilibrium stress on $\mathcal{P}$. This is indeed the case:

Theorem 4.3.2. *Let $\mathcal{P}^l$ be a polytopal surface in $\mathbb{R}^d$, and let $\mathcal{P}$ be its orthogonal projection to the horizontal affine hyperplane $\{x_d = 1\}$. Then the assignment of reals to $(d-2)$-faces of $\mathcal{P}$:*

$$\Omega_{fg} := \frac{\langle (a_g - a_f), n_{fg} \rangle}{\mathrm{Vol}^+_{d-2}(fg)}, \quad (fg) \in \mathcal{F}_{d-2}(\mathcal{P}) \tag{4.3.2}$$

is an equilibrium stress on $\mathcal{P}$ and

$$a_g - a_f = -\Omega_{fg} U_{fg}, \tag{4.3.3}$$

where $a_f \in \mathbb{R}^d$ defines the lifting in $\mathcal{P}^l$ of a facet f of $\mathcal{P}$ and $n_{fg} \in \{x_d = 0\} \subset \mathbb{R}^d$ is the positive unit normal to the $(d-2)$-face (fg) of $\mathcal{P}$ within the affine hyperplane $\{x_d = 1\}$.

Definition 4.3.3. *We call the stress Ω constructed in Theorem 4.3.2 the* canonical equilibrium stress *on the orthogonal projection $\mathcal{P}$ of $\mathcal{P}^l$.*

We remark that the notion of equilibrium stress is translationally invariant, thus Ω is an equilibrium stress on the orthogonal projection of $\mathcal{P}^l$ to a more natural hyperplane $\{x_d = 0\}$ as well. However, the Maxwell–Cremona lifting procedure starts with a homogenized flat embedding into $\{x_d = 1\}$ and U_{fg} in Eq. (4.3.3) is computed for the face (fg) realized in $\{x_d = 1\}$ as well. Thus, to avoid unnecessary complications, we work directly with the projection plane $\{x_d = 1\}$.

Proof of Theorem 4.3.2. First we prove the second part, that

$$a_g - a_f = -\Omega_{fg} U_{fg}.$$

The proof goes in two steps, (1) we first show that $a_g - a_f \parallel U_{fg}$ and (2) then we compute the coefficient. As usual for a point u in $\mathcal{P}$ we define by $h_f(u)$ the height of the vertical projection of the point u to the hyperplane spanned by the face f of $\mathcal{P}$, or in the notation of the vectors a_f we have $h_f(u) = \langle \mathrm{pr}_{\{x_d=1\}}(u), a_f \rangle$.

Step (1): For every point u in (fg), $h_f(u) = h_g(u)$, thus

$$\langle a_g - a_f, u \rangle = h_g(u) - h_f(u) = 0.$$

Moreover, from the definition of U_{fg}

$$\langle U_{fg}, u \rangle = \mathrm{Vol}_d((fg), u, 0) = 0$$

for any point u in (fg). Thus,

$$\langle a_g - a_f, u \rangle = \langle U_{fg}, u \rangle = 0$$

for any vector u in the hyperplane $(0,(fg))$ spanned by the origin and the face (fg). Since this hyperplane has maximal dimension, its orthogonal complement is one-dimensional and thus $a_g - a_f \parallel U_{fg}$.

Step (2): Let us now compute the constant c_{fg} such that $a_g - a_f = c_{fg}U_{fg}$. We consider the dot product of both sides with n_{fg} and get

$$\langle a_g - a_f, n_{fg}\rangle = \mathrm{Vol}^+_{d-2}(fg)\Omega_{fg}$$

by the definition of Ω_{fg} (Eq. (4.3.2)) on the left hand side and

$$c_{fg}\langle U_{fg}, n_{fg}\rangle = -c_{fg}\,\mathrm{Vol}^+_{d-2}(fg)$$

by Corollary 4.2.1 on the right hand side. Thus,

$$\mathrm{Vol}^+_{d-2}(fg)\Omega_{fg} = -c_{fg}\,\mathrm{Vol}^+_{d-2}(fg),$$

that shows that the coefficient in question is exactly $-\Omega_{fg}$ and

$$a_g - a_f = -\Omega_{fg}U_{fg}.$$

Now we move on to the first part of the theorem. Clearly, Ω_{fg} is a braced stress on $\mathcal{P}$: due to Eq. (4.3.3), for every cyclic sequence $(f_1, f_2, \ldots, f_n = f_1)$ of adjacent facets of $\mathcal{P}$

$$\sum_{i=1}^{n-1} \Omega_{f_i f_{i+1}} U_{f_i f_{i+1}} = -\sum_{i=1}^{n-1}(a_{f_{i+1}} - a_{f_i}) = 0.$$

By Lemma 4.2.4 every braced stress on a flat realization in the $\{x_d = 1\}$ affine hyperplane is an equilibrium stress, what finishes the proof. □

4.3.3 Full version of Maxwell–Cremona lifting theorem

Theorem 4.3.3. *Let $\mathcal{P}$ be a flat realization of a d-polytope P in $\mathbb{R}^{d-1}$. Then*

1. *The Maxwell–Cremona lifting procedure defines an isomorphism of the linear spaces of equilibrium stresses* $\mathrm{EQ}(\mathcal{P})$ *and of polyhedral liftings $L(\mathcal{P})$ of $\mathcal{P}$,*

$$\mathrm{MC} : \mathrm{EQ}(\mathcal{P}) \to L(\mathcal{P}).$$

2. *The inverse to the Maxwell–Cremona lifting is the operation* $\mathrm{CS} : L(\mathcal{P}) \to \mathrm{EQ}(\mathcal{P})$ *of computing the canonical equilibrium stress.*

Proof. 1. This holds due to Theorem 4.3.1 and the bijectivity, which follows from part 2 of the theorem.

2. First we notice that the canonical equilibrium stress is well-defined on the space of polyhedral liftings $L(\mathcal{P})$. Indeed, that follows from the definition of the canonical equilibrium stress Eq. (4.3.2), and from the fact that the set of differences $\{(a_g - a_f)\}_{(fg)\in\mathcal{F}_{d-2}(\mathcal{P})}$ in the Maxwell–Cremona lifting procedure does not depend on the choice of a representative of the equivalence class $L(\mathcal{P})$.

To finish the proof we show that

$$\mathrm{CS}\circ\mathrm{MC} = \mathrm{Id}_{\mathrm{EQ}(\mathcal{P})}\,.$$

Let $\Omega \in \mathrm{EQ}(\mathcal{P})$ be any equilibrium stress on $\mathcal{P}$; let $\mathcal{P}^l \in \mathrm{MC}(\Omega)$ be a Maxwell–Cremona lifting of $\mathcal{P}$ by Ω; and finally let $\Omega^c = \mathrm{CS}(\mathcal{P}^l)$ be the canonical equilibrium stress generated by the projection of $\mathcal{P}^l$ back onto $\mathcal{P}$. The introduced objects are depicted on Fig. 4.3.1. We show

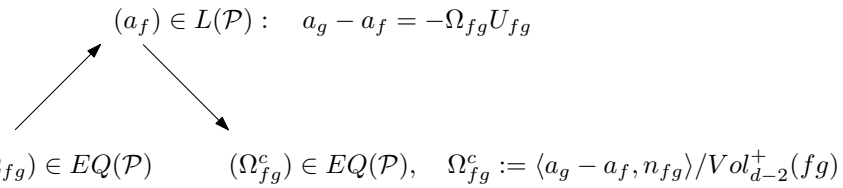

Figure 4.3.1: The way of an equilibrium stress through the Maxwell–Cremona lifting isomorphism.

that $\Omega^c = \Omega$. Indeed,

$$\Omega^c_{fg} = \frac{\langle a_g - a_f, n_{fg}\rangle}{\mathrm{Vol}^+_{d-2}(fg)} = -\frac{\langle \Omega_{fg} U_{fg}, n_{fg}\rangle}{\mathrm{Vol}^+_{d-2}(fg)} = -\Omega_{fg}\frac{\langle U_{fg}, n_{fg}\rangle}{\mathrm{Vol}^+_{d-2}(fg)} = \Omega_{fg}.$$

As usual, a_f stands for the vector defining the lifting in $\mathcal{P}^l$ of a facet f of $\mathcal{P}$. The second equation is the definition of the Maxwell–Cremona lifting procedure. The last equation is due to Lemma 4.2.2. □

4.3.4 Creasing formula for canonical equilibrium stress

Another, but equivalent approach to the canonical equilibrium stress is presented by Demaine and Schulz [10]. The authors introduce the notion of *creasing* to numerically operate with dihedral angles between facets. Authors mention there that this notion is inspired by the work of Rybnikov [32] though they don't explicitly connect the creasing with the notion of equilibrium stress. Below we accurately show that these notions coincide.

Creasing between two affine hyperplanes in $\mathbb{R}^d$

Definition 4.3.4. *Let f and g be two transversal affine hyperplanes in $\mathbb{R}^d$ and let (fg) be their intersection, an affine plane of dimension $d-2$. Let $u_1, \dots u_{d-1}$ span a full dimensional simplex X in (fg) and let $u_f \in f \setminus (fg)$ and $u_g \in g \setminus (fg)$. We define as creasing on X:*

$$c(f, g, X) := \frac{[u_1, \dots, u_{d-1}, u_f, u_g]}{[\![u_1, \dots u_{d-1}, u_f]\!][\![u_1, \dots, u_{d-1}, u_g]\!]}. \tag{4.3.4}$$

We use the *square bracket notation* for volumes: as usual by $[u_1, \dots u_{d+1}]$ we denote the oriented volume of the simplex spanned by these $d+1$ points in $\mathbb{R}^d$; and by $[\![u_1, \dots u_d]\!]$ we denote $[\bar{u}_1, \dots \bar{u}_d]$ where $\bar{u} = \pi(u)$ stands for the orthogonal projection of u to $\mathbb{R}^{d-1}$. In particular, for $u_i \in \{x_d = 1\}$

$$[\![u_1, \dots u_d]\!] = [u_1, \dots u_d, \mathbf{0}],$$

where $\mathbf{0}$ stands for the origin. In [10, Lemma 2] the following properties are observed:

Lemma 4.3.2. *In the setup of Definition 4.3.4*

1. *the creasing $c(f, g, X)$ is well-defined and does not depend on the choice of the points u_f and u_g;*
2. *$c(f, g, X) = -c(g, f, X)$;*
3. *$c(f, g, X) = \frac{h_f(u_g) - h_g(u_g)}{[\![u_1, \dots, u_{d-1}, u_g]\!]} \quad \forall u_g \in g \setminus (fg)$.*

Proof. We include the proof for completeness. The first two statements are straightforward and follow from simple computations with determinants. We prove the last one. For a hyperplane

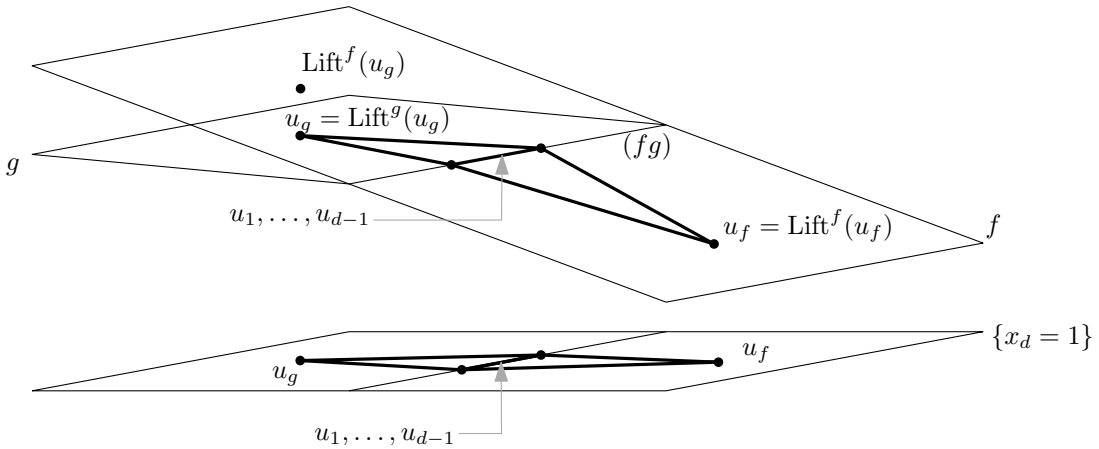

Figure 4.3.2: The creasing on the $(d-2)$-face (fg). We denote with $\text{Lift}^f(u) := (\pi(u), h_f(u))$ the lifting of a point u to the hyperplane f.

f we denote with $\text{Lift}^f(u) := (\pi(u), h_f(u))$ the vertical lifting of the point $u \in \mathbb{R}^d$ to f, see Fig. 4.3.2. Then

$$\begin{aligned}
[u_1, \dots u_{d-1}, u_f, u_g] &= \det \begin{pmatrix} u_1 & \dots & u_{d-1} & u_f & u_g \\ 1 & \dots & 1 & 1 & 1 \end{pmatrix} \\
&= \det \begin{pmatrix} u_1 & \dots & u_{d-1} & u_f & u_g - \text{Lift}^f(u_g) \\ 1 & \dots & 1 & 1 & 0 \end{pmatrix} \\
&\quad + \det \begin{pmatrix} u_1 & \dots & u_{d-1} & u_f & \text{Lift}^f(u_g) \\ 1 & \dots & 1 & 1 & 1 \end{pmatrix} \\
&= \det \begin{pmatrix} \bar{u}_1 & \dots & \bar{u}_{d-1} & \bar{u}_f & 0 \\ h_f(u_1) & \dots & h_f(u_{d-1}) & h_f(u_f) & h_g(u_g) - h_f(u_g) \\ 1 & \dots & 1 & 1 & 0 \end{pmatrix} + 0 \\
&= -(h_g(u_g) - h_f(u_g)) \det \begin{pmatrix} \bar{u}_1 & \dots & \bar{u}_{d-1} & \bar{u}_f \\ 1 & \dots & 1 & 1 \end{pmatrix} \\
&= (h_f(u_g) - h_g(u_g)) [\![u_1, \dots, u_{d-1}, u_f]\!].
\end{aligned}$$

The third transition holds since all the points $u_1, \dots u_{d-1}, u_f, \text{Lift}^f(u_g)$ lie in the affine hyperplane f, thus they are coplanar and

$$\det \begin{pmatrix} u_1 & \dots & u_{d-1} & u_f & \text{Lift}^f(u_g) \\ 1 & \dots & 1 & 1 & 1 \end{pmatrix} = \text{Vol}_d(u_1, \dots u_{d-1}, u_f, \text{Lift}^f(u_g)) = 0.$$

□

The creasing $c(f, g, X)$ is sensible to the orientation: the change of orientation on X changes the sign of $c(f, g, X)$. The orientation on facets of a polytope allows to define a robust version.

Creasing on ridges of polytope

Definition 4.3.5. *Let $\mathcal{P}^l$ be a realization of a d-polytope P as a polytopal surface in $\mathbb{R}^d$. Let $(fg) \in \mathcal{F}_{d-2}(P)$ be an oriented $(d-2)$-face separating facets f and g, let $X_{(fg)} = (u_1, \dots u_{d-1})$ be a $(d-2)$-simplex in (fg) oriented by the order on its vertices positively w.r.t the orientation*

on (fg). *Then* the creasing on the face (fg) *is*

$$c(fg) := \frac{\mathrm{Vol}^+_{d-2} X_{(fg)}}{\mathrm{Vol}^+_{d-2}(fg)} c(f,g,X_{(fg)}) = \frac{\mathrm{Vol}^+_{d-2} X_{(fg)}}{\mathrm{Vol}^+_{d-2}(fg)} \frac{[u_1,u_2,\dots u_{d-1},u_f,u_g]}{[\![u_1,\dots u_{d-1},u_f]\!][\![u_1,\dots u_{d-1},u_g]\!]}, \tag{4.3.5}$$

where $u_f \in f \setminus (fg)$ *and* $u_g \in g \setminus (fg)$.

In the next lemma we show that the canonical equilibrium stress that we defined in Definition 4.3.3 coincides with creasing:

Lemma 4.3.3. *Let* $\mathcal{P}^l$ *be a polytopal surface in* $\mathbb{R}^d$, *let* $\mathcal{P}$ *be its orthogonal projection to the horizonatal affine hyperplane* $\{x_d = 1\}$. *Let* $(fg) \in \mathcal{F}_{d-2}(\mathcal{P})$. *Then*

$$c(fg) = \Omega_{fg}$$

where $c(fg)$ *is the creasing as defined by Definition 4.3.5 and* Ω_{fg} *is the canonical equilibrium stress as defined by Definition 4.3.3.*

Proof. The right hand side of Eq. (4.3.5) is invariant under positive rescalings of the simplex $X_{(fg)}$, we pick $X_{(fg)}$ such that $\mathrm{Vol}^+_{d-2} X_{(fg)} = \mathrm{Vol}^+_{d-2}(fg)$, thus the scaling factor on the right hand side equals 1.

Let Ω be the canonical equilibrium stress as defined by Definition 4.3.3. Then for every pair of adjacent facets f and g,

$$a_g - a_f = -\Omega_{fg} U_{fg}, \quad (fg) \in \mathcal{F}_{d-2}(\mathcal{P}),$$

where a_f and a_g are as usual the vectors defining liftings of the facets f and g in $\mathcal{P}^l$. Then for every point $u \in \{x_d = 1\}$,

$$\langle a_g - a_f, u\rangle = -\Omega_{fg}\langle U_{fg}, u\rangle$$

or equivalently

$$h_g(u) - h_f(u) = -\Omega_{fg}\,\mathrm{Vol}_d((fg), u, \mathbf{0}).$$

Let the face (fg) be oriented by an ordered set of points $u_1, \dots u_{d-1}$, then the volume on the right hand side equals

$$\mathrm{Vol}_d((fg), u, \mathbf{0}) = [u_1, \dots u_{d-1}, u, \mathbf{0}] = [\![u_1, \dots u_{d-1}, u]\!],$$

where the first equation is due to the definition of volume of a simplex, thus

$$h_g(u) - h_f(u) = -\Omega_{fg}[\![u_1, \dots u_{d-1}, u]\!].$$

At least one of the facets f and g is not parallel to the affine hyperplane $\{x_d = 1\}$, w.l.o.g we assume that it is g (otherwise we recompute everything swapping f and g). The last equality holds for any point $u \in \{x_d = 1\}$. We pick any point $u_g \in \alpha_g \cap \{x_d = 1\}$ where α_g is the hyperplane supporting the facet g. Thus

$$\Omega_{fg} = -\frac{h_g(u_g) - h_f(u_g)}{[\![u_1 \dots u_{d-1}, u_g]\!]}$$

and the right hand side equals $c(fg)$ by Lemma 4.3.2. □

As a result of the observations of this subsection, the canonical equilibrium stress allows two points of view: through the reverse-engineering of Maxwell–Cremona lifting, Eq. (4.3.2) and as the creasing, Eq. (4.3.5).

Final version of creasing representation of canonical equilibrium stress

Below we wrap up the results of the creasing approach to the canonical equilibrium stresses on simplicial polytopes and give it a less technical, closed form:

Corollary 4.3.1. *Let $\mathcal{P}^l$ be a simplicial polytopal surface in $\mathbb{R}^d$ and $\mathcal{P}$ be its orthogonal projection to the $\{x_d = 0\}$ hyperplane. Then the canonical equilibrium stress equals creasing:*

$$\Omega_{fg} = \frac{[u_1, u_2, \dots u_{d-1}, u_f, u_g]}{[\![u_1, \dots u_{d-1}, u_f]\!][\![u_1, \dots u_{d-1}, u_g]\!]}, \tag{4.3.6}$$

where $(u_1, \dots u_{d-1})$ is a positively oriented set of points in (fg), and $u_f \in f \backslash (fg)$, $u_g \in g \backslash (fg)$. Eq. (4.3.6) can be given a less technical closed form:

$$\Omega_{fg} = \frac{[(f \cup g)]}{[\![f]\!][\![g]\!]}, \tag{4.3.7}$$

where facets f and g on the right hand side are taken with a positive orientation and $(f \cup g) = \mathrm{Conv}(f, g)$ with the orientation given by the ordered set of vertices $(f \cup g) = (u_1^f, u_2^f, \dots u_d^f, u_g)$ where $(u_1^f, u_2^f, \dots u_d^f)$ are vertices of f in a positive order.

Proof. We denote the vertices of (fg) in a positive order with $(u_1, \dots, u_{d-1})$ and let $u_f \in f \setminus (fg)$, $u_g \in g \setminus (fg)$. By the definition of creasing

$$\Omega_{fg} = \frac{[u_1, u_2, \dots u_{d-1}, u_f, u_g]}{[\![u_1, \dots u_{d-1}, u_f]\!][\![u_1, \dots u_{d-1}, u_g]\!]}.$$

By the definition of orientation on (fg),

$$\begin{aligned} &\mathrm{sign}_g(u_1, \dots u_{d-1}, u_g) > 0, \\ &\mathrm{sign}_f(u_1, \dots u_{d-1}, u_f) < 0, \end{aligned}$$

and thus

$$\begin{aligned} &[\![u_1, \dots u_{d-1}, u_g]\!] = [\![g]\!], \\ &[\![u_1, \dots u_{d-1}, u_f]\!] = -[\![f]\!], \\ &[\![u_1, \dots u_{d-1}, u_f, u_g]\!] = -[f, u_g] = -[(f \cup g)]. \end{aligned}$$

□

We remark, that it also follows from the proof above, that the orientation on $(f \cup g)$ does not depend on the order of f and g, and can be viewed using the common $(d-2)$-face (fg) as

$$\mathrm{sign}(f \cup g) = \mathrm{sign}((fg), u_f, u_g) = \mathrm{sign}((gf), u_g, u_f) = \mathrm{sign}(g \cup f).$$

Corollary 4.3.2. *Let $\mathcal{P}^l$ be a convex d-polytope such that its orthogonal projection $\mathcal{P}$ to the hyperplane $\{x_d = 0\}$ is a planar realization of $\mathcal{P}^l$. Then the canonical equilibrium stress on $\mathcal{P}$ is a positive equilibrium stress: $\Omega_{fg} > 0$ for every $(fg) \in \mathcal{F}_{d-2}(\mathcal{P}) : f, g \neq f_0$, where f_0 is the outerfacet of $\mathcal{P}$.*

Proof. This follows directly from the representation of Eq. (4.3.7). □

4.4 Lovász construction in $\mathbb{R}^d$

The main tool for constructing dual polytopes is, analogously to the 3d case, the Lovász duality procedure. The construction in $\mathbb{R}^d$ word for word repeats the procedure in $\mathbb{R}^3$.

Lemma 4.4.1. *Let $\mathcal{P}$ be a realization of a convex polytope P as a polytopal surface in $\mathbb{R}^d$ equipped with a braced stress Ω. Then every facet f of $\mathcal{P}$ can be assigned with a vector ϕ_f, so that for each adjacent facet g and the separating (d-2)-face (fg)*

$$\phi_g - \phi_f = \Omega_{fg} U_{fg}. \tag{4.4.1}$$

The set of vectors (ϕ_f) is uniquely defined up to translations of $\mathbb{R}^d$ and can be chosen so that

$$|\phi_f| \le \operatorname{diam}(\mathrm{Sk}_1(\mathcal{P}^*)) \max_{(fg)\in\mathcal{F}_{d-2}(\mathcal{P})} |\Omega_{fg}| \max_{u\in\mathcal{F}_0(\mathcal{P})} |u|^{d-1},$$

where $\mathrm{Sk}_1(\mathcal{P}^*)$ is the 1-skeleton of the polytope dual to $\mathcal{P}$ and $\operatorname{diam}(\mathrm{Sk}_1(\mathcal{P}^*))$ is the diameter of this graph (see remark below).

Before we proceed with the proof, we make a short remark on the diameter of the graph of a polytope. The question of an efficient bound on $\operatorname{diam}(\mathrm{Sk}_1(\mathcal{P}^*))$ in terms of the number of vertices n of the d-polytope $\mathcal{P}$ is open and is known under the name of *Hirsch conjecture*, which in 1957 initially conjectured that $\operatorname{diam}(\mathrm{Sk}_1(\mathcal{P}^*)) \le n-d$. This conjecture was disproved by Francisco Santos in 2010, see [33], and the best known general upper bound to date is

$$\operatorname{diam}(\mathrm{Sk}_1(\mathcal{P}^*)) = O(n^{\lfloor \log(d)\rfloor + 2}),$$

due to Kalai and Kleitman [18]. For a detailed overview of the subject we refer the reader to [19].

We now move on back to the lemma:

Proof of Lemma 4.4.1. To construct the family of vectors (ϕ_f), we start by assigning an arbitrary value to ϕ_{f_0} (for an arbitrary facet f_0); then we proceed iteratively using Eq. (4.4.1). To prove the consistency of the construction, we show that the differences $(\phi_g - \phi_f)$ sum to zero over every cycle Γ in the dual graph G^*. This is indeed straightforward from the definition of braced stress:

$$\sum_{(f,g)\in\Gamma} (\phi_g - \phi_f) = \sum_{(f,g)\in\Gamma} \Omega_{fg} U_{fg} = 0.$$

The vectors (ϕ_f) are unique up to the initial choice for ϕ_{f_0}. To bound $|\phi_f|$ we pick the origin as the initial value, $\phi_{f_0} := (0, \dots 0)^T$. Then, for every facet f, the value ϕ_f is bounded by

$$\phi_f \le \operatorname{diam}(\mathrm{Sk}_1(\mathcal{P}^*)) \max_{(fg)\in\mathcal{F}_{d-2}(\mathcal{P})} |\Omega_{fg}| \max_{u\in\mathcal{F}_0(\mathcal{P})} |u|^{d-1},$$

where $\operatorname{diam}(\mathrm{Sk}_1(\mathcal{P}^*))$ is the diameter of the graph of the polytope $\mathcal{P}^*$ dual to $\mathcal{P}$. □

The cone-convex realizations of polytopes in $\mathbb{R}^d$ directly generalize cone-convex embeddings of graphs in $\mathbb{R}^3$:

Definition 4.4.1. *We call a realization $\mathcal{P}$ of a d-polytope P in $\mathbb{R}^d$ as a polytopal surface* a cone-convex *realization if the cones over the facets of $\mathcal{P}$ are pointed, convex and pairwise interiorly disjoint.*

We remind that we call a cone *pointed* if it does not contain any whole line.

Lemma 4.4.2. *In the setup of Lemma 4.4.1 for a cone-convex embedding $\mathcal{P}$ and a positive braced stress Ω the vectors $(\phi_f)_{f\in\mathcal{F}_{d-1}(\mathcal{P})}$ are the vertices of a convex polytope dual to $\mathcal{P}$.*

Proof. The proof of this result word for word coincides with the original proof by Lovász for $d = 3$, Lemma 5 of [21]. □

4.5 Realizations of truncated polytopes

In this section we present an algorithm for realizing d-dimensional truncated polytopes on the integer grid $\mathbb{Z}^d$ of size polynomial in the number of vertices of the polytope. The section generalizes the presentation of the 3-dimensional algorithm of Sect. 2.5.2.

4.5.1 Truncated and stacked polytopes

Definition 4.5.1. A d-dimensional truncated polytope *is a d-polytope constructed from a d-dimensional simplex by a sequence of* truncation operations*, where each* truncation operation *cuts off one vertex of a polytope by introducing a new supporting hyperplane that separates this vertex from the other vertices of the polytope.*

Formally, let $\mathcal{P}$ be a convex d-polytope and u be a vertex of $\mathcal{P}$. Let α be any supporting hyperplane to $\mathcal{P}$ at the vertex u such that u is the only point in $\alpha \cap \mathcal{P}$, see Fig. 4.5.1. The hyperplane α is defined by some vector $v \in \mathbb{R}^d$ and a scalar $c \in \mathbb{R}$ so that $\alpha = \alpha_{v,c} = \{x \in \mathbb{R}^d : \langle x, v\rangle = c\}$ and w.l.o.g we assume that

$$\mathcal{P} \subset H^-_{v,c} = \{x \in \mathbb{R}^d : \langle x, v\rangle \leq c\}.$$

Since u is the only point in the intersection of α and $\mathcal{P}$, there exists some $\delta > 0$ such that u is the only vertex of $\mathcal{P}$ in

$$\mathbb{R}^d \setminus \{x \in \mathbb{R}^d : \langle x, v\rangle \leq c - \delta\}.$$

Then we define the result of the truncation of the vertex u from the polytope $\mathcal{P}$ as

$$\mathrm{Tr}(\mathcal{P}, u) = \mathcal{P} \cap \{x \in \mathbb{R}^d : \langle x, v\rangle \leq c - \delta\}.$$

Given the freedom of choice of the truncation plane, the truncation operation defines only the combinatorics of the resulting polytope.

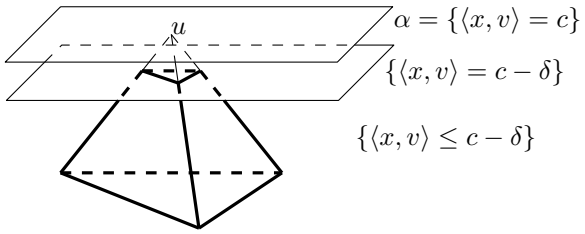

Figure 4.5.1: Truncation of a vertex u from a simplex in $\mathbb{R}^3$, the result of the truncation is marked bold.

As usual, to construct a realization of a polytope we start with constructing a cone-convex realization of its dual polytope equipped with an equilibrium stress. As in $\mathbb{R}^3$, the duals to truncated polytopes are stacked polytopes:

Let $\mathcal{P}$ be a convex polytope and $\mathcal{P}^*$ be a polytope dual to $\mathcal{P}$, let u be a vertex of $\mathcal{P}$ and $f_u = u^*$ be a facet of $\mathcal{P}^*$ dual to u. Then the operation on $\mathcal{P}^*$ that corresponds to truncating the vertex u of $\mathcal{P}$ is *stacking* a new vertex atop the facet $f_u = u^*$ of $\mathcal{P}^*$:

Definition 4.5.2. *Let $\mathcal{P}$ be a convex d-polytope with a facet f. The* stacking operation *atop the facet f adds to $\mathcal{P}$ one vertex u_f by gluing atop of f outside $\mathcal{P}$ a pyramid with base f and an apex — the new vertex u_f, such that the result after gluing is a convex polytope. We denote the resulting polytope with* $\mathrm{Stack}(\mathcal{P}, f, u_f)$*. In the above terms,* $\mathrm{Stack}(\mathcal{P}, f, u_f) = \mathrm{Conv}(\mathcal{P} \cup \{u_f\})$.

A stacked d-polytope *is a d-polytope produced from a d-simplex by a sequence of stacking operations.*

The truncation operation cuts off a vertex of a polytope and adds one new facet, thus the dual operation removes a facet of the dual polytope and adds a new vertex instead. Analogously to the truncation operation, the definition of *stacking* does not explicitly specify the location of the new vertex u_f, it only defines the combinatorics of the resulting polytope.

4.5.2 High level description of the algorithm

At the high level, the algorithm that realizes truncated polytopes on the grid is the following:

Step 1 Let $\mathcal{P}$ be a truncated polytope and $\mathcal{P}^*$ be its dual — a stacked polytope. Let the last stacking operation in some sequence of stacking operations that produce $\mathcal{P}^*$ from a simplex be the stacking of a vertex u_n to the facet f_{n-1} of the polytope $\mathcal{P}^*_{n-1}$ (clearly, $\mathcal{P}^*_{n-1}$ is a stacked d-polytope as well), thus $\mathcal{P}^* = \text{Stack}(\mathcal{P}^*_{n-1}, f_{n-1}, u_n)$. We temporarily remove the vertex u_n from $\mathcal{P}^*$ and construct a planar embedding of $\mathcal{P}^*_{n-1}$ onto the affine hyperplane $\{x_d = 1\} \subset \mathbb{R}^d$ equipped with a positive equilibrium stress Ω_{n-1} such that the facet f_{n-1} is the outerfacet of this planar embedding.

Step 2 We geometrically perform the last stacking of $\text{Stack}(\mathcal{P}^*_{n-1}, f_{n-1}, u_n)$ by putting the last vertex u_n at the point $(0, \dots 0, -d)^T \in \mathbb{R}^d$. We prove that the resulting realization of $\mathcal{P} = \text{Stack}(\mathcal{P}^*_{n-1}, f_{n-1}, u_n)$ is cone-convex and we expand the positive equilibrium stress Ω_{n-1} on $\mathcal{P}^*_{n-1}$ to a positive braced stress Ω on the whole $\mathcal{P}^* = \text{Stack}(\mathcal{P}^*_{n-1}, f_{n-1}, u_n)$.

Step 3 We use the construction of Lovász, Lemma 4.4.2, to transform the cone-convex embedding of $\mathcal{P}^*$ with the positive braced stress Ω to a realization of $\mathcal{P}$ as a convex polytope.

In the following we discuss these steps in more details.

4.5.3 Step 1: Realizations of stacked polytopes

Given a stacked polytope $\mathcal{P}$ we have to construct a planar realization of $\mathcal{P}$ with a prescribed outerfacet f, small integer coordinates, and with a small integer positive equilibrium stress. As a starting point we use the result by Demaine and Schulz [10]:

Lemma 4.5.1 (Demaine and Schulz [10], Theorem 1)**.** *Any stacked d-polytope with n vertices can be realized on the integer grid so that all the coordinates have size at most $10d^2R^2$, except for one axis, where the coordinates have size at most $6R^3$ where $R = n^{\lg(2d)}$.*

The construction of Demaine and Schulz also guaranties that the orthogonal projection $\mathcal{P}^{pr}$ of the constructed polytope onto the plane $\{x_d = 0\}$ is a planar realization of $\mathcal{P}$ inside a prescribed outerfacet f. However, the construction does not directly follow the standard Maxwell–Cremona lifting approach, to achieve better bounds the authors operate directly with liftings without handling equilibrium stresses.

Thus, Lemma 4.5.1 immediately provides us with a desired planar embedding $\mathcal{P}^{pr}$ of $\mathcal{P}$, but it does not generate an integer equilibrium stress on it. In this subsection we adapt the construction of Demaine and Schulz to produce a polynomial integer equilibrium stress for some scaling $(Cu^0_1, \dots Cu^0_n)$ of the planar embedding $\mathcal{P}^{pr}$ produced by Demaine and Schulz.

To construct stresses we follow the standard procedure:

1. We start with a realization $\mathcal{P}$ of the stacked polytope as a convex d-polytope with small integer coordinates produced by the method of Demaine and Schulz (Lemma 4.5.1);

2. We project $\mathcal{P}$ to the hyperplane $\{x_d = 0\}$ to a flat realization $\mathcal{P}^{pr}$ and compute the canonical equilibrium stress Ω^c;

3. We decompose the canonical equilibrium stress into a linear combination

$$\Omega^c = \sum_i \alpha_i \Omega^a_i$$

of *integer* equilibrium stresses Ω^a_i on parts ("building blocks") of the polytope $\mathcal{P}$. We call the stresses Ω^a_i the *atomic equilibrium stresses*;

4. We finally perturb the coefficients α_i of the linear combination to integers, preserving the signs of the resulting sum $\sum \alpha_i \Omega^a_i$.

Atomic equilibrium stress of a simplex

Definition 4.5.3. *Let $u_1, \dots u_{d+1} \in \mathbb{R}^{d-1}$ be the vertices of a d-simplex T in $\mathbb{R}^{d-1}$. Then the assignment of reals $\Omega^a : \mathcal{F}_{d-2}(T) \to \mathbb{R}$ to $(d-2)$-faces of T defined by*

$$\Omega^a_{fg} = \prod_{h \in \mathcal{F}_{d-1}(T), h \neq f,g} [h]$$

is called the atomic equilibrium stress *on T; where for $h_k \in \mathcal{F}_{d-1}(T)$ formed by all the vertices of T except u_k we denote with $[h_k]$ the signed volume of h_k:*

$$[h_k] = (-1)^{d+1-k}[(u_1, \dots, u_{d+1}) \setminus u_k],$$

where $(u_1, \dots, u_{d+1}) \setminus u_k$ is the ordered set of vertices with omitted vertex u_k.

Lemma 4.5.2. *The atomic equilibrium stress is an equilibrium stress.*

Proof. Let us consider any lifting $u^l_1, \dots, u^l_{d+1}$ of T into $\mathbb{R}^d$ such that $[u^l_1, \dots, u^l_{d+1}] > 0$, and denote the resulting simplex with $T^l = (u^l_1, \dots, u^l_{d+1})$. Then, $u_1, \dots, u_{d+1}$ is the orthogonal projection of T^l to $\{x_d = 0\}$ and thus possesses the canonical equilibrium stress.

We use the creasing formula Eq. (4.3.7) for the canonical equilibrium stress:

$$\Omega^c_{fg} = \frac{[f \cup g]}{[\![f]\!][\![g]\!]}.$$

We notice that for any $(d-2)$-face (fg) of T^l

$$[f \cup g] = [u^l_1, \dots u^l_{d+1}] = [T^l].$$

Indeed, let $f = h_k$ and $g = h_l$. Then $f = (u^l_1, \dots, u^l_{d+1}) \setminus u^l_k$ and $u^l_k \in g \setminus (fg)$ thus by the definition of $[f \cup g]$

$$\begin{aligned}[f \cup g] &= (-1)^{d+1-k}[(u^l_1 \dots u^l_{d+1}) \setminus u^l_k, u^l_k] \\ &= (-1)^{d+1-k}(-1)^{d+1-k}[u^l_1, \dots, u^l_{d+1}] = [T^l].\end{aligned}$$

Thus $[f \cup g]$ does not depend on the choice of facets f and g of T^l.

We rescale the canonical equilibrium stress to

$$\Omega = \frac{\prod_{h \in \mathcal{F}_{d-1}(T^l)} [\![h]\!]}{[T^l]} \Omega^c,$$

where all the facets $h \in \mathcal{F}_{d-1}(T^l)$ participate with positive orientation. Thus, Ω is an equilibrium stress on T and

$$\Omega_{fg} = \prod_{h \in \mathcal{F}_{d-1}(T^l), h \neq f,g} [\![h]\!],$$

where all the facets $h \in \mathcal{F}_{d-1}(T^l)$ participate with positive orientation.

To show that Ω_{fg} coincides with Ω^a_{fg} from the statement of the lemma, we explicitly compute the positive order on the vertices of $h \in \mathcal{F}_{d-1}(T^l)$: we show that for a facet $h_k = ((u^l_1, \dots u^l_{d+1}) \setminus u^l_k)$ of T^l that is formed by all the vertices except the vertex u^l_k

$$\operatorname{sign}_{h_k}((u^l_1, \dots u^l_{d+1}) \setminus u^l_k) = (-1)^{d+1-k}.$$

Indeed, for n_k being the outernormal to the facet h_k of T^l (we assume in the computation below that $k \neq d+1$, the case $k = d+1$ can be handled similarly)

$$\begin{aligned}
\operatorname{sign}_{h_k}((u^l_1, \dots, u^l_{d+1}) \setminus u^l_k) &= \operatorname{sign}((u^l_1 - u^l_{d+1}, \dots, u^l_d - u^l_{d+1}) \setminus u^l_k - u^l_{d+1}, n_k) \\
&= (-1)\operatorname{sign}((u^l_1 - u^l_{d+1}, \dots, u^l_d - u^l_{d+1}) \setminus u^l_k - u^l_{d+1}, u^l_k - u^l_{d+1}) \\
&= (-1)(-1)^{d-k}\operatorname{sign}(u^l_1 - u^l_{d+1}, \dots, u^l_d - u^l_{d+1}) \\
&= (-1)(-1)^{d-k}\operatorname{sign}([u^l_1, \dots, u^l_{d+1}]) \\
&= (-1)^{d+1-k}.
\end{aligned}$$

The first transition is the definition of orientation on a facet of a polytope, Eq. (4.1.2). The second transition holds since the vectors n_f and $u^l_k - u^l_{d+1}$ are oppositely directed w.r.t the facet h_k of T^l. The fourth transition is the definition of the oriented volume, and the last transition holds by the choice of lifting T^l. □

Decomposition into atomic stresses

Lemma 4.5.3. *Let $\mathcal{P} = (u_1, \dots u_n)$ be an embedding of a stacked d-polytope P onto $\mathbb{R}^d$. Let $\mathcal{P}$ be produced by the stacking sequence*

$$\begin{aligned}
\mathcal{P}_{d+1} &= (u_1, \dots u_{d+1}), && \text{— initial simplex,} \\
\mathcal{P}_{d+2} &= \operatorname{Stack}(\mathcal{P}_{d+1}, f_{d+1}, u_{d+2}), && f_{d+1} \in \mathcal{F}_{d-1}(\mathcal{P}_{d+1}), \\
&\dots \\
\mathcal{P} = \mathcal{P}_n &= \operatorname{Stack}(\mathcal{P}_{n-1}, f_{n-1}, u_n), && f_{n-1} \in \mathcal{F}_{d-1}(\mathcal{P}_{n-1}).
\end{aligned}$$

We denote the simplices that are being stacked with $T_i = \operatorname{Conv}(f_{i-1}, u_i)$. Let $\mathcal{P}^{pr}$ be the orthogonal projection of $\mathcal{P}$ to the hyperplane $\{x_d = 0\}$ and the stress Ω^c be the canonical equilibrium stress on this projection. Then, there exists a unique set of real coefficients α_i such that

$$\Omega^c = \sum_{d+1 \le i \le n} \alpha_i \Omega^a(T_i),$$

where $\Omega^a(T_i)$ is the atomic equilibrium stress on the simplex T_i.

Proof. We use Theorem 4.3.3 and conduct the proof by induction on the stacking sequence $(\mathcal{P}_i)$. The base for $\mathcal{P}_{d+1}$ is a direct consequence of Theorem 4.3.3.

We prove the induction step. Let Ω_{n-1} be the canonical equilibrium stress on the projection of $\mathcal{P}_{n-1}$. Then by the definition of the canonical equilibrium stress, Ω_{n-1} and Ω_n coincide on all the $(d-2)$-faces of $\mathcal{P}_n$ that are not faces of the simplex $T_n = \operatorname{Conv}(f_{n-1}, u_n)$ that is being stacked:

$$(\Omega_{n-1})_{(fg)} = (\Omega_n)_{(fg)} \quad \forall (fg) \in \mathcal{F}_{d-2}(\mathcal{P}_n) \setminus \mathcal{F}_{d-2}(T_n).$$

Thus, the difference between these canonical equilibrium stresses $\Omega_n - \Omega_{n-1}$ has its support on T_n. But this difference is an equilibrium stress on its support, thus $\Omega_n - \Omega_{n-1}$ is an equilibrium stress on T_n. The space of equilibrium stresses on a simplex is 1-dimensional, thus

$$\Omega_n - \Omega_{n-1} = \alpha_n \Omega^a(T_n).$$

□

Estimates, scaling, rounding

Lemma 4.5.4. *Let $\mathcal{P} = (u_1, \dots u_n)$ be an embedding of a stacked d-polytope P onto $\mathbb{R}^d$ with integer coordinates such that*

$$\begin{aligned} |x_i(u_j)| &< L && \forall 1 \le j \le n, 1 \le i < d, \\ |x_d(u_j)| &< M && \forall 1 \le j \le n. \end{aligned}$$

Then the orthogonal projection $\mathcal{P}^{pr}$ of $\mathcal{P}$ onto $\{x_d = 0\}$ possesses an equilibrium stress Ω that is integer and bounded by

$$|\Omega_{fg}| \le (n-d)(2L)^{(d-1)^2} \left((2L)^{3(d-1)}(2M) + 1 \right).$$

Moreover the signs of Ω coincide with the signs of the canonical equilibrium stress Ω^c on $\mathcal{P}$. In particular, when the projected realization $\mathcal{P}^{pr}$ is planar, Ω is a positive equilibrium stress.

Proof. We follow the plan announced at the beginning of the subsection. Let Ω^c be the canonical equilibrium stress for the projection $\mathcal{P}^{pr}$. We use Lemma 4.5.3 to decompose Ω^c onto a linear combination of atomic equilibrium stresses on the simplices forming $\mathcal{P}$ (and we also import the notation and conventions for stacking sequence from Lemma 4.5.3):

$$\Omega^c = \sum_{d+1 \le i \le n} \alpha_i \Omega^a(T_i).$$

Since the embedding $\mathcal{P}^{pr}$ has integer coordinates, all the atomic stresses $\Omega^a(T_i)$ are integral. To make the final equilibrium stress Ω^c integer we round the coefficients α_i. Though, after rounding the stress Ω^c should preserve signs. To achieve it, we scale Ω^c before rounding.

We start with estimating the bounds on Ω^c and $\Omega^a(T_i)$. For the canonical equilibrium stress Ω^c on $\mathcal{P}^{pr}$, for every $(d-2)$-face (fg)

$$\Omega^c_{fg} = \frac{[f \cup g]}{[\![f]\!][\![g]\!]} \ge \frac{1}{(2L)^{d-1}(2L)^{d-1}}.$$

And for the atomic equilibrium stresses on T_i

$$\begin{aligned} \Omega^a_{fg}(T_i) = \prod_{h \in \mathcal{F}_{d-1}(T_i), h \ne f,g} [\![h]\!] \le \\ \prod_{h \in \mathcal{F}_{d-1}(T_i), h \ne f,g} (2L)^{d-1} \le (2L)^{(d-1)^2}. \end{aligned}$$

The last inequality holds since any simplex has exactly $d+1$ (as many as vertices) facets.

We chose the integral scaling factor

$$C := (n-d)(2L)^{2(d-1)+(d-1)^2}$$

so that

$$C \ge (n-d) \frac{\max_{i,(fg)} |\Omega^a_{(fg)}(T_i)|}{\min_{(fg)} |\Omega^c_{(fg)}|}$$

and define the new coefficients and the new equilibrium stresses:

$$\begin{aligned} \alpha'_i &:= \lfloor C\alpha_i \rfloor, \\ \Omega' &:= \sum_{n+1 \le i \le d} \alpha'_i \Omega^a(T_i). \end{aligned}$$

To finish the construction we show that Ω' is positive, in other words that the scaling and rounding don't affect the sign of any of the stresses:

$$\begin{aligned}
|\Omega^c_{fg} - \frac{1}{C}\Omega'_{fg}| &\leq \sum_{d+1\leq i\leq n} |\alpha_i - \frac{1}{C}\alpha'_i||\Omega^a_{fg}(T_i)| \\
&\leq (n-d) \max_{d+1\leq i\leq n} |\alpha_i - \frac{1}{C}\alpha'_i| \max_{i,(fg)} |\Omega^a_{fg}(T_i)| \\
&\leq (n-d)\frac{1}{C} \max_{i,(fg)} |\Omega^a_{fg}(T_i)| \\
&\leq \min_{(fg)\in\mathcal{F}_{d-1}(\mathcal{P})} |\Omega^c_{fg}| \leq |\Omega^c_{fg}|.
\end{aligned}$$

The resulting equilibrium stress Ω' is thus integer and has the same signs as Ω^c. To finish the proof we bound it from above:

$$\begin{aligned}
|\Omega'_{fg}| &= \left| \sum_{d+1\leq i\leq n} \lfloor C\alpha_i \rfloor \Omega^a_{fg}(T_i) \right| \\
&\leq \left| \sum_{d+1\leq i\leq n} C\alpha_i \Omega^a_{fg}(T_i) \right| + \sum_{d+1\leq i\leq n} |\Omega^a_{fg}(T_i)| \\
&\leq C|\Omega^c_{fg}| + (n-d) \max_{d+1\leq i\leq n} |\Omega^a_{fg}(T_i)|.
\end{aligned}$$

To bound the last equation we bound $|\Omega^c_{fg}|$ from above:

$$\left|\Omega^c_{fg}\right| = \left| \frac{[f\cup g]}{[\![f]\!][\![g]\!]} \right| \leq |[f\cup g]| \leq (2L)^{d-1}(2M).$$

Thus finally

$$|\Omega'_{(fg)}| \leq (n-d)(2L)^{2(d-1)+(d-1)^2}(2L)^{d-1}(2M) + (n-d)(2L)^{(d-1)^2}.$$

□

We combine the result by Demaine and Schulz, Lemma 4.5.1, and the previous Lemma 4.5.4 for the final result on the planar realizations of stacked polytopes with equilibrium stresses:

Theorem 4.5.1. *Let P be a stacked d-polytope with n vertices. Then there exists an integer planar realization $\mathcal{P} = (u_i)_{1\leq i\leq n}$ of P in $\mathbb{R}^{d-1}$ and a positive integer equilibrium stress Ω on this realization such that*

$$\begin{aligned}
|\Omega_{fg}| &= n^{O(d^2 \lg(d))}, \\
|u_i| &= n^{O(\lg(d))}.
\end{aligned}$$

Proof. We feed the output of Lemma 4.5.1 into Lemma 4.5.4 to get

$$\begin{aligned}
|\Omega_{fg}| &\leq (n-d)(20d^2R^2)^{(d-1)^2}((20d^2R^2)^{3(d-1)}(12R^3)+1), \\
|u_i| &\leq 10d^2R^2,
\end{aligned}$$

where $R = n^{\lg(2d)}$. Since $d = n^{O(\lg(d))}$, the statement of the theorem holds. □

4.5.4 Step 2: Stacking of the missing vertex

Lemma 4.5.5 (Framework for truncated polytopes)**.** *Let $\mathcal{P}$ be a planar integer realization of a convex d polytope in $\mathbb{R}^{d-1}$ with simplicial outerfacet f. Let $\Omega_{\mathcal{P}}$ be a positive integer equilibrium stress for $\mathcal{P}$. Let* $\mathrm{Stack}(\mathcal{P}, f, u_0)$ *be the result of stacking a new vertex u_0 atop the facet f of $\mathcal{P}$. Then*

1. *There exists an integer cone-convex realization of* $\mathrm{Stack}(\mathcal{P}, f, u_0)$ *with an integer positive braced stress Ω_S such that*

$$\begin{aligned} |u| &\le d \max_{v \in \mathcal{F}_0(\mathcal{P})} |v| && \forall u \in \mathcal{F}_0(\mathrm{Stack}(\mathcal{P}, f, u_0)), \\ |\Omega_S(F)| &\le \max_{H \in \mathcal{F}_{d-2}(\mathcal{P})} |\Omega_P(H)| + 1 && \forall F \in \mathcal{F}_{d-2}(\mathrm{Stack}(\mathcal{P}, f, u_0)); \end{aligned}$$

2. *There exists an integer realization of the polytope dual to* $\mathrm{Stack}(\mathcal{P}, f, u_0)$ *as a convex polytope in $\mathbb{R}^d$ such that the coordinates of its vertices are bounded by*

$$|\phi| \le d^{d-1} \operatorname{diam}(\mathrm{Sk}_1(\mathrm{Stack}(\mathcal{P}, f, u_0)^*)) \left(\max_{H \in \mathcal{F}_{d-2}(\mathcal{P})} |\Omega_P(H)| + 1 \right) \max_{u \in \mathcal{F}_0(\mathcal{P})} |u|^{d-1}.$$

To proceed we need the following technical statement about braced stresses on a simplex:

Lemma 4.5.6. *Let $T = (u_1, \dots u_{d+1})$ be a simplex in $\mathbb{R}^d$ and let for some nonzero $\lambda_i \in \mathbb{R}$*

$$\sum_{1 \le i \le d+1} \lambda_i u_i = 0.$$

Then, the assignment

$$\Omega_{ij} := \frac{1}{\lambda_i} \frac{1}{\lambda_j}$$

is a braced stress on T, where with (ij) we denote the $(d-2)$-face of T spanned by all the vertices of T except u_i and u_j.

Proof. Let F be any $(d-3)$-face of T. We denote the three vertices that do not lie in F with u_i, u_j, u_k. Then, the $(d-2)$-faces in $\delta(F)$ are $F_{ij} = (F, u_k)$, $F_{jk} = (F, u_i)$ and $F_{ki} = (F, u_i)$. Thus,

$$\begin{aligned} \sum_{(f_i f_{i+1}) \in \delta(F)} \Omega_{f_i f_{i+1}} U_{f_i f_{i+1}} &= \Omega_{ij} U_{ij} + \Omega_{jk} U_{jk} + \Omega_{ki} U_{ki} \\ &= \frac{1}{\lambda_j \lambda_k} F \times u_i + \frac{1}{\lambda_i \lambda_k} F \times u_j + \frac{1}{\lambda_i \lambda_j} F \times u_k \\ &= \frac{1}{\lambda_i \lambda_j \lambda_k} F \times (\lambda_i u_i + \lambda_j u_j + \lambda_k u_k) \\ &= -\frac{1}{\lambda_i \lambda_j \lambda_k} F \times \sum_{m \ne i,j,k} \lambda_m u_m = 0, \end{aligned}$$

where the last equality holds because F is spanned exactly by the vertices $(u_m)_{m \ne i,j,k}$.

□

Proof of Lemma 4.5.5. The proof of this result mimics the proof of the 3-dimensional case, Lemma 2.5.1 and Theorem 2.5.2.

(1) We denote the vertices spanning the face F with $u_1, \dots u_d$. We scale the realization $\mathcal{P}$ with factor d so that

$$\frac{1}{d}(u_1 + \ldots + u_d) \in \mathbb{Z}^{d-1}$$

has integer coordinates, and translate it so that $\frac{1}{d}(u_1 + \ldots + u_d) = 0$. The new realization $\bar{\mathcal{P}}$ has integer coordinates as well. We embed $\bar{\mathcal{P}}$ onto the $\{x_d = 1\}$ hyperplane of $\mathbb{R}^d$ so that $\frac{1}{d}(u_1 + \ldots + u_d) = (0, \dots, 0, 1)^T$. To facilitate notation, we forget about the bar on $\bar{\mathcal{P}}$ and denote the vertices of $\bar{\mathcal{P}}$ as the vertices of the initial $\mathcal{P}$ with (u_i).

We put the new vertex u_0 of $\mathrm{Stack}(\mathcal{P}, f, u_0)$ at the point $(0, \dots 0, -d)^T$. Then

$$u_0 + \ldots + u_d = 0.$$

By Lemma 4.5.6 the stress $\Omega_T \equiv 1$ is a braced stress on the simplex $T = (u_0, \dots u_d)$.

So, the stress $\Omega_S = \mu\Omega_T + \Omega_P$ is a braced stress for $\mathrm{Stack}(P, f, u_0)$ for any real μ. We pick μ so that the braced stress Ω_S is positive. To do so we remind that all the entries of Ω_P are positive apart from those that correspond to $(d-2)$-faces of the outerfacet f, and all the entries of Ω_T equal 1, thus we pick

$$\mu := \max_{F \in \mathcal{F}_{d-2}(f)} |\Omega_P(F)| + 1.$$

The constructed embedding of $\mathrm{Stack}(\mathcal{P}, f, u_0)$ is cone-convex since it is a convex embedding of the simplex $(u_0, \dots u_d)$ with one facet refined in a convex way.

(2) We use the d-dimensional version of the Lovász duality transformation (Lemma 4.4.2) for the embedding of $\mathrm{Stack}(\mathcal{P}, f, u_0)$ with the stress Ω_S to construct an integer realization (ϕ_f) of the polytope dual to $\mathrm{Stack}(\mathcal{P}, f, u_0)$:

$$\begin{aligned}|\phi_f| &= \mathrm{diam}(\mathrm{Sk}_1(\mathrm{Stack}(\mathcal{P}, f, u_0)^*)) \max_{F \in \mathcal{F}_{d-2}(\mathrm{Stack}(\mathcal{P}, f, u_0))} |\Omega_S(F)| \max_{u \in \mathcal{F}_0(\mathrm{Stack}(\mathcal{P}, f, u_0))} |u|^{d-1} \\ &= \mathrm{diam}(\mathrm{Sk}_1(\mathrm{Stack}(\mathcal{P}, f, u_0)^*)) \left(\max_{F \in \mathcal{F}_{d-2}(\mathcal{P})} |\Omega_P(F)| + 1 \right) d^{d-1} \max_{u \in \mathcal{F}_0(\mathcal{P})} |u|^{d-1}.\end{aligned}$$

□

4.5.5 Step 3: Realizing truncated polytopes

Theorem 4.5.2. *Let P be a truncated polytope with n faces. Then there exists a realization (ϕ_f) of P as a convex polytope with integer coordinates bounded by*

$$|\phi_f| = n^{O(d^2 \lg(d))}.$$

Proof. The proof of this theorem mimics the proof of the 3d case, Theorem 2.5.3. Let P^* be the polytope dual to P. Then P^* is a stacked polytope with n vertices.

We follow the notation of Subsec. 4.5.3 and denote the last stacking operation (for some sequence of stacking operations producing P^*) as the stacking of the vertex u_n onto the face f_{n-1} of the polytope P^*_{n-1}, thus $P^* = \mathrm{Stack}(P^*_{n-1}, f_{n-1}, u_n)$.

The polytope P^*_{n-1} is a stacked polytope with $n-1$ vertices, and hence, by Theorem 4.5.1, there exists a planar embedding $(p_i)_{1 \le i \le n-1}$ of P^*_{n-1} into $\mathbb{R}^{d-1}$ with integer coordinates and a positive integer equilibrium stress $\Omega_{P^*_{n-1}}$ for this embedding satisfying the properties of Lemma 4.5.5 and such that

$$\begin{aligned}&|\Omega_{P^*_{n-1}}(F)| = n^{O(d^2 \lg(d))} && \forall F \in \mathcal{F}_{d-2}(P^*_{n-1}), \\ &|p_i| = n^{O(\lg(d))} && \forall p_i \in \mathcal{F}_0(P^*_{n-1}).\end{aligned}$$

We apply Lemma 4.5.5 and obtain an embedding (ϕ_f) of $P = (\text{Stack}(P_{n-1}, f_{n-1}, u_n))^*$ with the bound on the coordinates size

$$\begin{aligned}|\phi_f| &\leq d^{d-1} \operatorname{diam}(\text{Sk}_1(P)) \left(\max_{F \in \mathcal{F}_{d-2}(P^*_{n-1})} |\Omega_{P^*_{n-1}}(F)| + 1 \right) \max_{p_i \in \mathcal{F}_0(P^*_{n-1})} |p_i|^{d-1} \\ &= \operatorname{diam}(\text{Sk}_1(P)) n^{O(d^2 \lg(d))}.\end{aligned}$$

Every truncation operation increases the diameter of the skeleton of the polytope by no more than 1, and the diameter of the skeleton of a simplex is 1 as well. The polytope $\mathcal{P}$ is produced from a simplex by $n - d - 1$ truncation operations, thus

$$\operatorname{diam}(\text{Sk}_1(P)) \leq n - d$$

and the final estimate follows.

□

4.6 Duality transform for general simplicial polytopes

In this section we present a duality transform for general simplicial polytopes. It mimics the construction for 3-dimensional polytopes presented in Sect. 2.5.3.

4.6.1 Wheel-decomposition theorem

We begin the section with studying the space of braced stresses of a convex polytope: we introduce the d-dimensional generalization of the wheel and prove the d-dimensional version of the wheel-decomposition theorem. Analogously to the 3-dimensional case, the d-dimensional wheel-decomposition theorem explicitly describes a basis of the linear space of braced stresses of a polytopal surface.

We remind that in the 3-dimensional setup we call a *wheel* the graph of a pyramid. However, in $\mathbb{R}^d$ the combinatorics of a polytope is not predetermined by its graph, thus we abandoned graphs of polytopes and work directly with realizations of polytopes. The most natural generalization of the wheel to $\mathbb{R}^d$ is the d-dimensional pyramid itself. However, to keep the language consistent between the 3-dimensional and d-dimensional parts, we also introduce the notion of a d-dimensional wheel, which is the full synonym of the d-dimensional pyramid with a simplicial base.

Definition 4.6.1. *(1) Let B be a convex $(d-1)$-polytope in $\mathbb{R}^{d-1} \subset \mathbb{R}^d$. Let a be a point in $\mathbb{R}^d$ not in the hyperplane containing B. We call the polytope given by the convex hull* $\mathrm{Conv}(\{a\} \cup B)$ *the* pyramid *with the base B and apex a and we denote this pyramid with $P(a, B)$.*

(2) Let B be a simplicial $(d-1)$-polytope. A wheel $\mathrm{W}(a, B)$ *with the base B and apex a is the pyramid $P(a, B)$.*

We use only ridged realizations of wheels, thus we usually do not put any restrictions on how the base facet is realized: neither should it be realized as a convex $(d-1)$-polytope, nor should it lie in any hyperplane (does not have to be "flat"). This is another reason to introduce the notion of wheel, since the word "pyramid" bears a strong connotation with the flatness of the base. The following observation provides a motivation to study ridged realizations of wheels and stresses on them.

Lemma 4.6.1. *Let $\mathcal{P}$ be a simplicial d-polytope. For a vertex u of $\mathcal{P}$ let $N(u, \mathcal{P})$ be the polytopal complex defined by all the facets ($(d-1)$-simplices) of $\mathcal{P}$ that are incident to u. Then the $(d-2)$ skeleton of $N(u, \mathcal{P})$ is a ridged realization of a wheel with apex u and the base of this wheel can be oriented in a canonical way.*

For the vertex u_i of $\mathcal{P}$ we denote the wheel defined by $N(u_i, \mathcal{P})$ with W_i and we refer to this wheel as the subwheel of $\mathcal{P}$ centered at the vertex u_i.

Proof. We choose the euclidean coordinates in $\mathbb{R}^d$ so that the vertex $u = (0, 0 \dots 0)^T$ is the origin, the hyperplane $\{x_d = 0\}$ is a supporting hyperplane to $\mathcal{P}$ at u and the polytope $\mathcal{P}$ without the vertex u, $\mathcal{P} \setminus \{u\}$, lies in the upper halfspace $\{x_d > 0\}$.

Let $\alpha = \{x_d = 1\}$. For every $(d-1)$-simplex $T \in N(u, \mathcal{P})$ we consider its $(d-2)$-face that does not contain the vertex u, we denote this face with $B(T)$, thus $T = \mathrm{Conv}(\{u\} \cup B(T))$. We centrally project each of $B(T)$ for $T \in N(u, \mathcal{P})$ to α, thus every point $x \neq 0$ goes to $x/|x|$. We denote this projection of $B(T)$ with $B'(T)$. Then we construct the new simplex $T'(T) = \mathrm{Conv}(\{u\} \cup B'(T))$ for every $T \in N(u, \mathcal{P})$. The simplices $(T'(T))_{T \in N(u,\mathcal{P})}$ form a polytopal complex that we denote with $N'(u, \mathcal{P})$. The face lattice of $N'(u, \mathcal{P})$ is by construction equivalent to the face lattice of $N(u, \mathcal{P})$.

We construct $B := \mathrm{Conv}(\cup_{T \in N(u,\mathcal{P})} B'(T))$. Clearly, B is a convex $(d-1)$-polytope that lies in α, such that the $(d-2)$-faces of B are exactly all the simplices $B'(T)$ for $T \in N(u, \mathcal{P})$. Thus, by the definition of the wheel, the polytopal complex $N'(u, \mathcal{P})$ is the $(d-1)$-skeleton of

the wheel $\mathrm{W}(u, B)$ without the base facet B. Since the face structures of $N(u, \mathcal{P})$ and $N'(u, \mathcal{P})$ coincide, the statement of the lemma follows. The wheel $\mathrm{W}(u, B)$ is a convex polytope, thus its facet B is oriented through the outer normal vector. Clearly, different choices of the initial projection plane α produce wheels that are isomorphic preserving the orientation. □

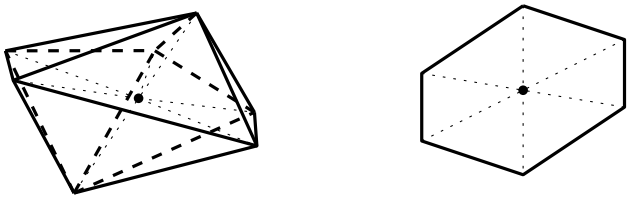

Figure 4.6.1: Depicted are flat realizations of wheels. Left: a 4-wheel with the 5-gonal bipyramid as the base. Right: a 3-wheel with the convex 6-gon as the base. The bases are bold. The apex is the point in the center.

In context of the previous lemma, every simplicial d-polytope $\mathcal{P}$ can be viewed as "covered" by wheels centered at its vertices. Considering all these wheels $(W_i)_{u_i \in \mathcal{F}_0(\mathcal{P})}$ simultaneously, every $(d-2)$-face F of $\mathcal{P}$ is covered exactly $d+1$ times: by 2 wheels for which the face F belongs to the base and $d-1$ wheels centered at $d-1$ vertices of F. The goal of this section is to show that every stress on $\mathcal{P}$ can be decomposed into a linear combination of elementary stresses on the wheels W_i. Before we proceed, we discuss the structure of a wheel in more details.

The structure of the $(d-2)$-faces of a wheel

Following the structure of the wheel, the $(d-2)$-faces of a wheel $\mathrm{W}(a, B)$ are by definition of two types (see Fig. 4.6.2): (1) the $(d-2)$-faces of the underlying base $F \in \mathcal{F}_{d-2}(B)$ and (2) the pyramids with apex a over the $(d-3)$-faces of the underlying base, $F = (a, f)$ with $f \in \mathcal{F}_{d-3}(B)$.

We distinguish between these two types in the definition of atomic stresses, see Definition 4.6.2.

The orientation on the $(d-2)$-faces of a wheel

For an oriented $(d-2)$-face $F \in \mathcal{F}_{d-2}(B)$ with vertices $F = (u_1^F, \dots u_{d-1}^F)$ and an additional point a we use the standard shortcut notation for the oriented volumes (for realizations in $\mathbb{R}^{d-1}$) and determinants (for realizations in $\mathbb{R}^d$):

$$\begin{aligned} [F, a] &= [u_1^F, \dots u_{d-1}^F, a], & a, u_i^F &\in \mathbb{R}^{d-1}, \\ \det(F, a) &= \det(u_1^F, \dots u_{d-1}^F, a), & a, u_i^F &\in \mathbb{R}^d. \end{aligned}$$

Analogously, for an oriented $(d-3)$-face $f \in \mathcal{F}_{d-3}(B)$ with vertices $f = (u_1^f, \dots u_{d-2}^f)$ and two additional points a, b we shortcut

$$\begin{aligned} [f, a, b] &= [u_1^f, \dots u_{d-2}^f, a, b], & a, b, u_i^f &\in \mathbb{R}^{d-1}, \\ \det(f, a, b) &= \det(u_1^f, \dots u_{d-2}^f, a, b), & a, b, u_i^f &\in \mathbb{R}^d. \end{aligned}$$

We suppose that every wheel comes with a chosen orientation of its base B. In other words, for every $(d-2)$-face of B a positive order of its vertices is chosen and this choice is consistent

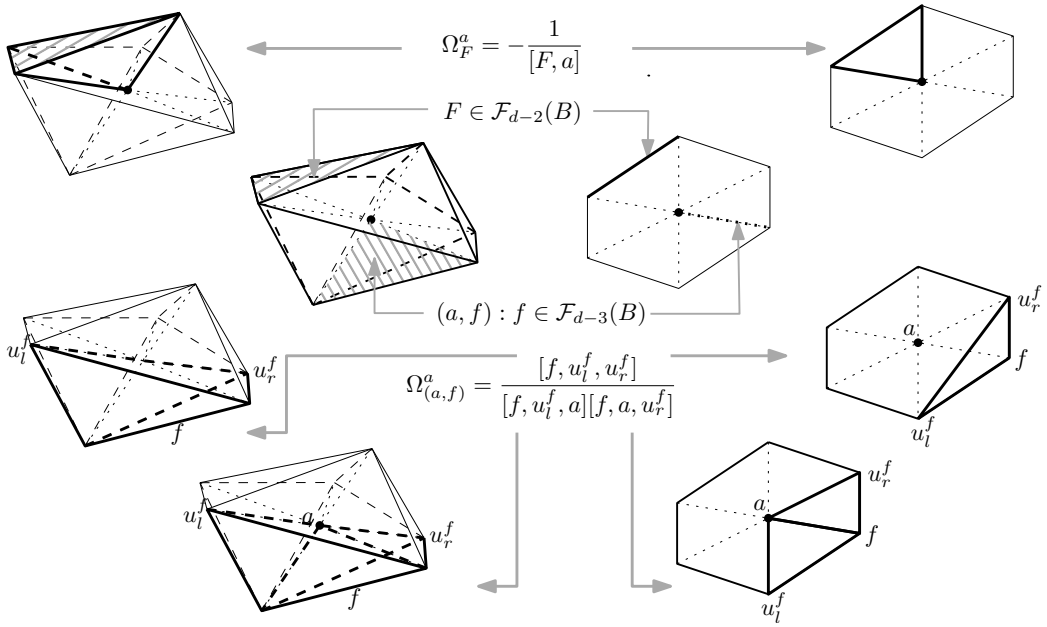

Figure 4.6.2: A 4-wheel (center left) and a 3-wheel (center right) with two types of $(d-2)$-faces. The $(d-1)$-faces whose volumes participate in the atomic equilibrium stresses on the corresponding $(d-2)$-faces are labeled directly on the picture.

throughout all the $(d-2)$-faces of B. If not explicitly specified otherwise, we assume every $F \in \mathcal{F}_{d-2}(B)$ that we consider with the *positive* orientation. Thus, $[F,a]$ (or, depending on the dimension of a realization, $\det(F,a)$) is well-defined.

The orientation on the base B of the wheel does not induce an orientation on its $(d-3)$-faces. However, for every choice of the orientation on a $(d-3)$-face $f \in \mathcal{F}_{d-3}(B)$, $f = (u^f_1, \dots u^f_{d-2})$, it defines an order on the pair of its two adjacent $(d-2)$-faces of B: We say that the $(d-2)$-face $F \in \mathcal{F}_{d-2}(B)$ is adjacent to f *on the left (right)* if $F = (u^f_1, \dots u^f_{d-2}, u^F)$ is a negative (positive) orientation on F, where u^F is the vertex of F not in f. We denote u^F with u^f_l (u^f_r). We call the vertex u^f_l (u^f_r) the *left (right) neighbour* of f in B,

Thus, for every $f \in \mathcal{F}_{d-3}(B)$ the determinant $[f,u^f_l,u^f_r]$ is well-defined. The sign of the product $[f,u^f_l,a][f,u^f_r,a]$ for any point a is also well-defined because the change of the order of vertices of f changes the signs of both factors.

Realizations of a wheel

Let W be any embedding of vertices of a d-wheel $\mathrm{W}(a,B)$ in $\mathbb{R}^{d-1}$ or $\mathbb{R}^d$. The $(d-2)$-faces of $\mathrm{W}(a,B)$ are of two types: the $(d-2)$-faces of the base and the pyramids with apex a over the $(d-3)$-faces of the base. Since the base B is a simplicial $(d-1)$-polytope, its $(d-2)$- and $(d-3)$-faces are simplices of corresponding dimensions. Thus, all the $(d-2)$-faces of $\mathrm{W}(a,B)$ are simplices and any embedding of the vertices of $\mathrm{W}(a,B)$ in $\mathbb{R}^{d-1}$ or $\mathbb{R}^d$ realizes every $(d-2)$-face of $\mathrm{W}(a,B)$ as a convex $(d-2)$-polytope. Thus, every embedding of vertices of a wheel in $\mathbb{R}^{d-1}$ ($\mathbb{R}^d$) defines a *ridged* embedding of this wheel, and for every embedding the notion of equilibrium (braced) stress is defined.

Atomic equilibrium and braced stresses on wheels

The analysis above allows us to define atomic stresses on a wheel:

Definition 4.6.2 (Atomic equilibrium stress on a wheel)**.** *Let W be a ridged realization of a d-wheel $\mathrm{W}(a,B)$ in $\mathbb{R}^{d-1}$. We call the* atomic equilibrium stress *the assignment of reals $\Omega^a : \mathcal{F}_{d-2}(W) \to \mathbb{R}$ to $(d-2)$-faces of W*

$$\Omega^a_F = \begin{cases} -\frac{1}{[F,a]}, & F \in \mathcal{F}_{d-2}(B), \\ \frac{[f,u^f_l,u^f_r]}{[f,u^f_l,a][f,u^f_r,a]}, & F=(a,f), f \in \mathcal{F}_{d-3}(B), \end{cases}$$

where $F \in \mathcal{F}_{d-2}(B)$ is considered with positive orientation and (f,u^f_l) and (f,u^f_r) are two $(d-2)$-faces of B adjacent to the $(d-3)$-face $f \in \mathcal{F}_{d-3}(B)$ of the base on the left and on the right correspondingly; see Fig. 4.6.2.

Definition 4.6.3 (Atomic braced stress on a wheel)**.** *Let W be a ridged realization of a d-wheel $\mathrm{W}(a,B)$ in $\mathbb{R}^d$. We call the* atomic braced stress *the assignment of reals $\Omega^a : \mathcal{F}_{d-2}(W) \to \mathbb{R}$ to $(d-2)$-faces of W*

$$\Omega^a_F = \begin{cases} -\frac{1}{\det(F,a)}, & F \in \mathcal{F}_{d-2}(B), \\ \frac{\det(f,u^f_l,u^f_r)}{\det(f,u^f_l,a)\det(f,u^f_r,a)}, & F=(a,f), f \in \mathcal{F}_{d-3}(B), \end{cases}$$

where $F \in \mathcal{F}_{d-2}(B)$ is considered with positive orientation and (f,u^f_l) and (f,u^f_r) are two $(d-2)$-faces of B adjacent to the $(d-3)$-face $f \in \mathcal{F}_{d-3}(B)$ of the base on the left and on the right correspondingly, see Fig. 4.6.2.

The two definitions above are clearly consistent with the equivalence between the spaces of braced and equilibrium stresses (Subsec. 4.2.3): for a flat realization of $\mathrm{W}(a,B)$ in $\mathbb{R}^{d-1} = \{x_d = 1\} \subset \mathbb{R}^d$ the atomic braced stress coincides with the atomic equilibrium stress. Thus in the definition above we use the same notation for the atomic equilibrium stress and for the atomic braced stress.

Link to the $d=3$ case. In the 3-dimensional case the base B is a k-gon $B=(u_1,\dots,u_k)$ and this notation implies orientation.

A $(d-2)$-face F of B is an edge (u_iu_{i+1}). Thus,

$$\Omega^a_F = -\frac{1}{[F,a]} = -\frac{1}{[u_i,u_{i+1},a]} \quad \forall F=(u_iu_{i+1}) \in \mathcal{F}_{d-2}(B).$$

A $(d-3)$-face f of B is a vertex u_i. It has two neighbours in B, u_{i-1} and u_{i+1}. The edge (u_iu_{i+1}) is positively oriented thus u_{i+1} is the right neighbour of u_i,

$$u_{i+1} = u^r_f.$$

The edge (u_iu_{i-1}) is negatively oriented thus u_{i-1} is the left neighbour of u_i,

$$u_{i-1} = u^l_f.$$

Thus,

$$\Omega^a_{(f,a)} = \frac{[f,u^f_l,u^f_r]}{[f,u^f_l,a][f,u^f_r,a]} = \frac{[u_i,u_{i-1},u_{i+1}]}{[u_i,u_{i-1},a][u_i,u_{i+1},a]} \quad \forall f=u_i \in \mathcal{F}_{d-3}(B).$$

Thus, the atomic stresses of a d-wheel is a direct generalization of the atomic stresses of a wheel in R^3.

Lemma 4.6.2. *(1) The atomic equilibrium stress on a ridged realization W of a d-wheel $\mathrm{W}(a,B)$ in $\mathbb{R}^{d-1}$ is an equilibrium stress on W. (2) The atomic braced stress on a ridged realization W of a d-wheel $\mathrm{W}(a,B)$ in $\mathbb{R}^d$ is a braced stress on W.*

Proof. (1) We construct the lifting W^l of W such that the base B stays in the hyperplane $\{x_d = 0\}$ and the apex a is lifted to $\{x_d = 1\}$. Then W is the orthogonal projection of W^l and thus W possesses the canonical equilibrium stress as defined by Eq. (4.3.5), which coincides with the atomic equilibrium stress on W.

(2) We pick any affine hyperplane α on distance 1 from the origin, such that none of the vectors representing the vertices of W is parallel to α. We centrally project W to α. We use Lemma 4.2.6 to rescale the atomic braced stress following the projection. A direct computation shows that after rescaling it equals the atomic equilibrium stress on the projection. By part (1) of the lemma, the latter is an equilibrium stress. Thus, by Lemma 4.2.5 it is also a braced stress. So, again by Lemma 4.2.6, it was a braced stress before rescaling as well. □

Similarly to the 3-dimensional case we define the *large atomic stresses* that are rescalings of the atomic stresses such that the stresses are integral for integral embeddings:

Definition 4.6.4 (Large atomic stress)**.** *(1) Let W be a ridged realization of a d-wheel $\mathrm{W}(a, B)$ in $\mathbb{R}^{d-1}$. We call the* large atomic equilibrium stress Ω^A *the rescaling of the atomic equilibrium stress Ω^a with the factor $\prod_{f\in\mathcal{F}_{d-1}(W),f\neq B}[f]$:*

$$\Omega^A = \left(\prod_{f\in\mathcal{F}_{d-1}(W),f\neq B} [f]\right)\Omega^a,$$

where the facets of W are taken with the positive orientation.

(2) Let W be a ridged realization of a d-wheel $\mathrm{W}(a, B)$ in $\mathbb{R}^d$. We call the large atomic braced stress Ω^A *the rescaling of the atomic braced stress Ω^a with the factor $\prod_{f\in\mathcal{F}_{d-1}(W)}\det(f)$:*

$$\Omega^A = \left(\prod_{f\in\mathcal{F}_{d-1}(W),f\neq B} \det(f)\right)\Omega^a,$$

where the facets of W are taken with the positive orientation.

Theorem 4.6.1 (Wheel-decomposition theorem)**.** *(1) Let Ω be an equilibrium stress on a ridged realization $\mathcal{P}$ of a d-polytope P in $\mathbb{R}^{d-1}$. Then*

$$\Omega = \sum_{1\le i\le n} \alpha_i\Omega^a(W_i), \quad \alpha_i \in \mathbb{R},$$

where $\Omega^a(W_i)$ is the atomic equilibrium stress on the wheel $W_i \subset \mathcal{P}$, centered at the vertex u_i of $\mathcal{P}$. The coefficients α_i are the heights of the corresponding vertices of $\mathcal{P}$ in any Maxwell–Cremona lifting of $\mathcal{P}$ by the stress Ω. The set of coefficients α_i is unique up to a "translation" transformation $\alpha_i \to \alpha_i + \langle u_i, v\rangle + c$ for any $v \in \mathbb{R}^{d-1}$ and $c \in \mathbb{R}$.

(2) Let Ω be a braced stress on a ridged realization $\mathcal{P}$ of a d-polytope P in $\mathbb{R}^d$. Then

$$\Omega = \sum_{1\le i\le n} \alpha_i\Omega^a(W_i), \quad \alpha_i \in \mathbb{R},$$

where $\Omega^a(W_i)$ is the atomic braced stress on the wheel $W_i \subset \mathcal{P}$, centered at the vertex u_i of $\mathcal{P}$. The set of coefficients α_i is unique up to a "translation" transformation $\alpha_i \to \alpha_i + \langle u_i, v\rangle$ for any $v \in \mathbb{R}^d$.

Proof. (1) This proof is identical to the proof of $d = 3$ dimensional version, Theorem 2.2.1.

(2) The proof follows the same pattern as the proof of part (2) of Lemma 4.6.2. We use Lemma 4.2.6 to transfer the question to some hyperplane α, and Lemma 4.2.5 to restate the question in terms of equilibrium stresses. It reduces part (2) to part (1). □

4.6.2 Duality transform for general simplicial polytopes

Lemma 4.6.3. *Let $\mathcal{P} = (u_i)_{1\le i\le n}$ be a convex simplicial d-polytope in $\mathbb{R}^d$ with integer coordinates, containing the origin in its interior. Then there exists an integral positive braced stress Ω for $\mathcal{P}$ such that its entries are bounded by*

$$|\Omega_{fg}| = O\left(d \max_{u\in\mathcal{F}_0(\mathcal{P})} |u|^{d(\Delta_{\mathrm{G}}{}^*+3)-2}\right),$$

where $\Delta_{\mathrm{G}}{}^*$ is the maximum over the vertices v of P of the number of facets of $\mathcal{P}$ adjacent to v.

Proof. The proof mimics the proof of 3-dimensional case. It goes through 3 steps:

(I) We construct the canonical braced stress Ω^c_{fg} for $\mathcal{P}$ and bound its entries;

(II) We use the wheel-decomposition theorem to decompose $\Omega^c = \sum_{1\le k\le n} \alpha_k \Omega^A(W_k)$ and bound the large atomic braced stresses;

(III) We define the final braced stress $\Omega := \sum_{1\le k\le n} \lfloor C\alpha_k \rfloor \Omega^a(W_k)$ with $C = (d+1)\frac{\max_{f,g,k}(\Omega^A_{fg}(W_k))}{\min_{f,g}(\Omega^c_{fg})}$ and check its correctness.

Throughout the proof we set $L := \max_{ij} |u_i - u_j|$.
Step (I): Let Ω^c be the canonical braced stress for $\mathcal{P}$:

$$\phi_g - \phi_f = \Omega^c_{fg} U_{fg}$$

for every pair of adjacent facets f and g. On the next steps we need to bound $|\Omega^c_{fg}|$. Obviously,

$$\frac{\max_{(fg)\in\mathcal{F}_{d-2}(\mathcal{P})} |\phi_g - \phi_f|}{\min_{(fg)\in\mathcal{F}_{d-2}(\mathcal{P})} |U_{fg}|} \ge |\Omega^c_{fg}| \ge \frac{\min_{(fg)\in\mathcal{F}_{d-2}(\mathcal{P})} |\phi_g - \phi_f|}{\max_{(fg)\in\mathcal{F}_{d-2}(\mathcal{P})} |U_{fg}|}.$$

To bound $|\Omega^c_{fg}|$ further we need a lower bound on $|\phi_g - \phi_f|$ (estimate (a)) and an upper bound on $|\phi_f|$ (estimate (b)).

Estimate (a): We remark that ϕ_f is the solution of the linear system

$$\langle \phi_f, u^f_1\rangle = 1, \langle \phi_f, u^f_2\rangle = 1, \dots, \langle \phi_f, u^f_d\rangle = 1,$$

where the vertices $u^f_1 u^f_2 \dots u^f_d$ belong to the face f. Thus, since (u^f_i) are integral,

$$\phi_f = \frac{1}{\det(u^f_1 u^f_2 \dots u^f_d)} Z_d$$

for Z_d being some vector in $\mathbb{Z}^d$. Similarly,

$$\phi_g = \frac{1}{\det(u^g_1 u^g_2 \dots u^g_d)} Z'_d,$$

where Z'_d is some vector in $\mathbb{Z}^d$. Thus, going to the common denominator,

$$|\phi_g - \phi_f| = \frac{1}{\det(u^f_1 u^f_2 \dots u^f_d)\det(u^g_1 u^g_2 \dots u^g_d)} Z''_d$$

for some third Z''_d in $\mathbb{Z}^d$. So, since $\phi_f \ne \phi_g$,

$$|\phi_g - \phi_f| \ge \frac{1}{\det(u^f_1 u^f_2 \dots u^f_d)\det(u^g_1 u^g_2 \dots u^g_d)} \ge \frac{1}{L^{2d}}. \tag{4.6.1}$$

Estimate (b): To bound $|\phi_f|$ from above we consider the pyramid over the face $f = (u_1^f u_2^f \dots u_d^f)$ with apex at the origin $\mathbf{0} = (0, 0, \dots, 0)^T$. Its (nonoriented) volume $\mathrm{Vol}_d^+(\mathbf{0}, u_1^f, u_2^f, \dots, u_d^f)$ can be computed as

$$\mathrm{Vol}_d^+(\mathbf{0}, u_1^f, u_2^f, \dots, u_d^f) = h_f \, \mathrm{Vol}_{d-1}^+(u_1^f, u_2^f, \dots, u_d^f),$$

where h_f is the height to the base f. Since all u_i^fs are integral, $\mathrm{Vol}_d^+(\mathbf{0}, u_1^f, u_2^f, \dots, u_d^f) \geq 1$. Trivially, $\mathrm{Vol}_{d-1}^+(u_1^f, u_2^f, \dots, u_d^f) \leq L^{d-1}$. Since ϕ_f is the polar vector for the hyperplane supporting the facet f, and $|h_f|$ is the distance from the origin to this hyperplane, $|h_f| = \frac{1}{|\phi_f|}$. Thus,

$$|\phi_f| \leq \frac{\mathrm{Vol}_{d-1}^+(u_1^f u_2^f \dots u_d^f)}{\mathrm{Vol}_d^+(\mathbf{0}, u_1^f, u_2^f, \dots, u_d^f)} \leq L^{d-1}. \tag{4.6.2}$$

Using the two bounds of Eq. (4.6.1) and Eq. (4.6.2) gives:

$$|\Omega_{fg}^c| \geq \frac{\min_{(fg)\in\mathcal{F}_{d-2}(\mathcal{P})} |\phi_g - \phi_f|}{\max_{(fg)\in\mathcal{F}_{d-2}(\mathcal{P})} |U_{fg}|} \geq \frac{1/L^{2d}}{L^{d-1}} = \frac{1}{L^{3d-1}},$$
$$|\Omega_{fg}^c| \leq \frac{\max_{(fg)\in\mathcal{F}_{d-2}(\mathcal{P})} |\phi_g - \phi_f|}{\min_{(fg)\in\mathcal{F}_{d-2}(\mathcal{P})} |U_{fg}|} \leq 2 \max_{f\in\mathcal{F}_{d-1}(\mathcal{P})} |\phi_f| \leq 2L^{d-1}.$$

We additionally used that $|U_{fg}| = \mathrm{Vol}_{d-1}^+(\mathbf{0}, (f, g)) \leq L^{d-1}$ and that U_{fg} is integral when f and g are simplices with integral vertices and thus $|U_{fg}| \geq 1$.

Step (II): We use the wheel-decomposition theorem (Theorem 4.6.1) to decompose Ω^c into a linear combination of the *large* atomic braced stresses of wheels, centered at the vertices of $\mathcal{P}$:

$$\Omega^c = \sum_{1\leq k\leq n} \alpha_k \Omega^A(W_k). \tag{4.6.3}$$

As a next step we bound the entries $|\Omega_{fg}^A|$ from above. By definition,

$$|\Omega_{fg}^A(W_k)| \leq \left(\max_{u_{i_1},\dots u_{i_d}\in\mathcal{F}_0(W_k)} \det(u_{i_1}, \dots u_{i_d}) \right)^{\deg^*(u_k)-1} \leq L^{d(\deg^*(u_k)-1)},$$

where we denote with $\deg^*(u_k)$ the number of facets of $\mathcal{P}$ adjacent to the vertex u_k.

Step (III): The large atomic braced stresses in the decomposition of Eq. (4.6.3) are integers. To make the whole sum integral we round the coefficients. Though, direct rounding may influence the sign of the resulting stresses. To overcome this effect we scale the coefficients before rounding. We pick the scaling factor

$$C := (d+1) \left\lceil \frac{\max_{f,g,k} |\Omega_{fg}^A(W_k)|}{\min_{f,g} |\Omega_{fg}^c|} \right\rceil$$

and construct

$$\Omega := \sum_{1\leq k\leq n} \lfloor C\alpha_k \rfloor \Omega^A(W_k).$$

The stress Ω is an integral braced stress for (u_i). It remains to prove that the signs of Ω_{fg} and Ω_{fg}^c coincide, which would validate that Ω is positive. Indeed,

$$|\Omega_{fg} - C\Omega_{fg}^c| = \left| \sum_{1\leq k\leq n} (\lfloor C\alpha_k \rfloor - C\alpha_k) \Omega_{fg}^A(W_k) \right|$$
$$\leq \sum_{1\leq k\leq n} |\Omega_{fg}^A(W_k)| \leq (d+1) \max_{(fg),k} |\Omega_{fg}^A(W_k)| \leq C \min_{(fg)} |\Omega_{fg}^c|.$$

The third transition holds since exactly $d+1$ wheels participate in the wheel-decomposition of every single $(d-2)$-face (fg): $(d-1)$ wheels with apexes in each of the vertices of (fg) and 2 wheels with apexes in the vertices of f and g that do not belong to (fg).

In the remainder of the proof we bound the entries of Ω. Due to the bounds on Ω^c and Ω^A, the constant C is bounded by

$$C \leq (d+1)L^{d(\Delta_G{}^*+2)-1}.$$

The constructed braced stress Ω is therefore bounded by

$$\begin{aligned}
|\Omega_{fg}| \leq & |C\Omega^c_{fg}| + (d+1)\max_{(fg),k} |\Omega^A_{fg}(W_k)| \\
\leq & |C| \max_{(fg)} |\Omega^c_{fg}| + (d+1)\max_{(fg),k} |\Omega^A_{fg}(W_k)| \\
\leq & (d+1)L^{d(\Delta_G{}^*+2)-1} 2L^{d-1} + (d+1)L^{d(\Delta_G{}^*-1)} \\
= & O\left(dL^{d(\Delta_G{}^*+3)-2}\right),
\end{aligned}$$

where we denote with $\Delta_G{}^* := \max_{v\in\mathcal{F}_0(\mathcal{P})}(\deg^*(v))$. □

The duality transform theorem is now a direct consequence of the Lovász duality construction of Lemma 4.4.2 and Lemma 4.6.3:

Theorem 4.6.2. *Let $\mathcal{P}$ be a simplicial polytope with n vertices in $\mathbb{R}^d$. Then there exists a realization $(\phi_f)_{f\in\mathcal{F}_{d-1}(\mathcal{P})}$ of the polytope $\mathcal{P}^*$ dual to $\mathcal{P}$ as a convex polytope with integer coordinates bounded by*

$$|\phi_f| = O\left(dn^{\lfloor\log(d)\rfloor+2}\max_{u\in\mathcal{F}_0(\mathcal{P})}|u|^{d(\Delta_G{}^*+4)-3}\right),$$

where $\Delta_G{}^*$ is the maximum over the vertices v of P of the number of facets of $\mathcal{P}$ adjacent to v.

Proof. We first use Lemma 4.6.3 to construct a positive integer braced stress Ω on $\mathcal{P}$ such that

$$\Omega_{fg} = O\left(d\max_{u\in\mathcal{F}_0(\mathcal{P})}|u|^{d(\Delta_G{}^*+3)-2}\right).$$

Then by Lemma 4.4.2 there exists a realization $(\phi_f)_{f\in\mathcal{F}_{d-1}(\mathcal{P})}$ of the dual polytope $\mathcal{P}^*$ as a convex polytope with integral vertices such that

$$|\phi_f| \leq \operatorname{diam}\left(\mathrm{Sk}_1(\mathcal{P}^*)\right)\max_{(fg)\in\mathcal{F}_{d-2}(\mathcal{P})}|\Omega_{fg}|\max_{u\in\mathcal{F}_0(\mathcal{P})}|u|^{d-1}.$$

We use the general bound on $\operatorname{diam}(\mathrm{Sk}_1(\mathcal{P}^*)$ due to Kalai and Kleitman [18]:

$$\operatorname{diam}\left(\mathrm{Sk}_1(\mathcal{P}^*)\right) = O\left(n^{\lfloor\log(d)\rfloor+2}\right)$$

and the statement of the theorem follows. □

Conclusion

In our work we presented some advances in finding polynomial size integral realizations of convex polytopes. Together with the previous work by Demaine and Schulz [9] on stacked polytopes, we are now aware of two large classes of polytopes that admit such realizations: the class of stacked and the class of truncated polytopes. However, the final answer to the question of whether every 3-dimensional polytope admits such a realization, or, if not, of classifying those polytopes that admit, still stays outrageously open.

In the introduction we observed that in context of our question a particularly perspective class of polytopes is the class of simplicial polytopes. We remind that this general belief is based on the observation, that every vertex of a simplicial polytope can be independently slightly perturbed so that the combinatorial structure of the polytope is not affected. In particular, stacked polytopes, the only previously known class of polytopes which allow small integral realizations, are simplicial.

One particularly interesting feature of our results is that our algorithms construct realizations of nonsimplicial polytopes. Indeed, truncated polytopes are simple polytopes, without any restrictions on the number of vertices in one face. Nevertheless, every truncated polytope can be realized on a grid of fixed polynomial in the number of vertices size. Moreover, we show how to transform an efficient realization of any simplicial polytope into a realization of its dual, which is in turn simple, however this transformation is efficient only for simplicial polytopes with bounded maximal vertex degree.

That weakens our belief in that the nonsimplicial polytopes are hopeless in the context of our question as well as that the simplicial polytopes are simpler to approach. Now, with an efficient duality transform in hand, any progress in realizing simplicial polytopes will immediately lead to a progress in realizing simple polytopes. However, we are not a single step closer to efficient realizations of polytopes that are neither simplicial nor simple. General handwaving apart, we consider the following directions of research as perspective:

- We are sure that the limits of applicability of the developed duality transform are not reached in our work. We remind that the Lovász duality rephrases the question of efficiently realizing a convex polytope to the question of finding a cone-convex realization of the dual graph with small integral coordinates and a small integral positive braced stress. We presented two constructions that build such realizations: one builds it for stacked polytopes "from scratch", another starts with a convex realization of a simplicial polytope and computes a small braced stress on it. We believe that there are more classes of polytopes, for which the cone-convex realizations with braced stresses of the dual graphs can be constructed from scratch, similar to the pair of truncated/stacked polytopes. This belief is strengthened by the fact that braced stresses represent a new tool, which is well-connected to equilibrium stresses, which in turn is a well-established and well-studied object.

- We believe that there is still room for the direct application of Tutte's stressed embeddings and the Maxwell–Cremona lifting. As we have mentioned in the review of the existing approaches, Chapter 1, this approach is used as a base for the best to date algorithm

for realizing an arbitrary 3d convex polytope with small integral coordinates [29], as well as for the best to date algorithm for realizing 3d convex polytopes with good vertex resolution [37]. We believe that further advances using these approaches are possible. In particular, we mention a new technology for locally adjusting stresses, developed in [37], which in our opinion may be successfully used in other setups operating with equilibrium and braced stresses.

- Another not yet investigated direction is the possibility of employing Colin de Verdière matrices. We remind that a Colin de Verdière matrix of a graph is defined in terms of spectral properties of the graph. For a 3-connected planar graph any Colin de Verdière matrix has rank 3 and thus defines an embedding of the underlying graph into $\mathbb{R}^3$ that can be scaled to a convex polytope in a canonical way. This technology was developed by Lovász [21] and we use the geometrical ideas of this work as the main source of inspiration in this thesis. However, we expect that the spectral ideas of Lovász' work can also be used. In particular, we expect that there exists a way to directly produce "efficient" Colin de Verdière matrices for special classes of polytopes.

- The example of the prismatoid presented in our work shows that not all the direct combinatorially-geometrical ideas are yet developed. We expect that larger classes of polytopes can be handled using available constructions for prismatoids, truncated, and stacked polytopes as some kinds of "building blocks".

- Additional motivation in favour of geometrical methods is provided by a recent development in realizing simplicial polytopes with two coordinates of polynomial size at the expense of the third coordinate by Pak and Wilson [27]. Their method combines combinatorial and purely geometrical ideas and does not involve any stresses.

To conclude, our greatest hope is that new results may be achieved by combining the geometrical, spectral, and stressed methods listed above.

Bibliography

[1] E. Andreev. On convex polyhedra in Lobačevskiĭ spaces. *Mathematics of the USSR-Sbornik*, 10(3):413, 1970.

[2] E. Andreev. On convex polyhedra of finite volume in Lobačevskiĭ space. *Sbornik: Mathematics*, 12(2):255–259, 1970.

[3] G. E. Andrews. A lower bound for the volume of strictly convex bodies with many boundary lattice points. *Transactions of the American Mathematical Society*, 106(2):270–279, 1963.

[4] D. Barnette and B. Grünbaum. Preassigning the shape of a face. *Pacific Journal of Mathematics*, 32(2):299–306, 1970.

[5] G. R. Brightwell and E. R. Scheinerman. Representations of planar graphs. *SIAM Journal on Discrete Mathematics*, 6(2):214–229, 1993.

[6] M. Chrobak and G. Kant. Convex grid drawings of 3-connected planar graphs. *International Journal of Computational Geometry & Applications*, 7(3):211–223, 1997.

[7] H. Crapo and W. Whiteley. Plane self stresses and projected polyhedra I: The basic pattern. *Structural Topology*, 20, 1993.

[8] H. de Fraysseix, J. Pach, and R. Pollack. How to draw a planar graph on a grid. *Combinatorica*, 10(1):41–51, 1990.

[9] E. D. Demaine and A. Schulz. Embedding stacked polytopes on a polynomial-size grid. In *Proc. 22nd ACM-SIAM Symposium on Discrete Algorithms (SODA)*, pages 1177–1187. ACM Press, 2011.

[10] E. D. Demaine and A. Schulz. Embedding stacked polytopes on a polynomial-size grid. `http://arxiv.org/abs/1403.7980v3`, 2016.

[11] I. Fáry. On straight lines representation of plane graphs. *Acta. Sci. Math. Szeged*, 11:229–233, 1948.

[12] S. Felsner. Convex drawings of planar graphs and the order dimension of 3-polytopes. *Order*, 18(1):19–37, 2001.

[13] B. Grünbaum. *Convex polytopes*, volume 221 of *Graduate Texts in Mathematics*. Springer-Verlag, New York, 2 edition, 2003.

[14] J. E. Hopcroft and P. J. Kahn. A paradigm for robust geometric algorithms. *Algorithmica*, 7(4):339–380, 1992.

[15] A. Igamberdiev, F. Nielsen, and A. Schulz. Small grid embeddings of prismatoids and the platonic solids. In *Graph Drawing*, page 530. Springer, 2013.

[16] A. Igamberdiev and A. Schulz. A duality transform for constructing small grid embeddings of 3d polytopes. In *Graph Drawing*, pages 173–184. Springer, 2013.

[17] I. Izmestiev. The Colin de Verdière number and graphs of polytopes. *Israel Journal of Mathematics*, 178(1):427–444, 2010.

[18] G. Kalai and D. J. Kleitman. A quasi-polynomial bound for the diameter of graphs of polyhedra. *Bull. Amer. Math. Soc*, 26(2):315–316, 1992.

[19] E. D. Kim and F. Santos. An update on the Hirsch conjecture. *Jahresbericht der Deutschen Mathematiker-Vereinigung*, 112(2):73–98, 2010.

[20] P. Koebe. *Kontaktprobleme der konformen Abbildung.* Hirzel, 1936.

[21] L. Lovász. Steinitz representations of polyhedra and the Colin de Verdière number. *J. Combin. Theory Ser. B*, 82(2):223–236, 2001.

[22] L. Lovász. Geometric representations of graphs. `http://www.cs.elte.hu/~lovasz/bookxx/geomrep.pdf`, 2014. Accessed 22.11.2015.

[23] J. C. Maxwell. On reciprocal figures and diagrams of forces. *The London, Edinburgh, and Dublin Philosophical Magazine and Journal of Science*, 27(182):250–261, 1864.

[24] B. Mohar. A polynomial time circle packing algorithm. *Discrete Mathematics*, 117(1):257–263, 1993.

[25] F. Müller-Hoissen, J. M. Pallo, and J. Stasheff. *Associahedra, Tamari lattices and related structures: Tamari memorial Festschrift*, volume 299. Springer Science & Business Media, 2012.

[26] S. Onn and B. Sturmfels. A quantitative Steinitz' theorem. In *Beiträge zur Algebra und Geometrie*, volume 35, pages 125–129, 1994.

[27] I. Pak and S. Wilson. A quantitative Steinitz theorem for plane triangulations. `http://arxiv.org/abs/1311.0558`, 2013.

[28] A. Ribó Mor. *Realization and counting problems for planar structures.* PhD thesis, Freie Universität Berlin, Germany, 2006.

[29] A. Ribó Mor, G. Rote, and A. Schulz. Small grid embeddings of 3-polytopes. *Discrete & Computational Geometry*, 45(1):65–87, 2011.

[30] J. Richter-Gebert. *Realization Spaces of Polytopes*, volume 1643 of *Lecture Notes in Mathematics.* Springer, 1996.

[31] J. Richter-Gebert and G. M. Ziegler. Realization spaces of 4-polytopes are universal. *Bull. Amer. Math. Soc.*, 32:403, 1995.

[32] K. A. Rybnikov. Stresses and liftings of cell-complexes. *Discrete & Computational Geometry*, 21(4):481–517, 1999.

[33] F. Santos. A counterexample to the Hirsch conjecture. *Annals of mathematics*, 176(1):383–412, 2012.

[34] W. Schnyder. Embedding planar graphs on the grid. In *Proc. 1st ACM-SIAM Symposium Discrete Algorithms (SODA)*, pages 138–148, 1990.

[35] O. Schramm. How to cage an egg. *Inventiones mathematicae*, 107(1):543–560, 1992.

[36] A. Schrijver. *Combinatorial optimization: polyhedra and efficiency*, volume 24. Springer Science & Business Media, 2003.

[37] A. Schulz. Drawing 3-polytopes with good vertex resolution. *Journal of Graph Algorithms and Applications*, 15(1):33–52, 2011.

[38] E. Steinitz. Polyeder und Raumeinteilungen. In *Encyclopädie der mathematischen Wissenschaften*, volume 3-1-2 (Geometrie), chapter 12, pages 1–139. B. G. Teubner, Leipzig, 1916.

[39] E. Steinitz. Über isoperimetrische Probleme bei konvexen Polyedern. *Journal für die reine und angewandte Mathematik*, 159:133–143, 1928.

[40] R. Tamassia. *Handbook of graph drawing and visualization*. CRC press, 2013.

[41] W. P. Thurston. The geometry and topology of three-manifolds. `http://library.msri.org/books/gt3m/`, 2002. Princeton University lecture notes.

[42] W. T. Tutte. How to draw a graph. *Proceedings London Mathematical Society*, 13(52):743–768, 1963.

[43] J. Van Leeuwen. *Handbook of theoretical computer science: Algorithms and complexity*, volume 1. Elsevier, 1990.

[44] W. Whiteley. Motions and stresses of projected polyhedra. *Structural Topology*, 7, 1982.

[45] H. Whitney. Congruent graphs and the connectivity of graphs. *Amer. J. Math.*, 54:150–168, 1932.

[46] G. M. Ziegler. *Lectures on polytopes*, volume 152 of *Graduate Texts in Mathematics*. Springer-Verlag, New York, 1995.